Precise predictions for Higgs physics in supersymmetric models

Dissertation

zur Erlangung des Doktorgrades
an der Fakultät für Mathematik,
Informatik und Naturwissenschaften

Fachbereich Physik
der Universität Hamburg

vorgelegt von

Ivan Sobolev
aus
Moskau, Russland

Hamburg

2020

Hiermit versichere ich an Eides statt, die vorliegende Dissertationsschrift selbst verfasst und keine anderen als die angegebenen Hilfsmittel und Quellen benutzt zu haben. Die eingereichte schriftliche Fassung entspricht der auf dem elektronischen Speichermedium. Die Dissertation wurde in der vorgelegten oder einer ähnlichen Form nicht schon einmal in einem früheren Promotionsverfahren angenommen oder als ungenügend beurteilt.

Hamburg, den 31. Mai 2020.

Gutachter der Dissertation:	Prof. Dr. Georg Weiglein Prof. Dr. Géraldine Servant
Zusammensetzung der Prüfungskommission:	Prof. Dr. Peter Schmelcher Prof. Dr. Georg Weiglein Prof. Dr. Géraldine Servant Prof. Dr. Sven-Olaf Moch Prof. Dr. Isabell Melzer-Pellmann
Vorsitzender der Prüfungskommission:	Prof. Dr. Peter Schmelcher
Datum der Disputation:	07.07.2020
Vorsitzender Fach-Promotionsausschusses PHYSIK:	Prof. Dr. Günter H.W. Sigl
Leiter des Fachbereichs PHYSIK:	Prof. Dr. Wolfgang Hansen
Dekan der Fakultät MIN:	Prof. Dr. Heinrich Graener

Abstract

In the Minimal Supersymmetric Standard Model (MSSM), the mass of the SM-like Higgs boson can be predicted in terms of the model parameters and therefore used as a precision observable to constrain the MSSM parameter space. The precise prediction of the lightest MSSM Higgs boson mass in scenarios with one or several heavy supersymmetric particles requires the resummation of higher-order logarithmic contributions obtained within an effective-field-theory (EFT) approach. By combining the EFT calculation with a fixed-order calculation, a precise prediction also for low and intermediary SUSY scales can be obtained. This method is called the hybrid approach and is implemented, for instance, in the publicly available code `FeynHiggs`.

We discuss various improvements to this hybrid framework. First, we consider the resummation of logarithmic contributions proportional to the bottom-Yukawa coupling, including two-loop Δ_b-resummation. For large $\tan\beta$, this can lead to large upward shifts of the Higgs mass compared to the existing fixed-order calculations. Second, we improve the implemented EFT calculation by fully taking into account the effect of the phases of complex soft SUSY-breaking parameters. In addition, we discuss the inclusion of partial $\mathrm{N^3LL}$ resummation.

After that, we turn to the case when there is a significant hierarchy between the gluino mass and the masses of the scalar top quarks. In such a situation, the current Higgs boson mass predictions so far have suffered from large theoretical uncertainties related to non-decoupling power-enhanced gluino contributions in the EFT employing the $\overline{\mathrm{DR}}$ renormalization scheme. We demonstrate that the theoretical predictions in the heavy gluino region are vastly improved by the introduction of a more suitable renormalization scheme for the EFT calculation. It is shown that within this scheme, the large gluino contributions are absorbed into the model parameters, resulting in reliable and numerically stable predictions in the heavy-gluino region.

The presented improvements will become publicly available as parts of `FeynHiggs`.

Zusammenfassung

Im minimalen supersymmetrischen Standardmodell (MSSM) kann die Masse des leichtesten Higgs-Bosons in Abhängigkeit von den Modellparametern vorhergesagt werden und daher als Präzisionsobservable verwendet werden, um den MSSM-Parameterraum einzuschränken. Die präzise Vorhersage der Masse des leichtesten MSSM-Higgs-Bosons in Szenarien mit einem oder mehreren schweren supersymmetrischen Teilchen erfordert die Resummation logarithmischer Beiträge höherer Ordnung, die im Rahmen eines EFT-Ansatzes (Effektive-Feld-Theorie) durchgeführt wird. Durch die Kombination der EFT-Rechnung mit einer Rechnung auf fester Ordnung kann eine präzise Vorhersage auch für niedrige und intermediäre SUSY-Skalen erhalten werden. Diese Methode wird als Hybridansatz bezeichnet und ist z.B. im öffentlich zugänglichen Code `FeynHiggs` implementiert.

In dieser Arbeit werden verschiedene Verbesserungen dieser Hybrid-Methode diskutiert. Zunächst wird die Resummation der logarithmischen Beiträge proportional zur Bottom-Yukawakopplung betrachtet, einschließlich von Δ_b-Resummation auf dem Zwei-Schleifen-Niveau. Bei großen $\tan\beta$ können diese Verbesserungen zu großen Verschiebungen der Higgs-Masse nach oben im Vergleich zu den bestehenden Berechnungen auf fester Ordnung führen. Weiterhin wird die EFT-Berechnung verbessert, indem die Auswirkungen der Phasen von komplexen soft SUSY-brechenden Parametern vollständig berücksichtigen berücksichtigt werden. Als weitere Verbesserung wird die Einbeziehung einer teilweisen $\mathrm{N^3LL}$-Resummation diskutiert.

Danach wird der Fall einer großen Hierarchie zwischen der Gluino-Masse und den Massen der skalaren Top-Quarks betrachtet. In diesem Fall weisen die bisherigen Higgs-Boson-Massenvorhersagen große theoretischen Unsicherheiten auf. Diese werden durch nicht-entkoppelnde und durch die Gluino-Masse potentiell verstärkte Beiträge im EFT-Ergebnis als Konsequenz der Verwendung des $\overline{\mathrm{DR}}$-Renormierungsschemas hervorgerufen. Es wird demonstriert, dass die theoretischen Vorhersagen in der Parameterregion mit schweren Gluinos durch die Einführung eines geeigneteren Renormierungsschemas für die EFT-Berechnung erheblich verbessert werden. In diesem Schema werden die großen Gluino-Beiträge in die Modellparameter absorbiert. Dadurch sind zuverlässige und numerisch stabile Vorhersagen in der Parameterregion mit schweren Gluinos möglich.

Die vorgestellten Verbesserungen werden als Teil des Programms `FeynHiggs` öffentlich zugänglich sein.

This thesis is based on the publications:

- H. Bahl, I. Sobolev and G. Weiglein, *Improved determination of the light MSSM Higgs boson mass for large* $\tan\beta$*, complex input parameters and large* M_{SUSY}, DESY 20-085, to appear.
- H. Bahl, I. Sobolev and G. Weiglein, *Precise prediction for the mass of the light MSSM Higgs boson for the case of a heavy gluino*, *Phys. Lett.* **B808** (2020)

Other publications by the author:

- E. Bagnaschi *et al.*, *Supersymmetric Models in Light of Improved Higgs Mass Calculations*, *Eur.Phys.J.***C79** (2019) no.2, 149.
- S.V. Demidov, I.V. Sobolev, *Low scale supersymmetry at the LHC with jet and missing energy signature*, `arXiv:1709.03830`.
- M. Chala, G. Nardini, I. Sobolev, *Unified explanation for dark matter and electroweak baryogenesis with direct detection and gravitational wave signatures*, *Phys. Rev.* **D94** (2016), no. 5, 055006.
- S.V. Demidov, I.V. Sobolev, *Lepton flavor-violating decays of the Higgs boson from sgoldstino mixing*, *JHEP* **1608** (2016) 030.

Contents

Introduction

In July 2012 two experiments at the Large Hadron Collider (LHC), ATLAS [1] and CMS [2], announced the discovery of a new particle with a mass of around $M_h \sim 125$ GeV . To date, this has been the last discovery of a new particle whose existence is explainable within the Standard Model (SM) of particle physics, a theory which describes the three fundamental forces of Nature: the electromagnetic, weak, and strong interactions. Subsequent analyses of the data collected during Run I and Run II of the LHC indicate that the properties of this particle are, within current theoretical and experimental uncertainties, compatible with those of the SM Higgs boson [3].

So far, the SM has been successful in describing almost all experimental results in high-energy physics. However, it has several problems which make us believe that the SM should be embedded into a more fundamental theory. For example, it does not account for neutrino oscillations, nor for the evidence for Dark Matter (DM) and does not predict the correct amount of the baryon-antibaryon asymmetry of the Universe. On top of that, if the SM is considered as a low-energy approximation of a more complete theory, the mass of the SM Higgs boson is unprotected against potentially large radiative corrections originating from physics at high mass scales. The latter problem is often called the *naturalness* or the *hierarchy* problem. The unnaturally small size of the Higgs mass suggests that new degrees of freedom should show up at energies of the order of the TeV scale. Numerous beyond the SM (BSM) models have been put forward to address one or more of the shortcomings of the SM.

Supersymmetry (SUSY) - a symmetry relating fermions to bosons - is among the most prominent and attractive concepts for building BSM models since it can address several of the problems of the SM. The minimal realization of supersymmetry, the Minimal Supersymmetric extension of the Standard Model (MSSM) is one of the best-studied extensions of the SM. In this model, the number of degrees of freedom is doubled by adding a boson to each SM fermionic degree of freedom, and a fermion to each SM boson. Loop corrections to scalar masses now contain contributions both from the SM particles and their superpartners, which come with different signs and

cancel each other in the case of exact supersymmetry. The MSSM endowed with an additional symmetry, called R-parity, provides a natural DM candidate – the lightest supersymmetric particle (LSP). The MSSM also provides additional sources of $\mathcal{CP}$-violation, which can give rise to the correct amount of the baryon-antibaryon asymmetry of the Universe.

To realize SUSY not only the doubling of the particle content of the SM is required. In addition, the SM Higgs sector has to be extended by adding a second Higgs doublet. This results in five physical degrees of freedom: at lowest order, these are two $\mathcal{CP}$-even, one $\mathcal{CP}$-odd, and two charged Higgs bosons. The tree-level Higgs potential is determined only by two parameters: the mass of the $\mathcal{CP}$-odd Higgs boson m_A and the ratio of the vacuum expectation values of the two Higgs doublets, $\tan\beta = v_2/v_1$. The tree-level mass of the lightest Higgs boson, which typically plays the role of the SM-like Higgs boson, is bounded from above by the mass of the Z-boson. However, it can acquire sizeable radiative corrections and can reach the measured value of $M_h \sim 125$ GeV. Consequently, the physical mass of the lightest Higgs boson is correlated with other parameters of the theory and can be used as a powerful constraint on the MSSM parameter space.

The Higgs boson mass has been measured with a sub-percent precision [3–5], and according to the current projections, it might be possible to further reduce the uncertainty down to as low as 10-20 MeV at the high luminosity (HL) phase of the LHC [6]. In order to exploit precision for constraining the parameter space of the MSSM, one needs very precise theoretical prediction for the mass of the SM-like Higgs boson. This can be achieved by computing quantum corrections to the Higgs boson mass that incorporate numerically sizeable contributions. The evaluation of these quantum corrections can be performed in different frameworks. In the most direct approach, quantum corrections to the Higgs self-energy are calculated diagrammatically in the full theory (for recent works see [7–12]). This approach has the advantage of capturing all corrections at a specific order in perturbation theory.

In light of the absence of any direct evidence for supersymmetric particles at the LHC, the ATLAS and CMS experiments have pushed the lower bounds on the masses of some of them, mainly scalar top quarks and gluinos, into the TeV range. If the scale of the SUSY particles is much larger than the electroweak scale, large logarithms emerge in the fixed-order corrections spoiling the convergence of the perturbative expansion. In such situations, effective field theory (EFT) techniques allow the resummation of these large logarithmic corrections (for recent works see [13–20]). Without including higher-dimensional operators into the low-energy EFT, terms suppressed by the SUSY scale are, however, missed in this approach. Therefore, the

EFT approach can lose its accuracy if one or more SUSY particles have masses that are comparable to the electroweak scale.

To obtain a precise prediction for the SM-like Higgs boson mass for low, intermediary as well as high SUSY scales, both approaches – the fixed-order and the EFT approach – can be combined. Such a hybrid approach has been implemented into the publicly available code `FeynHiggs` [16, 20–24] (similar approaches have been considered in [25–28]).

In this thesis, we will consider various improvements to the incorporated EFT calculation as well as its combination with the implemented fixed-order calculation. Among those considered are the resummation of large logarithms proportional to the bottom Yukawa coupling (including two-loop Δ_b resummation [29–31]), the extension of the EFT calculation to fully take into account complex input parameters as well as the inclusion of partial N^{3}LL resummation.

In addition, we discuss the prediction for the SM-like Higgs mass for scenarios in which the gluino is much heavier than the stops. Currently, appropriate EFT methods for the calculation of the mass of the SM-like Higgs boson have been developed for different patterns of possible SUSY spectra, including split-SUSY type scenarios where the mass of the gluino is much lighter than the masses of the squarks [32, 33]. However, no proper EFT treatment of the case where the gluino is significantly heavier than the squarks is available up till now. It has been known for a while that the two-loop QCD corrections to the Higgs mass computed in the $\overline{\text{DR}}$ scheme contain contributions that are enhanced by powers of the gluino mass $|M_3|$ [34]. Since the EFT result is parametrized in the $\overline{\text{DR}}$ scheme, large theoretical uncertainties in the Higgs-mass prediction, obtained in the EFT approach, occur for values of $|M_3| \gtrsim 2M_{\text{SUSY}}$ [35]. This can be a serious drawback for realistic analyses of SUSY phenomenology since the LHC searches have pushed the experimental bounds on the gluino mass to the region above ~ 2 TeV, while the superpartners of the top quark are still allowed to have masses around the TeV scale [36–44]. We show how the contributions enhanced by powers of $|M_3|$ can be absorbed by the choice of a suitable renormalization scheme for the EFT calculation, called the $\overline{\text{MDR}}$ scheme. This leads to a drastic reduction of the theoretical uncertainty.

Thesis outline

This thesis is organized as follows. In **Chapter 1**, we give a short overview of the Standard Model of particle physics focusing on the electroweak symmetry breaking by the Higgs mechanism, and we outline the shortcomings of the Standard Model. **Chapter 2** introduces the concept of supersymmetry and explains how the most

general $N = 1$ supersymmetric Lagrangian can be built. After that, we describe the different sectors of the MSSM at the tree-level. In **Chapter 3**, we briefly review methods for higher-order calculations and describe the renormalization of the relevant MSSM sectors. **Chapter 4** describes different methods for the computation of higher-order corrections to the SM-like Higgs mass: the fixed-order approach, the effective field theory approach and the hybrid approach. We review each method in detail and its current status. In **Chapter 5**, we explain how the NNLL resummation of logarithms proportional to the bottom Yukawa coupling is incorporated into the hybrid framework used in the publicly available code `FeynHiggs`. We also discuss the derivation of the leading two-loop QCD and the mixed Yukawa-QCD threshold corrections to the bottom Yukawa coupling. The extension of the EFT calculation to the case of complex input parameters is discussed in **Chapter 6**. We explain the implementation of partial N^{3}LL resummation in **Chapter 7**. In **Chapter 8**, we discuss how corrections that are enhanced by powers of the gluino mass arise and how they can be resummed by a suitable choice of the renormalization scheme. Finally, the conclusions are given in **Chapter 9**. Supplementary material is given in App. A – App. D.

Chapter 1

The Standard Model of Particle Physics

In this Chapter, we provide a brief review of the Standard Model of particle physics. After describing the gauge and the Yukawa sectors in Sections 1.1–1.3 we turn to the discussion of the shortcomings of the Standard Model in Sec. 1.5.

1.1 Gauge symmetries

The Standard Model (SM) of particle physics is the minimal renormalizable quantum field theory describing almost all experimental data from collider experiments. It is a gauge theory with the group $G_{\rm SM} = SU(3)_C \otimes\ SU(2)_L \otimes\ U(1)_Y$. The group can be split into two pieces. The color group $SU(3)_C$ describes strong interactions with the coupling constant g_3. The corresponding gauge fields are gluons $G^a_\mu, (a = 1, \ldots, 8)$, and they transform in the adjoint representation of the group. $SU(2)_L \otimes\ U(1)_Y$ describes electroweak interactions. Here $SU(2)_L$ is a weak isospin group with three gauge bosons denoted as $W^a_\mu, (a = 1, 2, 3)$, and the gauge coupling g. The remaining $U(1)_Y$ group is called the hypercharge group. The corresponding gauge boson is B_μ and the gauge coupling is g'.

Demanding invariance of the SM Lagrangian under the gauge transformations implies that we need to replace the derivatives ∂_μ in the kinetic terms by the covariant derivatives D_μ in the following way,

$$\partial_\mu \to D_\mu = \partial_\mu - ig_3\frac{\lambda_a}{2}G^a_\mu + ig\frac{\sigma^a}{2}W^a_\mu - ig'\frac{Y}{2}B_\mu, \tag{1.1.1}$$

where λ_a are Gell-Mann matrices σ_a are Pauli matrices and Y is a hypercharge. Using this notation we can write down the gauge-invariant kinetic term for a fermion field ψ,

$$\mathcal{L}_{\text{kin}}^{\text{fermion}} = i\bar{\psi}\not{D}\psi, \tag{1.1.2}$$

with $\bar{\psi} \equiv \psi^\dagger\gamma_0$, $\not{D} \equiv \gamma^\mu D_\mu$, and γ^μ are the Dirac matrices. The kinetic term for the gauge fields has the following form

$$\mathcal{L}_{\text{gauge}} = -\frac{1}{4}F^a_{\mu\nu}F^{a\mu\nu} = -\frac{1}{4}G^a_{\mu\nu}G^{\mu\nu a} - \frac{1}{4}W^a_{\mu\nu}W^{\mu\nu a} - \frac{1}{4}B_{\mu\nu}B^{\mu\nu}, \tag{1.1.3}$$

where the gauge-invariant quantities $G^a_{\mu\nu}$, $W^a_{\mu\nu}$ and $B_{\mu\nu}$ are the field strength tensors

$$G^a_{\mu\nu} = \partial_\mu G^a_\nu - \partial_\nu G^a_\mu + g_3 f^{abc} G^b_\mu G^c_\nu, \tag{1.1.4}$$

$$W^a_{\mu\nu} = \partial_\mu W^a_\nu - \partial_\nu W^a_\mu + g\epsilon^{abc} W^b_\mu W^c_\nu, \tag{1.1.5}$$

$$B_{\mu\nu} = \partial_\mu B_\nu - \partial_\nu B_\mu, \tag{1.1.6}$$

and f^{abc} and ϵ^{abc} are the structure constants of $SU(3)$ and $SU(2)$, respectively, (i.e. $[\sigma^a, \sigma^b] = 2i\epsilon^{abc}\sigma^c$ and $[\lambda^a, \lambda^b] = 2if^{abc}\lambda^c$). W- and B-bosons mix after electroweak symmetry breaking into the $W^\pm$-, and Z-bosons as well as the photon. This issue will be considered in more detailed in the next Section.

1.2 Electroweak symmetry breaking

It is a well-established experimental fact that the weak interaction is a short-range force, so that its mediators have to be massive particles. A simple realization of a theory of massive vector bosons with a mass term [1]

$$\mathcal{L}_B = -\frac{1}{4}(\partial_\mu B_\nu - \partial_\nu B_\mu)^2 + \frac{M_B^2}{2}B_\mu B^\mu \tag{1.2.1}$$

leads to an unphysical behaviour of the vector bosons at large momenta which spoils the renormalizability and the unitarity of the theory. Moreover, it is known that the weak interaction does not preserve parity. More precisely, only left-handed fermions transform according to the $SU(2)_L$ gauge group.[2] This forbids the existence of a fermion mass term. Indeed, since for some fermionic field ψ its left-handed and right-handed part transform differently, the term

$$-M_F\bar{\psi}\psi = -M_F(\bar{\psi}_L\psi_R + \bar{\psi}_R\psi_L) \tag{1.2.2}$$

[1] For the illustration, we consider the case of an Abelian vector boson theory. The same arguments apply for the non-Abelian case as well.

[2] It is for this reason we use the index L for the $SU(2)_L$ subgroup of G_{SM}.

would clearly violate gauge invariance. However, most of the SM particles (except for gluons, photons and neutrinos) are massive.

These problems can be solved by the Brout–Englert–Higgs (BEH) mechanism [45–48] via introducing an $SU(2)_L$ scalar doublet Φ with hypercharge $Y = 1$ which triggers spontaneous breaking of $SU(2)_L \otimes U(1)_Y$. This complex field, called Higgs field, can be written as follows

$$\Phi(x) = \begin{pmatrix} \phi^+(x) \\ \phi^0(x) \end{pmatrix}. \tag{1.2.3}$$

The notations in this formula are chosen according to the Gell-Mann–Nishijima formula

$$Q = I^3 + \frac{Y}{2}, \tag{1.2.4}$$

where Q is the electric charge, I^3 is the third component of the isospin vector, $I^3 = \frac{\sigma^3}{2}$, and Y is the hypercharge. Indeed,

$$Q\ \Phi(x) = \begin{pmatrix} \phi^+(x) \\ 0 \end{pmatrix}, \tag{1.2.5}$$

so $\phi^+(x)$ has electric charge $+1$ and $\phi^0(x)$ is electrically neutral. The most general renormalizable gauge-invariant Lagrangian for the field Φ reads

$$\mathcal{L}_H = D_\mu \Phi^\dagger D^\mu \Phi - V(\Phi), \tag{1.2.6}$$

where the scalar potential of the field has the form

$$V(\Phi) = -\mu^2 \Phi^\dagger \Phi + \frac{\lambda}{2}(\Phi^\dagger \Phi)^2. \tag{1.2.7}$$

In this expression the dimensionless coupling constant λ is called Higgs quartic coupling, and the parameter μ^2 is the Higgs mass parameter. The sign of the quartic coupling, $\lambda > 0$, is fixed by requiring that the potential is bounded from below. Indeed, if lambda was less than zero, then for arbitrarily large values of $\Phi^\dagger\Phi$ the potential $V(\Phi)$ would take large negative values, so it would not have a global minimum. The sign of the μ^2 parameter determines the shape of the potential. For $\mu^2 < 0$ it has a global minimum at $\Phi = 0$, and electroweak gauge symmetry is not broken. For $\mu^2 > 0$ the global minimum of the potential is at $\Phi^\dagger\Phi = v^2$, where v is called the vacuum expectation value (vev) of the Higgs field. The vacuum expectation value of Φ can be written as

$$\langle \Phi \rangle = e^{iU(x)} \begin{pmatrix} 0 \\ v \end{pmatrix}. \tag{1.2.8}$$

The phase factor $e^{iU(x)}$ can be rotated away by choosing a unitary gauge. Inserting Eq. (1.2.8) into Eq. (1.2.7) and demanding that $\langle\Phi\rangle$ is a global minimum of the potential, we obtain $v = \sqrt{\frac{\mu^2}{\lambda}}$. Now, the complex scalar field can be expanded around the vacuum expectation value,

$$\Phi(x) = \begin{pmatrix} \phi^+(x) \\ v + \frac{1}{\sqrt{2}}\left(h(x) + i\chi(x)\right) \end{pmatrix}, \tag{1.2.9}$$

where the electrically charged field $\phi^+(x)$ (and its charge conjugate $\phi^-(x)$) together with the electrically neutral $\chi(x)$ are would-be Goldstone bosons. They are unphysical degrees of freedom and are not present in the unitary gauge. The fourth one, $h(x)$, is a physical Higgs field whose potential reads

$$V_{\text{Higgs}}(h) = \frac{m_h^2}{2}h^2 + \frac{m_h^2}{2\sqrt{2}v}h^3 + \frac{m_h^2}{16v^2}h^4, \tag{1.2.10}$$

where

$$m_h^2 = 2\mu^2 = 2\lambda v^2 \tag{1.2.11}$$

is the Higgs boson mass. Being a free parameter in the Standard Model, it together with the vacuum expectation value v completely fixes the tree-level potential of the theory.

The Higgs field vacuum expectation value also gives masses to the gauge bosons. To show this, let us act with the covariant derivative (1.1.1) on (1.2.8) assuming the unitary gauge (i.e. $e^{iU(x)} = 1$),

$$D_\mu\Phi = \begin{pmatrix} \partial_\mu\phi^+ \\ \frac{1}{\sqrt{2}}(\partial_\mu h + i\partial_\mu\chi) \end{pmatrix} + \frac{v}{2}\begin{pmatrix} g(iW_\mu^1 + W_\mu^2) \\ -i(g'B_\mu + gW_\mu^3) \end{pmatrix}. \tag{1.2.12}$$

The Higgs field kinetic term then reads

$$\begin{aligned}(D_\mu\Phi)^\dagger(D_\mu\Phi) = \left|\partial_\mu\phi^+\right|^2 + \frac{(\partial_\mu h)^2}{2} + \frac{(\partial_\mu\chi)^2}{2} + \frac{g^2v^2}{4}\left|W_\mu^1 + iW_\mu^2\right|^2 \\ + \frac{v^2}{4}\left(gW_\mu^3 + g'B_\mu\right)^2 + \ldots,\end{aligned} \tag{1.2.13}$$

where the dots represent interactions between scalar and gauge fields. Redefining the fields in the following way

$$W_\mu^\pm = \frac{W_\mu^1 \mp iW_\mu^2}{\sqrt{2}},\ Z_\mu = \frac{gW_\mu^3 + g'B_\mu}{\sqrt{g^2+g'^2}},\ A_\mu = \frac{gW_\mu^3 - g'B_\mu}{\sqrt{g^2+g'^2}} \tag{1.2.14}$$

we can diagonalize the vector boson mass matrices and rewrite the respective mass terms from Eq. (1.2.13) as

$$(D_\mu\Phi)^\dagger(D_\mu)\Phi = M_W^2 W_\mu^+ W^{\mu,-} + \frac{M_Z^2}{2} Z_\mu Z^\mu + \dots, \tag{1.2.15}$$

with

$$M_W^2 = \frac{g^2 v^2}{2}, \quad M_Z^2 = \frac{(g^2+g'^2)v^2}{2}. \tag{1.2.16}$$

Due to the electroweak symmetry breaking (EWSB) the Goldstone bosons $\phi^\pm(x)$ and $\chi(x)$ become the longitudinal components of the $W^\pm$ and Z gauge bosons. Finally, A_μ from Eq. (1.2.14) does not have a mass term. It describes a photon field which corresponds to the unbroken $U(1)_{em}$ group. The redefinition performed in Eq. (1.2.14), $(W_\mu^3, B_\mu) \to (A_\mu, Z_\mu)$, can be seen as a transformation

$$\begin{pmatrix} Z_\mu \\ A_\mu \end{pmatrix} = \begin{pmatrix} c_\mathrm{w} & s_\mathrm{w} \\ -s_\mathrm{w} & c_\mathrm{w} \end{pmatrix} \begin{pmatrix} W_\mu^3 \\ B_\mu \end{pmatrix}, \tag{1.2.17}$$

where the mixing angle θ_W (also called weak mixing angle) is defined as

$$s_\mathrm{w} \equiv \sin\theta_W = \frac{g'}{\sqrt{g^2+g'^2}}, \quad c_\mathrm{w} \equiv \cos\theta_W = \frac{g}{\sqrt{g^2+g'^2}} = \frac{M_W}{M_Z}. \tag{1.2.18}$$

The weak mixing angle θ_W also relates the electroweak couplings g and g' to the electic charge e of the electron,

$$e = g'\cos\theta_W = g\sin\theta_W = \frac{gg'}{\sqrt{g^2+g'^2}}. \tag{1.2.19}$$

Finally, the Higgs vacuum expectation value v can be related to Fermi's constant G_F which is measured with very high precision in the muon decay, $\mu^- \to e^-\nu_e\bar{\nu}_\mu$ [49],

$$v = \left(2\sqrt{2}G_F\right)^{-1/2} \simeq 174 \text{ GeV}. \tag{1.2.20}$$

Throughout the thesis, we will often use

$$\alpha = \frac{e^2}{4\pi}, \quad \alpha_s = \frac{g_3^2}{4\pi} \tag{1.2.21}$$

instead of g_3 and e.

1.3 Fermion sector of the SM

The fermion sector of the Standard Model consists of three generations. Each of them includes two leptons and two quarks (up-type and down-type). Leptons and

neutrinos are not charged under $SU(3)_C$, while the quarks transform according to the fundamental representation of this group. As we mentioned in Sec.1.2, explicit mass terms for fermions are forbidden by gauge symmetry since left- and right-handed fermions transform differently under the gauge transformations. Similar to the problem of vector boson masses discussed in the previous Section, this problem is also solved by the Higgs mechanism. To realize this, we need to add terms in the Lagrangian $\mathcal{L}_{\rm SM}$ which include fermion-Higgs field interactions.

From experimental studies of weak decays, we know that only left-handed fermions couple to the $SU(2)_L$ gauge bosons. Accordingly, one can construct an $SU(2)_L$ doublet consisting of one left-handed charged lepton and one neutrino

$$L_L = \begin{pmatrix} \nu_L \\ l_L \end{pmatrix} . \tag{1.3.1}$$

From the Gell-Mann–Nishijima relation (Eq. (1.2.4)), the hypercharge of this doublet is determined to be equal to $Y_L = -1$. Right-handed leptons are singlets with respect to $SU(2)_L$, so from the same relation it follows that their hypercharge is equal to $Y_{e_R} = -2$. Analogously, left-handed quarks form a doublet

$$Q_L = \begin{pmatrix} u_L \\ d_L \end{pmatrix} . \tag{1.3.2}$$

Quarks have fractional electric charges: $Q(u_L) = \frac{2}{3}$ and $Q(d_L) = -\frac{1}{3}$. The corresponding hypercharge is $Y_{Q_L} = \frac{1}{3}$. Finally, right-handed quarks transform trivially under $SU(2)_L$ and have hypercharges $Y(u_R) = \frac{4}{3}$ and $Y(d_R) = -\frac{2}{3}$. Keeping in mind the quantum numbers of the fermions and the Higgs field, we can write down the most general renormalizable terms involving fermion-Higgs interactions. These are:

$$\mathcal{L}_{\rm Yuk} \supset -\overline{Q}_L \mathbf{Y}_d \Phi d_R - \overline{Q}_L \mathbf{Y}_u \left(i\sigma^2 \Phi^* \right) u_R - \overline{L}_L \mathbf{Y}_l \Phi e_R + \text{h.c.} . \tag{1.3.3}$$

In the broken phase, using the unitary gauge, one gets

$$\mathcal{L}_{\rm Yuk} \supset -\overline{d}_{L,i} \mathbf{Y}_{d,ij} d_{R,j} \, (v + H) - \overline{u}_{L,i} \mathbf{Y}_{u,ij} u_{R,j} (v + H) - \overline{l}_{L,i} \mathbf{Y}_{l,ij} l_{R,j} (v + H) + \text{h.c.}, \tag{1.3.4}$$

where $\mathbf{Y}_{d,u,l}$ are arbitrary non-diagonal 3×3 complex matrices. To obtain the physical fields, we have to go to the mass eigenstate basis. This can be achieved by performing the following field transformations

$$\begin{aligned} &u_L \to V_L^u u_L, \quad d_L \to V_L^d d_L, \quad l_L \to V_L^l l_L, \\ &u_R \to V_R^u u_R, \quad d_R \to V_R^d d_R, \quad l_R \to V_R^l l_R \, . \end{aligned} \tag{1.3.5}$$

The six rotation matrices $V_{L,R}^{u,d,l}$ can be chosen in such a way that they diagonalize the matrices $\mathbf{Y}_{d,u,l}$,

$$\begin{aligned} V_L^d(v\mathbf{Y}_d)V_R^{d,\dagger} &= M_d = \mathrm{diag}\,(m_d, m_s, m_b)\,, \\ V_L^u(v\mathbf{Y}_u)V_R^{u,\dagger} &= M_u = \mathrm{diag}\,(m_u, m_c, m_t)\,, \\ V_L^l(v\mathbf{Y}_l)V_R^{l,\dagger} &= M_l = \mathrm{diag}\,(m_e, m_\mu, m_\tau)\,. \end{aligned} \tag{1.3.6}$$

In this basis Eq. (1.3.4) takes the form

$$\mathcal{L}_{\mathrm{Yuk}} \supset -\sum_f m_f \overline{f} f - \sum_f y_f \overline{f} f H, \tag{1.3.7}$$

where the summation runs over all charged leptons and quarks and we have introduced a Yukawa coupling for each fermion, $y_f = \frac{m_f}{v}$. The matrices $V_{L,R}^l$, which rotate the lepton fields, are unphysical. Unless Dirac right-handed neutrinos are included in the model, they cancel in all vertices. This is not the case for the quarks. Indeed, the interaction between the left-handed quarks and the W-bosons originates from the kinetic term for Q_L,

$$\mathcal{L}_{\mathrm{Yuk}} \supset i\overline{Q}_{L,i}\not{D}Q_{L,i} \supset -\frac{g}{\sqrt{2}}\overline{Q}_{L,i}\begin{pmatrix} 0 & \gamma^\mu W_\mu^+ \\ \gamma^\mu W_\mu^- & 0 \end{pmatrix} Q_{L,i} = -\frac{g}{\sqrt{2}}\overline{u}_{L,i}\gamma^\mu d_{L,i} W_\mu^+ + \mathrm{h.c.}\,. \tag{1.3.8}$$

After the transformation defined in Eq. (1.3.5) it takes the form

$$-\frac{g}{\sqrt{2}}\overline{u}_{L,j}V_{L,ji}^{u,\dagger}\gamma^\mu V_{L,ik}^d d_{L,k} W_\mu^+ + \mathrm{h.c.} = -\frac{g}{\sqrt{2}}\overline{u}_{L,j}\left(V_L^{u,\dagger}V_L^d\right)_{jk} W_\mu^+ d_{L,k} + \mathrm{h.c.}\,. \tag{1.3.9}$$

The product of the two unitary matrices in the brackets, $V_L^{u,\dagger}V_L^d$, is called Cabibbo-Kobayashi-Maskawa (CKM) matrix [50, 51]. This matrix has four free parameters: three mixing angles and a phase. This phase is the only source of $\mathcal{CP}$-violation in the Standard Model [52].[3]

The SM Lagrangian

The full Lagrangian of the Standard Model has the form,

$$\mathcal{L}_{\mathrm{SM}} = \mathcal{L}_{\mathrm{gauge}} + \mathcal{L}_{\mathrm{Yuk}} + \mathcal{L}_H + \mathcal{L}_{\mathrm{fix}} + \mathcal{L}_{\mathrm{FP}}. \tag{1.3.10}$$

[3] In the version of the SM, that we consider in this thesis, only left-handed massless neutrinos are present. However, the phenomenon of neutrino oscillations points at small but non-zero neutrino masses [53–58]. The SM can be extended in a minimal way to accommodate massive neutrinos by introducing the right-handed neutrino fields. The neutrino mixing matrix, which is analogous to the one in the quark sector, is called Pontecorvo–Maki–Nakagawa–Sakata (PMNS) matrix.

The first three terms in this sum, $\mathcal{L}_{\text{gauge}}$, $\mathcal{L}_{\text{Yuk}}$ and $\mathcal{L}_H$, were described in Sec. 1.1, 1.2 and 1.3, respectively. The other two emerge after the quantization of the theory. So far, we have been working in the unitary gauge since it has the advantage of setting the Goldstone bosons to zero and thus eliminating them completely from the Lagrangian. However, it complicates the computation of radiative corrections in the Standard Model. For this reasion, in practice often another of gauges. In the class of R_ξ-gauges, the gauge-fixing term can be written in the following way,

$$\begin{aligned}\mathcal{L}_{\text{fix}} = &-\frac{1}{2\xi_A}\left(\partial^\mu A_\mu\right)^2 - \frac{1}{2\xi_Z}\left(\partial^\mu Z_\mu - M_Z\xi'_Z\chi\right)^2 - \\ &- \frac{1}{\xi_W}\left(\partial^\mu W^+_\mu - iM_W\xi'_W\phi^+\right)\left(\partial^\mu W^-_\mu + iM_W\xi'_W\phi^-\right)\end{aligned} \tag{1.3.11}$$

with ξ_A, ξ_Z, ξ'_Z, ξ_W, ξ'_W being gauge-fixing parameters. One can simplify Eq. (1.3.11) by setting $\xi'_W = \xi_W$ and $\xi'_Z = \xi_Z$ (*'t-Hooft gauge*) which cancels the gauge boson-Goldstone mixing terms emerging from $|D_\mu\Phi|^2$. Sometimes, it is also convenient to set $\xi_A = \xi_W = \xi_Z = 1$ (*'t-Hooft-Feynman gauge*). Finally, the last term of Eq. (1.3.10) contains Faddeev-Popov ghosts fields [59]. These are unphysical degrees of freedom which appear only as virtual particles. The gauge-fixing terms (Eq. (1.3.11)) break the invariance of $\mathcal{L}_{\text{SM}}$ under local gauge transformations. However, there is a generalization of the latter, called BRST transformations [60–63],

$$\delta_{\text{BRST}}\left(\mathcal{L}_{\text{fix}} + \mathcal{L}_{\text{FP}}\right) = 0 \tag{1.3.12}$$

and therefore $\delta_{\text{BRST}}\mathcal{L}_{\text{SM}} = 0$. Gauge and BRST invariance make the SM renormalizable [64] which means that it can be treated consistenly as a quantum field theory with all the quantum effects being evaluated within its framework.

1.4 Global symmetries of the Standard Model

Besides the gauge symmetries, the SM Lagrangian, as defined in Eq. (1.3.10), is endowed with several global symmetries. First of all, it is invariant under simultaneous transformations of all quark fields

$$q \to e^{i\frac{\beta}{3}}q, \quad \overline{q} \to e^{-i\frac{\beta}{3}}\overline{q}, \tag{1.4.1}$$

where β is an abitrary real number. This is the baryon number symmetry $U(1)_B$. Due to this symmetry, the proton is stable in the SM. By definition, each quark carries baryon number $+\frac{1}{3}$, and the baryon number of each antiquark is $-\frac{1}{3}$. Then the baryon

number of a state, containing N_q quarks and $N_{\bar{q}}$ antiquarks, can be defined as

$$B = \frac{1}{3}\left(N_q - N_{\bar{q}}\right). \tag{1.4.2}$$

For instance, the baryon number of proton is +1, the baryon number of a meson is 0. Secondly, in the SM with massless neutrinos the lepton numbers of each individual generation are conserved. This symmetry corresponds to the following phase rotations of lepton and neutrino fields,

$$\begin{aligned}
U(1)_{L_e}: &\quad (\nu_e, e) \to e^{i\beta_e}(\nu_e, e), \quad (\overline{\nu}_e, \overline{e}) \to e^{-i\beta_e}(\overline{\nu}_e, \overline{e}), \\
U(1)_{L_\mu}: &\quad (\nu_\mu, \mu) \to e^{i\beta_\mu}(\nu_\mu, \mu), \quad (\overline{\nu}_\mu, \overline{\mu}) \to e^{-i\beta_\mu}(\overline{\nu}_\mu, \overline{\mu}), \\
U(1)_{L_\tau}: &\quad (\nu_\tau, \tau) \to e^{i\beta_\tau}(\nu_\tau, \tau), \quad (\overline{\nu}_\tau, \overline{\tau}) \to e^{-i\beta_\tau}(\overline{\nu}_\tau, \overline{\tau}).
\end{aligned} \tag{1.4.3}$$

The observed neutrino oscillations [53–58] indicate a violation of these numbers. In the extension of the SM which includes three Dirac right-handed neutrinos, these three symmetries are no longer exact. However, the special case of the transformations (1.4.3) with $\beta_e = \beta_\mu = \beta_\tau$ leaves the Lagrangian of the SM invariant if the right-handed neutrinos are added to it. Both symmetries $U(1)_B$ and $U(1)_L$ are violated by sphaleron processes [65] but the difference $B - L$ is still conserved.

1.5 Problems of the Standard Model

So far, the Standard Model was remarkably successful in explaining most of the experimental results in high-energy physics. It successfully predicted the outcome of many high-precision experiments. Many of them are so precise that the calculation of sophisticated higher-order corrections for obtaining a precise theory prediction is needed. As an example, the mass of the W-boson in the SM only fits together with the measured Higgs mass after the inclusion of the complete two-loop and leading higher-order corrections to M_W.[4]

Despite its great success, there are reasons to believe that the Standard Model is not the ultimate theory of Nature. In particular, there is no complete description of gravity within the framework of the SM. One can use the semiclassical description based on the expansion of the Einstein-Hilbert Lagrangian

$$\mathcal{L}_{EH} = M_{\mathrm{Pl}}^2 \sqrt{-g} R, \tag{1.5.1}$$

[4] The inclusion of only pure one-loop corrections would imply that the favored region for the Higgs-boson mass of the SM would be much higher than 125 GeV [66–69]. More examples of precision tests of the SM can be found in [70].

around the Minkowski metric $g_{\mu\nu} = \eta_{\mu\nu} + \frac{1}{M_{\rm Pl}} h_{\mu\nu}$, where $M_{\rm Pl}$ is the Planck mass, $M_{\rm Pl} = 10^{19}$ GeV. This description works well for low energies, but it is clear that it has to break down at the latest at scales close to $M_{\rm Pl}$.

Quantum gravity is not the only motivation for physics beyond the SM. There are many others which we will list below.

Dark matter

Starting from the 1930s, there has been plenty of evidence for the existence of Dark Matter (DM) – a non-luminous substance, which amounts to approximately 25% of the total energy density of the Universe. Historically, the first evidence was obtained by Fritz Zwicky [71], who applied the virial theorem to the Coma Cluster and was able to prove the existence of the unseen mass there. Later, in the 1970s, the velocity distributions in spiral galaxies were observed by Vera Rubin, Kent Ford and Ken Freeman [72,73]. It turned out that these distributions (also known as rotation curves) were falling off for large distances smoother than expected. Another convincing evidence for the existence of DM is the observation of a cluster of galaxies, called Bullet cluster (1E0657-558), passing through another cluster [74]. The observations in the X-ray range revealed that the hot gas, which forms most of the baryonic matter in both clusters decelerates during this collision. On the other hand it was also possible to chart the gravitational potential of the clusters after the collision by using gravitational lensing. This revealed that most of the unseen mass in both clusters passed through without interaction. The existence of DM is also supported by the precise measurement of the anisotropies of the cosmic microwave background (CMB) radiation [75]. However, not much is known about the nature of Dark Matter, except for the fact that it interacts gravitationally. One of the most popular solutions to this puzzle is the existence of new particles that interact at most weakly with the particles we know.

The origin of neutrino masses

In the Standard Model, only left-handed and massless neutrinos were present. However, as already said above, there is striking evidence that neutrinos do have a small mass. In principle, one can add the right-handed neutrinos consistently to the theory in such a way that they acquire their mass through the interaction with the Higgs field. However, the upper bounds on the neutrino mass, set by the Troitsk ν-mass [76] and KATRIN experiments [77], and also by the Planck CMB observation [75], do not exceed $\mathcal{O}(1)$ eV. Thus the natural question arises in this approach: if the neutrino masses are generated via the same mechanism as for the other particles, why are

these masses are so small? In principle, there is another way to generate the neutrino masses via the 5-dimensional Weinberg operator [78],

$$\mathcal{L}_\nu \supset \frac{c_{ij}}{2\Lambda}(\bar{L}_i^c \cdot H)(H^T \cdot L_j), \tag{1.5.2}$$

which after the EWSB yields Majorana mass terms for the neutrinos,

$$\mathcal{L}_\nu \supset \frac{1}{2}(m_\nu)_{ij}\bar{\nu}_i^c \nu_j. \tag{1.5.3}$$

But the presence of the cut-off scale Λ in the expression (1.5.2) signals that some new physics has to emerge at the scale Λ. For the neutrino masses to be compatible with the current bounds, this scale has to be $\Lambda \geq 10^{15}$ GeV. The Majorana nature of neutrinos can reveal itself in the neutrinoless double-beta decay which is extensively being searched for [79].

Hierarchy problem

The shortcomings we mentioned above hint that the Standard Model of particle physics has to be extended in some way. And even if there is no new physics below the Planck scale, the SM breaks down at the latest at $M_{\rm Pl}$. Therefore, in any case the Standard Model is most likely a low energy limit of some more complete theory and the Higgs boson mass acquires radiative corrections after integrating out heavy particles from this ultraviolet (UV) theory. If no additional symmetry is imposed, these corrections would behave like $m_h^2 \sim \Lambda_{\rm NP}^2$ (see also discussion in Sec. 2.2), where $\Lambda_{\rm NP}$ is the scale of new physics. If $\Lambda_{\rm NP}$ is of the order of the Grand Unified Theory (GUT) scale $\Lambda_{\rm NP} \sim 10^{16}$GeV or the Planck scale, then we expect the Higgs boson mass to be approximately of the same order. So, the question is, why the Higgs boson mass is so small? This question might be posed a bit differently. Namely, why is the weak scale so smaller than the Planck scale and what stabilizes this huge hierarchy? This is the essence of the Hierarchy problem (also called Naturalness problem) [80–82].

Unification of gauge couplings

The renormalization group analysis of the scale dependence of the three gauge couplings g, g', g_3 shows that they almost meet at the scale around 10^{16} GeV in the SM. This is not a problem of the model itself, but this observation suggests that at these energies the SM goes over into a Grand Unified Theory (GUT) – a theory with an extended gauge group [83, 84] (popular choices for such groups are $SU(5), SO(10)$ and E_6). Many of these models include additional heavy fermionic degrees of freedom, which on the one hand tackle the neutrino mass problem, but, on the other hand, lead

to large corrections to the Higgs potential as discussed in the context of the hierarchy problem above.

Baryon asymmetry of the Universe

The Standard Model cannot explain, why there is much more matter than antimatter in the observable Universe [75, 85]. To generate such an asymmetry, three conditions (called *Sakharov conditions*) [86] must be met. One of them is the existence of $\mathcal{CP}$-violation. While $\mathcal{CP}$-violation is present in the SM in the quark sector, more sources of it are needed to account for the observed asymmetry.

Numerous theories have been put forward to tackle the problems mentioned above. In particular, many ideas were proposed to solve the Hierarchy problem. In this thesis we focus on the minimal supersymmetric extension of the Standard Model. This model is endowed with a new symmetry which relates bosonic and fermionic degrees of freedom – supersymmetry (SUSY). In the next Chapter we will introduce the concept of SUSY and describe the minimal supersymmetric extension of the Standard Model.

Chapter 2

The Minimal Supersymmetric Standard Model

In this chapter we provide a brief review of the Minimal Supersymmetric Standard Model. Sections 2.1 – 2.4 are largely based on the Refs. [87–89]. In Section 2.5 we will mostly follow the notations and conventions of [90, 91].

2.1 Notations and conventions

Let us first introduce the notations and conventions which we will extensively use throughout the chapter. First, for the Minkowski metric the "mostly minus" convention is used

$$g^{\mu\nu} = g_{\mu\nu} = \text{diag}\,(+1, -1, -1, -1)\,. \tag{2.1.1}$$

Supersymmetric theories are more conveniently written in terms of two-component spinors. To introduce them, we first recap some facts from the representation theory of the Lorentz algebra. It is known that the Lorentz algebra is isomorphic to a direct sum of two $SU(2)$ algebras

$$SO(1,3) \simeq SU(2)_L \oplus SU(2)_R. \tag{2.1.2}$$

The objects which transform only under $SU(2)_L$ and lie in the trivial representation of $SU(2)_R$ are called left-handed Weyl spinors χ_α. In the same manner, the right-handed Weyl spinor $\bar{\xi}_{\dot{\alpha}}$, which transforms only under $SU(2)_R$, can be constructed. Left- and right-handed Weyl spinors correspond to two different irreducible representations of the Lorentz group, denoted as $\left(\frac{1}{2}, 0\right)$ and $\left(0, \frac{1}{2}\right)$, respectively. The Hermitian conjugate of a left-handed Weyl spinor is a right-handed Weyl spinor and vice versa. The spinor

indices can be raised and lowered by making use of the totally antisymmetric tensor

$$\epsilon_{\alpha\beta} = \epsilon_{\dot{\alpha}\dot{\beta}} = \begin{pmatrix} 0 & -1 \\ 1 & 0 \end{pmatrix}, \quad \epsilon^{\alpha\beta} = \epsilon^{\dot{\alpha}\dot{\beta}} = \begin{pmatrix} 0 & 1 \\ -1 & 0 \end{pmatrix}. \tag{2.1.3}$$

By definition,

$$\chi^{\alpha} = \epsilon^{\alpha\beta}\chi_{\beta}, \quad \bar{\xi}^{\dot{\alpha}} = \epsilon^{\dot{\alpha}\dot{\beta}}\bar{\xi}_{\dot{\beta}}. \tag{2.1.4}$$

The four-component Dirac spinor Ψ_D in this notation can be written in the following way

$$\Psi_D = \begin{pmatrix} \xi_{\alpha} \\ \left(\chi^{\dagger}\right)^{\dot{\alpha}} \end{pmatrix} = \begin{pmatrix} \Psi_{D,L} \\ \Psi_{D,R} \end{pmatrix}. \tag{2.1.5}$$

Next, to define several commutation relations in the supersymmetry algebra, we will need Pauli matrices with one Lorentz and two spinor indices [5]

$$\begin{aligned} &\sigma^{\mu}_{\alpha\dot{\beta}} = \left(\mathbf{1}_{2\times 2}, \sigma^1, \sigma^2, \sigma^3\right), \quad \bar{\sigma}^{\mu\ \dot{\alpha}\beta} = \left(\mathbf{1}_{2\times 2}, -\sigma^1, -\sigma^2, -\sigma^3\right), \\ &\text{with} \quad \sigma^1 = \begin{pmatrix} 0 & 1 \\ 1 & 0 \end{pmatrix}, \quad \sigma^2 = \begin{pmatrix} 0 & -i \\ i & 0 \end{pmatrix}, \quad \sigma^3 = \begin{pmatrix} 1 & 0 \\ 0 & -1 \end{pmatrix}. \end{aligned} \tag{2.1.6}$$

We will also need sigma matrices with two Lorentz indices. These are [6]

$$\left(\sigma^{\mu\nu}\right)_{\alpha}{}^{\beta} = \frac{i}{4}\left(\sigma^{\mu}\bar{\sigma}^{\nu} - \sigma^{\nu}\bar{\sigma}^{\mu}\right)_{\alpha}{}^{\beta}, \tag{2.1.7}$$

$$\left(\bar{\sigma}^{\mu\nu}\right)^{\dot{\alpha}}{}_{\dot{\beta}} = \frac{i}{4}\left(\bar{\sigma}^{\mu}\sigma^{\nu} - \bar{\sigma}^{\nu}\sigma^{\mu}\right)^{\dot{\alpha}}{}_{\dot{\beta}}. \tag{2.1.8}$$

Weyl spinors are regarded as Grassmann variables (i.e., $\psi_1\xi_2 = -\xi_2\psi_1$). Using this fact and the definitions for the spinors with upper indices (Eq. (2.1.4)), we can construct $SU(2)_{L,R}$-invariant bilinear products[7],

$$\chi\xi = \chi^{\alpha}\xi_{\alpha} \equiv \xi\chi = \left(\bar{\chi}\bar{\xi}\right)^{\dagger}, \tag{2.1.9}$$

$$\bar{\chi}\bar{\sigma}^{\mu}\xi = \bar{\chi}_{\dot{\alpha}}\bar{\sigma}^{\mu\ \dot{\alpha}\beta}\xi_{\beta} = \left(\bar{\xi}\bar{\sigma}^{\mu}\chi\right)^{\dagger}, \tag{2.1.10}$$

$$\chi\sigma^{\mu}\bar{\xi} = \chi^{\alpha}\sigma^{\mu}_{\alpha\dot{\beta}}\bar{\xi}^{\dot{\beta}} = \left(\xi\sigma^{\mu}\bar{\chi}\right)^{\dagger}. \tag{2.1.11}$$

Finally, we will need to integrate over Grassmann variables and take derivatives with respect to them. The latter are defined as follows,

$$\partial_{\alpha}\theta^{\beta} = \delta^{\beta}_{\alpha}, \quad \partial_{\alpha}\bar{\theta}^{\dot{\beta}} = 0, \quad \partial_{\dot{\alpha}}\bar{\theta}^{\dot{\beta}} = \delta^{\dot{\beta}}_{\dot{\alpha}}, \quad \partial_{\dot{\alpha}}\theta^{\beta} = 0, \tag{2.1.12}$$

[5] Here, we follow the conventions of [88, 92]. The σ^{μ} used in [89] have a different sign with respect to ours for $\mu = 1, 2, 3$.

[6] In [89] the factor $\frac{1}{4}$ instead of $\frac{i}{4}$ is used.

[7] Note, that, due to the grassmannian nature of Weyl spinors the quantity $\theta^2 = \theta \cdot \theta$ is non-zero: $\theta^2 = -2\theta_1\theta_2$

while for the integration we introduce the following integration measures,

$$d^2\theta = -\frac{1}{4} d\theta^\alpha d\theta^\beta \, \epsilon_{\alpha\beta}, \quad d^2\bar{\theta} = -\frac{1}{4} d\bar{\theta}_{\dot{\alpha}} d\bar{\theta}_{\dot{\beta}} \, \epsilon^{\dot{\alpha}\dot{\beta}}. \tag{2.1.13}$$

This definition, in particular, implies that integration over a Grasmann variable θ acts as a projector on the corresponding integrand: it returns the terms proportional to θ^2. For example, if $F = a + \psi\theta + c\theta^2$, then

$$\int d^2\theta \; F = c. \tag{2.1.14}$$

The definitions (2.1.14) and (2.1.13) allow for integration by parts. Indeed, since $\partial_\alpha F = \psi_\alpha + 2c\theta_\alpha$, the following integral vanishes:

$$\int d^2\theta \; \partial_\alpha F = 0. \tag{2.1.15}$$

2.2 Supersymmetry algebra

Supersymmetry (SUSY) – a symmetry between fermions and bosons – was initially proposed more than 40 years ago in the papers [93–95]. Before that, the Coleman-Mandula theorem [96] was formulated, which states that if G is a symmetry group of the S-matrix and contains the Poincaré group $\mathcal{P}$ as a subgroup, then it can be represented as a direct product of the latter and an internal symmetry group. To put it differently, the Poincaré algebra can be combined with any other continuous symmetry of the S-matrix only in a trivial way. A bypass around this theorem was found by Haag, Łopuszański and Sohnius [97], who showed that the Poincaré algebra can be nontrivially extended by introducing generators which belong to representations $\left(\frac{1}{2}, 0\right)$ and $\left(0, \frac{1}{2}\right)$ of the Lorentz group. In addition, this extension requires the introduction of anticommutators aside from the commutators in the algebras $\mathcal{P}$ and G. This extension of the symmetry group of the S-matrix turns out to be the only possible one in relativistic quantum field theories in four space-time dimensions.

Generators of the supersymmetric algebra, which we will denote as Q^I_α and $\left(\overline{Q}^I_{\dot{\alpha}}\right)$, $(I = 1 \ldots N)$, transform a fermionic state into a bosonic one and vice versa. Schematically,

$$\overline{Q}^I_{\dot{\alpha}} \left|\text{boson}\right\rangle = \left|\text{fermion}\right\rangle \quad \text{and} \quad Q^I_\alpha \left|\text{fermion}\right\rangle = \left|\text{boson}\right\rangle. \tag{2.2.1}$$

They commute with the momentum operator P_μ and internal symmetries,

$$\left[Q^I_\alpha, P_\mu\right] = 0, \quad \left[Q^I_\alpha, G\right] = 0, \quad \left[\overline{Q}^I_{\dot{\alpha}}, P_\mu\right] = 0, \quad \left[\overline{Q}^I_{\dot{\alpha}}, G\right] = 0, \tag{2.2.2}$$

but do not commute with the angular momentum operator,

$$\left[M_{\mu\nu}, Q^I_\alpha\right] = -(\sigma_{\mu\nu})_\alpha{}^\beta Q^I_\beta, \quad \left[M_{\mu\nu}, \overline{Q}^{I,\dot\alpha}\right] = -(\bar\sigma_{\mu\nu})^{\dot\alpha}{}_{\dot\beta}\overline{Q}^{I,\dot\beta}. \tag{2.2.3}$$

The commutation relations (Eqs. (2.2.2)–(2.2.3)) imply that in the supersymmetric theories one deals with multiplets of particles (called supermultiplets), each consisting of particles with the same mass and quantum numbers with respect to G but different spin. Fermions and bosons within multiplets are superpartners to each other. The total number of fermionic and bosonic degrees of freedom in one multiplet is equal. For completeness, we also present the anticommutation relations for the SUSY generators,

$$\left\{Q^I_\alpha, \overline{Q}^J_{\dot\beta}\right\} = 2\sigma^\mu_{\alpha\dot\beta}P_\mu\delta^{IJ}, \quad \left\{Q^I_\alpha, Q^J_\beta\right\} = \epsilon_{\alpha\beta}Z^{IJ}, \quad \left\{\overline{Q}^I_{\dot\alpha}, \overline{Q}^J_{\dot\beta}\right\} = \epsilon_{\dot\alpha\dot\beta}\left(Z_{IJ}\right)^* \\ \text{with} \quad Z^{JI} = -Z^{IJ}, \tag{2.2.4}$$

where Z^{IJ} are called *central charges*.

Already at this point, it is possible to understand how SUSY helps to solve the Hierarchy problem (see Sec. 1.5) without going into details of the concrete supersymmetric model. Recall, that the problem arises when the Standard Model is regarded as a low energy effective theory and hence has a cut-off $\Lambda_{\rm NP} \leq M_{\rm Pl}$. Let us assume that in the UV-completion of the Standard Model the Higgs boson couples with a coupling constant y to a heavy scalar field S, which has mass $M \sim \Lambda_{\rm NP}$,

$$\mathcal{L}_{\rm UV} \supset -\frac{M^2S^2}{2} - yH^\dagger HS^2. \tag{2.2.5}$$

Then after integrating out these heavy particles, the correction to the Higgs boson mass reads [8]

$$\Delta m_h^2 \simeq C\frac{y^2}{16\pi^2}M^2 + \cdots, \tag{2.2.6}$$

where ellipsis denotes terms not enhanced by M^2, and C is a numerical factor which depends on the details of the model and is expected to be $C \sim \mathcal{O}(1)$. In supersymmetric theories, there is a fermionic superpartner of S (let us call it F) with exactly the same mass and the same coupling constant to the Higgs boson. The contribution of F to Δm_h^2 will be exactly equal to the contribution of S but will have an opposite sign. So, in case of exact supersymmetry, there will be no correction to the Higgs mass at all. Due to the non-renormalization theorem, this property holds at all orders of perturbation theory [98]. However, the non-observation of superpartners

[8] In the formula (2.2.6) the factor $(16\pi^2)^{-1}$ comes from the one-loop diagrams. If there is no direct coupling between the unknown heavy particles and the Standard Model Higgs boson in $\mathcal{L}_{\rm UV}$, then this coupling can in principle be generated at higher loop orders. In this case, the right-hand side of the formula (2.2.6) has to be multiplied by additional factors of $(16\pi^2)^{-1}$.

of the Standard Model particles indicates that SUSY must be broken at low energies. We will come back to the discussion of this issue in Section 2.4.2.

In this thesis, we will consider only $N = 1$ supersymmetric extensions of the Standard Model, which implies that $Z^{IJ} \equiv 0$. In order to build such an extension, all the SM fields have to be put into some SUSY multiplets. A convenient way to describe these multiplets is the superfield formalism, which is described in the next section.

2.3 Superfields

Superfields are generalizations of the normal fields used in quantum field theory. More precisely, a superfield is a function of superspace coordinates: the four coordinates of the Minkowski space, x^μ, and the two Majorana spinors, θ^α and $\bar{\theta}_{\dot{\alpha}}$. Since the latter have only two indices each, and since Grassmann variables θ_α and $\bar{\theta}_{\dot{\beta}}$ anticommute, any term involving product of more than two θ's (or $\bar{\theta}$'s) would vanish. Thus the most general superfield $S(x^\mu, \theta_\alpha, \bar{\theta}_{\dot{\alpha}})$ in $N = 1$ supersymmetry can be written as a quadratic polynomial in θ and $\bar{\theta}$:

$$\begin{aligned} S(x^\mu, \theta_\alpha, \bar{\theta}_{\dot{\alpha}}) = f(x) + \psi(x)\theta + \bar{\omega}(x)\bar{\theta} + B(x)\theta^2 + C(x)\bar{\theta}^2 \\ + (\bar{\theta}\bar{\sigma}^\mu\theta)\ A_\mu(x) + \gamma(x)\theta\bar{\theta}^2 + \bar{\lambda}(x)\bar{\theta}\theta^2 + \frac{1}{2}\theta^2\bar{\theta}^2 D(x), \end{aligned} \tag{2.3.1}$$

where $f(x), B(x), C(x)$ and $D(x)$ are scalar fields, $\psi(x), \gamma(x)$ are left-handed Majorana spinors, $\bar{\omega}(x), \bar{\lambda}(x)$ are right-handed Majorana spinors and $A_\mu(x)$ is a vector field. Global supersymmetric transformations in superspace formalism coincide with translations in coordinates $\theta, \bar{\theta}$:

$$S(x + i\epsilon\sigma^\mu\bar{\theta} + i\bar{\epsilon}\bar{\sigma}\theta, \theta + \epsilon, \bar{\theta} + \bar{\epsilon}) - S(x, \theta, \bar{\theta}) = \delta_{\epsilon,\bar{\epsilon}} S = -i\left(\epsilon Q + \bar{\epsilon}\overline{Q}\right) S, \tag{2.3.2}$$

where the generators Q_α and $\overline{Q}_{\dot{\alpha}}$ have the following representation,

$$Q_\alpha = i\partial_\alpha - \left(\sigma^\mu\bar{\theta}\right)_\alpha \partial_\mu, \quad \overline{Q}_{\dot{\alpha}} = -i\bar{\partial}_{\dot{\alpha}} + (\theta\sigma^\mu)_{\dot{\alpha}}\, \partial_\mu. \tag{2.3.3}$$

These generators contain only derivatives: one with respect to θ ($\bar{\theta}$) and one which acts on the Minkowski coordinates. This implies that the quantity (2.3.2) is a total derivative and vanishes upon integration over the full superspace. This means in turn that the full integral of any superfield $S(x^\mu, \theta_\alpha, \bar{\theta}_{\dot{\alpha}})$ is a supersymmetric invariant quantity,

$$\delta_{\epsilon,\bar{\epsilon}} \int d^4x\ d^2\theta\ d^2\bar{\theta}\ S(x^\mu, \theta_\alpha, \bar{\theta}_{\dot{\alpha}}) = 0. \tag{2.3.4}$$

This fact can in principle be used to build supersymmetric invariant actions. However, not any superfield is suitable for the construction of phenomenologically viable Lagrangians. After all, the end result should describe gauge-invariant renormalizable interactions of the fields, which have canonically normalized kinetic terms. Furthermore, it is useful to identify the building blocks, from which the Lagrangian with desired properties can be constructed. Technically speaking, these building blocks are superfields, which correspond to the irreducible representations of the SUSY algebra. The superfield $S(x,\theta,\bar{\theta})$ defined in Eq. (2.3.1) is too generic to be such a building block. It can be shown [88, 89] that only two types of such superfields supersymmetry are needed for $N=1$ supersymmetry, which also turn out to be sufficient to encompass all fermionic and bosonic degrees of freedom of the Standard Model and to reproduce correct interactions between them. These are the (anti-)chiral and vector superfields.

In order to define chiral and anti-chiral superfields we need to introduce the generalized covariant derivatives,

$$D_\alpha = \partial_\alpha - i(\sigma^\mu\bar{\theta})_\alpha\partial_\mu, \quad \bar{D}_{\dot{\alpha}} = -\partial_{\dot{\alpha}} + i(\theta\sigma^\mu)_{\dot{\alpha}}\partial_\mu. \tag{2.3.5}$$

Then the chiral Φ and anti-chiral $\bar{\Phi}$ superfields are defined through

$$\bar{D}_{\dot{\alpha}}\Phi = 0, \quad D_\alpha\bar{\Phi} = 0. \tag{2.3.6}$$

These conditions are consistent with supersymmetric transformations. This means, that if Φ is a chiral superfield, then $\delta_{\epsilon,\bar{\epsilon}}\Phi$ is a chiral superfield as well, where the transformation with the infinitesimal parameters ϵ and $\bar{\epsilon}$ is defined in Eq. (2.3.2). It can be shown [88, 89] that the following superfield is the solution of the left constraint in Eq. (2.3.6),

$$\begin{aligned}\Phi(x,\theta,\bar{\theta}) &= \phi(x) + \sqrt{2}\theta\psi(x) + i(\bar{\theta}\bar{\sigma}^\mu\theta)\partial_\mu\phi(x) + \theta^2 F(x) \\ &- \frac{i}{\sqrt{2}}\theta^2(\bar{\theta}\bar{\sigma}^\mu\partial_\mu\psi(x)) - \frac{1}{4}\theta^2\bar{\theta}^2\Box\phi(x).\end{aligned} \tag{2.3.7}$$

Here, ϕ is a complex scalar field, ψ is a left-handed Majorana fermion and F is an unphysical auxiliary field, which is needed to have an equal number of fermionic and bosonic degrees of freedom off-shell. In turn, the solution of the right constraint is the Hermitian conjugate of (2.3.7): $\bar{\Phi}(x,\theta,\bar{\theta}) = \Phi^\dagger(x,\theta,\bar{\theta})$. A supersymmetric Lagrangian for a theory containing chiral fields Φ_i, $(i=1,\ldots,M)$ reads

$$\mathcal{L}_{\text{SUSY}} = \int d^2\theta d^2\bar{\theta} \sum_{i=1}^{M} \Phi_i^\dagger\Phi_i + \int d^2\theta\, W(\{\Phi_i\}) + \int d^2\bar{\theta}\, \overline{W}(\{\Phi_i^\dagger\}). \tag{2.3.8}$$

The first term in (2.3.8), $\sum_{i=1}^{M} \Phi_i^\dagger \Phi_i$, is called the Kähler potential. It yields the kinetic terms for the fields of the theory,

$$\mathcal{L}_{\text{kin}} = \int d^2\theta d^2\bar{\theta} \sum_{i=1}^{M} \Phi_i^\dagger \Phi_i = \partial^\mu \phi_i^\dagger \partial_\mu \phi_i + i\bar{\psi}_i \bar{\sigma}^\mu \partial_\mu \psi_i + F_i^\dagger F_i. \tag{2.3.9}$$

The two other terms in Eq. (2.3.8) yield the mass terms for the particles and also describe interactions between them. Note, that the function W, called superpotential, is a holomorphic function of $\{\Phi_i\}$, i.e. it depends only on the chiral (and not on the anti-chiral) fields. Other requirements originate from the renormalizability of the theory. In order for the theory to be renormalizable, the superpotential has to be at most a cubic funcion of the superfields. For instance, the superpotential for the model of chiral superfields alone, called Wess-Zumino model, can be written as follows [99],

$$W = L^i \Phi_i + \frac{1}{2} M^{ij} \Phi_i \Phi_j + \frac{1}{6} y^{ijk} \Phi_i \Phi_j \Phi_k. \tag{2.3.10}$$

In components the corresponding piece of the Lagrangian reads

$$\mathcal{L}_{\text{interaction}} = \int d^2\theta\, W(\{\Phi_i\}) + \text{h.c.} = \left\{ \frac{\partial W}{\partial \Phi_i} F_i - \frac{1}{2} \frac{\partial^2 W}{\partial \Phi_i \partial \Phi_j} \psi_i \psi_j \right\} \Bigg|_{\Phi \to \phi} + \text{h.c.}, \tag{2.3.11}$$

where the chiral superfields have to be replaced with there scalar components. From Eqs. (2.3.9) and (2.3.11) we can derive equations of motion for the auxiliary fields F and $F^\dagger$, solve them and insert the solutions back in the Lagrangian. This yields the potential for the scalar fields,

$$V_F(\{\phi_i^\dagger, \phi_i\}) = \sum_i^M \left| \frac{\partial W}{\partial \Phi_i} \right|^2 \Bigg|_{\Phi \to \phi}. \tag{2.3.12}$$

We will call this scalar potential "F-term" since it was generated by the auxiliary fields F_i. Next, the second term in Eq. (2.3.11) gives masses to the fermionic degrees of freedom ψ_i, with the mass matrix being equal to M^{ij}, as well as the Yukawa interactions between complex scalar fields ϕ_i and fermions with the coupling constants y^{ijk}. The second type of superfields which is needed to build supersymmetric extensions of the Standard Model is the vector superfield, which describes gauge interactions in supersymmetric theories. These superfields are defined by the following equation,

$$V^\dagger = V. \tag{2.3.13}$$

Applying this condition to the superfield in the most general form, Eq. (2.3.1) results into the conditions for the component fields,

$$f^* = f, \quad D^* = D, \quad \psi = \omega, \quad B^* = C, \quad A^*_\mu = A_\mu, \quad \gamma = \lambda. \tag{2.3.14}$$

So, the vector field can be written in the following form

$$\begin{aligned} V(x^\mu, \theta_\alpha, \bar{\theta}_{\dot{\alpha}}) = f + \psi\theta + \bar{\psi}\bar{\theta} + B\theta^2 + B^*\bar{\theta}^2 \\ + (\bar{\theta}\bar{\sigma}^\mu\theta)A_\mu + \lambda\theta\bar{\theta}^2 + \bar{\lambda}\bar{\theta}\theta^2 + \frac{1}{2}\theta^2\bar{\theta}^2 D. \end{aligned} \tag{2.3.15}$$

This expression is suffcient for building Abelian supersymmetric gauge theories. In order to study models, that are based on the non-Abelian gauge groups, we have to promote the vector superfield to an element of the corresponding Lie algebra. For a semi-simple Lie group G we get

$$V = V_a T^a, \quad a = 1, \ldots, \dim\, G, \tag{2.3.16}$$

where T^a are group generators and V_a are vector superfields. Supersymmetric gauge theories admit a wider class of symmetries in comparison to their non-supersymmetric counterparts. To be more specific, they are invariant under non-linear super-gauge transformations, which for a group G read

$$e^{2gV} \to e^{2ig\Lambda^\dagger} e^{2gV} e^{-2ig\Lambda}, \tag{2.3.17}$$

where Λ is a chiral superfield and g is a gauge coupling associated with the gauge group. Using this gauge freedom, we can eliminate the fields f, ψ and B from the first line of Eq. (2.3.15). This particular gauge choice is called Wess-Zumino gauge [100],

$$V(x^\mu, \theta_\alpha, \bar{\theta}_{\dot{\alpha}})^a_{\mathrm{WZ}} = (\bar{\theta}\bar{\sigma}^\mu\theta)A^a_\mu + \lambda^a\theta\bar{\theta}^2 + \bar{\lambda}^a\bar{\theta}\theta^2 + \frac{1}{2}\theta^2\bar{\theta}^2 D^a. \tag{2.3.18}$$

So, the physical degrees of freedom in the vector supermultiplet are the gauge field A^a_μ and its superpartner called gaugino λ^a. The field D^a is an auxilliary non-propagating field and it vanishes after applying the equations of motion. The Wess-Zumino gauge is convenient because it simplifies all calculations. Indeed, since each term in Eq. (2.3.18) contains at least one power of θ or $\bar{\theta}$, all powers V^n with n greater than 3 vanish. For example, the term e^V from Eq. (2.3.17) simply reads

$$e^{2gV}\Big|_{\mathrm{WZ}} = 1 + 2gV + 2g^2V^2. \tag{2.3.19}$$

Using the vector superfields, we can construct super-field strengths,

$$\mathcal{W}_\alpha = -\frac{1}{4}\bar{D}_{\dot{\alpha}}\bar{D}^{\dot{\alpha}}\left(e^{-V}D_\alpha e^V\right), \quad \overline{\mathcal{W}}_{\dot{\alpha}} = -\frac{1}{4}D^\alpha D_\alpha\left(e^{-V}\bar{D}_{\dot{\alpha}}e^V\right), \tag{2.3.20}$$

where D and $\bar{D}$ are the covariant derivatives defined in (2.3.5). Using them we can build the renormalizable Lagrangian of a supersymmetric gauge theory,

$$\begin{aligned}\mathcal{L}_{\text{supergauge}} &= \int d^2\theta\left(\frac{1}{4}\mathcal{W}^{a,\alpha}\mathcal{W}^a_\alpha\right) + \text{h.c.} \\ &= -\frac{1}{4}F^{a\mu\nu}F^a_{\mu\nu} + i\bar{\lambda}^a\bar{\sigma}^\mu D_\mu\lambda^a + \frac{1}{2}D^aD^a.\end{aligned} \tag{2.3.21}$$

In order to couple the matter and gauge fields together, we have to define how chiral superfields transform under the gauge group G. If a chiral supermultiplet lies in the representation R of group G, then we can expect that it transforms under the supergauge transformations in the following way, [9]

$$\Phi \to \Phi' = e^{2ig\Lambda}\Phi, \tag{2.3.22}$$

where now the chiral superfield Λ can be written as a sum over generators T^a_R: $\Lambda = \Lambda^a T^a_R$. The Kähler potential we considered before in this section, $\Phi^\dagger\Phi$, is not invariant under the supergauge transformations (for the sake of brevity we consider here only one chiral field). Indeed, $\Phi^\dagger\Phi \to \Phi^\dagger e^{-2ig\Lambda^\dagger}e^{2ig\Lambda}\Phi$. To compensate for the factor $e^{-2ig\Lambda^\dagger}e^{2ig\Lambda}$, we have to modify the Kähler potential accordingly,

$$\Phi^\dagger\Phi \to \Phi^\dagger e^{2gV}\Phi. \tag{2.3.23}$$

In Wess-Zumino gauge the terms proportional to $\theta^2\bar{\theta}^2$ in the new Kähler potential read:

$$\Phi^\dagger e^{2gV}\Phi\Big|_{\theta^2\bar{\theta}^2} = D_\mu\phi^\dagger D^\mu\phi + i\bar{\psi}\bar{\sigma}^\mu D_\mu\psi + F^\dagger F - \sqrt{2}g(\phi^\dagger\lambda\psi + \bar{\psi}\bar{\lambda}\phi) + g\phi^\dagger D\phi. \tag{2.3.24}$$

We see that the Kähler potential not only substitutes the ordinary derivatives, ∂_μ, with the covariant ones, D_μ, but also introduces new vertices involving the fermion ψ, its superpartner ϕ and the gaugino λ. Collecting all pieces together, we arrive at the generalization of Eq. (2.3.8). In the case that the chiral superfields are charged under some gauge group, the Lagrangian is given by

$$\mathcal{L}_{\text{SUSY}} = \int d^2\theta d^2\bar{\theta}\ \sum_{i=1}^{M}\Phi_i^\dagger e^{2gV}\Phi_i + \left[\int d^2\theta\left(\frac{1}{4}\mathcal{W}^{a,\alpha}\mathcal{W}_{a,\alpha} + W(\{\Phi_i\})\right) + \text{h.c.}\right]. \tag{2.3.25}$$

[9] Note, that the product of two chiral superfields is also a chiral superfield. So, this transformation does not change the properties of the superfield Φ.

Using the same procedure as we applied to obtain the F-terms (see Eq. (2.3.12)), we get the piece of the scalar potential which is generated via auxiliary fields D and thus called "D-term"

$$V_D(\{\phi_i^\dagger, \phi_i\}) = \frac{g^2}{2} \sum_{a=1}^{\dim G} D^a D^a = \frac{g^2}{2} \sum_{a=1}^{\dim G} \left(\phi_i^\dagger \, T_R^a \, \phi_i\right)^2 . \tag{2.3.26}$$

2.4 Superpotential of the MSSM

The Minimal Supersymmetric Standard Model (MSSM) [101–103] is the minimal extension of the Standard Model which realizes supersymmetry. In the previous section, we have seen that a renormalizable supersymmetric Lagrangian contains two main pieces: the Kähler potential and the superpotential. While the first one is fully fixed by the particle content of the model, the second one has to be a holomorphic function of the chiral superfields (see Eq. (2.3.8) in Sec. 2.3). Besides, it can be at most a cubic polynomial in order to ensure the renormalizability of the model.

Let us start the description of the MSSM with its particle content. To ensure invariance under the SUSY transformation, we need to promote all the SM fields to superfields. For the gauge bosons, this is done by introducing a vector superfield for every SM gauge field. In this way, the superpartners of the gauge bosons are introduced into the model. These are the gluinos (superpartners of gluons), the winos (superpartners of W-bosons) and the binos (superpartners of B-bosons).

For the SM fermions, the procedure is a bit more elaborate. Indeed, all the SM fermions are Dirac particles, which means that they can be decomposed into a left-handed and a right-handed Weyl spinor according to Eq. (2.1.5). Due to this representation, the quantum numbers of chiral superfields have to be assigned in such a way that they would include either the left-handed fermions or the Hermitian conjugates of the right-handed fermions. For example, in the Standard Model, the left-handed electron and neutrino are combined into the $SU(2)$ doublet, whereas the right-handed electron is an $SU(2)$ singlet. So, the latter must be included into a superfield, denoted as $\bar{e}$ [10], which contains $e_R^\dagger$ and its superpartner $\widetilde{e}_R^*$, called selectron. The hypercharge of the latter is $+2$, and the electric charge equals $+1$. The left-handed neutrino and electron are included into the superfield, denoted as L, which lies in the fundamental representation of the $SU(2)_L$ group, has hypercharge equal to -1 and contains, apart from the mentioned particles, the scalar particle $\widetilde{\nu}_L$ (called sneutrino) and $\widetilde{e}_L$. The same procedure applies to the left- and right-handed quarks. The

[10] The bar here is a part of the name and does not denote Hermitian conjugation. Furthermore, the generation index, which is not written explicitly, is always implicitly assumed in the formulas.

Superfield		Component fields			$SU(3)_C \otimes SU(2)_L \otimes U(1)_Y$
		spin 0	spin 1/2	spin 1	
Chiral superfields					
		$R=-1$	$R=+1$		
(s)quarks, $i=1\dots3$	$Q_{L,i}$	$(\widetilde{u}_{L,i}\ \ \widetilde{d}_{L,i})$	$(u_{L,i}\ \ d_{L,i})$	-	$(\mathbf{3},\mathbf{2},\frac{1}{3})$
	$\overline{u}_i$	$\widetilde{u}^*_{R,i}$	$u^\dagger_{R,i}$	-	$(\overline{\mathbf{3}},\mathbf{1},-\frac{4}{3})$
	$\overline{d}_i$	$\widetilde{d}^*_{R,i}$	$d^\dagger_{R,i}$	-	$(\overline{\mathbf{3}},\mathbf{1},\frac{2}{3})$
(s)leptons, $i=1\dots3$	L_i	$(\widetilde{\nu}_{L,i}\ \ \widetilde{l}_{L,i})$	$(\nu_{L,i}\ \ l_{L,i})$	-	$(\mathbf{1},\mathbf{2},-1)$
	$\overline{l}_i$	$\widetilde{l}^*_{R,i}$	$l^\dagger_{R,i}$	-	$(\mathbf{1},\mathbf{1},2)$
		$R=+1$	$R=-1$		
Higgs, higgsinos	$\mathcal{H}_1$	$(H_1^0\ \ H_1^-)$	$(\widetilde{H}_1^0\ \ \widetilde{H}_1^-)$	-	$(\mathbf{1},\mathbf{2},-1)$
	$\mathcal{H}_2$	$(H_2^+\ \ H_2^0)$	$(\widetilde{H}_2^+\ \ \widetilde{H}_2^0)$	-	$(\mathbf{1},\mathbf{2},+1)$
Vector superfields					
			$R=-1$	$R=+1$	
gluino, gluon	V_G^a	-	$\widetilde{g}^a$	$G^a_\mu,\ a=1\dots8$	$(\mathbf{8},\mathbf{1},0)$
winos, W-bosons	V_W^a	-	$\widetilde{W}^a$	$W^i_\mu,\ i=1\dots3$	$(\mathbf{1},\mathbf{3},0)$
bino, B-boson	V_B	-	$\widetilde{B}$	B_μ	$(\mathbf{1},\mathbf{1},0)$

Table 2.1: Chiral and vector supermultiplets in the Minimal Supersymmetric Standard Model.

notations for the superfields and their quantum numbers are summarized in Table 2.1 [11]

Additional care has to be taken for the symmetry-breaking sector. Being a scalar particle, it has to be included in a chiral multiplet. However, supersymmetric extensions of the Standard Model require at least two such fields. There are two reasons for that. First, in the SM, one Higgs field is enough to provide masses for both up- and down-type quarks: after EWSB the field Φ gives masses to the down-type quarks, whereas its conjugate, $i\sigma^2\Phi^*$, gives masses to the up-type quarks. In supersymmetric theories, the superpotential must be a function only of a chiral field but not its conjugate, thus at least two Higgs doublets are needed. Another reason why a second Higgs doublet is needed are the gauge anomalies. It is known that chiral anomalies have to cancel in order to render the theory renormalizable. In the SM quark and lepton contributions to the chiral anomalies cancel within each generation. However, the Higgs chiral superfield $\mathcal{H}_1$ includes a left-handed fermion (called Higgsino) whose contribution is uncompensated unless a second Higgs doublet $\mathcal{H}_2$ with opposite hypercharge is added. The non-gauge interactions are described

[11] The quantum number denoted as R is R-parity. We will introduce it in Sec. 2.4.1.

by the following R-parity conserving (see Sec. 2.4.1) superpotential,

$$W_{\rm MSSM} = \bar{u}_i\, \mathbf{h}_{u,ij}\, (Q_j \cdot \mathcal{H}_2) - \bar{d}_i\, \mathbf{h}_{d,ij}\, (Q_j \cdot \mathcal{H}_1) - \bar{l}_i\, \mathbf{h}_{l,ij}\, (L_j \cdot \mathcal{H}_1) + \mu\, (\mathcal{H}_1 \cdot \mathcal{H}_2)\,, \tag{2.4.1}$$

where the $SU(2)$-invariant product of two superfields is defined by

$$\Phi_1 \cdot \Phi_2 = \epsilon_{ji} \Phi_1^i \Phi_2^j, \tag{2.4.2}$$

with ϵ being the totally antisymmetric 2×2 tensor defined in Eq. (2.1.3). Apart from the last μ-term, which gives masses to the Higgsinos, this expression resembles the Higgs-fermion interactions in the SM (see Eq. (1.3.4) in Sec. 1.3) with the only difference that now there are two Higgs doublets instead of one and these are superfields instead of ordinary fields. In this basis [12] the vertices are essentially the same as in the SM, just two out of three particles involved in the interaction in any vertex must be replaced by their superpartners. The aforementioned μ parameter is in general a complex number. As in the Standard Model, the MSSM Yukawa couplings, $\mathbf{h}_{u,d,e}$, are in general 3×3 complex-valued matrices which can be diagonalized by bi-unitary transformations.

2.4.1 *R*-parity

The superpotential $W_{\rm MSSM}$, defined in Eq. (2.4.1), does not exhaust all possible gauge-invariant renormalizable interactions of superfields. For example, the following terms are renormalizable and compatible with all symmetries of the MSSM,[13]

$$W_{\rm NR} = \lambda^{ijk}\, (L_i \cdot L_j)\, \bar{l}_k + \lambda'^{ijk}\, (L_i \cdot Q_j)\, \bar{d}_k + \mu'^i\, (L_i \cdot \mathcal{H}_2) + \lambda''^{ijk} \bar{u}_i \bar{d}_j \bar{d}_k. \tag{2.4.3}$$

Let us consider the first term in this expression. According to the Table 2.1, under the lepton number transformation (Eq. (1.4.3) in Sec. 1.4) the superfields L_i, L_j and e_k transform as $L_i \to e^{i\beta} L_i$, $L_j \to l^{i\beta} L_j$, $\bar{l}_k \to e^{-i\beta} \bar{l}_k$ and thus

$$(L_i \cdot L_j)\, \bar{l}_k \to e^{i\beta}\, (L_i \cdot L_j)\, \bar{l}_k. \tag{2.4.4}$$

So, this term violates lepton number. The same can be said about the second term, $(L_i \cdot Q_j)\, \bar{d}_k$, and the third one, $(L_i \cdot \mathcal{H}_2)$. The last term in Eq. (2.4.3) violates baryon number. In combination, they allow, as an example, for the proton decay $p^+ \to e^+ \pi^0$ via the exchange of a squark. This process is, however, highly constrained: the proton

[12] The fields from Table 2.1 mix with each other as a consequence of electroweak symmetry breaking and hence do not form a physical basis of the MSSM. In the physical basis the vertices will no longer have the same coupling constants as the corresponding vertices in the SM but will also involve the mixing matrices (see Sec. 2.5).

[13] The invariance of the last term under $SU(3)_C$ implies that λ''^{ijk} must be antisymmetric in j and k. $SU(2)_L$ symmetry enforces antisymmetry of λ^{ijk} and λ'^{ijk} with respect to their first two indices. See [104] for more details.

lifetime should be at least 1.67×10^{34} years [105]. So, the appearance of the operators in Eq. (2.4.4) in the MSSM superpotential is potentially problematic. In order to protect the MSSM from the appearance of these terms in the superpotential, a new symmetry, called R-parity, is introduced

$$R = (-1)^{3(B-L)+2s}, \tag{2.4.5}$$

where B is the baryon number, L is the lepton number and s is the spin of the particle. This symmetry admits the superpotential in Eq. (2.4.1), but not the terms in Eq. (2.4.3). All fermions in the SM have either $3(B-L) = 1$ (quarks) or $B - L = -3$ (leptons). Either way, the combination $3(B-L)+2s$ is an even number and $R = 1$. Higgs and gauge bosons have $B = L = 0$, hence $R = 1$ for them. On the other hand, the spin of the SUSY particles differs by $\frac{1}{2}$ from the spin of their SM counterparts. Thus, for them $R = -1$. R-parity conservation has two consequences:

- Supersymmetric particles can only be produced in pairs at colliders,

- the lightest neutral SUSY particle with $R = -1$ (also called LSP) is absolutely stable and hence is an attractive candidate for Dark Matter [106, 107] (see Section 1.5).

2.4.2 Supersymmetry breaking

As we already noticed in Sec. 2.2, SUSY can at best be realized as a broken symmetry at low energies. This SUSY breaking cannot occur in the MSSM itself [88] but requires an additional "hidden sector" [108–110]. This sector interacts with the visible one (the MSSM sector) only via the exchange of particles, called "messengers". Many different mechanisms of SUSY breaking have been discussed in the literature: e.g. gravity-mediated breaking [111–114], gauge-mediated breaking [115–117], breaking via exchange of gauginos [118, 119]. In this thesis we will not focus on a particular mechanism of SUSY breaking. Instead, we will parametrize the effect of it in the MSSM Lagrangian via the set of operators which explicitly violate supersymmetry. The crucial point here is that these terms should not reintroduce the Hierarchy problem discussed in Sections 1.5 and 2.2. For that, they should leave the relations between dimensionless couplings unmodified, or in other words, the field operators should have mass dimension less than four, as shown in [120]. The part of the MSSM

Lagrangian, which contains these terms (also called *soft* terms) reads

$$\begin{aligned}\mathcal{L}_{\text{soft}} = &-\frac{1}{2}\left(M_3\widetilde{g}^a\widetilde{g}^a + M_2\widetilde{W}^i\widetilde{W}^i + M_1\widetilde{B}\widetilde{B} + \text{h.c.}\right)\\ &- (m^2_{\tilde{q}})_{ij}\widetilde{q}^*_{L,i}\widetilde{q}_{L,j} - (m^2_{\tilde{u}})_{ij}\widetilde{u}^*_{R,i}\widetilde{u}_{R,j} - (m^2_{\tilde{d}})_{ij}\widetilde{d}^*_{R,i}\widetilde{d}_{R,j}\\ &- (m^2_{\tilde{l}_L})_{ij}\widetilde{l}^*_{L,i}\widetilde{l}_{L,j} - (m^2_{\tilde{l}_R})_{ij}\widetilde{l}^*_{R,i}\widetilde{l}_{R,j}\\ &- \widetilde{m}^2_1 H_1^\dagger H_1 - \widetilde{m}^2_2 H_2^\dagger H_2 - \left(m^2_{12}H_1\cdot H_2 + \text{h.c.}\right)\\ &- \Big[(\mathbf{h}_u\mathbf{A}_u)_{ij}\,(\widetilde{q}_{L,i}\cdot H_2)\,\widetilde{u}^*_{R,j} + (\mathbf{h}_d\mathbf{A}_d)_{ij}\,(H_1\cdot\widetilde{q}_{L,i})\,\widetilde{d}^*_{R,j}\\ &+ (\mathbf{h}_l\mathbf{A}_l)_{ij}\left(H_1\cdot\widetilde{l}_{L,i}\right)\widetilde{l}^*_{R,j} + \text{h.c.}\Big]\,.\end{aligned} \tag{2.4.6}$$

The first line of Eq. (2.4.6) contains (in general, complex) soft masses of the gluino M_3, winos M_2 and bino M_1 which break the mass degeneracy between them and the respective gauge bosons. The second and third lines introduce soft breaking masses for the "left" squarks $(m^2_{\tilde{q}})_{ij}$ [14], for the "right" up-type, $(m^2_{\tilde{u}})_{ij}$ and down-type squarks, $(m^2_{\tilde{d}})_{ij}$, for the "left" sleptons, $(m^2_{\tilde{l}_L})_{ij}$ and "right" sleptons, $(m^2_{\tilde{l}_R})_{ij}$ [15]. In these notations i and j are generation indices. So all these soft breaking masses are in fact 3×3 matrices. The fourth line introduces the soft breaking masses for the Higgs doublets. As we will see in the subsequent Section these terms are necessary to trigger EWSB. Finally, the terms in the last two lines determine the trilinear couplings between the Higgs doublets and squarks. They are proportional to the elements of 3×3 complex-valued matrices $\mathbf{h}_u\mathbf{A}_u$, $\mathbf{h}_d\mathbf{A}_d$ or $\mathbf{h}_l\mathbf{A}_l$. In this thesis we will assume that the minimal flavour violation (MFV) scenario is realized [121–123]. In this scenario, all matrices $m^2_{\tilde{q}}, m^2_{\tilde{u}}, m^2_{\tilde{d}}, m^2_{\tilde{l}_L}, m^2_{\tilde{l}_R}, \mathbf{h}_u\mathbf{A}_u, \mathbf{h}_d\mathbf{A}_d$ and $\mathbf{h}_l\mathbf{A}_l$ are diagonal. There are fourteen parameters in the MSSM which can be complex valued. These are: the gaugino masses $M_{1,2,3}$, the Higgssino mass parameter μ, the Higgs soft-breaking mass m_{12} and the trilinear couplings A_f with $f\in\{u,d,c,s,t,b,e,\mu,\tau\}$. However, not all of the associated phases are physical; two of them can be absorbed by a redefinition of the fields as shown in [124].

2.5 Mass eigenstates

The MSSM fields, listed in Table 2.1, mix with each other to form physical states as shown in Table 2.2 In this Section we will examine different sectors of the MSSM at the tree-level, deriving the expressions for their masses and mixing matrices. To shorten the expression, in the next Subsections the following abbreviations will be

[14] Squarks and sleptons are scalar particles and don't possess such a property as chirality. "Left" and "right" sparticles in this context denote superpartners of a corresponding left- and right-handed fermion.

[15] In the latter case, the soft mass is given only to selectrons, smuons and staus.

name	spin	gauge eigenstates	mass eigenstates
Higgs bosons	0	$\phi_{1,2},\ \chi_{1,2},\ \phi_1^-,\ \phi_2^+$	$h,\ H,\ A,\ H^\pm$
Goldstone bosons	0	$\chi_{1,2},\ \phi_1^-,\ \phi_2^+$	$G,\ G^\pm$
squarks	0	$\widetilde{q}_{L,R}$	$\widetilde{q}_{1,2}$
sleptons	0	$\widetilde{l}_{L,R}, \widetilde{\nu}_{l_{L,R}}$	$\widetilde{l}_{1,2}, \widetilde{\nu}_{l_{1,2}}$
neutralinos	1/2	$\widetilde{B},\ \widetilde{H}^0_{1,2},\ \widetilde{W}^0$	$\widetilde{\chi}^0_{1,2,3,4}$
charginos	1/2	$\widetilde{H}^\pm_{1,2},\ \widetilde{W}^\pm$	$\widetilde{\chi}^\pm_{1,2}$
gluino	1/2	$\widetilde{g}$	$\widetilde{g}$

Table 2.2: Gauge and mass eigenstates of the MSSM.

introduced

$$s_x \equiv \sin x, \quad c_x \equiv \cos x, \quad t_x \equiv \tan x, \tag{2.5.1}$$

for a generic angle x.

2.5.1 Higgs sector

As we discussed in Sec. 2.2, the scalar potential in a supersymmetric theory emerges after integrating out the auxiliary F- and D-fields. The F-term in the Higgs potential in the MSSM originates from the $\mu\,\mathcal{H}_1\cdot\mathcal{H}_2$ term in $W_{\rm SUSY}$ (see Eq. (2.4.1)) and reads

$$V_F = |\mu|^2 \left(H_1^\dagger H_1 + H_2^\dagger H_2\right). \tag{2.5.2}$$

The D-terms emerge after integrating out the D-fields from the $SU(2)_L$ and $U(1)_Y$ vector superfields. Together they read (see Eq. (2.3.26))

$$V_D = \frac{g^2}{8}\sum_{i=1}^{3}\left(H_1^\dagger \sigma^i H_1 + H_2^\dagger \sigma^i H_2\right)^2 + \frac{g'^2}{8}\left(H_1^\dagger H_1 - H_2^\dagger H_2\right). \tag{2.5.3}$$

In addition to them, there are the soft-breaking terms defined in Eq. (2.4.6)

$$V_{\rm soft} = \tilde{m}_1^2 H_1^\dagger H_1 + \tilde{m}_2^2 H_2^\dagger H_2 + \left(m_{12}^2 H_1\cdot H_2 + \text{h.c.}\right). \tag{2.5.4}$$

The sum of the contributions in Eqs. (2.5.2)–(2.5.4) can be rewritten in the following form

$$\begin{aligned} V_H &= V_F + V_D + V_{\rm soft}, \\ V_H &= m_1^2 H_1^\dagger H_1 + m_2^2 H_2^\dagger H_2 + (m_{12}^2 H_1\cdot H_2 + \text{h.c.}) \\ &\quad + \frac{1}{8}(g^2+g'^2)(H_1^\dagger H_1 - H_2^\dagger H_2)^2 + \frac{1}{2}g^2\left|H_1^\dagger H_2\right|^2, \end{aligned} \tag{2.5.5}$$

where $m_i^2 = \tilde{m}_i^2 + |\mu|^2$. It can be shown [88] that by making use of appropriate $SU(2)_L$ transformations, one can choose a minimum for the Higgs potential such that the vevs of the charged components of the Higgs doublets vanish, $\langle H_1^- \rangle = \langle H_2^+ \rangle \equiv 0$. As in the Standard Model, the Higgs potential gives rise to the spontaneous symmetry breaking $SU(2)_L \times U(1)_Y \to U(1)_{\text{em}}$. The two Higgs doublets can be parametrized in terms of excitations around their vacuum expectation values

$$H_1 = \begin{pmatrix} v_1 + \frac{1}{\sqrt{2}}(\phi_1 - i\chi_1) \\ -\phi_1^- \end{pmatrix}, \quad H_2 = e^{i\xi} \begin{pmatrix} \phi_2^+ \\ v_2 + \frac{1}{\sqrt{2}}(\phi_2 + i\chi_2) \end{pmatrix}, \tag{2.5.6}$$

with real and positive vacuum expectation values v_1, v_2 and ξ being a relative $\mathcal{CP}$-violating phase. After plugging this expression into Eq. (2.5.5), we get the following representation of the Higgs potential

$$\begin{aligned} V_H = \text{const} &- T_{\phi_1}\phi_1 - T_{\phi_2}\phi_2 - T_{\chi_1}\chi_1 - T_{\chi_2}\chi_2 \\ &+ \frac{1}{2}\begin{pmatrix}\phi_1, \phi_2, \chi_1, \chi_2\end{pmatrix} \mathbf{M}_{\phi\phi\chi\chi} \begin{pmatrix} \phi_1 \\ \phi_2 \\ \chi_1 \\ \chi_2 \end{pmatrix} + \begin{pmatrix}\phi_1^-, \phi_2^-\end{pmatrix} \mathbf{M}_{\phi^\pm\phi^\pm} \begin{pmatrix} \phi_1^+ \\ \phi_2^+ \end{pmatrix} + \cdots, \end{aligned} \tag{2.5.7}$$

where the ellipsis stands for the cubic and quartic terms which we do not list here. The coefficients of the linear terms (called *tadpoles*) read

$$T_{\phi_1} = -\sqrt{2}(m_1^2 v_1 - c_{\xi'}|m_{12}^2|v_2 + \frac{1}{4}(g^2 + g'^2)(v_1^2 - v_2^2)v_1), \tag{2.5.8a}$$

$$T_{\phi_2} = -\sqrt{2}(m_2^2 v_2 - c_{\xi'}|m_{12}^2|v_1 - \frac{1}{4}(g^2 + g'^2)(v_1^2 - v_2^2)v_2), \tag{2.5.8b}$$

$$T_{\chi_1} = \sqrt{2}\ s_{\xi'}|m_{12}^2|v_2 = -T_{\chi_2}\frac{v_2}{v_1}, \tag{2.5.8c}$$

$$\text{where } \xi' = \xi + \arg\left(m_{12}^2\right).$$

In analogy to the Standard Model, after inserting expression (2.5.6) into the Higgs kinetic term in the Lagrangian, we obtain expressions for the masses of the W and Z-bosons (see Eqs.(1.2.13)–(1.2.16) in Sec. 1.2),

$$M_W^2 = \frac{g^2(v_1^2 + v_2^2)}{2}, \quad M_Z^2 = \frac{(g^2 + g'^2)(v_1^2 + v_2^2)}{2}. \tag{2.5.9}$$

Comparison of Eq. (2.5.9) with Eq. (1.2.16) yields $v = \sqrt{v_1^2 + v_2^2} \approx 174$ GeV. The ratio of the Higgs vacuum expectation values is denoted as $\tan\beta$,

$$\tan\beta = \frac{v_2}{v_1}. \tag{2.5.10}$$

Since $v_{1,2} > 0$, the angle β can be chosen to be in the interval $0 < \beta < \frac{\pi}{2}$. The real, symmetric 4×4-matrix $\mathbf{M}_{\phi\phi\chi\chi}$ and the hermitian 2×2-matrix $\mathbf{M}_{\phi^\pm\phi^\pm}$ contain the following elements,

$$\mathbf{M}_{\phi\phi\chi\chi} = \begin{pmatrix} \mathbf{M}_\phi & \mathbf{M}_{\phi\chi} \\ \mathbf{M}_{\phi\chi}^\dagger & \mathbf{M}_\chi \end{pmatrix}, \tag{2.5.11a}$$

$$\mathbf{M}_\phi = \begin{pmatrix} m_1^2 + \frac{1}{4}(g'^2+g^2)(3v_1^2 - v_2^2) & -c_{\xi'}\,|m_{12}^2| - \frac{1}{2}(g^2+g'^2)v_1v_2 \\ -c_{\xi'}\,|m_{12}^2| - \frac{1}{2}(g^2+g'^2)v_1v_2 & m_2^2 + \frac{1}{4}(g^2+g'^2)(3v_2^2 - v_1^2) \end{pmatrix}, \tag{2.5.11b}$$

$$\mathbf{M}_{\phi\chi} = \begin{pmatrix} 0 & s_{\xi'}\,|m_{12}^2| \\ -s_{\xi'}\,|m_{12}^2| & 0 \end{pmatrix}, \tag{2.5.11c}$$

$$\mathbf{M}_\chi = \begin{pmatrix} m_1^2 + \frac{1}{4}(g^2+g'^2)(v_1^2 - v_2^2) & -c_{\xi'}\,|m_{12}^2| \\ -c_{\xi'}\,|m_{12}^2| & m_2^2 + \frac{1}{4}(g^2+g'^2)(v_2^2 - v_1^2) \end{pmatrix}, \tag{2.5.11d}$$

$$\mathbf{M}_{\phi^\pm\phi^\pm} = \begin{pmatrix} m_1^2 + \frac{1}{4}g'^2(v_1^2 - v_2^2) + \frac{1}{4}g^2(v_1^2 + v_2^2) & -e^{i\xi'}|m_{12}^2| - \frac{1}{2}g^2v_1v_2 \\ -e^{-i\xi'}|m_{12}^2| - \frac{1}{2}g^2v_1v_2 & m_2^2 + \frac{1}{4}g'^2(v_2^2 - v_1^2) + \frac{1}{4}g^2(v_1^2 + v_2^2) \end{pmatrix}. \tag{2.5.11e}$$

Minimization of the potential requires that all tadpoles vanish,

$$\begin{aligned} &v_1\left(m_1^2 - c_{\xi'}|m_{12}^2|\tan\beta + \frac{M_Z^2}{2}c_{2\beta}\right) = 0, \\ &v_2\left(m_2^2 - c_{\xi'}|m_{12}^2|\cot\beta - \frac{M_Z^2}{2}c_{2\beta}\right) = 0, \\ &v_1 s_{\xi'}|m_{12}^2| = 0, \\ &v_2 s_{\xi'}|m_{12}^2| = 0. \end{aligned} \tag{2.5.12}$$

At this point it is possible to see why without the soft-breaking masses spontaneous EWSB cannot take place in the MSSM. Indeed, in the limit $m_1^2 \to |\mu|^2$, $m_2^2 \to |\mu|^2, m_{12}^2 \to 0$, the solution of the system of equations (2.5.12) is $v_1 = v_2 \equiv 0$.

In the presence of soft-breaking parameters, the last two equations yield $\xi' = 0$. This implies that the off-diagonal entries of the matrix $\mathbf{M}_{\phi\chi}$ vanish and hence there

is no mixing between $\mathcal{CP}$-even and $\mathcal{CP}$-odd particles at the tree-level. Moreover, by making use of Peccei–Quinn transformation [125,126], the phase of m_{12} can be rotated away, yielding $\xi = 0$. From the first two equations, we can express the Z-boson mass as

$$M_Z^2 = \frac{\tilde{m}_1^2 - \tilde{m}_2^2}{\cos 2\beta} - \tilde{m}_1^2 - \tilde{m}_2^2 - 2|\mu|^2. \tag{2.5.13}$$

The parameters on the right-hand side of this equation have different origins. The Higgsino mass parameter, μ, appears in the superpotential of the MSSM W_{MSSM} (see Eq. (2.4.1)), whereas the masses $\tilde{m}_1^2$ and $\tilde{m}_2^2$ are soft-breaking parameters. The question of why so seemingly unrelated parameters combine to yield the electroweak quantity M_Z^2 is the essence of the "μ-problem" of the MSSM [127]. A solution to this problem is given in the Next-to-Minimal Supersymmetric Standard Model (NMSSM) [128], where μ is generated by the vacuum expectation value of an additional Higgs singlet which itself depends on the soft breaking parameters. In this thesis, however, we will only discuss the MSSM.

The matrices $\mathbf{M}_{\phi\phi\chi\chi}$ and $\mathbf{M}_{\phi^\pm\phi^\pm}$ can be diagonalized by unitary transformations

$$\begin{pmatrix} h \\ H \end{pmatrix} = \mathbf{R}_\alpha \begin{pmatrix} \phi_1 \\ \phi_2 \end{pmatrix}, \quad \begin{pmatrix} A \\ G \end{pmatrix} = \mathbf{R}_{\beta_n} \begin{pmatrix} \chi_1 \\ \chi_2 \end{pmatrix}, \quad \begin{pmatrix} H^\pm \\ G^\pm \end{pmatrix} = \mathbf{R}_{\beta_c} \begin{pmatrix} \phi_1^\pm \\ \phi_2^\pm \end{pmatrix}, \tag{2.5.14}$$

where

$$\mathbf{R}_x = \begin{pmatrix} -s_x & c_x \\ c_x & s_x \end{pmatrix}. \tag{2.5.15}$$

Note that since $\mathcal{CP}$-even and $\mathcal{CP}$-odd states do not mix with each other at the tree-level, they are diagonalized by two different matrices. The Higgs potential in the new basis reads

$$\begin{aligned} V_H =& \text{const} - T_h \cdot h - T_H \cdot H - T_A \cdot A - T_G \cdot G \\ &+ \frac{1}{2} \begin{pmatrix} h & H & A & G \end{pmatrix} \cdot \begin{pmatrix} m_h^2 & m_{hH}^2 & m_{hA}^2 & m_{hG}^2 \\ m_{hH}^2 & m_H^2 & m_{HA}^2 & m_{HG}^2 \\ m_{hA}^2 & m_{hH}^2 & m_A^2 & m_{AG}^2 \\ m_{hG}^2 & m_{HG}^2 & m_{AG}^2 & m_G^2 \end{pmatrix} \cdot \begin{pmatrix} h \\ H \\ A \\ G \end{pmatrix} \\ &+ \begin{pmatrix} H^- & G^- \end{pmatrix} \cdot \begin{pmatrix} m_{H^\pm}^2 & m_{H^-G^+}^2 \\ m_{G^-H^+}^2 & m_{G^\pm}^2 \end{pmatrix} \cdot \begin{pmatrix} H^+ \\ G^+ \end{pmatrix} + \dots, \end{aligned} \tag{2.5.16}$$

where the entries of the mass matrices have the following form:

$$\begin{aligned}
m_h^2 =& M_Z^2 s_{\alpha+\beta}^2 + m_A^2 \frac{c_{\alpha-\beta}^2}{c_{\beta-\beta_n}^2} \\
&+ \frac{e s_{\alpha-\beta_n}}{2 s_{\mathrm{w}} M_W c_{\beta-\beta_n}^2} \left[T_H c_{\alpha-\beta} s_{\alpha-\beta_n} + \frac{T_h}{2} \left(c_{2\alpha-\beta-\beta_n} + 3 c_{\beta-\beta_n} \right) \right], && \text{(2.5.17a)} \\
m_{hH}^2 =& - M_Z^2 s_{\alpha+\beta} c_{\alpha+\beta} + m_A^2 \frac{s_{\alpha-\beta} c_{\alpha-\beta}}{c_{\beta-\beta_n}^2} \\
&+ \frac{e}{2 s_{\mathrm{w}} M_W c_{\beta-\beta_n}^2} \left[T_H s_{\alpha-\beta} s_{\alpha-\beta_n}^2 - T_h c_{\alpha-\beta} c_{\alpha-\beta_n}^2 \right], && \text{(2.5.17b)} \\
m_H^2 =& M_Z^2 c_{\alpha+\beta}^2 + m_A^2 \frac{s_{\alpha-\beta}^2}{c_{\beta-\beta_n}^2} \\
&+ \frac{e c_{\alpha-\beta_n}}{2 s_{\mathrm{w}} M_W c_{\beta-\beta_n}^2} \left[-T_h s_{\alpha-\beta} c_{\alpha-\beta_n} + \frac{T_H}{2} \left(c_{2\alpha-\beta-\beta_n} - 3 c_{\beta-\beta_n} \right) \right], && \text{(2.5.17c)} \\
m_{hA}^2 =& m_{HG}^2 = \frac{e}{2 s_{\mathrm{w}} M_W} T_A \frac{s_{\alpha-\beta_n}}{c_{\beta-\beta_n}}, && \text{(2.5.17d)} \\
m_{hG}^2 =& - m_{HA}^2 = \frac{e}{2 s_{\mathrm{w}} M_W} T_A \frac{c_{\alpha-\beta_n}}{c_{\beta-\beta_n}}, && \text{(2.5.17e)} \\
m_{AG}^2 =& - m_A^2 t_{\beta-\beta_n} - \frac{e}{2 s_{\mathrm{w}} M_W c_{\beta-\beta_n}} \left(T_H s_{\alpha-\beta_n} + T_h c_{\alpha-\beta_n} \right), && \text{(2.5.17f)} \\
m_G^2 =& m_A^2 t_{\beta-\beta_n}^2 + \frac{e}{2 s_{\mathrm{w}} M_W c_{\beta-\beta_n}^2} \left(-T_H c_{\alpha+\beta-2\beta_n} + T_h s_{\alpha+\beta-2\beta_n} \right), && \text{(2.5.17g)} \\
m_{H^- G^+}^2 =& - m_{H^\pm}^2 t_{\beta-\beta_c} - \frac{e}{2 s_{\mathrm{w}} M_W} \left(T_H \frac{s_{\alpha-\beta_c}}{c_{\beta-\beta_c}} + T_h \frac{c_{\alpha-\beta_c}}{c_{\beta-\beta c}} + i \frac{T_A}{c_{\beta-\beta_n}} \right), && \text{(2.5.17h)} \\
m_{G^- H^+}^2 =& \left(m_{H^- G^+}^2 \right)^*, && \text{(2.5.17i)} \\
m_{G^\pm}^2 =& m_{H^\pm}^2 t_{\beta-\beta_c}^2 + \frac{e}{2 s_{\mathrm{w}} M_W c_{\beta-\beta_c}^2} \left(-T_H c_{\alpha+\beta-2\beta_c} + T_h s_{\alpha+\beta-2\beta_c} \right). && \text{(2.5.17j)}
\end{aligned}$$

The eight independent parameters of the tree-level Higgs potential in Eq. (2.5.7) $(m_1^2, m_2^2, \xi, |m_{12}^2|, v_1, v_2, g, g')$ were replaced by $(T_h, T_H, T_A, m_A^2, e, M_W, M_Z, t_\beta)$ [16]. Since the tadpoles $T_{h,H,A}$ vanish at the mininum of the Higgs potential, the off-diagonal elements $m_{hA}^2, m_{HG}^2, m_{hG}^2$ and m_{HA}^2 are automatically equal to zero. Next, the requirement that $m_{AG}^2 = m_{H^- G^+}^2 \equiv 0$ gives

$$\beta_c = \beta_n \equiv \beta. \tag{2.5.18}$$

The latter condition sets the masses of Goldstone bosons to zero [17]

$$m_G^2 = m_{G^\pm}^2 \equiv 0. \tag{2.5.19}$$

[16] Despite the fact that the phase ξ equals zero at the tree level, it has to be renormalized at higher-orders. That is why it is treated as an independent parameter [91, 129, 130].

[17] Computation of higher order corrections requires the gauge fixing in full analogy to the Standard Model, see Eq. (1.3.11) in Section 1.3. In 't-Hooft gauge the Goldstone bosons have the following masses $m_G^2 = \xi_Z M_Z^2$, $m_{G^\pm}^2 = \xi_W M_W^2$.

Using Eq. (2.5.18), it can be shown that the following relation holds between the masses of the $\mathcal{CP}$-odd and charged Higgs bosons,

$$m^2_{H^\pm} = m^2_A + M^2_W. \tag{2.5.20}$$

The remaining non-zero off-diagonal element is m^2_{hH}. Taking into account that $T_H = T_h \equiv 0$ and the Eq. (2.5.18), it can be rewritten as

$$m^2_{hH} = \frac{c_{2\alpha+2\beta}c_{2\alpha-2\beta}}{4}\left(m^2_A(t_{2\alpha} - t_{2\beta}) + M^2_Z(t_{2\alpha} + t_{2\beta})\right). \tag{2.5.21}$$

For this expression to vanish, the mixing angle α has to satisfy the equation

$$t_{2\alpha} = t_{2\beta}\,\frac{m^2_A + M^2_Z}{m^2_A - M^2_Z}. \tag{2.5.22}$$

The solution, which lies inside the interval $-\frac{\pi}{2} < \alpha < 0$ [18], can be written as follows:

$$\alpha = -\frac{1}{2}\arcsin\left\{\frac{(m^2_A + M^2_Z)s_{2\beta}}{\sqrt{(m^2_A + M^2_Z)^2 - 4m^2_A M^2_Z c^2_{2\beta}}}\right\}, \tag{2.5.23}$$

After inserting the expression for α into Eqs. (2.5.17a) and (2.5.17c), we obtain the two remaining eigenvalues of the matrix $\mathbf{M}_{\phi\phi\chi\chi}$:

$$m^2_{h/H} = \frac{1}{2}\left[m^2_A + M^2_Z \mp \sqrt{(m^2_A + M^2_Z)^2 - 4m^2_A M^2_Z c^2_{2\beta}}\right]. \tag{2.5.24}$$

To summarize, let us make several comments. First of all, contrary to the Standard Model, the MSSM contains five physical Higgs bosons instead of one: three neutral bosons h, H, A, and two charged bosons, $H^\pm$. Another important difference to the SM, is that the masses of h and H can be predicted in terms of the other parameters of the theory. In fact, at lowest order they are determined only by two parameters: m_A and t_β. By analyzing the expression (2.5.24), we notice that the mass of the lightest Higgs boson m_h is bounded from above by the Z-boson mass,

$$m_h < M_Z|\cos 2\beta| \leq M_Z, \tag{2.5.25}$$

and hence lower than the mass of the particle discovered at the LHC [1, 2]. Let us note that, in this statement we implicitly identified the light MSSM Higgs boson, h, with the particle discovered at the LHC. In principle the heavier Higgs boson, H, can be identified with the observed signal as well. The MSSM scenarios, realizing this possibility were considered in the papers [131–138], but as shown in [138], this scenario is already strongly constrained by the experimental data. That is why in

[18] This choice correponds to the convention $m_h < m_H$.

this thesis we will identify the lightest Higgs boson, h, with the particle discovered at the LHC.

Being bounded by the Z-boson mass at lowest order, the mass of the lightest Higgs boson, m_h, gets sizeable higher-order corrections from other MSSM sectors which can lift its value such that it agrees with the measured value. Also, higher-order corrections make the Higgs boson mass dependent on many other parameters of the model. In the next chapters, we will address different aspects of radiative corrections to the Higgs mass, and in order to distinguish between the tree-level mass and the physical mass we will be using the capitalized M_h for the latter.

Moreover, as we already mentioned before, the Higgs sector preserves $\mathcal{CP}$ at the lowest order, but the $\mathcal{CP}$-violation can occur at the higher-orders of perturbation theory. If this is the case, then $\mathcal{CP}$-even states h, H mix with $\mathcal{CP}$-odd Higgs boson A, and m_A is no longer an eigenvalue of $\mathbf{M}_{\phi\phi\chi\chi}$. In this case, the mass of the charged Higgs boson $m_{H^\pm}$ is used as an input parameter instead of m_A.

As in the Standard Model (see Sec. 1.3), the fermion masses are generated via interactions with the Higgs fields. While in the Standard Model one Higgs field was enough to give masses to both up- and down-type fermions, the holomorphicity of the MSSM superpotential leads to the requirement of two Higgs doublets to achieve the same in the MSSM (see Sec. 2.4). By taking the θ^2 coefficient of Eq. (2.4.1) and retaining only the Higgs-fermion-fermion terms, we get

$$\begin{aligned}\mathcal{L}_{\text{Yuk}}^{\text{MSSM}} = &- (\mathbf{h}_l)_{ij}\bar{l}_{i,R}(iH_1^T\sigma^2)L_{j,L} - (\mathbf{h}_d)_{ij}\bar{d}_{i,R}(iH_1^T\sigma^2)Q_{j,L} \\ &- (\mathbf{h}_u)_{ij}\bar{u}_{i,R}(-iH_2^T\sigma^2)Q_{j,L} + \text{h.c.}\,.\end{aligned} \tag{2.5.26}$$

After electroweak symmetry breaking the fermions get masses

$$m_{e,\mu,\tau} = h_{e,\mu,\tau}v_1 = h_{e,\mu,\tau}c_\beta v, \tag{2.5.27a}$$

$$m_{d,s,b} = h_{d,s,b}v_1 = h_{d,s,b}c_\beta v, \tag{2.5.27b}$$

$$m_{u,c,t} = h_{u,c,t}v_2 = h_{u,c,t}s_\beta v. \tag{2.5.27c}$$

A small remark should be made here. The ratio of the bottom and top Yukawa couplings $\frac{h_b}{h_t} = \frac{m_b}{m_t}\tan\beta$ is proportional to the ratio of vevs, $\tan\beta$. Sufficiently large values of $\tan\beta \sim \frac{m_t}{m_b} \sim 40$ may compensate for the suppression of the mass ratio m_b/m_t and can potentially make the bottom Yukawa coupling as large as the top Yukawa coupling [19]. Moreover, the MSSM bottom Yukawa coupling gets SUSY-QCD corrections which are also proportional to $\tan\beta$. The latter, in turn, can either

[19] It is worth mentioning, that in the *decoupling limit*, i.e. when $M_A \gg M_Z$ the coupling of the light Higgs boson to bottom quarks behaves SM-like. Thus, the enhancement of the Yukawa coupling does not lead to an enhancement of this coupling in the mentioned limit [139].

suppress the coupling or enhance it even more. We will consider this in detail in Sec. 3.2.3.

2.5.2 Sfermion sector

After electroweak symmetry breaking the mass matrix of the sfermions is generated,

$$\mathcal{L}_{\tilde{f}} \supset -\begin{pmatrix} \widetilde{f}_L^\dagger & \widetilde{f}_R^\dagger \end{pmatrix} \mathbf{M}_{\tilde{f}} \begin{pmatrix} \widetilde{f}_L \\ \widetilde{f}_R \end{pmatrix}, \tag{2.5.28}$$

$$\text{with} \quad \mathbf{M}_{\tilde{f}} = \begin{pmatrix} m^2_{\tilde{f}_L} + m_f^2 + M_Z^2(I_3^f - Q_f s_{\rm w}^2)c_{2\beta} & m_f\, X_f^* \\ m_f\, X_f & m^2_{\tilde{f}_R} + m_f^2 + M_Z^2 Q_f s_{\rm w}^2 c_{2\beta} \end{pmatrix},$$

where I_3^f is the weak isospin, Q_f is the electric charge, and m_f is the mass of the corresponding fermion ($s_{\rm w} = \sin\theta_W$). The complex variable X_f in the off-diagonal entries of $\mathbf{M}_{\tilde{f}}$ is defined as

$$X_f \;\; = \;\; A_f - \mu^* \kappa. \tag{2.5.29}$$

In this expression A_f is the soft-breaking trilinear coupling (see Eq. (2.4.6)) and $\kappa = \frac{1}{t_\beta}$ for $f \in \{u, c, t\}$ and $\kappa = t_\beta$ for $f \in \{d, s, b, e, \mu, \tau\}$. Due to the $SU(2)_L$ symmetry, the soft-breaking masses $m^2_{\tilde{f}_L}$ are the same for up- and down-type sfermions (for example, $m_{\tilde{t}_L} = m_{\tilde{b}_L}$). The matrix $\mathbf{M}_{\tilde{f}}$ is diagonalized by a unitary transformation

$$\mathbf{U}_{\tilde{f}} \mathbf{M}_{\tilde{f}} \mathbf{U}_{\tilde{f}}^\dagger = \text{diag}(m^2_{\tilde{f}_1}, m^2_{\tilde{f}_2}), \quad \text{with} \quad \mathbf{U}_{\tilde{f}} = \begin{pmatrix} c_{\tilde{f}} & s_{\tilde{f}} \\ -s^*_{\tilde{f}} & c_{\tilde{f}} \end{pmatrix}, \quad \mathbf{U}_{\tilde{f}} \mathbf{U}_{\tilde{f}}^\dagger = \mathbb{1}, \tag{2.5.30}$$

Here $c_{\tilde{f}} \equiv \cos\theta_{\tilde{f}}$ is real, whereas $s_{\tilde{f}} \equiv e^{-i\phi_{X_f}} \sin\theta_{\tilde{f}}$ can be complex with the phase

$$\phi_{s_{\tilde{f}}} = -\phi_{X_f} = \arg\left(X_f^*\right) \;. \tag{2.5.31}$$

The mixing angle $\theta_{\tilde{f}}$ is defined from the equation

$$\tan 2\theta_{\tilde{f}} = \frac{2 m_f |X_f|}{\mathbf{M}_{\tilde{f}_{11}} - \mathbf{M}_{\tilde{f}_{22}}}. \tag{2.5.32}$$

As a convention it can be chosen to be in the interval $-\frac{\pi}{4} < \theta_{\tilde{f}} < \frac{\pi}{4}$. The eigenvalues of $\mathbf{M}_{\tilde{f}}$ are given by

$$m^2_{\tilde{f}_{1,2}} = m_f^2 + \frac{1}{2}\Big[m^2_{\tilde{f}_L} + m^2_{\tilde{f}_R} + I_3^f M_Z^2 c_{2\beta} \tag{2.5.33}$$

$$\mp \ \mathrm{C}\ \sqrt{\left[m^2_{\tilde{f}_L} - m^2_{\tilde{f}_R} + M_Z^2 c_{2\beta}(I_3^f - 2Q_f s^2_{\mathrm{w}})\right]^2 + 4m_f^2 |X_f|^2}\ \Big],$$

where

$$\mathrm{C} = \mathrm{sign}\left\{m^2_{\tilde{f}_L} - m^2_{\tilde{f}_R} + M_Z^2(I_3^f - 2Q_f s^2_{\mathrm{w}})\right\}. \tag{2.5.34}$$

The product of $c_{\tilde{f}}$ and $s_{\tilde{f}}$ fulfills the relation

$$c_{\tilde{f}}\ s_{\tilde{f}} = \frac{m_f X_f^*}{m^2_{\tilde{f}_2} - m^2_{\tilde{f}_1}}, \tag{2.5.35}$$

which will be used later in Chapter 3.

2.5.3 Neutralino/chargino sector

The charged Higgsinos $\widetilde{H}_1^-, \widetilde{H}_2^+$ and the winos $\widetilde{W}^\pm$ have the following mass term

$$\mathcal{L}_{\tilde{\chi}^\pm} \supset -\frac{1}{2}\begin{pmatrix}\widetilde{W}^+ & \widetilde{H}_2^+\end{pmatrix}\mathbf{X}^T\begin{pmatrix}\widetilde{W}^- \\ \widetilde{H}_1^-\end{pmatrix} + \begin{pmatrix}\widetilde{W}^- & \widetilde{H}_1^-\end{pmatrix}\mathbf{X}\begin{pmatrix}\widetilde{W}^+ \\ \widetilde{H}_2^+\end{pmatrix} + \mathrm{h.c.}, \tag{2.5.36}$$

where $\mathbf{X}$ is a 2×2 complex matrix

$$\mathbf{X} = \begin{pmatrix} M_2 & \sqrt{2}s_\beta\, M_W \\ \sqrt{2}c_\beta\, M_W & \mu \end{pmatrix}. \tag{2.5.37}$$

This martix can be diagonalized by a bi-unitary transformation

$$\begin{pmatrix} m_{\tilde{\chi}_1^\pm} & 0 \\ 0 & m_{\tilde{\chi}_2^\pm}\end{pmatrix} = \mathbf{U}^*\,\mathbf{X}\,\mathbf{V}^\dagger, \tag{2.5.38}$$

where the mass eigenvalues read

$$\begin{aligned} m_{\tilde{\chi}^\pm_{1,2}} =& \frac{1}{2}\Big[|M_2|^2 + |\mu|^2 + 2M_W^2 \\ & \mp\sqrt{\left(|M_2|^2 + |\mu|^2 + 2M_W^2\right)^2 - 4|\mu M_2 - M_W^2 s_{2\beta}|^2}\Big]. \end{aligned} \tag{2.5.39}$$

The matrices $\mathbf{U},\ \mathbf{V}$ transform Higgsinos and winos into the mass eigenstates called *charginos* $\widetilde{\chi}^\pm_{1,2}$

$$\begin{pmatrix}\widetilde{\chi}_1^+ \\ \widetilde{\chi}_2^+\end{pmatrix} = \mathbf{V}\begin{pmatrix}\widetilde{W}^+ \\ \widetilde{H}_2^+\end{pmatrix}, \quad \begin{pmatrix}\widetilde{\chi}_1^- \\ \widetilde{\chi}_2^-\end{pmatrix} = \mathbf{U}\begin{pmatrix}\widetilde{W}^- \\ \widetilde{H}_1^-\end{pmatrix}. \tag{2.5.40}$$

The mass eigenvalues in Eq. (2.5.39) are real and positive numbers. In case that the mass parameters M_2 and μ are complex numbers, their phases enter the mixing matrices $\mathbf{U}$ and $\mathbf{V}$ and eventually the chargino-fermion-sfermion vertices.

The neutral Higgsinos $\widetilde{H}^0_{1,2}$, the wino $\widetilde{W}^0$ and the bino acquire the following mass term after electroweak symmetry breaking

$$\mathcal{L}_{\tilde{\chi}^0} \supset -\frac{1}{2}\widetilde{\psi}_0^T\,\mathbf{Y}\,\widetilde{\psi}_0 + \text{h.c.}, \tag{2.5.41}$$

where $\widetilde{\psi}_0^T = \left(\widetilde{B}^0 \quad \widetilde{W}^0 \quad \widetilde{H}^0_1 \quad \widetilde{H}^0_2\right)$, and the mass matrix is given by

$$\mathbf{Y} = \begin{pmatrix} M_1 & 0 & -M_Z\, s_\mathrm{w} c_\beta & M_Z\, s_\mathrm{w} s_\beta \\ 0 & M_2 & M_Z\, c_\mathrm{w} c_\beta & M_Z\, c_\mathrm{w} s_\beta \\ -M_Z\, s_\mathrm{w} c_\beta & M_Z\, c_\mathrm{w} c_\beta & 0 & -\mu \\ M_Z\, s_\mathrm{w} s_\beta & M_Z\, c_\mathrm{w} s_\beta & -\mu & 0 \end{pmatrix}. \tag{2.5.42}$$

This matrix is symmetric, so it can be diagonalized by a Takagi transformation [140, 141] with a matrix $\mathbf{N}$

$$\begin{pmatrix} \widetilde{\chi}^0_1 \\ \widetilde{\chi}^0_2 \\ \widetilde{\chi}^0_3 \\ \widetilde{\chi}^0_4 \end{pmatrix} = \mathbf{N} \begin{pmatrix} \widetilde{B}^0 \\ \widetilde{W}^0 \\ \widetilde{H}^0_1 \\ \widetilde{H}^0_2 \end{pmatrix}, \quad \mathbf{N}^*\,\mathbf{Y}\,\mathbf{N}^\dagger = \mathrm{diag}\left(m_{\widetilde{\chi}^0_1}, m_{\widetilde{\chi}^0_2}, m_{\widetilde{\chi}^0_3}, m_{\widetilde{\chi}^0_4}\right). \tag{2.5.43}$$

The mass eigenstates $\widetilde{\chi}^0_i$ are called *neutralinos*. As in the aforementioned case of charginos the mass eigenvalues are assumed to be real and positive. If the supersymmetric parameters $M_{1,2}$ and μ are complex numbers, their phases enter the mixing matrix N and therefore appear in the neutralino-fermion-sfermion vertices. These mass eigenvalues are the roots of a fourth-order equation and thus in the most general case with complex μ, M_1 and M_2 they have very lengthy expressions. Compact solutions can be found only in special cases, e.g. when $M_1 = M_2$ and $\tan\beta = 1$ [142], when the mass parameters and there splittings are much large than the Z-boson mass, $|M_{1,2}|^2, |\mu|^2 \gg M_Z^2$, $\quad ||M_{1,2}| - |\mu||^2 \gg M_Z^2$ [142, 143] or when $M_1 = M_2 = \mu \gg M_Z$ [144].

In this thesis, we will refer to neutralinos and charginos generically as *electroweakinos*.

2.5.4 Gluino sector

Only soft-breaking terms contribute to the mass of the gluinos (see Eq. (2.4.6) in Sec. 2.4.2),

$$\mathcal{L}_{\tilde{g}} \supset -\frac{1}{2}\left(M_3\,\tilde{g}^a\tilde{g}^a + M_3^*\,\bar{\tilde{g}}^a\bar{\tilde{g}}^a\right). \tag{2.5.44}$$

The gluino mass parameter M_3 in general is a complex parameter with an absolute value $m_{\tilde{g}} = |M_3|$ and phase ϕ_{M_3}. Its phase can be absorbed by redefining the gluino field. Thereby, the original Weyl spinors $\tilde{g}^a$ and $\bar{\tilde{g}}^a$ are replaced by λ^a and $\bar{\lambda}^a$

$$\tilde{g}^a \to e^{i\frac{\phi_{M_3}}{2}}\tilde{g}^a, \quad \bar{\tilde{g}}^a \to e^{-i\frac{\phi_{M_3}}{2}}\bar{\tilde{g}}^a. \tag{2.5.45}$$

In terms of the new fields, the mass term (Eq. (2.5.44)) can be written as follows,

$$\mathcal{L}_{\tilde{g}} \supset -\frac{m_{\tilde{g}}}{2}\left(\tilde{g}^a\tilde{g}^a + \bar{\tilde{g}}^a\bar{\tilde{g}}^a\right). \tag{2.5.46}$$

The gluino phase, being eliminated from Eq. (2.5.44), appears in quark-squark-gluino vertices [145] (see also Eq. (2.3.24) from Sec. 2.3),

$$\begin{aligned}\mathcal{L}_{q\tilde{q}\tilde{g}} \supset &-\sqrt{2}g_3\left(e^{-\frac{i\phi_{M_3}}{2}}\tilde{q}_L^\dagger T^a\tilde{g}^a q_L + e^{\frac{i\phi_{M_3}}{2}}\,q_L^\dagger T^a\bar{\tilde{g}}^a\tilde{q}_L\right)\\ &-\sqrt{2}g_3\left(e^{-\frac{i\phi_{M_3}}{2}}\tilde{q}_R^\dagger T^a\tilde{g}^a q_R + e^{\frac{i\phi_{M_3}}{2}}\,q_R^\dagger T^a\bar{\tilde{g}}^a\tilde{q}_R\right),\end{aligned} \tag{2.5.47}$$

where g_3 is the strong coupling and T_a are the $SU(3)_C$ generators.

Chapter 3

Higher-order corrections

This chapter reviews the main aspects of higher-order corrections needed for the discussion of the radiative corrections to the Higgs masses in the MSSM. The introductory Section 3.1 is based on the Review [146]. The one-loop renormalization of the MSSM sectors relevant for this thesis follows the conventions of the Refs. [9, 11, 34, 90, 91, 147–151].

3.1 Regularization and Renormalization

The experimental precision achieved at modern colliders demands high-precision computation of observables like cross-sections, decay widths, branching ratios, and many others. The calculations of these observables are based on the fact that the Lagrangian of the model, within which these calculations are carried out, can be split into two parts. The first part contains terms quadratic in the fields and describes the propagation of free particles. The second part contains terms of higher powers in the fields. These terms are proportional to dimensional or dimensionless *coupling constants* [20] and describe interactions between the different fields of the model. If these coupling constants are small enough, which will always be assumed in this thesis, this part can be treated as a perturbation to the free part of the Lagrangian. Therefore, the expression for some observable $\widehat{O}$ can be written as a series in the coupling constant g,

$$\widehat{O} = \widehat{O}_0 + g\,\widehat{O}_1 + g^2\widehat{O}_2 + \dots . \tag{3.1.1}$$

Each term in this series can be represented by a graph called *Feynman graph* or *Feynman diagram* [152–154]. Very often, the leading term, $\widehat{O}_0$, corresponds to the graphs, in which two vertices are connected by at most one path, i.e., to the *tree graphs*. If this is the case, then the leading result is referred to as a "tree-level" result. [21] The

[20] We already introduced electroweak and strong coupling constants in Chapters 1 and 2.
[21] We already used this term for the description of the different MSSM sectors (see Sec. 2.5).

higher-order terms in Eq. (3.1.1), $\widehat{O}_n$ (where $n \geq 1$), correspond to *loop diagrams*, i.e. to graphs where two vertices are connected by more than one path. An example of a one-loop diagram is presented in Fig. 3.1. Each part of the exemplary one-loop diagram in Fig. 3.1 corresponds to a specific expression. For example in Fig. 3.1, the internal line with momentum k corresponds to the propagator [22]

$$\frac{i}{k^2 - m^2 + i0}, \tag{3.1.2}$$

with $+i0$ being an infinitesimal shift from the real axis. External lines yield a factor of 1 and vertices a factor of ig, where g is a coupling constant in the Lagrangian. For each momentum, which is not constrained by the momentum conservation law (e.g. k in Fig. 3.1) there is an integration with the measure

$$\int_{\mathbb{R}^4} \frac{d^4k}{(2\pi)^4}. \tag{3.1.3}$$

Applying these rules to the diagram in Fig. 3.1, we arrive at the expression

$$I(p) = (ig)^2 \int_{\mathbb{R}^4} \frac{d^4k}{(2\pi)^4} \frac{i^2}{(k^2 - m^2 + i0)((p+k)^2 - m^2 + i0)}. \tag{3.1.4}$$

For large k, the integrand behaves like $\sim \frac{1}{k^4}$, implying that the integral diverges logarithmically. The problem of ultraviolet (UV) divergent integrals in quantum field theories is addressed via the two-step procedure of *regularization* and *renormalization* which we consider in the next two Sections. Theories, in which all divergences arising from the loop diagrams can be consistently canceled order by order by renormalization, are called renormalizable. Both the SM and the MSSM belong to this class of theories [64]. An important theorem which has been proven by Bogolyubov and Parasyuk [155], and independently by Hepp and Zimmermann [156, 157], states that the divergent parts of any loop integral are polynomials in the external momenta after subtracting all possible subdivergences.

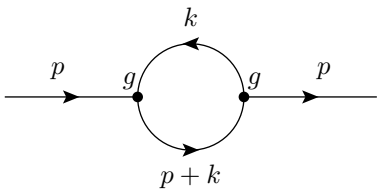

Figure 3.1: Example of the one-loop diagram

[22] We assume that the inner lines of the diagram in Fig. 3.1 describe the propagation of the spin-0 particles.

Note that in models with massless particles, e.g., Quantum Electrodynamics (QED), Quantum Chromodynamics (QCD), divergences of another type might occur. Unlike the UV divergences, they are caused by the behavior of the integrand at small momenta. Therefore, they are called infrared (IR) divergences. In this thesis, we will discuss only UV divergences.

3.1.1 Regularization

As a first step, a divergent integral is regularized by introducing a fictitious regularization parameter in such a way that the integral converges. The most intuitive option is to introduce a cut-off for the integral, i.e., to restrict the domain of integration to $|\vec{k}| < \Lambda$. In this regularization scheme, the divergences will manifest themselves as powers and logarithms of Λ. The cut-off scheme, being conceptually simple, is not Lorentz and gauge invariant, which makes it hard to use in the SM and MSSM calculations.

A more neat modification of the cut-off regularization is the Pauli-Villars (PV) regularization. In this approach, every propagator is replaced by

$$\frac{i}{k^2 - m^2 + i0} \to \frac{i}{k^2 - m^2 + i0} - \frac{i}{k^2 - \Lambda^2 + i0}, \tag{3.1.5}$$

which in turn changes its behavior at large momenta k^2 such that the integral becomes finite. PV regularization works in Abelian gauge theories, but is not very useful in the non-Abelian case [158]. But even in the Abelian case, this method requires many fictitious particles to perform calculations beyond one-loop order and thus becomes quickly impractical.

A widely used regularization scheme (due to its applicability in gauge theories and its simplicity), is a *dimensional regularization* (DREG). It is based on the analytic continuation of the integrals from four-dimensional to D-dimensional Minkowski space [159–162]. For a one-loop integral, DREG is employed as follows

$$\int_{\mathbb{R}^4} \frac{d^4k}{(2\pi)^4} f(k, \{m_i\}) \to \mu_R^{4-D} \int_{\mathbb{R}^D} \frac{d^Dk}{(2\pi)^D} f(k, \{m_i\}) = \Delta a_{-1} + a_0 + a_1\epsilon + \mathcal{O}(\epsilon^2), \tag{3.1.6}$$

where $D = 4 - 2\epsilon$. [23] Δ is a numerical factor which encodes the divergence,

$$\Delta = \frac{1}{\epsilon} - \gamma_E + \log 4\pi, \tag{3.1.7}$$

with $\gamma_E \approx 0.577$ being Euler–Mascheroni constant. In Eq. (3.1.6) the *regularization scale* μ_R is introduced to preserve the overall dimension of the integral. As can be

[23] Note, that sometimes in the literature ϵ is defined as $D = 4 - \epsilon$.

seen from Eq. (3.1.6), the divergence manifests itself as a pole $\sim \frac{1}{\epsilon}$. At higher-orders the expansion in ϵ may start with a different power of Δ, e.g. Δ^2 for the two-loop integral, Δ^3 for the three-loop and so on.

Dimensional regularization cannot be applied directly in supersymmetric theories. Since additional degrees of freedom for vector bosons are introduced in the transition to D dimensions, the number of bosonic degrees of freedom no longer equals to the number of the fermionic ones. Thus, in supersymmetric theories a modified version of DREG – *dimensional reduction* (DRED) – is often used [163, 164]. Contrary to the method of dimensional regularization, only the momenta are treated as D dimensional objects, whereas all the fields and γ-matrices remain four-dimensional. It was shown by means of explicit checks that DRED preserves SUSY up to the three-loop level in the gaugeless limit (see Sec. 3.2.1) and up to the one-loop order if electroweak couplings are taken into account [165–167]. This scheme is applicable to all cases considered in this thesis.

3.1.2 Renormalization

Regularization introduces unphysical regularization parameters into the theory. For example, in case of DREG/DRED these are the regularization scale μ_R and ϵ. By means of renormalization this dependence on unphysical parameters is eliminated, and the connection between the parameters of the theory and physical observables is established. All parameters in the Lagrangian of a theory (also called *bare parameters*) are replaced by a sum of renormalized parameters and *counterterms*. For example, for a mass m and a coupling constant g the renormalization transformations take the following form,

$$\begin{aligned} m_0 &= m + \delta m = m + \delta^{(1)} m + \delta^{(2)} m + \dots, \\ g_0 &= g + \delta g = g + \delta^{(1)} g + \delta^{(2)} g + \dots, \end{aligned} \tag{3.1.8}$$

where the ellipsis denotes higher-order counterterms. The renormalized parameters m and g in Eq. (3.1.8) are finite quantities, while the counterterms $\delta^{(i)} g$ and $\delta^{(i)} m$ contain the dependence on the regularization parameters at the i-th order of perturbation theory. Renormalization of the bare parameters is sufficient to render all S-matrix elements finite. To renormalize Green functions, the renormalization transformation has to be applied also to the fields of the theory. For a field ϕ, this reads

$$\phi_0 = \sqrt{Z_\phi}\, \phi, \text{ with } Z_\phi = 1 + \delta^{(1)} Z_\phi + \delta^{(2)} Z_\phi + \dots. \tag{3.1.9}$$

In this equation the quanity Z_ϕ is a field renormalization constant.

After the renormalization transformation, the Lagrangian can be split into two parts,

$$\mathcal{L}(\phi_0, m_0, g_0) = \mathcal{L}(\phi, m, g) + \mathcal{L}_{\rm CT}(\phi, m, g, \delta Z_\phi, \delta m, \delta g). \tag{3.1.10}$$

The first term on the right-hand side of the Eq. (3.1.10) has the same functional dependence on the fields and the parameters as the original Lagrangian. The second term, $\mathcal{L}_{\rm CT}$, contains the counterterms which are needed to absorb the divergences arising from Feynman integrals. Note that since the counterterms are at least of one-loop order, tree-level diagrams with counterterm insertions are at least of one-loop order; one-loop diagrams with counterterms are at least of two-loop order and etc.

3.1.3 Renormalization schemes

The renormalization constants for the masses and the coupling constants are defined via the physical observables. For instance, one can compute a theory prediction for such an observable $\widehat{O}_1^{\rm th}$ in terms of a coupling constant g, [24]

$$\widehat{O}_1^{\rm th} \equiv \widehat{O}_1^{\rm th}(g, \delta g). \tag{3.1.11}$$

Since in general the loop integrals needed to compute $\widehat{O}_1^{\rm th}$ are UV divergent, the result also depends on the counterterm δg. Since $\widehat{O}_1$ is an observable, it can be related to some measurable quantity, $\widehat{O}_1^{\rm exp}$,

$$\widehat{O}_1^{\rm exp} = \widehat{O}_1^{\rm th}(g, \delta g). \tag{3.1.12}$$

The counterterm can be determined via inverting this equation

$$\delta g = f(\widehat{O}_1^{\rm exp}, g). \tag{3.1.13}$$

Using this relation between the counterterm and the measurable quantity $\widehat{O}_1^{\rm exp}$, we can compute another observable $\widehat{O}_2$,

$$\widehat{O}_2 = \widehat{O}_2(g, \delta g) = \widehat{O}_2(g, f(\widehat{O}_1^{\rm exp}, g)). \tag{3.1.14}$$

The relation between the observables (3.1.14) does not contain divergences and is regulator independent [25] up to a given order of perturbation theory [146, 168].

So far, for the sake of brevity we only considered the determination of the counterterm for a single coupling constant g. In general, to fix n counterterms in a model, n physical observables are needed. The relations between the parameters of the theory

[24] The computation of an observable involves the calculation of the matrix element for some process, and that is why it also depends on some incoming and outgoing momenta $\{p_i\}$, which are omitted for the sake of brevity.

[25] The relation between different observables in the theory is also gauge-independent.

and the observables form a *renormalization scheme*. In the following chapters we will mostly deal with parameters defined either in the on-shell (OS), the $\overline{\text{MS}}$ or the $\overline{\text{DR}}$ schemes. [26]

$\overline{\text{MS}}$/$\overline{\text{DR}}$ scheme

First, we consider the *minimal subtraction* (MS) scheme. In this scheme, all counterterms consist only of a divergent part. I.e., at the n-th loop order they are polynomials in $\frac{1}{\epsilon}$ with the highest possible power equal to n. In this thesis, we will use the modified version of this scheme, i.e., the $\overline{\text{MS}}$ scheme where the constant $-\gamma_E + \log 4\pi$ is subtracted together with the divergent part. In other words, the two schemes are related by the replacement,

$$\frac{1}{\epsilon} \to \Delta \,. \tag{3.1.15}$$

The $\overline{\text{DR}}$ (DR) scheme is defined in the same way as the $\overline{\text{MS}}$ scheme, the only difference being that DRED is used instead of DREG to regularize the divergent integrals. The final result of a calculation in the $\overline{\text{DR}}$ or $\overline{\text{MS}}$ scheme in general still depends on the scale μ_R, which was introduced during the regularization (see Eq. (3.1.6)). Since the relation between different physical observables should not depend on any of the auxiliary parameters at the given order of perturbation theory, the renormalized parameters in the $\overline{\text{MS}}$ or $\overline{\text{DR}}$ scheme have to depend on the scale μ_R. [27] This dependence is given by the so-called β-functions of the couplings and masses, which will be considered in Section 3.1.4.

On-shell (OS) scheme

At tree level the propagator of a particle with mass m has a pole at $p^2 = m^2$ (see Eq. (3.1.2)). At higher orders of perturbation theory the propagator gets contributions from loop diagrams which can be resummed via the so-called "Dyson resummation". For the scalar particle ϕ this reads,

$$\begin{aligned} \Delta_\phi(p^2) &= \frac{i}{p^2 - m^2} + \frac{i}{p^2 - m^2}\, i\widehat{\Sigma}(p^2)\, \frac{i}{p^2 - m^2} + \dots \\ &= \quad + \quad + \quad + \dots = \frac{i}{p^2 - m^2 + \widehat{\Sigma}(p^2)} \quad , \end{aligned} \tag{3.1.16}$$

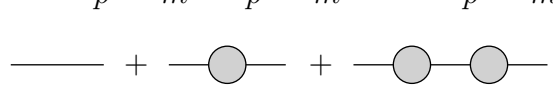

where the line denotes a tree-level propagator, and the grey circle denotes the renormalized self-energy $i\widehat{\Sigma}(p^2)$. The expression for the latter reads at one-loop

[26] In Chapter 7 we will discuss a $\overline{\text{DR}}'$ scheme, and in Chapter 8 we will introduce the (modified) $\overline{\text{MDR}}$ renormalization scheme.

[27] That is why it is also called *renormalization scale*.

order

$$\widehat{\Sigma}(p^2) = \Sigma(p^2) - \delta m^2 + (p^2 - m^2)\delta Z_\phi, \tag{3.1.17}$$

where $\Sigma(p^2)$ is unrenormalized self-energy of the particle. The on-shell condition for the propagator $\Delta_\phi(p^2)$ requires that it has a pole at $p^2 = m^2$ with a residue which is equal to unity. The first condition implies that the mass counterterm is equal to the unrenormalized self-energy, evaluated at $p^2 = m^2$,

$$\widehat{\Sigma}(m^2) \stackrel{!}{=} 0 \Longrightarrow \delta m^2 = \Sigma(m^2). \tag{3.1.18}$$

Expanding the equation (3.1.17) around $p^2 = m^2$,

$$\widehat{\Sigma}(p^2) = (p^2 - m^2)(\delta Z_\phi + \Sigma'(m^2)) + \mathcal{O}((p^2 - m^2)^2), \tag{3.1.19}$$

(where the prime denotes the derivative with respect to the momentum squared), and inserting the result back into the equation (3.1.16) yields

$$\Delta_\phi(p^2) = \frac{i}{(p^2 - m^2)(1 + \delta Z_\phi + \Sigma'(m^2) + \mathcal{O}(p^2 - m^2))}. \tag{3.1.20}$$

The requirement that the residue of $\Delta_\phi(p^2)$ equals unity when $p^2 \to m^2$ leads to the condition for the field renormalization constant,

$$\delta Z_\phi = -\Sigma'(m^2) \iff \widehat{\Sigma}'(m^2) = 0. \tag{3.1.21}$$

If the particle ϕ is unstable, its self-energy, $\widehat{\Sigma}(p^2)$, develops an imaginary part for $p^2 = m^2$, since the particles which run in the loop go on-shell, i.e. their squared momentum becomes equal to their mass squared. In this case, the condition (3.1.18) should be modified to

$$\delta m^2 = \operatorname{Re}\Sigma(m^2) \tag{3.1.22}$$

at one-loop order. Dyson resummation can also be applied to fermion fields. In this case one gets for a fermion field ψ with mass m,

$$\Delta_\psi(p^2) = i\left(\not{p} - m + \widehat{\Sigma}_f(p)\right)^{-1}, \tag{3.1.23}$$

where the renormalized fermion self-energy is related to the unrenormalized one via

$$\widehat{\Sigma}_f(p) = \Sigma_f(p) + (\not{p} - m)\delta Z_\psi - \delta m. \tag{3.1.24}$$

The unrenormalized fermion self-energy, in turn, can be decomposed as,

$$\Sigma_f(p) = \not{p} P_L \Sigma_f^L(p^2) + \not{p} P_R \Sigma_f^R(p^2) + m_f \Sigma_f^S(p^2) + m_f \gamma_5 \Sigma_f^P(p^2). \tag{3.1.25}$$

It can be shown [146] that the OS mass counterterm in this case reads

$$\delta m = \frac{m}{2}\,\mathrm{Re}\left[\Sigma_f^L(m^2) + \Sigma_f^R(m^2) + 2\Sigma_f^S(m^2)\right]. \tag{3.1.26}$$

The renormalized self-energy of the vector field with a tree-level mass M_V in R_ξ gauge with the gauge parameter ξ_V can be written as follows,

$$\begin{aligned}\widehat{\Sigma}^V_{\mu\nu}(p) = &-\left[\left(g_{\mu\nu} - \frac{p_\mu p_\nu}{p^2}\right)\Sigma_T^V(p^2) + \frac{p_\mu p_\nu}{p^2}\Sigma_L^V(p^2)\right] \\ &-\left[\left(g_{\mu\nu} - \frac{p_\mu p_\nu}{p^2}(1-\xi_V)\right)p^2 - g_{\mu\nu}M_V^2\right]\delta Z_V \\ &+\left(g_{\mu\nu}\delta M_V^2 + q_\mu q_\nu \delta Z_V\right),\end{aligned} \tag{3.1.27}$$

where $\Sigma_T^V(p^2)$ and $\Sigma_L^V(p^2)$ are the unrenormalized transversal and longitudinal self-energies, respectively. The OS conditions for the mass and field renormalization constants involve only the transversal part [146],

$$\delta M_V^2 = \mathrm{Re}\ \Sigma_T^V(M_V^2), \quad \delta Z_V = -\Sigma_T^{V\prime}(M_V^2). \tag{3.1.28}$$

For the renormalisation of a vector field V in a gauge theory the gauge-fixing parameter ξ_V can be renormalized as follows,

$$\xi_V \to \xi_V\left(1 + \frac{1}{2}\delta Z_{\xi_V}\right) \tag{3.1.29}$$

The divergent of the counterterm for ξ_V is related to the divergent part of the vector field renormalization constant [169],

$$\delta\xi_V|_{\mathrm{div}} = \delta Z_V|_{\mathrm{div}}\,. \tag{3.1.30}$$

So far, we have discussed the OS scheme for the mass and the field renormalization constants. Similar renormalization prescriptions can be used for a coupling constant. In this case, the counterterm can be fixed via a process that involves the coupling constant. For example, the OS prescription for the electric charge is chosen such that all quantum corrections to the Thompson scattering vanish on-shell and for zero momentum transfer [146]. The usage of the OS scheme completely eliminates the dependence on the regularization scale μ_R.

Conversion between different schemes

Suppose that a parameter p is defined in the renormalization schemes I and II. Then the bare parameter p^0 is a scheme-independent quantity and it can be related to the

renormalized parameters in both schemes according to Eq. (3.1.8),

$$p^0 = p^I + \delta p^I = p^{II} + \delta p^{II}. \tag{3.1.31}$$

From this relation, we can express the parameter in scheme II in terms of the parameter in scheme I,

$$p^{II} = p^I + (\delta p^{II} - \delta p^I). \tag{3.1.32}$$

Note, that the divergent part of the counterterms in both schemes is the same to render the result of the computation finite. Thus the shift of the parameter p between different schemes, $(\delta p^{II} - \delta p^I)$, is a finite quantity.

3.1.4 Renormalization group equation

As we already mentioned, a physical result should not depend on the regularization scale μ_R introduced in Section 3.1.1 to preserve the correct dimension of the loop integrals (see Eq. (3.1.6)). This issue can be seen also from a slightly different angle. The action of a theory in D dimensions is given by an integral of the Lagrangian over the Minkowski space,

$$S = \int d^D x \, \mathcal{L}. \tag{3.1.33}$$

The action is a dimensionless quantity, $[S] = E^0$, therefore the Lagrangian has an energy dimension

$$[\mathcal{L}] = E^D. \tag{3.1.34}$$

This implies that the coupling constants change their dimensionality when going from 4-dimensional to D-dimensional space. For example, the electric charge becomes a dimensional quantity,

$$[e] = E^{\frac{4-D}{2}} = E^{\epsilon}. \tag{3.1.35}$$

Another example is the ϕ^4 theory defined as,

$$\mathcal{L} = \frac{(\partial_\mu \phi)^2}{2} - \frac{m^2 \phi^2}{2} - \frac{\lambda \phi^4}{4!}, \tag{3.1.36}$$

where the quartic coupling has the following energy dimension in D dimensions

$$[\lambda] = E^{4-D} = E^{2\epsilon}. \tag{3.1.37}$$

In a theory with N coupling constants the relation between bare and renormalized coupling constants can be written as,

$$g_{0i} = Z_{g_i} g_i = \mu_R^{2b_i \epsilon} \widetilde{Z}_{g_i} g_i, \quad \text{where} \quad i = 1 \dots N, \tag{3.1.38}$$

where $Z_{g_i} = \dfrac{\delta g_i}{g_i}$ (see Eq. (3.1.8)), and the scaling factor, $\mu_R^{2b_i\epsilon}$, is explicitly pulled out, so that the renormalized coupling g_i remains a dimensionless quantity even in D dimensions (with $D \neq 4$). The constant b_i shows the scaling of the coupling constant g_i in D dimensions. For instance, it equals $1/2$ for the electron charge in QED. The renormalization constants $\widetilde{Z}_{g_i}$, being equal to unity at the tree level, are computed order by order

$$\widetilde{Z}_{g_i} = 1 + \delta\widetilde{Z}_{g_i}^{(1)} + \delta\widetilde{Z}_{g_i}^{(2)} + \dots . \tag{3.1.39}$$

In the $\overline{\text{MS}}/\overline{\text{DR}}$-scheme, the renormalization constants $\widetilde{Z}_{g_i}^{(k)}$, $k = 1, 2, \dots$ are proportional to Δ^k and do not depend explicitly on the renormalization scale. In this case, the dependence of the coupling constant g_i on the renormalization scale can be derived, by making use of the fact that the bare coupling does not depend on the regularization scale,

$$\begin{aligned} \frac{dg_{0i}}{d\log\mu_R^2} &= \left(\frac{\partial}{\partial\log\mu_R^2} + \sum_j \beta_j \frac{\partial}{\partial g_j}\right)\left(\mu_R^{2b_i\epsilon}\widetilde{Z}_{g_i}g_i\right) \\ &= \mu_R^{2b_i\epsilon}\left(b_i\epsilon + \sum_j \beta_j\frac{\partial}{\partial g_i}\right)\left(\widetilde{Z}_{g_j}g_j\right) \overset{!}{=} 0. \end{aligned} \tag{3.1.40}$$

where the *beta-function* of the coupling g_i is defined as,

$$\beta_{g_i} = \frac{dg_i}{d\log\mu_R^2}, \tag{3.1.41}$$

and in the second equality we have used the fact that in the $\overline{\text{MS}}/\overline{\text{DR}}$-schemes $\frac{\partial\widetilde{Z}_{g_i}}{\partial\log\mu_R^2} \equiv 0$. The last equality in (3.1.40) can be rewritten as

$$b_i\epsilon + \sum_j \beta_j \frac{\partial\log(\widetilde{Z}_{g_i}g_i)}{\partial g_j} = 0. \tag{3.1.42}$$

By solving this linear system of equations and then taking the limit $\epsilon \to 0$, one can derive all β-functions order by order.

3.1.4.1 Collins-Wilczek-Zee scheme

Contrary to the electric charge, the strong coupling constant cannot be renormalized on-shell, since at low energies it becomes so large that the QCD becomes non-perturbative. Therefore, it is only possible to determine the running coupling at scales where this coupling is small enough. On the other hand, the β-function for the coupling constant in the $\overline{\text{MS}}/\overline{\text{DR}}$ schemes does not depend on any masses and thus the heavy particles do not decouple in the low-energy regime, as it would be guaranteed

by the Appelquist-Carazzone theorem (also called decoupling theorem) [170].[28] Non-decoupling of heavy particles with mass M leads to the appearance of large logarithms $\sim \log \frac{M^2}{\mu_R^2}$ in the result, if the process is computed at low energies, $\mu_R \ll M$. To avoid this issue, the $\overline{\text{MS}}/\overline{\text{DR}}$ scheme for the running coupling has to be modified in such a way that the heavy particles decouple properly in the low-energy regime. This is achieved in the Collins-Wilczek-Zee scheme [171, 172], which is defined at lowest order as

$$\alpha_s^{\text{CWZ}}(\mu_R) = \alpha_s^{\overline{\text{MS}}/\overline{\text{DR}}}(\mu_R)\left(1 + \frac{\alpha_s(\mu_R)}{4\pi}\log\frac{\mu_R^2}{M^2}\,\beta_0^{\text{H}}\right), \tag{3.1.43}$$

where β_0^{H} is the contribution of the particle with mass $M > \mu_R$ to the β-function of the strong coupling, and the relation between the coefficient β_0 and the lowest order beta-function β reads,

$$\frac{d\alpha_s}{d\log\mu_R^2} = -\frac{\alpha_s^2}{4\pi}\beta_0 \equiv \beta. \tag{3.1.44}$$

For example, in the Standard Model the leading-order beta-function reads [173, 174],

$$\beta = -\frac{\alpha_s^2}{12\pi}(33 - 2n_f), \tag{3.1.45}$$

where n_f is the number of active flavours, i.e the number of quarks which are not heavier than μ_R. From Eqs. (3.1.43) and (3.1.45), one can find the leading-order relation between $\alpha_s^{(n_f+1)}$ and $\alpha_s^{(n_f)}$ in the Standard Model,[29]

$$\alpha_s^{(n_f)}(\mu_R) = \alpha_s^{(n_f+1)}(\mu_R)\left(1 + \frac{\alpha_s^{(n_f+1)}(\mu_R)}{6\pi}\log\frac{\mu_R^2}{m_q^2}\right), \tag{3.1.46}$$

where m_q is the mass of the heavy-flavour quark. Higher-order corrections to this relation up to four-loop order were computed in [175, 176]. In the MSSM similar matching relations are known up to two-loop order [177, 178].

3.2 Renormalization of the MSSM

3.2.1 Higgs sector

In Sec. 2.5.1 we outlined that the Higgs scalar potential before minimization is defined by eight independent parameters, which can be conveniently chosen to be

$$T_h, T_H, T_A, m_A^2 \text{ (or } m_{H^\pm}^2), e, M_W, M_Z, t_\beta, \tag{3.2.1}$$

[28] This theorem is valid only for the momentum subtraction schemes.
[29] Each quark gives a contribution to the leading-order beta-function which reads $\beta_0 = -\frac{2}{3}$.

where in the $\mathcal{CP}$-concerving case either m_A^2 or $m_{H^\pm}^2$ can be chosen as input parameters for the calculation of the Higgs masses. In the $\mathcal{CP}$-violating case[30] the off-diagonal entries of the mass matrix $\mathbf{M}_{\phi\phi\chi\chi}$, which mix different $\mathcal{CP}$-eigenstates and are equal to zero at tree level, acquire corrections at the loop-level. Thus, m_A^2 is not a suitable on-shell parameter anymore. In this case, the mass of the charged Higgs boson, $m_{H^\pm}^2$, is used.

The parameters in Eq. (3.2.1) are renormalized as described in Sec. 3.1.2, [31]

$$\begin{aligned} &M_Z^2 \to M_Z^2 + \delta M_Z^2, \quad M_W^2 \to M_W^2 + \delta M_W^2, \\ &t_\beta \to t_\beta(1+\delta t_\beta), \quad T_i \to T_i + \delta T_i, \ (i = h, H, A), \\ &e \to e + \delta e, \quad m_{H^\pm}^2 \to m_{H^\pm}^2 + \delta m_{H^\pm}^2. \end{aligned} \tag{3.2.2}$$

The entries of the mass matrices in Eq. (2.5.16) are renormalized accordingly,

$$m_{ij}^2 \to m_{ij}^2 + \delta m_{ij}^2, \quad i,j = h, H, A, G, G^\pm, H^\pm. \tag{3.2.3}$$

Although the mixing angles α, β_n, β_c are related to the angle β at tree level, they are not renormalized. After inserting the expressions in Eqs. (3.2.2) into the Eqs. (2.5.17a)–(2.5.17j) and keeping only the one-loop terms, we obtain the following counterterms for the mass matrices,

$$\begin{aligned} \delta^{(1)} m_h^2 = {} & \delta^{(1)} m_A^2 c_{\alpha-\beta}^2 + \delta^{(1)} M_Z^2 s_{\alpha+\beta}^2 \\ & + \frac{e}{2 s_\mathrm{w} M_W} \left(\delta^{(1)} T_H c_{\alpha-\beta} s_{\alpha-\beta}^2 + \delta^{(1)} T_h s_{\alpha-\beta}(1 + c_{\alpha-\beta}^2) \right) \\ & + \delta^{(1)} t_\beta \left(m_A^2 s_{2\alpha-2\beta} + M_Z^2 s_{2\alpha+2\beta} \right) s_\beta c_\beta, \end{aligned} \tag{3.2.4a}$$

$$\begin{aligned} \delta^{(1)} m_{hH}^2 = {} & \frac{1}{2} \left(\delta^{(1)} m_A^2 s_{2\alpha-2\beta} - \delta^{(1)} M_Z^2 s_{2\alpha+2\beta} \right) \\ & + \frac{e}{2 s_\mathrm{w} M_W} \left(\delta^{(1)} T_H s_{\alpha-\beta}^3 - \delta^{(1)} T_h c_{\alpha-\beta}^3 \right) \\ & - \delta^{(1)} t_\beta \left(m_A^2 c_{2\alpha-2\beta} + M_Z^2 c_{2\alpha+2\beta} \right) s_\beta c_\beta, \end{aligned} \tag{3.2.4b}$$

$$\begin{aligned} \delta^{(1)} m_H^2 = {} & \delta^{(1)} m_A^2 s_{\alpha-\beta}^2 + \delta^{(1)} M_Z^2 c_{\alpha+\beta}^2 \\ & - \frac{e}{2 s_\mathrm{w} M_W} \left(\delta^{(1)} T_H c_{\alpha-\beta}(1 + s_{\alpha-\beta}^2) + \delta^{(1)} T_h s_{\alpha-\beta} c_{\alpha-\beta}^2 \right) \\ & - \delta^{(1)} t_\beta \left(m_A^2 s_{2\alpha-2\beta} + M_Z^2 s_{2\alpha+2\beta} \right) s_\beta c_\beta, \end{aligned} \tag{3.2.4c}$$

$$\delta^{(1)} m_{hA}^2 = \delta^{(1)} m_{HG}^2 = \frac{e}{2 s_\mathrm{w} M_W} \delta^{(1)} T_A s_{\alpha-\beta}, \tag{3.2.4d}$$

$$\delta^{(1)} m_{hG}^2 = -\delta^{(1)} m_{HA}^2 = \frac{e}{2 s_\mathrm{w} M_W} \delta^{(1)} T_A c_{\alpha-\beta}, \tag{3.2.4e}$$

[30] Recall, that there is no $\mathcal{CP}$-violation in the Higgs sector at tree level but it may be induced via loop contributions from the other sectors od the MSSM.

[31] Sometimes, a different convention for the δt_β counterterm is used: $t_\beta \to t_\beta + \delta t_\beta$.

$$\delta^{(1)} m_{AG}^2 = -\frac{e}{2 s_{\mathrm{w}} M_W} \left(\delta^{(1)} T_H s_{\alpha-\beta} + \delta^{(1)} T_h c_{\alpha-\beta} \right) - \delta^{(1)} t_\beta m_A^2 s_\beta c_\beta, \tag{3.2.4f}$$

$$\delta^{(1)} m_G^2 = \frac{e}{2 s_{\mathrm{w}} M_W} \left(-\delta^{(1)} T_H c_{\alpha-\beta} + \delta^{(1)} T_h s_{\alpha-\beta} \right), \tag{3.2.4g}$$

$$\delta^{(1)} m_{H^- G^+}^2 = -\frac{e}{2 s_{\mathrm{w}} M_W} (\delta^{(1)} T_H s_{\alpha-\beta} + \delta^{(1)} T_h c_{\alpha-\beta} + i\, \delta^{(1)} T_A) - \delta^{(1)} t_\beta m_{H^\pm}^2 s_\beta c_\beta, \tag{3.2.4h}$$

$$\delta^{(1)} m_{G^- H^+}^2 = (\delta^{(1)} m_{H^- G^+}^2)^*, \tag{3.2.4i}$$

$$\delta^{(1)} m_{G^\pm}^2 = \frac{e}{2 s_{\mathrm{w}} M_W} (-\delta^{(1)} T_H c_{\alpha-\beta} + \delta^{(1)} T_h s_{\alpha-\beta}). \tag{3.2.4j}$$

In the Eqs. (3.2.4a) – (3.2.4c), the counterterm for the $\mathcal{CP}$-odd Higgs boson mass, $\delta^{(1)} m_A^2$, can be expressed in terms of $\delta^{(1)} m_{H^\pm}^2$ and $\delta^{(1)} M_W^2$ by using the tree-level formula in Eq. (2.5.20),

$$\delta^{(1)} m_A^2 = \delta^{(1)} m_{H^\pm}^2 - \delta^{(1)} M_W^2. \tag{3.2.5}$$

Note that at the one-loop level the renormalization of the electric charge is not needed since it always appears as a coefficient of the tadpole-terms, which are zero after the minimization of the Higgs potential. The Higgs fields are renormalized to guarantee the finiteness of the Green functions [32],

$$H_i \to \sqrt{Z_{H_i}} = \left(1 + \frac{1}{2} \delta^{(1)} Z_{H_i} \right) H_i. \tag{3.2.6}$$

Using the relation between the gauge and mass eigenstates, given in the Eqs. (2.5.14), one can find the renormalization constants in the mass basis,

$$\delta^{(1)} Z_{hh} = s_\alpha^2 \delta^{(1)} Z_{H_1} + c_\alpha^2 \delta^{(1)} Z_{H_2}, \tag{3.2.7a}$$

$$\delta^{(1)} Z_{hH} = \delta^{(1)} Z_{Hh} = -s_\alpha c_\alpha \left(\delta^{(1)} Z_{H_1} - \delta^{(1)} Z_{H_2} \right), \tag{3.2.7b}$$

$$\delta^{(1)} Z_{HH} = c_\alpha^2 \delta^{(1)} Z_{H_1} + s_\alpha^2 \delta^{(1)} Z_{H_2}, \tag{3.2.7c}$$

$$\delta^{(1)} Z_{AA} = s_\beta^2 \delta^{(1)} Z_{H_1} + c_\beta^2 \delta^{(1)} Z_{H_2}, \tag{3.2.7d}$$

$$\delta^{(1)} Z_{AG} = \delta^{(1)} Z_{GA} = -s_\beta c_\beta \left(\delta^{(1)} Z_{H_1} - \delta^{(1)} Z_{H_2} \right), \tag{3.2.7e}$$

$$\delta^{(1)} Z_{GG} = \delta^{(1)} Z_{G^\pm G^\pm} = c_\beta^2 \delta^{(1)} Z_{H_1} + s_\beta^2 \delta^{(1)} Z_{H_2}, \tag{3.2.7f}$$

$$\delta^{(1)} Z_{H^\pm H^\pm} = s_\beta^2 \delta^{(1)} Z_{H_1} + c_\beta^2 \delta^{(1)} Z_{H_2}, \tag{3.2.7g}$$

$$\delta^{(1)} Z_{H^- G^+} = \delta^{(1)} Z_{G^- H^+} = -s_\beta c_\beta \left(\delta^{(1)} Z_{H_1} - \delta^{(1)} Z_{H_2} \right). \tag{3.2.7h}$$

As a consequence of $\mathcal{CP}$-conservation at the tree-level and the choice of the renormalization constants for the Higgs doublets (see Eq. (3.2.6)), the field renormalization

[32] This choice is sufficient to render all the Green functions with external Higgs fields finite. Sometimes, it is helpful to also introduce the finite off-diagonal elements $\delta^{(1)} Z_{H_1 H_2}$ and $\delta^{(1)} Z_{H_2 H_1}$. See the discussion in [16, 24].

constants for the transition between $\mathcal{CP}$-even and $\mathcal{CP}$-odd states are equal to zero, [33]

$$\delta^{(1)} Z_{hA} = \delta^{(1)} Z_{hG} = \delta^{(1)} Z_{HA} = \delta^{(1)} Z_{HG} = 0. \tag{3.2.8}$$

The expression for the one-loop renormalized self-energy with external Higgs bosons, evaluated at external momentum p^2, in terms of the previously defined quantities reads,

$$\begin{aligned} \widehat{\Sigma}^{(1)}_{ij}(p^2) = \Sigma^{(1)}_{ij}(p^2) + \left(p^2 - \frac{m_i^2 + m_j^2}{2}\right) \delta^{(1)} Z_{ij} - \delta^{(1)} m^2_{ij}, \\ i,j \in \{h, H, A, G, H^\pm, G^\pm\}. \end{aligned} \tag{3.2.9}$$

where $\Sigma^{(1)}_{ij}(p^2)$ is the unrenormalized self-energy.

The one-loop counterterms for the tadpoles are determined by the requirement that the renormalized one-loop corrected tapoles, $\widehat{T}^{(1)}_i$, are equal to zero,

$$\widehat{T}^{(1)}_i = T^{(1)}_i + \delta^{(1)} T_i \stackrel{!}{=} 0 \Longrightarrow \delta^{(1)} T_i = -T^{(1)}_i, \quad i \in \{h, H, A\}, \tag{3.2.10}$$

where $T^{(1)}_i$ is the unrenormalized tadpole with external Higgs i. These conditions imply that the vacuum expectation values v_1 and v_2 remain unchanged at the one-loop level. The masses of the vector bosons are renormalized in the on-shell scheme,

$$\delta^{(1)} M_Z^2 = \text{Re}\ \Sigma^{T,(1)}_{ZZ}(M_Z^2), \quad \delta^{(1)} M_W^2 = \text{Re}\ \Sigma^{T,(1)}_{WW}(M_W^2), \tag{3.2.11}$$

where $\Sigma^{T,(1)}_{ZZ}$ and $\Sigma^{T,(1)}_{WW}$ are the transversal parts of the unrenormalized one-loop self-energies for the Z- and W-bosons, respectively (see Eq. (3.1.28)). Accordingly, the counterterm for the weak mixing angle reads,

$$\delta^{(1)} s_\text{w} = \frac{c_\text{w}^2}{2 s_\text{w}} \left(\frac{\delta^{(1)} M_Z^2}{M_Z^2} - \frac{\delta^{(1)} M_W^2}{M_W^2} \right). \tag{3.2.12}$$

The charged Higgs boson mass is also renormalized on-shell,[34]

$$\delta^{(1)} m^2_{H^\pm} = \text{Re}\ \Sigma^{(1)}_{H^\pm H^\pm}(m^2_{H^\pm}). \tag{3.2.13}$$

Using Eqs. (3.2.7a) and (3.2.7c), it is possible to relate the field renormalization constants for the physical Higgs bosons and the field renormalization constants for the Higgs doublets,

$$\delta^{(1)} Z_{H_1} = \delta^{(1)} Z_{HH}\Big|_{\alpha=0}, \quad \delta^{(1)} Z_{H_2} = \delta^{(1)} Z_{hh}\Big|_{\alpha=0}. \tag{3.2.14}$$

[33] This statement holds for all orders of perturbation theory.

[34] For the MSSM without $\mathcal{CP}$-violation m_A can be chosen as input parameter, and the counterterm for $m^2_{H^\pm}$ is fixed by the Eq. (3.2.5).

To define the renormalization constant for the ratio of the vacuum expectation values, $\tan\beta$, it is necessary to define the renormalization constants for the vacuum expectation values $v_{1,2}$. Since they appear in the expressions for the Higgs doublets (see Eq. (2.5.6)), they are renormalized in the following way,

$$v_i \to \sqrt{Z_{H_i}}\,(v_i + \delta v_i) = v_i + \delta^{(1)} v_i + \frac{\delta^{(1)} Z_{H_i}}{2} v_i + \ldots, \quad i = 1, 2, \tag{3.2.15}$$

where the ellipsis denotes contributions from higher-order counterterms. By combining the definition of the δt_β counterterm, given in Eq. (3.2.2), and the expression in Eq. (3.2.15), we derive the one-loop counterterm for t_β,

$$\delta^{(1)} t_\beta = \frac{1}{t_\beta}\delta^{(1)}\left(\frac{v_2}{v_1}\right) = \frac{\delta^{(1)} v_2}{v_2} - \frac{\delta^{(1)} v_1}{v_1} + \frac{1}{2}\left(\delta^{(1)} Z_{H_2} - \delta^{(1)} Z_{H_1}\right). \tag{3.2.16}$$

There is no obvious relation of t_β to any physical observable. Therefore, it is convenient to renormalize t_β and the field renormalization constants in the $\overline{\text{DR}}$ scheme. Furthermore, as was shown in [179–181], this scheme choice contrary to the OS definition of the field renormalization constants gives numerically stable and gauge-independent results at the one-loop level. With the additional observation that [182–185],

$$\left.\frac{\delta^{(1)} v_1}{v_1}\right|_{\text{div}} = \left.\frac{\delta^{(1)} v_2}{v_2}\right|_{\text{div}}, \tag{3.2.17}$$

this definition gives

$$\delta^{(1)} t_\beta = \frac{1}{2}\left(\delta^{(1)} Z_{H_2}^{\overline{\text{DR}}} - \delta^{(1)} Z_{H_1}^{\overline{\text{DR}}}\right) \tag{3.2.18}$$

where

$$\delta^{(1)} Z_{H_1}^{\overline{\text{DR}}} = -\left.\Sigma'^{(1)}_{HH}(p^2)\right|_{\alpha=0}^{\text{div}}, \quad \delta^{(1)} Z_{H_2}^{\overline{\text{DR}}} = -\left.\Sigma'^{(1)}_{hh}(p^2)\right|_{\alpha=0}^{\text{div}}, \tag{3.2.19}$$

and the derivatives of unrenormalized self-energies can be evaluated at arbitrary momentum, since the UV-divergent part does not depend on it. This completes the one-loop renormalization of the Higgs sector of the MSSM.

3.2.1.1 Gaugeless limit

Two-loop calculations in the Higgs sector and therefore also the two-loop renormalization of this sector is often performed in the *gaugeless limit*. This limit corresponds to vanishing electroweak gauge couplings while keeping the electroweak mixing angle constant,

$$g \to 0, \quad g' \to 0, \quad s_{\text{w}} = \text{const}. \tag{3.2.20}$$

In this limit the tree-level masses of the Higgs boson read

$$m_h^2 = 0, \quad m_H^2 = m_A^2, \quad m_{H^\pm}^2 = m_A^2. \tag{3.2.21}$$

In the R_ξ gauge the masses of the Goldstone bosons are proportional to the masses of the W- and Z-bosons. Thus, they are equal to zero in the gaugeless limit,

$$m_G^2 = m_{G^\pm}^2 \equiv 0. \tag{3.2.22}$$

Eq. (2.5.22), which defines the mixing angle α, has the following form in the limit $M_Z \to 0$,

$$t_{2\alpha} = t_{2\beta}. \tag{3.2.23}$$

Taking into account that $-\frac{\pi}{2} < \alpha < 0$ and $0 < \beta < \frac{\pi}{2}$, the mixing angle α reads

$$\alpha = \frac{\pi}{2} - \beta \tag{3.2.24}$$

in the gaugeless limit. The explicit expressions for the two-loop counterterms in the gaugeless limit can be found in Section 6.2 of [186]. The renormalization of the Higgs sector at the two-loop level is described in detail in [91, 129, 130, 187]. Two-loop corrections to the Higgs boson masses require the renormalization of the other MSSM sectors. We will describe only those which will be relevant for the next chapters. Moreover, the renormalization of these sectors is performed in the gaugeless limit.

3.2.2 Top/stop sector

In the gaugeless limit the mass matrix of the stop squarks takes the following form (see Eq. (2.5.28) in Section 2.5.2)

$$\mathbf{M}_{\tilde{t},\mathrm{gl}} = \begin{pmatrix} m_{\tilde{t}_L}^2 + m_t^2 & m_t\, X_t^* \\ m_t\, X_t & m_{\tilde{t}_R}^2 + m_t^2 \end{pmatrix}. \tag{3.2.25}$$

We renormalize the parameters appearing in this matrix as follows,[35]

$$\begin{aligned} &m_{\tilde{t}_{L/R}}^2 \to m_{\tilde{t}_{L/R}}^2 + \delta^{(1)} m_{\tilde{t}_{L/R}}^2, \\ &X_t \to X_t + \delta^{(1)} X_t, \\ &m_t \to m_t + \delta^{(1)} m_t. \end{aligned} \tag{3.2.26}$$

[35] See [91, 129, 130, 151] for a detailed discussion of the renormalization scheme presented in this Section.

In this way the stop mass matrix $\mathbf{M}_{\tilde{t}}$ acquires the counterterm [36]

$$\delta^{(1)}\mathbf{M}_{\tilde{t}} = \begin{pmatrix} \delta^{(1)}m^2_{\tilde{t}_L} + \delta^{(1)}m^2_t & X_t^*\,\delta^{(1)}m_t + m_t\,\delta^{(1)}X_t^* \\ X_t\,\delta^{(1)}m_t + m_t\,\delta^{(1)}X_t & \delta^{(1)}m^2_{\tilde{t}_R} + \delta^{(1)}m^2_t \end{pmatrix} . \tag{3.2.27}$$

Using the tree-level transformation matrix $\mathbf{U}_{\tilde{t}}$, which relates gauge and mass eigenstates (see Eq. (2.5.30)), we define

$$\mathbf{U}_{\tilde{t}}\,\delta^{(1)}\mathbf{M}_{\tilde{t}}\,\mathbf{U}^\dagger_{\tilde{t}} = \begin{pmatrix} \delta^{(1)}m^2_{\tilde{t}_1} & \delta^{(1)}m^2_{\tilde{t}_{12}} \\ \delta^{(1)}m^2_{\tilde{t}_{21}} & \delta^{(1)}m^2_{\tilde{t}_2} \end{pmatrix} , \tag{3.2.28}$$

where $\delta^{(1)}m^2_{\tilde{t}_{21}} = (\delta^{(1)}m^2_{\tilde{t}_{12}})^*$. The counterterms for the diagonal elements of this matrix, $m^2_{\tilde{t}_1}$ and $m^2_{\tilde{t}_2}$, can be fixed via the on-shell condition,

$$\delta^{(1)}m^2_{\tilde{t}_1} = \mathrm{Re}\;\Sigma^{(1)}_{\tilde{t}_1\tilde{t}_1}(m^2_{\tilde{t}_1}), \quad \delta^{(1)}m^2_{\tilde{t}_2} = \mathrm{Re}\;\Sigma^{(1)}_{\tilde{t}_2\tilde{t}_2}(m^2_{\tilde{t}_2}). \tag{3.2.29}$$

The counterterm for the off-diagonal entry is fixed via the symmetric on-shell condition,

$$\delta^{(1)}m^2_{\tilde{t}_{12}} = \frac{1}{2}\,\widetilde{\mathrm{Re}}\left[\Sigma^{(1)}_{\tilde{t}_1\tilde{t}_2}(m^2_{\tilde{t}_1}) + \Sigma^{(1)}_{\tilde{t}_1\tilde{t}_2}(m^2_{\tilde{t}_2})\right], \tag{3.2.30}$$

where the symbol $\widetilde{\mathrm{Re}}$ takes the real part of the loop integrals and does not affect the couplings. Rotating back to the gauge-eigenstate basis, the counterterms for the soft-breaking parameters read,

$$\begin{aligned}
\delta^{(1)}X_t &= \frac{1}{m_t}\Big[\mathbf{U}_{\tilde{t}_{11}}\mathbf{U}^*_{\tilde{t}_{12}}\left(\delta^{(1)}m^2_{\tilde{t}_1} - \delta^{(1)}m^2_{\tilde{t}_2}\right) \\
&\quad + \delta^{(1)}m^2_{\tilde{t}_{12}}\mathbf{U}_{\tilde{t}_{21}}\mathbf{U}^*_{\tilde{t}_{12}} + \delta^{(1)}m^2_{\tilde{t}_{21}}\mathbf{U}_{\tilde{t}_{11}}\mathbf{U}^*_{\tilde{t}_{22}} - X_t\delta^{(1)}m_t\Big], && \text{(3.2.31a)}\\
\delta^{(1)}m^2_{\tilde{t}_L} &= \delta^{(1)}m^2_{\tilde{t}_1}|\mathbf{U}_{\tilde{t}_{11}}|^2 + \delta^{(1)}m^2_{\tilde{t}_2}|\mathbf{U}_{\tilde{t}_{12}}|^2 \\
&\quad + \delta^{(1)}m^2_{\tilde{t}_{12}}\mathbf{U}_{\tilde{t}_{21}}\mathbf{U}^*_{\tilde{t}_{11}} + \delta^{(1)}m^2_{\tilde{t}_{21}}\mathbf{U}_{\tilde{t}_{11}}\mathbf{U}^*_{\tilde{t}_{21}} - 2m_t\,\delta^{(1)}m_t, && \text{(3.2.31b)}\\
\delta^{(1)}m^2_{\tilde{t}_R} &= \delta^{(1)}m^2_{\tilde{t}_1}|\mathbf{U}_{\tilde{t}_{12}}|^2 + \delta^{(1)}m^2_{\tilde{t}_2}|\mathbf{U}_{\tilde{t}_{22}}|^2 \\
&\quad + \delta^{(1)}m^2_{\tilde{t}_{12}}\mathbf{U}_{\tilde{t}_{22}}\mathbf{U}^*_{\tilde{t}_{12}} + \delta^{(1)}m^2_{\tilde{t}_{21}}\mathbf{U}_{\tilde{t}_{12}}\mathbf{U}^*_{\tilde{t}_{22}} - 2m_t\,\delta^{(1)}m_t\,. && \text{(3.2.31c)}
\end{aligned}$$

Before discussing the renormalization of the top-quark mass, let us make a remark on the renormalization of the off-diagonal entries of the matrix $\mathbf{M}_{\tilde{t}}$. We have used X_t as a free parameter, while the entries of the transformation matrix $\mathbf{U}_{\tilde{t}}$ were set to their tree-level values. Sometimes, a slightly different, although completely equivalent approach is used [150]. Namely, instead of renormalizing the X_t parameter the angle

[36] From now on, the subscript "gl" will be omitted for brevity.

$\theta_{\tilde{t}}$ and the phase ϕ_{X_t} of the rotation matrix $\mathbf{U}_{\tilde{t}}$ are renormalized,

$$\theta_{\tilde{t}} \to \theta_{\tilde{t}} + \delta^{(1)}\theta_{\tilde{t}}, \quad \phi_{X_t} \to \phi_{X_t} + \delta^{(1)}\phi_{X_t}. \tag{3.2.32}$$

At the first step, the original mass matrix is expressed in terms of θ_t and ϕ_{X_t} as,

$$\mathbf{M}_{\tilde{t}} = \begin{pmatrix} \cos^2\theta_{\tilde{t}}\, m^2_{\tilde{t}_1} + \sin^2\theta_{\tilde{t}}\, m^2_{\tilde{t}_2} & (m^2_{\tilde{t}_1} - m^2_{\tilde{t}_2}) \sin\theta_{\tilde{t}}\, \cos\theta_{\tilde{t}}\, e^{-i\phi_{X_t}} \\ (m^2_{\tilde{t}_1} - m^2_{\tilde{t}_2}) \sin\theta_{\tilde{t}}\, \cos\theta_{\tilde{t}}\, e^{i\phi_{X_t}} & \cos^2\theta_{\tilde{t}}\, m^2_{\tilde{t}_2} + \sin^2\theta_{\tilde{t}}\, m^2_{\tilde{t}_1} \end{pmatrix}. \tag{3.2.33}$$

Using the definition of the counterterms, given in Eq.(3.2.32), the counterterms for the entries of the original mass matrix can then be written as,

$$\delta^{(1)}\mathbf{M}_{\tilde{t}_{11}} = \cos^2\theta_{\tilde{t}}\, \delta^{(1)}m^2_{\tilde{t}_1} + \sin^2\theta_{\tilde{t}}\, \delta^{(1)}m^2_{\tilde{t}_2} + (m^2_{\tilde{t}_2} - m^2_{\tilde{t}_1}) \sin 2\theta_{\tilde{t}}\, \delta^{(1)}\theta_{\tilde{t}}, \tag{3.2.34a}$$

$$\begin{aligned}\delta^{(1)}\mathbf{M}_{\tilde{t}_{12}} &= (\delta^{(1)}m^2_{\tilde{t}_1} - \delta^{(1)}m^2_{\tilde{t}_2}) \sin\theta_{\tilde{t}} \cos\theta_{\tilde{t}}\, e^{-i\phi_{X_t}} \\ &\quad + (m^2_{\tilde{t}_1} - m^2_{\tilde{t}_2})(\delta^{(1)}\theta_{\tilde{t}}\, \cos 2\theta_{\tilde{t}} - i\delta^{(1)}\phi_{X_t} \sin\theta_{\tilde{t}}\, \cos\theta_{\tilde{t}})\, e^{-i\phi_{X_t}},\end{aligned} \tag{3.2.34b}$$

$$\begin{aligned}\delta^{(1)}\mathbf{M}_{\tilde{t}_{21}} &= (\delta^{(1)}m^2_{\tilde{t}_1} - \delta^{(1)}m^2_{\tilde{t}_2}) \sin\theta_{\tilde{t}} \cos\theta_{\tilde{t}}\, e^{i\phi_{X_t}} \\ &\quad + (m^2_{\tilde{t}_1} - m^2_{\tilde{t}_{22}})(\delta^{(1)}\theta_{\tilde{t}}\, \cos 2\theta_{\tilde{t}} + i\delta^{(1)}\phi_{X_t} \sin\theta_{\tilde{t}}\, \cos\theta_{\tilde{t}})\, e^{i\phi_{X_t}},\end{aligned} \tag{3.2.34c}$$

$$\delta^{(1)}\mathbf{M}_{\tilde{t}_{22}} = \cos^2\theta_{\tilde{t}}\, \delta^{(1)}m^2_{\tilde{t}_2} + \sin^2\theta_{\tilde{t}}\, \delta^{(1)}m^2_{\tilde{t}_1} + (m^2_{\tilde{t}_1} - m^2_{\tilde{t}_2}) \sin 2\theta_{\tilde{t}}\, \delta^{(1)}\theta_{\tilde{t}}\,. \tag{3.2.34d}$$

By transforming the counterterm matrix, $\delta^{(1)}\mathbf{M}_{\tilde{t}}$, to the mass eigenstates basis, we arrive at the following expression,

$$\delta^{(1)}m^2_{\tilde{t}_{12}} = e^{-i\phi_{X_t}}(m^2_{\tilde{t}_1} - m^2_{\tilde{t}_2})(\delta^{(1)}\theta_{\tilde{t}} - i\delta^{(1)}\phi_{X_t} \sin\theta_{\tilde{t}}\, \cos\theta_{\tilde{t}}). \tag{3.2.35}$$

This relation between $\delta^{(1)}m^2_{\tilde{t}_{12}}$ and $\delta^{(1)}\theta_{\tilde{t}}$ as well as $\delta^{(1)}\phi_{X_t}$, together with Eq. (3.2.30), yields the generalization of the condition

$$\delta^{(1)}\theta_{\tilde{t}} = \frac{\mathrm{Re}\,\Sigma^{(1)}_{\tilde{t}_1\tilde{t}_2}(m^2_{\tilde{t}_1}) + \mathrm{Re}\,\Sigma^{(1)}_{\tilde{t}_1\tilde{t}_2}(m^2_{\tilde{t}_2})}{2(m^2_{\tilde{t}_1} - m^2_{\tilde{t}_2})}, \tag{3.2.36}$$

which is valid for MSSM scenarios without $\mathcal{CP}$-violation in the stop sector [34, 147, 148, 188, 189]. If the stop sector exhibits $\mathcal{CP}$-violation it is instead more convenient to use the expressions in Eqs. (3.2.31a)–(3.2.31c). We will adopt the prescription of Eqs. (3.2.31a)–(3.2.31c) throughout this thesis.

The top-quark mass can be renormalized in the on-shell scheme,

$$\delta^{(1)}m_t = \frac{m_t}{2}\, \mathrm{Re}\left[\Sigma^{(1),L}_t(m^2_t) + \Sigma^{(1),R}_t(m^2_t) + 2\,\Sigma^{(1),S}_t(m^2_t)\right], \tag{3.2.37}$$

where Σ^L_t, Σ^R_t and Σ^S_t are the coefficients in the Lorentz decomposition of the top-quark self-energy (see Eq. (3.1.25)). In the context of the Higgs mass calculation, it

is sometimes more preferable to use the running $\overline{\text{MS}}$ mass, defined in the Standard Model, $\overline{m}_t \equiv m_t^{\overline{\text{MS}},\text{SM}}(m_t^{\text{OS}})$. This mass is related to the on-shell one via the following relation,

$$\overline{m}_t = m_t^{\text{OS}}(1 + \delta^{\text{SM}}). \tag{3.2.38}$$

The explicit one-loop formulas for δ^{SM} can be found in [190]. This parametrization allows to take into account leading QCD corrections to the Higgs potential beyond the two-loop order, as shown in [187,191]. Furthermore, this choice is more convenient for the resummation of the logarithmic contributions to the Higgs mass, which will be considered in the next Chapter.

In the forthcoming parts of this thesis, we will sometimes use the $\overline{\text{DR}}$ scheme for the soft-breaking parameters of the stop sector. In this case, only the UV-divergent part has to be kept in Eqs. (3.2.31a)–(3.2.31c).

3.2.3 Bottom/sbottom sector

The renormalization of the sector containing a bottom quark and two sbottoms is more involved as the stop sector due to the following reason. As we already pointed out at the end of Section 2.5.1, the quantum corrections to any observable, which are proportional to the MSSM bottom Yukawa coupling, are only significant in the parameter region where $\tan\beta$ is large. It may also happen that in this region of parameter space, the mentioned corrections are not just large but the dominant corrections to an observable. In this regard, special attention has to be paid to the choice of the renormalization scheme, since an inappropriate scheme choice may lead to artificially enhanced contributions and eventually the breakdown of the perturbative series. Comparisons of different renormalization schemes for the bottom/sbottom sector were performed in Refs. [148,149,189,192–195]. For instance, it was found out that the renormalization of the bottom/sbottom sector in complete analogy to the top/stop sector yields numerically unstable results. In this Section, we will describe two schemes which we were considered to be well-behaved in the Refs. [189,195] and which will be later used in the thesis.

3.2.3.1 Renormalization Scheme 1 (RS1)

The first scheme was originally used in [148,149] in the context of the two-loop corrections to the lightest Higgs mass.[37] These corrections were derived in the MSSM

[37] An analogous scheme but for arbitrary values of $\tan\beta$ is referred to as "A_b^{OS}, θ_b^{OS}" in Ref. [189] and **RS6** in Ref. [195].

without $\mathcal{CP}$-violation (rMSSM) and in the limit $\tan\beta \to \infty$, or equivalently,

$$v_1 \to 0, \quad v_2 \to v. \tag{3.2.39}$$

Both sbottom masses are fixed on-shell,

$$\delta m_{\tilde{b}_i} = \text{Re}\ \Sigma_{\tilde{b}_i\tilde{b}_i}(m^2_{\tilde{b}_i}), \quad i = 1, 2. \tag{3.2.40}$$

The trilinear soft-breaking parameter A_b is fixed via the $(\tilde{b}_1^*\tilde{b}_2 A)$ vertex function $\Lambda_{12A}(p_1^2, p_2^2, p_A^2)$. At the tree level and in the limit $t_\beta \to \infty$ (i.e. $s_\beta \to 1$) this vertex has the following form in the Lagrangian,

$$\mathcal{L} \supset \frac{i}{\sqrt{2}}\, \tilde{A}_b\, (\tilde{b}_1^*\tilde{b}_2 A) + \text{h.c.}, \quad \text{where} \quad \tilde{A}_b = h_b A_b. \tag{3.2.41}$$

The renormalization condition is given by

$$\hat{\Lambda}^{(1)}_{12A}(m^2_{\tilde{b}_1}, m^2_{\tilde{b}_1}, 0) + \hat{\Lambda}^{(1)}_{12A}(m^2_{\tilde{b}_2}, m^2_{\tilde{b}_2}, 0) \stackrel{!}{=} 0, \tag{3.2.42}$$

where the renormalized one-loop three-point function $\hat{\Lambda}^{(1)}_{12A}(p_1^2, p_2^2, p_A^2)$ can be expressed in terms of the unrenormalized one in the following way,

$$\begin{aligned}\hat{\Lambda}^{(1)}_{12A}(p_1^2, p_2^2, p_A^2) = \Lambda^{(1)}_{12A}(p_1^2, p_2^2, p_A^2) + \frac{i}{\sqrt{2}}\, \delta^{(1)}\tilde{A}_b + \\ + i\, \frac{\tilde{A}_b}{2} \left(\delta^{(1)} Z_{\tilde{b}_{11}} + \delta^{(1)} Z_{\tilde{b}_{22}} + \delta^{(1)} Z_{AA}\right),\end{aligned} \tag{3.2.43}$$

where $\delta^{(1)} Z_{\tilde{b}_{11}}$, $\delta^{(1)} Z_{\tilde{b}_{22}}$ and $\delta^{(1)} Z_{AA}$ are the field renormalization constants for the sbottoms $\tilde{b}_{1,2}$ and the $\mathcal{CP}$-odd Higgs boson, respectively. The renormalization constant for $\tilde{A}_b$ is derived from Eqs. (3.2.42) and (3.2.43),

$$\begin{aligned}\delta^{(1)}\tilde{A}_b = -\frac{i}{\sqrt{2}} \left(\Lambda^{(1)}_{12A}(m^2_{\tilde{b}_1}, m^2_{\tilde{b}_1}, 0) + \Lambda^{(1)}_{12A}(m^2_{\tilde{b}_2}, m^2_{\tilde{b}_2}, 0)\right) \\ - \frac{\tilde{A}_b}{2} \left(\delta^{(1)} Z_{\tilde{b}_{11}} + \delta^{(1)} Z_{\tilde{b}_{22}} + \delta^{(1)} Z_{AA}\right).\end{aligned} \tag{3.2.44}$$

The field renormalization constants of the sbottoms are chosen in the following way to ensure the infrared finiteness of the three-point function (see the discussion in Section 3 of [149]),

$$\delta^{(1)} Z_{\tilde{b}_{ii}} = -\frac{\text{Re}\ \Sigma^{(1)}_{ii}(m^2_{\tilde{b}_1}) - \text{Re}\ \Sigma^{(1)}_{ii}(m^2_{\tilde{b}_2})}{m^2_{\tilde{b}_1} - m^2_{\tilde{b}_2}}, \quad i = 1, 2. \tag{3.2.45}$$

In the same way, the counterterm $\delta^{(1)} Z_{AA}$ reads [38]

$$\delta^{(1)} Z_{AA} = -\frac{\text{Re}\,\Sigma^{(1)}_{AA}(m^2_{\tilde{b}_1}) - \text{Re}\,\Sigma^{(1)}_{AA}(m^2_{\tilde{b}_2})}{m^2_{\tilde{b}_1} - m^2_{\tilde{b}_2}}. \tag{3.2.46}$$

For the mixing angle of the sbottoms, θ_b, the condition, analogous to the condition in Eq. (3.2.36), is used,

$$\delta^{(1)}\theta_{\tilde{b}} = \frac{\text{Re}\,\Sigma^{(1)}_{\tilde{b}_1\tilde{b}_2}(m^2_{\tilde{b}_1}) + \text{Re}\,\Sigma^{(1)}_{\tilde{b}_1\tilde{b}_2}(m^2_{\tilde{b}_2})}{2(m^2_{\tilde{b}_1} - m^2_{\tilde{b}_2})}. \tag{3.2.47}$$

By using this condition and the relation in Eq. (2.5.34), derived at the end of Section 2.5.2, the counterterm for the bottom quark mass can be derived. In the limit $t_\beta \to \infty$ the relation in Eq. (2.5.34) takes the form

$$s_{2\theta_b} = \frac{2 m_b\, \mu\, t_\beta}{m^2_{\tilde{b}_2} - m^2_{\tilde{b}_1}}. \tag{3.2.48}$$

Therefore the counterterm for the bottom mass in this scheme has the following form,

$$\delta^{(1)} m_b = m_b \left(\frac{\delta^{(1)} m^2_{\tilde{b}_2} - \delta^{(1)} m^2_{\tilde{b}_1}}{m^2_{\tilde{b}_2} - m^2_{\tilde{b}_1}} + \frac{\delta^{(1)} s_{2\theta_b}}{s_{2\theta_b}} - \frac{\delta^{(1)}\mu}{\mu} - \delta^{(1)} t_\beta \right), \tag{3.2.49}$$

where $\delta^{(1)}\mu$ is the counterterm for the Higgsino mass parameter μ, which will be derived in Section 3.2.5. The actual bottom quark mass, which is used in the calculation is given by the formula

$$\widehat{m}_b = m_b^{\overline{\text{DR}},\text{MSSM}}(Q) \left(1 + \frac{\delta^{(1)} m^2_{\tilde{b}_2} - \delta^{(1)} m^2_{\tilde{b}_1}}{m^2_{\tilde{b}_2} - m^2_{\tilde{b}_1}} + \frac{\delta^{(1)} s_{2\theta_b}}{s_{2\theta_b}} - \frac{\delta^{(1)}\mu}{\mu} - \delta^{(1)} t_\beta \right) \Bigg|_{\text{fin}}. \tag{3.2.50}$$

Note that this quantity is scale independent at the one-loop level if the Higgsino mass parameter μ is renormalized in the $\overline{\text{DR}}$ scheme which will be assumed throughout this thesis. Due to the $SU(2)_L$ symmetry, the bilinear soft-breaking parameters $m_{\tilde{b}_L}$ and $m_{\tilde{t}_L}$ are equal at the tree level. This relation is broken at the one-loop level. Indeed, the counterterms for $m_{\tilde{t}_L}$ and $m_{\tilde{b}_L}$ read

$$\begin{aligned} \delta^{(1)} m^2_{\tilde{t}_L} &= \cos^2\theta_{\tilde{t}}\, \delta^{(1)} m^2_{\tilde{t}_1} + \sin^2\theta_{\tilde{t}}\, \delta^{(1)} m^2_{\tilde{t}_2} \\ &\quad + (m^2_{\tilde{t}_2} - m^2_{\tilde{t}_1}) \sin 2\theta_{\tilde{t}}\, \delta^{(1)}\theta_{\tilde{t}} - 2\, m_t\, \delta^{(1)} m_t, \qquad (3.2.51a) \\ \delta^{(1)} m^2_{\tilde{b}_L} &= \cos^2\theta_{\tilde{b}}\, \delta^{(1)} m^2_{\tilde{b}_1} + \sin^2\theta_{\tilde{b}}\, \delta^{(1)} m^2_{\tilde{b}_2} \\ &\quad + (m^2_{\tilde{b}_2} - m^2_{\tilde{b}_1}) \sin 2\theta_{\tilde{b}}\, \delta^{(1)}\theta_{\tilde{b}} - 2\, m_b\, \delta^{(1)} m_b, \qquad (3.2.51b) \end{aligned}$$

[38] While the definition of the field renormalization constant given in Eq. (3.2.45) is crucial for sbottoms to cancel the IR singularities associated with gluon radiation, it is not needed for the $\mathcal{CP}$-odd Higgs boson [196]. Instead also the definition in Eq. (3.2.7d) could be used.

which in general are not equal to each other. In the following, we will assume that $m^2_{\tilde{t}_L}$ is given as an input parameter. Then the renormalized soft sbottom mass $m^2_{\tilde{b}_L}$ is given by

$$m^2_{\tilde{b}_L} = m^2_{\tilde{t}_L} + \delta^{(1)} m^2_{\tilde{t}_L} - \delta^{(1)} m^2_{\tilde{b}_L}. \tag{3.2.52}$$

3.2.3.2 Renormalization Scheme 2 (RS2)

Another renormalization scheme, which will be described in this Section, was used in Refs. [9, 11, 189] (see also [195, 197]). [39] As in the mentioned references, we will consider the most general case of the MSSM with $\mathcal{CP}$ violation. Contrary to the **RS1** scheme, in this scheme the soft breaking masses $m_{\tilde{b}_L}$ and $m_{\tilde{t}_L}$ are equal at the one-loop level. This implies

$$\delta^{(1)} m^2_{\tilde{b}_L} = \delta^{(1)} m^2_{\tilde{t}_L}. \tag{3.2.53}$$

The consequence of this relation is that only one of the sbottom masses can be set on-shell. As a matter of convention, the mass of the second sbottom is defined in the on-shell scheme,

$$\delta^{(1)} m^2_{\tilde{b}_2} = \text{Re}\ \Sigma_{\tilde{b}_2\tilde{b}_2}(m^2_{\tilde{b}_2}). \tag{3.2.54}$$

The mass of the bottom quark is treated as an independent parameter and is renormalized in the $\overline{\text{DR}}$ scheme,

$$\delta^{(1)} m_b = \frac{m_b}{2}\ \text{Re}\left[\Sigma^{(1),L}_b(m^2_b) + \Sigma^{(1),R}_t(m^2_b) + 2\ \Sigma^{(1),S}_t(m^2_b)\right]\Big|_{\text{div}}. \tag{3.2.55}$$

The trilinear soft-breaking parameter A_b is also defined in the $\overline{\text{DR}}$ scheme. Using the relation, analogous to the one in the Eq. (3.2.31a), $\delta^{(1)} A_b$ can be related to the counterterms of the sbottom mass matrix after rotating back to the gauge eigenstate basis,

$$\begin{aligned}
\delta^{(1)} A_b^{\overline{\text{DR}}} = \frac{1}{m_b}\Big[&\left(\delta^{(1)} m^{2,\,\overline{\text{DR}}}_{\tilde{b}_1} - \delta^{(1)} m^{2,\,\overline{\text{DR}}}_{\tilde{b}_2}\right) \mathbf{U}_{\tilde{b}_{11}} \mathbf{U}^*_{\tilde{b}_{12}} \\
&+ \delta^{(1)} m^{2,\,\overline{\text{DR}}}_{\tilde{b}_{12}}\ \mathbf{U}_{\tilde{b}_{21}} \mathbf{U}^*_{\tilde{b}_{12}} + \delta^{(1)} m^{2,\,\overline{\text{DR}}}_{\tilde{b}_{21}}\ \mathbf{U}_{\tilde{b}_{11}} \mathbf{U}^*_{\tilde{b}_{22}}\Big] \\
&- (A_b - \mu^*\ t_\beta)\ \frac{\delta^{(1)} m_b^{\overline{\text{DR}}}}{m_b} + t_\beta\ \delta^{(1)} \mu^{*,\,\overline{\text{DR}}} + \mu^*\ t_\beta\ \delta^{(1)} t_\beta^{\overline{\text{DR}}},
\end{aligned} \tag{3.2.56}$$

where $\delta^{(1)} t_\beta^{\overline{\text{DR}}}$ is defined by Eq.(3.2.18) and the counterterm for the Higgsino mass parameter, $\delta^{(1)} \mu^{*,\,\overline{\text{DR}}}$, will be defined in Section 3.2.5. The renormalization constants in the expression above, $\delta^{(1)} m^{2,\,\overline{\text{DR}}}_{\tilde{b}_1}$, $\delta^{(1)} m^{2,\,\overline{\text{DR}}}_{\tilde{b}_2}$ and $\delta^{(1)} m^{2,\,\overline{\text{DR}}}_{\tilde{b}_{12}}$, are also fixed in the $\overline{\text{DR}}$

[39] This scheme is referred to as "$A_b^{\overline{\text{DR}}}$, $\theta_b^{\overline{\text{DR}}}$" in Ref. [189] and **RS2** in Ref. [195].

scheme,

$$\begin{aligned}
\delta^{(1)} m^{2,\,\overline{\rm DR}}_{\tilde{b}_1} &= \Sigma^{(1)}_{\tilde{b}_1\tilde{b}_1}(m^2_{\tilde{b}_1})\Big|_{\rm div}\,, \quad \delta^{(1)} m^{2,\,\overline{\rm DR}}_{\tilde{b}_2} = \Sigma^{(1)}_{\tilde{b}_2\tilde{b}_2}(m^2_{\tilde{b}_2})\Big|_{\rm div}\,, \\
\delta^{(1)} m^{2,\,\overline{\rm DR}}_{\tilde{b}_{12}} &= \frac{1}{2}\left(\Sigma^{(1)}_{\tilde{b}_1\tilde{b}_2}(m^2_{\tilde{b}_1})\Big|_{\rm div} + \Sigma^{(1)}_{\tilde{b}_1\tilde{b}_2}(m^2_{\tilde{b}_2})\Big|_{\rm div}\right).
\end{aligned} \tag{3.2.57}$$

Eqs. (3.2.53)–(3.2.57) fix the renormalization conditions for all parameters of the sector.

3.2.4 Bottom quark mass in the MSSM

Both schemes, which we discussed in the previous Section, require the calculation of the bottom quark mass in the $\overline{\rm DR}$ scheme in the full MSSM at some renormalization scale Q. Fits of experimental data, however, extract the running mass defined in the SM at the scale m_b [4],

$$m_b^{\overline{\rm MS},\rm SM}(m_b) = 4.18^{+0.04}_{-0.03}\ \text{GeV}. \tag{3.2.58}$$

The relation between $m_b^{\overline{\rm DR},\rm MSSM}$ and $m_b^{\overline{\rm MS},\rm SM}$ can be obtained in the following manner [189]. The on-shell mass of the bottom quark is related at the one-loop level to the running mass in the SM via the following relation (see Eq. (3.1.32)),

$$m_b^{\rm OS} = m_b^{\overline{\rm DR},\rm SM}(Q) - (\delta^{(1)} m_b^{\rm OS})^{\rm SM}\Big|_{\rm fin}\,, \tag{3.2.59}$$

where the superscript "OS, SM" means that only diagrams containing only SM particles contribute to the expression of the counterterm. Similarly, the on-shell bottom mass and the running mass in the full MSSM are related via

$$m_b^{\rm OS} = m_b^{\overline{\rm DR},\rm MSSM}(Q) - (\delta^{(1)} m_b^{\rm OS})^{\rm MSSM}\Big|_{\rm fin}\,. \tag{3.2.60}$$

After equating the Eqs. (3.2.59) and (3.2.60), we obtain the one-loop relation between $m_b^{\overline{\rm DR},\rm SM}(Q)$ and $m_b^{\overline{\rm DR},\rm MSSM}(Q)$,

$$\begin{aligned}
m_b^{\overline{\rm DR},\rm MSSM}(Q) &= m_b^{\overline{\rm DR},\rm SM}(Q) + (\delta^{(1)} m_b^{\rm OS})^{\rm MSSM}\Big|_{\rm fin} - (\delta^{(1)} m_b^{\rm OS})^{\rm SM}\Big|_{\rm fin} = \\
&= m_b^{\overline{\rm DR},\rm SM}(Q) + (\delta^{(1)} m_b^{\rm OS})^{\rm n/SM},
\end{aligned} \tag{3.2.61}$$

where the superscript "n/SM" means that only diagrams containing at least one non-SM particle contribute to the quantity. In addition to this, the one-loop relation between the bottom masses defined in the $\overline{\rm DR}$ and the $\overline{\rm MS}$ schemes has to be taken

into account [198, 199]

$$m_b^{\overline{\rm DR}}(Q) = m_b^{\overline{\rm MS}}(Q)\left(1 - \frac{\alpha_s(Q)}{3\pi}\right). \tag{3.2.62}$$

As was pointed out in Ref. [139], the difference between the SM bottom mass and the bottom mass in the full MSSM, $(\delta^{(1)} m_b^{\rm OS})^{\rm n/SM}$, grows linearly with $\tan\beta$ and for sufficiently high values of $\tan\beta$ can reach values of $\mathcal{O}(m_b)$. Moreover, it does not vanish in the limit when all superpartners of the SM particles have masses much heavier than the electroweak scale. These $\tan\beta$-enhanced terms in $(\delta^{(1)} m_b^{\rm OS})^{\rm n/SM}$ are usually denoted as Δ_b, [40]

$$(\delta^{(1)} m_b^{\rm OS})^{\rm n/SM} = m_b\ \Delta_b + m_b\ \epsilon_b. \tag{3.2.63}$$

The occurence of these large corrections leads to the necessity of computing the relation between $m_b^{\overline{\rm DR},\rm MSSM}(Q)$ and $m_b^{\overline{\rm DR},\rm SM}(Q)$ beyond the one-loop order. As was proven in [139, 200], all higher-order corrections to $(\delta^{(1)} m_b^{\rm OS})^{\rm n/SM}$ obey the following property: at n-th order of perturbation theory the leading t_β-enhanced contribution to $(\delta m_b^{\rm OS})^{\rm n/SM}$ is proportional to the one-loop result, namely,

$$(\delta^{(n)} m_b^{\rm OS})^{\rm n/SM} = m_b\ \Delta_b^n + \ldots, \tag{3.2.64}$$

where the ellipsis denotes the terms which either contain $\tan\beta$ to a power less than n or which are additionally suppressed by powers of $m_b/M_{\rm SUSY}$ (where $M_{\rm SUSY}$ denotes the mass scale of the non-SM particles), or both. This property makes it possible to sum the leading contributions to $(\delta m_b^{\rm OS})^{\rm n/SM}$ at all orders of perturbation theory and leads to the result,

$$m_b^{\overline{\rm DR},\rm MSSM}(Q) = m_b^{\overline{\rm MS},\rm SM}(Q)(1+\epsilon_b)\sum_{n=0}^{\infty}\Delta_b^n = m_b^{\overline{\rm MS},\rm SM}(Q)\frac{1+\epsilon_b}{1-\Delta_b}, \tag{3.2.65}$$

where the transition between $\overline{\rm DR}$ and $\overline{\rm MS}$ schemes (Eq. (3.2.62)) was included in ϵ_b. [41] The "scalar" part of the bottom mass counterterm, $\Sigma_b^S(m_b^2)$, (see Eq. (3.1.26)) contains pieces which are $\tan\beta$-enhanced compared to $\Sigma_b^L(m_b^2)$ and $\Sigma_b^R(m_b^2)$. Therefore the quantity Δ_b can be expressed by

$$\Delta_b = \Sigma_b^{\rm n/SM,S}(m_b)\Big|_{t_\beta\to\infty}. \tag{3.2.66}$$

[40] It should be noted that in the calculation of low-energy observables, (i.e. the decay $h \to \bar{b}b$), Δ_b drops out if all non-SM particles are much heavier than the EW scale as expected from the decoupling theorem.

[41] In principle, there are also terms in $(\delta m_b^{\rm OS})^{\rm n/SM}$ which are proportional to $m_b^2\tan^2\beta$ coming from the diagrams with the virtual charged Higgs boson $H^\pm$ and the top-quark. They are, however, numerically irrelevant and thus included into ϵ_b.

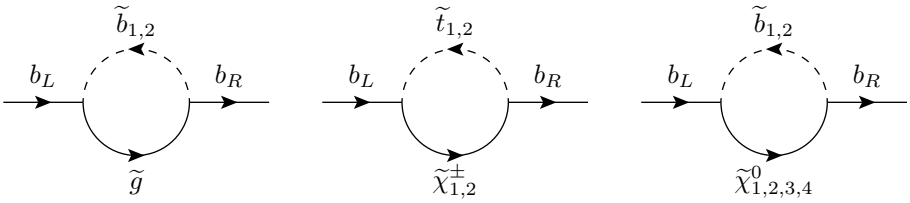

Figure 3.2: Diagrams contributing to Δ_b at the leading order

It gets contributions from the diagrams depicted in Fig. 3.2. The left diagram yields contributions proportional to α_s, while the second and third diagrams yield terms of $\mathcal{O}(\alpha, \alpha_t)$. It can be shown [200] that the divergent part of $\Sigma_b^{\mathrm{n/SM},S}(m_b)$ cancels in the limit $t_\beta \to \infty$. The explicit expressions for Δ_b were originally computed in [139, 191, 200, 201] and can be found (together with expressions for ϵ_b) in App. A in the limit where all non-SM particles are heavier than m_t. The leading two-loop QCD contributions to Δ_b have been computed in Refs. [29–31]. Inclusion of these corrections allows one to resum contributions of $\mathcal{O}(\alpha_s^n \tan^{n-1}\beta)$ and $\mathcal{O}(\alpha_s \alpha_t^{n-1} \tan^{n-1}\beta)$ in the relation between $m_b^{\overline{\mathrm{DR}},\mathrm{MSSM}}$ and $m_b^{\overline{\mathrm{MS}},\mathrm{SM}}$ at all orders of perturbation theory (see Chapters 5 and 6 for details).

3.2.5 Electroweakino sector

In the gaugeless limit the mass matrices of charginos and neutralinos have the following form,

$$\mathbf{Y}_{\mathrm{gl}} = \begin{pmatrix} M_1 & 0 & 0 & 0 \\ 0 & M_2 & 0 & 0 \\ 0 & 0 & 0 & -\mu \\ 0 & 0 & -\mu & 0 \end{pmatrix}, \quad \mathbf{X}_{\mathrm{gl}} = \begin{pmatrix} M_2 & 0 \\ 0 & \mu \end{pmatrix}. \tag{3.2.67}$$

The eigenvalues of these matrices read

$$\begin{aligned} &m_{\tilde{\chi}_1^0} = |M_1|, \quad m_{\tilde{\chi}_2^0} = |M_2|, \quad m_{\tilde{\chi}_{3,4}^0} = |\mu|, \\ &m_{\tilde{\chi}_1^\pm} = |M_2|, \quad m_{\tilde{\chi}_2^\pm} = |\mu|. \end{aligned} \tag{3.2.68}$$

Therefore, the counterterm for the Higgsino mass parameter μ can be related to the mass counterterms $\delta^{(1)} m_{\tilde{\chi}_2^\pm}$ [91, 129, 130]. In this thesis, we renormalize this parameter in the $\overline{\mathrm{DR}}$ scheme,

$$\delta^{(1)}\mu = \frac{\mu}{2} \left[\Sigma^{(1),L}_{\tilde{\chi}_2^\pm}(|\mu|^2) + \Sigma^{(1),R}_{\tilde{\chi}_2^\pm}(|\mu|^2) + 2\, \Sigma^{(1),S}_{\tilde{\chi}_2^\pm}(|\mu|^2) \right]\Big|_{\mathrm{div}}. \tag{3.2.69}$$

3.2.6 Vacuum expectation value

The vacuum expectation value v can be expressed in terms of the parameters $(M_W,\ s_\mathrm{w},\ e)$ (see Eq. (2.5.9)),

$$v^2 = \frac{2s_\mathrm{w}^2 M_W^2}{e^2}. \tag{3.2.70}$$

Thus the renormalization transformation applied to v^2 yields

$$v^2 \to v^2 \left(\frac{\delta^{(1)} M_W^2}{M_W^2} + \frac{2\delta^{(1)} s_\mathrm{w}}{s_\mathrm{w}} - \frac{\delta^{(1)} e^2}{e^2} - \delta^{(1)} Z_{hh} \right), \tag{3.2.71}$$

where the one-loop counterterm for s_w was derived in Eq. (3.2.12). In the gaugeless limit this counterterm is finite and $\frac{\delta^{(1)} e^2}{e^2} = 0$. That is why the relation between the $\overline{\mathrm{MS}}$ vev (an analogous relation is valid for the $\overline{\mathrm{DR}}$ vev) and the vev defined via M_W, s_w and e (we will refer to this vev as v_OS) is given by

$$v_{\overline{\mathrm{MS}}}^2 = v_\mathrm{OS}^2 \left(1 + \frac{\delta^{(1)} M_W^2}{M_W^2}\bigg|_\mathrm{fin} + \frac{2\delta^{(1)} s_\mathrm{w}}{s_\mathrm{w}} \right) \tag{3.2.72}$$

in the gaugeless limit. Instead of v_OS in this thesis we will use a different definition for the vacuum expectation value (see also Eq. (1.2.20)),

$$v_{G_F} = \left(2\sqrt{2} G_F \right)^{-1/2}. \tag{3.2.73}$$

The relation between the two definition is given by

$$v_\mathrm{OS}^2 = v_{G_F}^2 \left(1 + \Delta^{(1)} r \right), \tag{3.2.74}$$

where Δr includes all non-QED corrections to the muon decay amplitude [202, 203]. The MSSM contributions to Δr can be found in [67, 69, 204, 205]. In the gaugeless limit [91, 129, 130]

$$\Delta^{(1)} r = -\frac{2\delta^{(1)} s_\mathrm{w}}{s_\mathrm{w}}. \tag{3.2.75}$$

From Eqs. (3.2.72)–(3.2.75) the leading-order relation between $v_{\overline{\mathrm{MS}}}$ and v_{G_F} is obtained,

$$v_{\overline{\mathrm{MS}}}^2 = v_{G_F}^2 \left(1 + \frac{\delta^{(1)} M_W^2}{M_W^2}\bigg|_\mathrm{fin} \right). \tag{3.2.76}$$

Chapter 4

Higgs boson masses in the MSSM

This chapter provides a review of different methods for the Higgs mass calculation in the MSSM. In Sec. 4.1, we review the main idea and the current status of the fixed-order method which is based on the perturbative calculation of the Higgs boson self-energies at a given order. Sec. 4.2 contains a review of the EFT method which is best applicable in the case of a large hierarchy in the MSSM spectrum and allows to resum large logarithms in the expression for the SM-like Higgs mass by means of numerical integration of the system of RGEs. In Sec. 4.3, we consider the hybrid approach which serves as a merger of the fixed-order and the EFT approaches. It enables to make a precise prediction for the Higgs boson mass both for light- and heavy SUSY scenarios. This approach requires the conversion of input parameters from the scheme used in the fixed-order calculation to the $\overline{DR}$ scheme. The conversion formula may contain two sources of large logarithms: logarithms related to the RGE running of the top mass and other types of logarithms which appear only in certain SUSY scenarios and are absent in the others. This issue is studied in Sec. 4.4.

4.1 Feynman diagrammatic approach

As was already pointed out in Section 2.5.1, the tree-level mass of the lightest Higgs boson of the MSSM cannot be larger than the mass of the Z-boson, but it receives sizable quantum corrections. The loop-corrected masses of the neutral Higgs bosons are the poles of the 3 x 3 propagator matrix [42]

$$\Delta_{hHA}(p^2) = -\left(\widehat{\Gamma}_{hHA}(p^2)\right)^{-1}, \tag{4.1.1}$$

[42] In principle, in determining the loop-corrected masses one has to take into account the mixing of the Higgs bosons with the Goldstone and the gauge bosons. So, in general, a 6 x 6 matrix has to be considered. However, the mixing of the neutral Higgs bosons with Goldstone and gauge boson yields subleading two-loop contributions to the Higgs-boson masses and is therefore neglected in this thesis.

where

$$\widehat{\Gamma}_{hHA}(p^2) = i\left[p^2\mathbb{1} - \mathbf{M}(p^2)\right]. \tag{4.1.2}$$

In other words, they satisfy the equation

$$\det\,\widehat{\Gamma}_{hHA}(M_i^2) = 0. \tag{4.1.3}$$

The mass matrix $\mathbf{M}(p^2)$ in Eq. (4.1.2) has the following form

$$\mathbf{M}(p^2) = \begin{pmatrix} m_h^2 - \widehat{\Sigma}_{hh}(p^2) & -\widehat{\Sigma}_{hH}(p^2) & -\widehat{\Sigma}_{hA}(p^2) \\ -\widehat{\Sigma}_{hH}(p^2) & m_H^2 - \widehat{\Sigma}_{HH}(p^2) & -\widehat{\Sigma}_{HA}(p^2) \\ -\widehat{\Sigma}_{hA}(p^2) & -\widehat{\Sigma}_{HA}(p^2) & m_A^2 - \widehat{\Sigma}_{AA}(p^2) \end{pmatrix}, \tag{4.1.4}$$

where $\widehat{\Sigma}_{ij}(p^2)$ are the renormalized self-energies with external Higgs bosons, $i,\ j \in \{h,\ H,\ A\}$, and m_h, m_H, m_A are the tree-level masses. The diagonal elements of the propagator matrix $\Delta_{hHA}(p^2)$ can be rewritten in a form which resembles the dressed propagator (see Eq. (3.1.16)) of a single scalar particle without mixing,

$$\Delta_{ii}(p^2) := (\Delta_{hHA}(p^2))_{ii} = \frac{i}{p^2 - m_i^2 + \widehat{\Sigma}_{ii}^{\text{eff}}(p^2)}, \tag{4.1.5}$$

where the "effective" self-energy can be expressed via the elements of the matrix $\widehat{\Gamma}_{hHA}$ ($\widehat{\Gamma}_{ij} := (\widehat{\Gamma}_{hHA})_{ij}$),

$$\widehat{\Sigma}_{ii}^{\text{eff}}(p^2) = \widehat{\Sigma}_{ii}(p^2) - i\frac{2\widehat{\Gamma}_{ij}(p^2)\widehat{\Gamma}_{jk}(p^2)\widehat{\Gamma}_{ki}(p^2) - \widehat{\Gamma}_{ki}^2(p^2)\widehat{\Gamma}_{jj}(p^2) - \widehat{\Gamma}_{ij}^2(p^2)\widehat{\Gamma}_{kk}(p^2)}{\widehat{\Gamma}_{jj}(p^2)\widehat{\Gamma}_{kk}(p^2) - \widehat{\Gamma}_{jk}^2(p^2)}. \tag{4.1.6}$$

with $i,\ j$ and k all being different from each other. It can be shown that the inverse of any element of the matrix $\Delta_{hHA}(p^2)$ is proportional to the determinant of $\widehat{\Gamma}_{hHA}(p^2)$ [206],

$$(\Delta_{ii})^{-1} = \frac{\det\,\widehat{\Gamma}_{hHA}(p^2)}{\left(p^2 - m_j^2 + \widehat{\Sigma}_{jj}(p^2)\right)\left(p^2 - m_k^2 + \widehat{\Sigma}_{kk}(p^2)\right) - \widehat{\Sigma}_{jk}^2(p^2)}, \tag{4.1.7a}$$

$$(\Delta_{ij})^{-1} = \frac{\det\,\widehat{\Gamma}_{hHA}(p^2)}{\widehat{\Sigma}_{ik}(p^2)\widehat{\Sigma}_{jk}(p^2) - \left(p^2 - m_k^2 + \widehat{\Sigma}_{kk}(p^2)\right)\widehat{\Sigma}_{ij}(p^2)}, \tag{4.1.7b}$$

so any of them can be used to determine the poles of the matrix $\Delta_{hHA}(p^2)$. For instance, the poles $\mathcal{M}_i^2$ satisfy the equation

$$\mathcal{M}_i^2 - m_i^2 + \widehat{\Sigma}_{ii}^{\text{eff}}(\mathcal{M}_i^2) = 0, \quad i \in \{h,\ H,\ A\}. \tag{4.1.8}$$

The poles $\mathcal{M}_i^2$ are in general complex numbers and can be written as,

$$\mathcal{M}_i^2 = M_i^2 - i\, M_i\, \Gamma_i, \tag{4.1.9}$$

where M_i is the loop-corrected mass of a Higgs boson and Γ_i its width. In general, equation (4.1.8) cannot be solved analytically, but an approximate solution can be obtained by a perturbative expansion of the effective self-energy, $\widehat{\Sigma}_{ii}^{\text{eff}}(p^2)$ in the number of loops,

$$\widehat{\Sigma}_{ii}^{\text{eff}}(p^2) = \widehat{\Sigma}_{ii}^{(1)}(p^2) + \widehat{\Sigma}_{ii}^{(2)}(p^2) - \frac{\left[\widehat{\Sigma}_{ij}^{(1)}(p^2)\right]^2}{p^2 - m_j^2} - \frac{\left[\widehat{\Sigma}_{ik}^{(1)}(p^2)\right]^2}{p^2 - m_k^2} + \ldots, \tag{4.1.10}$$

where the superscript attached to the renormalized self-energies denotes the loop order, at which the respective self-energy is computed, and the ellipsis denotes contributions of three-loop order and higher. The ansatz for the loop-corrected mass, $\mathcal{M}_i^2$, can also be represented as a series,

$$\mathcal{M}_i^2 = m_i^2 + \Delta\mathcal{M}_i^{2,(1)} + \Delta\mathcal{M}_i^{2,(2)} + \ldots, \tag{4.1.11}$$

where m_i^2 is a tree-level mass, and $\mathcal{M}_i^{2,(k)}$ is a quantum correction to it at the k-th order of perturbation theory.

By inserting the ansatz (4.1.11) into the equation (4.1.8) and equating the corresponding loop orders, we obtain the expressions for $\mathcal{M}_i^{2,(1)}$ and $\mathcal{M}_i^{2,(2)}$,

$$\Delta\mathcal{M}_i^{2,(1)} = -\widehat{\Sigma}_{ii}^{(1)}(m_i^2), \tag{4.1.12a}$$

$$\Delta\mathcal{M}_i^{2,(2)} = -\widehat{\Sigma}_{ii}^{(2)}(m_i^2) + \widehat{\Sigma}_{ii}^{(1)}(m_i^2)\, \widehat{\Sigma}_{ii}^{(1)'}(m_i^2) + \frac{\left[\widehat{\Sigma}_{ij}^{(1)}(m_i^2)\right]^2}{m_i^2 - m_j^2} + \frac{\left[\widehat{\Sigma}_{ik}^{(1)}(m_i^2)\right]^2}{m_i^2 - m_k^2}, \quad \text{where } j,k \neq i. \tag{4.1.12b}$$

A few comments are in order. In general, the expansion of $\widehat{\Sigma}_{ii}^{\text{eff}}(p^2)$ in the number of loops is problematic. In particular, the denominators in Eq. (4.1.12b) become small for $m_i^2 \sim m_j^2$ and $m_i^2 \sim m_k^2$. In this case, the loop expansion is not well-defined and one needs the full expression given by Eq. (4.1.5) without further approximations to determine the complex poles. In this thesis we focus on the decoupling limit, $m_A \gg M_Z$, where the loop expansion is well-defined for the lightest Higgs boson and we will use it. However, it is worth noting that even in this case the expansion does not work for the bosons H and A. Here, by the lightest Higgs boson we mean the Higgs boson which has the smallest tree-level mass. The higher-order corrections, in

principle, might change the hierarchy of masses.[43] This, however, does not happen in the mentioned limit.

The complex pole of the lightest Higgs boson has the following form up to the two-loop order,

$$\mathcal{M}_h^2 = m_h^2 - \widehat{\Sigma}_{hh}^{(1)}(m_h^2) - \widehat{\Sigma}_{hh}^{(2)}(m_h^2) + \widehat{\Sigma}_{hh}^{(1)}(m_h^2)\ \widehat{\Sigma}_{hh}^{(1)'}(m_h^2) + \frac{\left[\widehat{\Sigma}_{hH}^{(1)}(m_h^2)\right]^2}{m_h^2 - m_H^2} + \frac{\left[\widehat{\Sigma}_{hA}^{(1)}(m_h^2)\right]^2}{m_h^2 - m_A^2}\,. \tag{4.1.13}$$

In the decoupling limit, $m_A \gg M_Z$ the last two terms in Eq. (4.1.13) are suppressed by the masses of the heavy Higgs bosons and therefore can be neglected.[44] Additionally, since the tree-level mass of the SM-like Higgs boson is smaller than the Z-boson mass, only light quarks and leptons can contribute to the imaginary part of $\widehat{\Sigma}_{hh}(m_h^2)$ in the Feynman gauge. This imaginary part is numerically irrelevant for the prediction of the Higgs boson mass and will be neglected in this thesis. Applying the above-mentioned approximations, the mass of the lightest Higgs boson reads up to the two-loop order

$$(M_h^2)_{\rm FD} = m_h^2 - \widehat{\Sigma}_{hh}^{(1)}(m_h^2) - \widehat{\Sigma}_{hh}^{(2)}(m_h^2) + \widehat{\Sigma}_{hh}^{(1)}(m_h^2)\ \widehat{\Sigma}_{hh}^{(1)'}(m_h^2). \tag{4.1.14}$$

In the method called *Feynman-diagrammatic (FD)* or *fixed-order (FO)* approach the contributions to the self-energies $\widehat{\Sigma}_{ij}(p^2)$ from all particles of the theory are computed at a given order. For instance, full one-loop corrections to $\widehat{\Sigma}_{ij}(p^2)$, including the momentum dependence, have been computed in the framework of the MSSM with [90] and without $\mathcal{CP}$-violation [183, 184, 208].

The leading two-loop corrections to the Higgs masses are of $\mathcal{O}(\alpha_t\alpha_s)$ (more precisely, of $\mathcal{O}(m_t^2\alpha_t\alpha_s)$). They have been computed in the approximation of vanishing external momenta and vanishing electroweak gauge couplings in the $\overline{\rm DR}$ scheme [209, 210] and in the mixed $\overline{\rm DR}$/OS scheme[45] [34, 187] in the MSSM without $\mathcal{CP}$-violation. The generalization of these corrections to the case of the MSSM with $\mathcal{CP}$-violation has been performed in [150]. The corresponding two-loop corrections for non-zero external momentum have been computed in the rMSSM [211] and in the complex MSSM (cMSSM) [7, 211, 212].

Other sizable two-loop contributions to the Higgs masses are of $\mathcal{O}(\alpha_t^2)$ (more accurately, of $\mathcal{O}(m_t^2\alpha_t^2)$). This correction has also been derived in the limit of vanishing external momenta and vanishing electroweak gauge couplings for the case of

[43] The main issue in this context is that it is not possible to make a unique assignment of which loop-corrected state should correspond to which tree-level state. In fact, all assignments are equivalent to each other as long as one keeps the full expression of the propagator matrix wirthout additional approximations. A detailed discussion of this issue can be found in [206, 207].

[44] These terms are taken into account in Refs. [16, 19].

[45] The mixed $\overline{\rm DR}$/OS scheme employed in [34, 147, 187] implies the renormalization of $\tan\beta$ and the Higgsino mass parameter μ in the $\overline{\rm DR}$ scheme. The other parameters are renormalized OS.

the MSSM with real parameters in the pure $\overline{\text{DR}}$ scheme [213], in the mixed $\overline{\text{DR}}$/OS scheme [147] and in the cMSSM in the mixed $\overline{\text{DR}}$/OS scheme [91, 129, 130].

For large $\tan\beta$ the contributions involving down-type fermions are sizable. In this case a careful choice of the renormalization scheme for the bottom/sbottom sector is needed to avoid numerically unstable results (see the discussion in Sec. 3.2.3 and in Refs. [189, 195]). The corrections to the Higgs boson masses of order $\mathcal{O}(\alpha_b\alpha_s)$ (of order $\mathcal{O}(m_b^2\alpha_b\alpha_s)$) in the rMSSM and in the limit of vanishing external momenta have been evaluated in Refs. [149, 189]. The mixed two-loop corrections to the Higgs masses involving top and bottom Yukawa couplings of order $\mathcal{O}(\alpha_t\alpha_b + \alpha_b^2)$ (i.e. of order $\mathcal{O}(m_t^2\alpha_t\alpha_b + m_b^2\alpha_t\alpha_b + m_b^2\alpha_b^2)$) have been computed in the rMSSM [148] and cMSSM [9]. Contributions involving the τ-Yukawa coupling, $\mathcal{O}(\alpha_\tau\alpha_b + \alpha_\tau^2)$ for the rMSSM have been computed in [148, 214]. Finally, the complete two-loop QCD corrections to Higgs boson masses in the cMSSM, taking into account the full momentum dependence as well as all contributions involving the Yukawa couplings, $\mathcal{O}(\sqrt{\alpha_{q_1}}\sqrt{\alpha_{q_2}}\alpha_s)$, where $q_{1,2} = t, b, c, s, u, d$, and the gauge couplings, $\mathcal{O}(\alpha\alpha_s)$, have been computed in [11]. The full two-loop effective potential in the cMSSM has been computed in [215]. This result was used to derive two-loop $\mathcal{O}(\alpha\alpha_s)$ corrections to the Higgs in the approximation of zero momenta [216, 217]. The two-loop corrections to the SM-like Higgs mass in the case of non-minimal flavor violation were computed in [218].

Three-loop corrections have been computed at order $\mathcal{O}(\alpha_t\alpha_s^2)$ (i.e. of order $\mathcal{O}(m_t^2\alpha_t\alpha_s^2)$) in the limit of vanishing external momenta for the rMSSM in [10, 219, 220] and in [12] (see also Chapter 7).

The main advantage of the FO approach is that it allows one to take into account all contributions from different MSSM sectors at a given order of perturbation theory, i.e., both logarithmic and non-logarithmic terms, as well as all terms suppressed by the ratio v/M_{SUSY}. However, if there is a strong hierarchy of scales present in the mass spectrum, the logarithms of the ratio of these scales emerge in the result of the calculation. These logarithms (which we will call "large logarithms" in the forthcoming parts of this thesis) spoil the convergence of the perturbation series and lead to large theoretical uncertainties of the final result.

A prime example of such large logarithms appears in the dominant one-loop contributions originating from the (s)top sector to the SM-like Higgs boson in scenarios where all non-SM particles are much heavier than the electroweak scale [214],

$$M_h^2 = M_Z^2\cos^2 2\beta + \frac{3m_t^4}{4\pi^2 v^2}\left[\log\frac{M_S^2}{m_t^2} + \frac{X_t^2}{M_S^2} - \frac{X_t^4}{12\,M_S^4}\right] + \mathcal{O}\left(\frac{m_t^2}{M_S^2}\right), \tag{4.1.15}$$

where $M_S^2 = m_{\tilde{t}_1}m_{\tilde{t}_2}$. Similar logarithmic terms arise at higher-orders; at n-th order of perturbation theory the corrections to the Higgs masses contain $\log^k\frac{M_S^2}{m_t^2}$ terms,

where $k = 1 \ldots n$. The method which allows to resum these logarithms to all orders of perturbation theory will be discussed in the next Section.

4.2 Effective field theory (EFT) approach

Another method for the calculation of the Higgs masses is the *effective field theory (EFT)* approach. The effective field theory method is applied in various areas of physics and in general treats the case of a hierarchy between the different scales of a theory. Its basic idea is that physics at low energy scales should not depend on physics at high scales [170]. More formally, in this approach, all degrees of freedom are categorized into "light" and "heavy" degrees of freedom. All "heavy" degrees of freedom are decoupled or integrated out. For example, a particle with the mass M is decoupled at the scale $Q \sim M$. Below this scale the low energy EFT, containing only the light degrees of freedom, describes all interactions between light particles.

To ensure that the EFT and the full theory give rise to the same predictions at the high scale, the masses and couplings in the EFT encode the physics of the full theory. Schematically, this dependence can be written as an expansion in the loop-counting factor $\kappa = (16\pi^2)^{-1}$,

$$g_{eff}(Q = M) = g_{\text{tree}} + \kappa\ \Delta g^{1l} + \kappa^2\ \Delta g^{2l} + \ldots\Big|_{Q=M}. \tag{4.2.1}$$

The tree-level coupling constant g_{tree}, as well as the *threshold corrections* Δg^{1l} and Δg^{2l} are obtained by demanding that predictions for physical observables calculated in the full theory and the EFT are equal to each other order by order in perturbation theory. This procedure is called *matching*. Given the value of the coupling constant g_{eff} at scale $Q = M$, one can calculate its value at low energies by making use of the renormalization group equations (see Sec. 3.1.4). This procedure is called *matching*. Given the value of the coupling constant g_{eff} at the scale $Q = M$, one can calculate its value at low energies by making use of the renormalization group equations (see Sec. 3.1.4).

In this thesis we will mostly consider the scenario (also called "Heavy SUSY" scenario) in which all soft-breaking parameters together with the $\mathcal{CP}$-odd Higgs boson mass m_A lie around some characteristic scale M_{SUSY} which is much heavier than the electroweak scale, $M_{\text{SUSY}} \gg m_t$.[46] We will use the geometric mean of the stop soft breaking masses as a definition for M_{SUSY},

$$M_{\text{SUSY}} = \sqrt{m_{\tilde{t}_L} m_{\tilde{t}_R}}. \tag{4.2.2}$$

[46] In App. A we also present threshold corrections to the couplings in the split-SUSY scenario, in which all stop and sbottom masses are much heavier than the gaugino masses.

In this setup all non-SM particles are integrated out at $M_{\rm SUSY}$, and at energies $Q < M_{\rm SUSY}$ the physics is described by the SM interactions. The coupling constants, however, are fixed by the boundary condition at $M_{\rm SUSY}$. For instance, the quartic coupling, λ, is not a free parameter anymore. Instead, it is fixed at the scale $M_{\rm SUSY}$. The tree-level matching relation can be derived from Eq. (2.5.24) in the limit $m_A \gg M_Z$,

$$m_h^2 = M_Z^2 \cos^2 2\beta + \mathcal{O}\left(\frac{M_Z^2}{m_A^2}\right). \tag{4.2.3}$$

From this relation and Eqs. (1.2.11) and (1.2.16) we obtain the tree-level matching condition for the Higgs quartic coupling,

$$\lambda(M_{\rm SUSY}) = \frac{1}{4}(g^2 + g'^2)c_{2\beta}^2, \tag{4.2.4}$$

where all parameters on the right-hand side are evaluated in the $\overline{\rm DR}$ scheme at the scale $M_{\rm SUSY}$. We will choose the electroweak scale to be equal to the top pole mass,

$$M_t \equiv m_t^{\rm OS}. \tag{4.2.5}$$

At this scale, the running $\overline{\rm MS}$ top and bottom Yukawa,[47] electroweak and strong gauge couplings are fixed. The running top Yukawa and electroweak gauge couplings are extracted at the electroweak scale from the top, W-, Z-boson pole masses, and the Fermi constant G_F via

$$\begin{aligned}
y_t^{\overline{\rm MS},{\rm SM}}(M_t) &= \frac{M_t}{v_{G_F}}(1+\Delta y_t),\\
g^{\overline{\rm MS},{\rm SM}}(M_t) &= \sqrt{2}\frac{M_W}{v_{G_F}}(1+\Delta g),\\
g'^{\,\overline{\rm MS},{\rm SM}}(M_t) &= \sqrt{2}\frac{\sqrt{M_Z^2 - M_W^2}}{v_{G_F}}(1+\Delta g'),\\
v^2_{\overline{\rm MS},{\rm SM}}(M_t) &= v^2_{G_F}(1+(\delta v^2)^{\rm SM}).
\end{aligned} \tag{4.2.6}$$

where v_{G_F} is defined via Eq. (1.2.20), and Δy_t, Δg, $\Delta g'$ and $\delta v^{2,{\rm SM}}$ are sometimes called "threshold corrections at the electroweak scale". The explicit leading order expressions for them can be found in Ref. [190]. The strong gauge coupling is determined at the scale M_Z with 5 active flavours, and the input bottom mass is given at the scale m_b, i.e. $m_b^{\overline{\rm MS},{\rm SM}}(m_b)$ [4]. By means of the RGEs one computes $\alpha_s(M_t)$ and $m_b^{\overline{\rm MS},{\rm SM}}(M_t)$ and thus the bottom Yukawa coupling at this scale.

Knowing the boundary conditions for the couplings (g, g', g_3, y_t, y_b) at M_t and for λ at $M_{\rm SUSY}$, one can solve the system of the renormalization group equations for

[47] In this thesis we do not consider contributions to the Higgs mass from quarks of the first and the second generations.

these couplings to find the value of λ at the electroweak scale, $\lambda(M_t)$. After that, the running Higgs mass can be obtained,

$$\left(m_h^{\overline{\rm MS},\rm SM}\right)^2 = 2\,\lambda(M_t) v^2_{\overline{\rm MS},\rm SM}(M_t). \tag{4.2.7}$$

The pole mass can be found from the SM pole equation (see Sec. 4.1),

$$M_h^2 - \left(m_h^{\overline{\rm MS},\rm SM}\right)^2 + \widetilde{\Sigma}_{hh}^{\overline{\rm MS},\rm SM}(M_h^2) = 0, \tag{4.2.8}$$

where the quantity $\widetilde{\Sigma}_{hh}^{\overline{\rm MS},\rm SM}$ denotes the following combination of the SM Higgs self-energy and the tadpole, renormalized in the $\overline{\rm MS}$ scheme in the Standard Model,

$$\widetilde{\Sigma}_{hh}^{\overline{\rm MS},\rm SM}(p^2) = \widehat{\Sigma}_{hh}^{\overline{\rm MS},\rm SM}(p^2)\Big|_{\rm fin} - \frac{1}{\sqrt{2} v_{\overline{\rm MS},\rm SM}} T_h^{\overline{\rm MS},\rm SM}\Big|_{\rm fin}. \tag{4.2.9}$$

The approximate solution of Eq. (4.2.8) up to terms of three-loop order reads

$$\begin{aligned}(M_h^2)_{\rm EFT} &= 2\lambda(M_t) v^2_{\overline{\rm MS},\rm SM}(M_t) - \widetilde{\Sigma}_{hh}^{\overline{\rm MS},\rm SM,(1)}(m_h^2) - \widetilde{\Sigma}_{hh}^{\overline{\rm MS},\rm SM,(2)}(m_h^2) \\ &- \widetilde{\Sigma}'^{\overline{\rm MS},\rm SM,(1)}_{hh}(m_h^2) \cdot \left[2\lambda(M_t) v^2_{\overline{\rm MS},\rm SM}(M_t) - \widetilde{\Sigma}_{hh}^{\overline{\rm MS},\rm SM,(1)}(m_h^2) - m_h^2\right] + \mathcal{O}(\kappa^3),\end{aligned} \tag{4.2.10}$$

where m_h is the tree-level Higgs mass in the decoupling limit, $m_A \gg M_Z$, given by Eq. (4.2.3).

The system of the RGEs in general can only be solved numerically or iteratively order by order in the loop-counting factor κ. For example, the scale dependence of the quartic coupling λ is given by the equation

$$\frac{d\lambda}{dt} = \beta_\lambda(t), \qquad t = \log Q^2, \tag{4.2.11}$$

where Q is the renormalization scale. The β-function (see Sec. 3.1.4) on the right-hand side is given as a power series in loops,

$$\beta_\lambda(t) = \sum_{n=1}^{\infty} \kappa^n \beta_\lambda(t) = \kappa\ \beta_\lambda^{(1)}(t) + \kappa^2\ \beta_\lambda^{(2)}(t) + \ldots, \tag{4.2.12}$$

It can be expanded in a Taylor series around $\widetilde{t} = \log M^2_{\rm SUSY}$,

$$\begin{aligned}\beta_\lambda(t) &= \sum_{n=1}^{\infty} \kappa^n \sum_{m=0}^{\infty} \frac{\beta_\lambda^{(n,m)}(\widetilde{t})}{m!}(t-\widetilde{t})^m, \quad \text{with} \\ \beta_\lambda^{(n,m)}(t) &\equiv \frac{d^m \beta_\lambda^{(n)}(t)}{dt^m}, \quad \beta_\lambda^{(n,0)} \equiv \beta_\lambda^{(n)}.\end{aligned} \tag{4.2.13}$$

Note that the quantity $\beta_\lambda^{(n,m)}(t)$ is of $\mathcal{O}(\kappa^m)$. For example,

$$\beta_\lambda^{(n,1)}(t) \equiv \frac{d\beta_\lambda^{(n)}}{dt} = \sum_g \frac{\partial \beta_\lambda^{(n)}}{\partial g} \frac{dg}{dt} = \sum_g \frac{\partial \beta_\lambda^{(n)}}{\partial g} \left(\kappa \beta_g^{(1)} + \dots\right), \tag{4.2.14}$$

where the summation on the right-hand side runs over all coupling constants which enter the expression for $\beta_\lambda^{(n)}$. Plugging the expression in Eq. (4.2.13) into Eq. (4.2.11), we can find the solution for $\lambda(t)$ as a series in κ,

$$\lambda(M_t) = \lambda(M_{\rm SUSY}) + \sum_{n=1}^{\infty} \sum_{m=0}^{\infty} \kappa^n \frac{(-1)^{m+1}}{(m+1)!} \beta_\lambda^{(n,m)}(M_{\rm SUSY}) L^{m+1}, \tag{4.2.15}$$

where $L = \log \frac{M_{\rm SUSY}^2}{M_t^2}$. Each term on the right-hand side is of $\mathcal{O}(\kappa^{m+n})$. Therefore, the one-loop beta-function, $\beta_\lambda^{(1)}$, allows the resummation of all terms in the expression for $\lambda(M_t)$ which are proportional to $(\kappa L)^{m+1}$ via the numerical solution of Eq. (4.2.11). These terms are called "leading logarithms" (LL). The two-loop beta-function allows the resummation of the terms which are proportional to $\kappa(\kappa L)^{m+1}$. They are called "next-to-leading logarithms" (NLL).

The derivatives $\beta_\lambda^{(n,m)}$ on the right-hand side of Eq. (4.2.15) can be expressed in terms of the couplings evaluated at the scale $M_{\rm SUSY}$. For example, the Higgs self-coupling, $\lambda(M_{\rm SUSY})$, is given at the leading order by Eq. (4.2.4). Higher order corrections to this relation do not contain large logarithms and therefore generate non-logarithmic and subleading logarithmic corrections to $\lambda(M_t)$. For instance, one-loop threshold corrections generate terms which are proportional to $\kappa^n(\kappa L)^{m+1}$ with $n \geq 1$, two-loop threshold corrections yield terms of order $\kappa^n(\kappa L)^{m+1}$ where $n \geq 2$, etc. With that, we can conclude that in order to resum N^{n}LL logarithms, the $n+1$-th order beta function, $\beta_\lambda^{(n+1)}$, and the n-th order threshold correction to λ at $M_{\rm SUSY}$ are needed.

Some care has to be taken regarding the parametrization of the threshold corrections. The threshold corrections to λ can be parametrized in terms of the SM or the MSSM couplings defined at $M_{\rm SUSY}$. The two are related via an expression analogous to Eq. (4.2.1). The threshold corrections to the respective couplings do not contain large logarithms, so in principle both parametrizations are valid and equivalent as long as the sum, given in Eq. (4.2.15), is truncated at some finite order in n. However, there are cases when one of the parametrizations is preferable to the other one. As we already mentioned in Sec. 3.2.4, the relation between the bottom mass in the SM and in the MSSM contains terms which grow linearly with $\tan\beta$ and potentially can be numerically important. These terms can be summed up to all orders of perturbation theory [139, 200]. This suggests that it is more appropriate to express the one- and

two-loop threshold corrections to λ in terms of the MSSM bottom Yukawa coupling. At the strict two-loop level, this parametrization is equivalent to the parametrization via the SM bottom Yukawa coupling, but beyond this order of perturbation theory, it consistently captures all the higher-order terms leading in the large $\tan\beta$ limit. The application of the two resummations (RG resummation of large logarithms and Δ_b resummation) at the same time does not cause any double counting as long as large logarithms are absent in Δ_b. As will be discussed in Chapters 5 and 6, Δ_b does not contain large logarithms if it is properly parametrized. Similar arguments can be applied for the top Yukawa coupling. In the following chapters of this thesis we will however express the threshold corrections to λ in terms of the SM top Yukawa coupling. A detailed analysis of the numerical impact of different parametrizations of the threshold corrections to λ, involving y_t, can be found in [221].

Full one-loop threshold corrections to $\lambda(M_{\text{SUSY}})$ have been computed in [32]. Two-loop corrections are known at orders [48] $\mathcal{O}(\alpha_t^2\alpha_s)$ [33], $\mathcal{O}(\alpha_t^3)$ [13], $\mathcal{O}((\alpha_t+\alpha_b)^3+(\alpha_b^2+\alpha_t^2)\alpha_s+\alpha_b^2\alpha_\tau+\alpha_b\alpha_\tau^2+\alpha_\tau^3)$ [15] and $\mathcal{O}((\alpha_t+\alpha_b)\alpha\alpha_s)$ [18]. Three-loop corrections of $\mathcal{O}(\alpha_t^2\alpha_s^2)$ have been calculated in [17]. The numerical effects of the inclusion of several dimension-6 operators have been studied in [15]. All these corrections have been computed in the MSSM without $\mathcal{CP}$-violation. In Chapter 6 we will discuss the derivation and numerical impact of the two-loop threshold corrections of order $\mathcal{O}((\alpha_t+\alpha_b)^3+(\alpha_b^2+\alpha_t^2)\alpha_s)$ in the MSSM with $\mathcal{CP}$-violation.

The EFT approach allows the resummation of large logarithms appearing in the fixed-order calculation but it is not applicable if $M_{\text{SUSY}} \sim M_t$. Therefore, in order to provide a reliable prediction for the Higgs-boson masses in both low- and high-scale MSSM scenarios, the resummation of the leading and subleading logarithms can be combined with the fixed-order results in the MSSM in the so-called *hybrid approach* which will be considered in the next Section.

4.3 Hybrid approach

In the hybrid approach, the logarithms that are resummed in the EFT approach are added to the pole equation for the SM-like Higgs boson [21–23], [49]

$$p^2 - m_h^2 + \widehat{\Sigma}_{hh}^{\text{MSSM}}(p^2) + \Delta_{hh}^{\text{EFT}} = 0, \tag{4.3.1}$$

[48] In this convention the dominant one-loop threshold correction is of $\mathcal{O}(\alpha_t^2)$ and it yields the correction to the SM-like Higgs mass of $\mathcal{O}(m_t^2\alpha_t)$. Another possible convention often utilized in the literature is to use the same order for the quartic coupling as for the Higgs mass. In that convention the dominant one-loop correction to the Higgs self-coupling would be of $\mathcal{O}(\alpha_t)$ instead of $\mathcal{O}(\alpha_t^2)$.

[49] Eq. (4.3.1) is only valid in the decoupling limit, $m_A \gg M_Z$. If $m_A \sim M_Z$, the effective field theory below M_{SUSY} is a Two-Higgs-Doublet Model (THDM). This case was considered in [16].

where $\Delta_{hh}^{\rm EFT}$ includes the EFT result – i.e., the result for the $\overline{\rm MS}$ Higgs mass – and *subtraction terms*,

$$\Delta_{hh}^{\rm EFT} = -2\,\lambda(M_t) v^2_{\overline{\rm MS},\rm SM}(M_t) - \left[\Delta M_h^2\right]_{\rm sub} \,. \tag{4.3.2}$$

The latter are needed to avoid double counting of the terms which are already present in the FO result. These include *logarithmic terms*, i.e. terms which include large logarithms, $\log \frac{M^2_{\rm SUSY}}{M_t^2}$, and *non-logarithmic terms* which include non-logarithmic contributions as well as logarithms of small mass ratios. The logarithms can be extracted by means of perturbatively solving the system of RGEs up to a given order,

$$\left[\Delta M_h^2\right]^{\log}_{\rm sub} = -2\,\lambda(M_t) v^2_{\overline{\rm MS},\rm SM}(M_t)\Big|_{\rm logs} \,. \tag{4.3.3}$$

The subtraction of the non-logaritmic terms is slightly more subtle. The non-logarithmic SUSY correction to the SM-like Higgs mass in the EFT approach up to the two-loop order yields (see Sec. 4.2),[50]

$$\left[M_h^{2,\rm EFT}\right]_{\rm non-log} = 2 v^2_{\overline{\rm MS},\rm SM}(M_t)\left(\lambda_{\rm tree}(M_{\rm SUSY}) + \Delta\lambda^{1l} + \Delta\lambda^{2l}\right), \tag{4.3.4}$$

where the tree-level quartic coupling $\lambda_{\rm tree}(M_{\rm SUSY})$ and the one- and two-loop threshold corrections to it are expressed in terms of the $\overline{\rm MS}$ or the $\overline{\rm DR}$ couplings at $M_{\rm SUSY}$. On the other hand, the FO result already contains exactly the same expression, but parametrized via different couplings. Therefore, the expression in Eq. (4.3.4) parametrized in terms of the FO couplings has to be subtracted to avoid double-counting of the non-logarithmic terms [35]. Schematically,

$$\left[\Delta M_h^2\right]^{\rm non-log}_{\rm sub} = -\left[M_h^{2,\rm EFT}\right]_{\rm non-log}\Big|_{p^{\rm EFT}\to p^{\rm FO}+\Delta p} \,, \tag{4.3.5}$$

where p is a parameter for which a different renormalization scheme is used in the FO and in the EFT calculation. The finite shift between different renormalization schemes in the one-loop threshold corrections generates two-loop terms which have to be added to the non-logarithmic subtraction terms. For instance, in `FeynHiggs` the FO result is parametrized by default via $\overline{m}_t$ and v_{G_F}, while the one- and two-loop threshold corrections to $\lambda(M_{\rm SUSY})$ are expressed in terms of $m_t^{\overline{\rm MS},\rm SM}(M_{\rm SUSY})$ and $v_{\overline{\rm MS},\rm SM}(M_{\rm SUSY})$. The one-loop threshold correction to λ of order $\mathcal{O}(\alpha_t^2)$ generates the following non-logarithmic terms in the expression for the mass of the SM-like Higgs

[50] We only have to subtract the non-SM corrections since the SM terms as well as the terms of the form $\widehat{\Sigma}^{\rm SM\prime}_{hh}(m_h^2)\widehat{\Sigma}^{\rm non-SM}_{hh}(m_h^2) + \widehat{\Sigma}^{\rm SM}_{hh}(m_h^2)\widehat{\Sigma}^{\rm n/SM\prime}_{hh}(m_h^2)$ are generated by solving the pole eq in Eq. (4.3.1) and do not lead to any double counting.

boson,

$$\begin{aligned}
\left[M_h^{2,\mathrm{EFT}}\right]_{\mathrm{non-log}} \supset\; & 12\,\kappa\, v^2_{\overline{\mathrm{MS}},\mathrm{SM}}(M_t)\left(y_t^{\overline{\mathrm{MS}},\mathrm{SM}}(M_{\mathrm{SUSY}})\right)^4\left(\frac{X_t^2}{M_{\mathrm{SUSY}}^2}-\frac{X_t^4}{12\,M_{\mathrm{SUSY}}^4}\right) = \\
&= 12\,\kappa\, v^2_{\overline{\mathrm{MS}},\mathrm{SM}}(M_t)\left[\frac{m_t^{\overline{\mathrm{MS}},\mathrm{SM}}(M_{\mathrm{SUSY}})}{v_{\overline{\mathrm{MS}},\mathrm{SM}}(M_{\mathrm{SUSY}})}\right]^4\left(\frac{X_t^2}{M_{\mathrm{SUSY}}^2}-\frac{X_t^4}{12\,M_{\mathrm{SUSY}}^4}\right) = \\
&= 12\,\kappa\frac{\overline{m}_t^4}{v^2_{\overline{\mathrm{MS}},\mathrm{SM}}(M_t)}\left(\frac{X_t^2}{M_{\mathrm{SUSY}}^2}-\frac{X_t^4}{12\,M_{\mathrm{SUSY}}^4}\right)+\mathrm{logs} = \\
&= 12\,\kappa\frac{\overline{m}_t^4}{v^2_{G_F}}\left(1-(\delta^{(1)}v^2)^{\mathrm{SM}}\right)\left(\frac{X_t^2}{M_{\mathrm{SUSY}}^2}-\frac{X_t^4}{12\,M_{\mathrm{SUSY}}^4}\right)+\mathrm{logs}+\ldots,
\end{aligned} \tag{4.3.6}$$

where the ellipsis denotes terms of three-loop order and higher, and $(\delta^{(1)}v^2)^{\mathrm{SM}}$ is a threshold correction to the vacuum expectation value at the electroweak scale (see Eqs. (4.2.6) and (3.2.76)). The higher-order logarithmic terms (denoted as "logs" in Eq. (4.3.6)) come from the running of $m_t^{\overline{\mathrm{MS}},\mathrm{SM}}$ and $v_{\overline{\mathrm{MS}},\mathrm{SM}}$ from M_{SUSY} down to M_t. At the one- and two-loop level, they are included in the logarithmic subtraction terms. The remaining terms in the fourth line of Eq. (4.3.6) have to be subtracted, i.e.

$$\left[\Delta M_h^2\right]_{\mathrm{sub}}^{\mathrm{non-log}} \supset -12\,\kappa\frac{\overline{m}_t^4}{v^2_{G_F}}\left(1-(\delta^{(1)}v^2)^{\mathrm{SM}}\right)\left(\frac{X_t^2}{M_{\mathrm{SUSY}}^2}-\frac{X_t^4}{12\,M_{\mathrm{SUSY}}^4}\right). \tag{4.3.7}$$

`FeynHiggs` also allows the use of the OS top mass m_t^{OS} in the fixed-order result. In this case an additional term has to be added to Eq. (4.3.7) due to the reparametrization $\overline{m}_t \leftrightarrow m_t^{\mathrm{OS}}$.

As we already mentioned in Sec. 3.2.2, we use either the OS or the $\overline{\mathrm{DR}}$ scheme for the renormalization of the top/stop sector of the MSSM. If the $\overline{\mathrm{DR}}$ scheme is used, then we will assume that the parameters $(m_{\tilde{t}_L}, m_{\tilde{t}_R}, X_t)$ are given at the scale M_{SUSY} and can be directly used in the EFT calculation. If they are given in the OS scheme, they have to be converted to the $\overline{\mathrm{DR}}$ scheme at this scale. In this case a bit more attention is needed since the formula which relates a parameter in the two schemes may contain large logarithms in the heavy SUSY limit, $v/M_{\mathrm{SUSY}} \to 0$. The explicit evaluation of the one-loop counterterms $\delta^{(1)}m^2_{\tilde{t}_1}$, $\delta^{(1)}m^2_{\tilde{t}_2}$ and $\delta^{(1)}m^2_{\tilde{t}_{12}}$ at $\mathcal{O}(\alpha_t)$, $\mathcal{O}(\alpha_b)$, and $\mathcal{O}(\alpha_s)$ shows that only the conversion formula for X_t contains large logarithms (the explicit expressions are given in the App. B.) As argued in [21,22], one only has to take into account the logarithmic terms in the relation between X_t^{OS} and $X_t^{\overline{\mathrm{DR}}}(M_{\mathrm{SUSY}})$. Indeed, this one-loop formula correctly reproduces large logarithms which are present in the fixed-order calculation, while the one-loop non-logarithmic terms contribute at the same order as the subleading logarithmic terms in the two-loop conversion

formula for X_t. The two-loop relation between $X_t^{\rm OS}$ and $X_t^{\overline{\rm DR}}$ in the heavy SUSY limit is however not known in the literature. [51]

Finally, the numerical iterative solution of the Eq. (4.3.1) requires the employment of the so-called "heavy-OS" scheme for the Higgs field renormalization constants. This scheme helps to cancel the momentum-dependent contributions of heavy particles that arise in the iterative solution of Eq. (4.3.1). More details on this issue can be found in [24].

4.4 Conversion of X_t

The counterterm for the off-diagonal entry of the stop mass matrix, $m_t X_t$, is given in Eq. (3.2.31a) in terms of the counterterms $\delta^{(1)}m^2_{\tilde{t}_1}$, $\delta^{(1)}m^2_{\tilde{t}_2}$ and $\delta^{(1)}m^2_{\tilde{t}_{12}}$,

$$\delta^{(1)}(m_t X_t) = \mathbf{U}_{\tilde{t}_{11}}\mathbf{U}^*_{\tilde{t}_{12}}\left(\delta^{(1)}m^2_{\tilde{t}_1} - \delta^{(1)}m^2_{\tilde{t}_2}\right) + \delta^{(1)}m^2_{\tilde{t}_{12}}\mathbf{U}_{\tilde{t}_{21}}\mathbf{U}^*_{\tilde{t}_{12}} + \delta^{(1)}m^2_{\tilde{t}_{21}}\mathbf{U}_{\tilde{t}_{11}}\mathbf{U}^*_{\tilde{t}_{22}}. \tag{4.4.1}$$

In the EFT approach the X_t parameter is normally defined in the $\overline{\rm DR}$ scheme [52] at the scale $M_{\rm SUSY}$, while in the FO approach in the case of on-shell input parameters we use the relations in Eq. (3.2.29)–Eq. (3.2.30) for $\delta^{(1)}m^2_{\tilde{t}_1}$, $\delta^{(1)}m^2_{\tilde{t}_2}$ and $\delta^{(1)}m^2_{\tilde{t}_{12}}$. The relation between the two schemes can be written as follows (see Eq. (3.1.32)),

$$(m_t X_t)^{\rm OS} = (m_t X_t)^{\overline{\rm DR}}(M_{\rm SUSY}) - \delta^{(1)}(m_t X_t)\Big|_{\rm fin}. \tag{4.4.2}$$

Dividing both sides of this equation by $m_t^{\rm OS}$ we obtain,

$$X_t^{\rm OS} = X_t^{\overline{\rm DR}}(M_{\rm SUSY})\,\frac{m_t^{\overline{\rm DR},\rm MSSM}(M_{\rm SUSY})}{m_t^{\rm OS}} - \frac{1}{m_t^{\rm OS}}\,\delta^{(1)}(m_t X_t)\Big|_{\rm fin}. \tag{4.4.3}$$

Both terms on the right-hand side of the Eq. (4.4.3) can contain large logarithms but these logarithms are of a different origin.

Let us start our discussion with the first term. The relation between the OS and the running top mass can be derived using a procedure similar to the one used in Sec. 3.2.4 for the derivation of Δ_b terms. Namely,

$$\begin{aligned} &m_t^{\overline{\rm DR},\rm MSSM}(M_{\rm SUSY}) = m_t^{\rm OS} + \delta^{(1)}m_t^{\rm OS}\Big|_{\rm fin} = \\ &= m_t^{\rm OS} + (\delta^{(1)}m_t^{\rm OS})^{\rm SM}\Big|_{\rm fin} + (\delta^{(1)}m_t^{\rm OS})^{\rm n/SM}\Big|_{\rm fin}, \end{aligned} \tag{4.4.4}$$

[51] Two-loop relations between running and pole squark masses have been computed in Ref. [222]. However, the mixing of squarks is neglected in this paper. The two-loop counterterms $\delta^{(1)}m^2_{\tilde{t}_1}$, $\delta^{(1)}m^2_{\tilde{t}_2}$ and $\delta^{(1)}m^2_{\tilde{t}_{12}}$ can also be computed by means of the `TLDR` package [223]. This however lies beyond the scope of this thesis.

[52] In Chapter 8 we will discuss an alternative renormalization scheme: the $\overline{\rm MDR}$ scheme.

where the finite part of the OS counterterm has been split into a SM and a non-SM part. The latter contains contributions from diagrams with at least one non-SM particle. Both parts have to be evaluated at the renormalization scale $Q = M_{\rm SUSY}$. The non-SM part does not contain large logarithms (see Eqs. (B.1.2e), (B.1.5e), (B.2.2d) and (B.2.4d)). On the other hand the SM part contains contributions only from the light particles – quarks, gluons, SM-like Higgs and Goldstones – evaluated at the heavy scale, $Q = M_{\rm SUSY}$. Therefore, it contains large logarithms. They can be extracted from Eqs. (B.1.2f) and (B.1.5f) by replacing each Passarino-Veltman function B_0 [224, 225] in the mentioned expressions by a large logarithm. This follows from the fact that the Passarino-Veltman functions used in Eqs. (B.1.2f) and (B.1.5f) contain the following renormalization-scale-dependent pieces,[53]

$$\log\frac{Q^2}{m_q^2} \quad \text{where} \quad q = t, b \quad \text{or} \quad \log\frac{Q^2}{|m_t^2 - m_b^2|}\,. \tag{4.4.5}$$

Since $Q = M_{\rm SUSY}$, these terms give rise to large logarithms. The described procedure yields,

$$(\delta^{(1)} m_t^{\rm OS})^{\rm SM}\big|_{\rm fin} \supset m_t^{\rm OS}\left(1 - \left(\frac{\alpha_s}{\pi} - \frac{3\alpha_t}{16\pi} + \frac{3\alpha_b}{16\pi}\right)\log\frac{M_{\rm SUSY}^2}{M_t^2} + \text{nonlog}\right), \tag{4.4.6}$$

where "nonlog" is used as a placeholder for terms which do not contain large logarithms, but can contain "small logarithms", i.e. logarithms of the top mass over the bottom mass or of the ratios $m_A/M_{\rm SUSY}$, $|M_3|/M_{\rm SUSY}$, $|\mu|/M_{\rm SUSY}$. As we already mentioned in Sec. 3.2.1, sometimes it is preferable to use the running $\overline{\rm MS}$ mass, defined in the SM, $\overline{m}_t \equiv m_t^{\overline{\rm MS},{\rm SM}}(M_t)$. This case corresponds to a different definition of X_t, which we will denote as $X_t^{\rm FO}$,

$$X_t^{\rm FO} = X_t^{\overline{\rm DR}}(M_{\rm SUSY})\,\frac{m_t^{\overline{\rm DR},{\rm MSSM}}(M_{\rm SUSY})}{\overline{m}_t} - \frac{1}{\overline{m}_t}\,\delta^{(1)}(m_t X_t)\big|_{\rm fin}\,. \tag{4.4.7}$$

The quantity $\delta^{(1)}(m_t X_t)$ is proportional to the top mass at the one-loop level in the heavy SUSY limit (see Eqs. (B.1.2d), (B.1.5d), (B.2.2c) and (B.2.4c)). Therefore, the top quark mass drops out of the ratio $\frac{1}{m_t}\delta^{(1)}(m_t X_t)$ up to higher-order terms. This means that this ratio is the same for both $m_t^{\rm OS}$ and $m_t^{\overline{\rm MS},{\rm SM}}(M_t)$. The first term on the right-hand side of Eq. (4.4.7) differs from the corresponding term in Eq. (4.4.3). However, the relation between $\overline{m}_t$ and $m_t^{\rm OS}$ does not contain large logarithms, since it arises from the diagrams with light particles evaluated at M_t. Therefore, large logarithms in the relation between $X_t^{\rm FO}$ and $X_t^{\overline{\rm DR}}(M_{\rm SUSY})$ are the same as in Eq. (4.4.6). In fact, these logarithms can be extracted from the running of

[53] The explicit form of Passarino-Veltman functions can be found e.g. in [146].

the top mass in the SM. They can be resummed by using the top mass defined in the $\overline{\text{MS}}$ or the $\overline{\text{DR}}$ scheme at M_{SUSY} either in the full MSSM or in the SM.

Now let us proceed with the second term in Eq. (4.4.3). We will now demonstrate that this term contains large logarithms if the soft-breaking masses of the squarks are degenerate,

$$m_{\tilde{t}_L} = m_{\tilde{t}_R} = m_{\tilde{b}_L} = m_{\tilde{b}_R} \equiv M_{\text{SUSY}}. \tag{4.4.8}$$

Explicit evaluation of the counterterm $\delta^{(1)}(m_t X_t)\big|_{\text{fin}}$ in this case shows that it contains the following terms in the limit $M_{\text{SUSY}} \gg M_t$ (see Eq. (B.2.2c)),

$$\begin{aligned}
\delta^{(1)}(m_t X_t)\big|_{\text{fin}} &= \frac{\alpha_t}{4\pi}\, m_t X_t\, |\widehat{X}_t|^2\, \log\frac{M_{\text{SUSY}}^2}{2m_t|X_t|} \\
&+ \frac{e^{i\phi_{X_t}} M_{\text{SUSY}}}{64\pi^2 v^2} \left(m_t|\widehat{X}_t| - m_b|\widehat{X}_b|\right)^3 \log\frac{M_{\text{SUSY}}^2}{|m_t|X_t| - m_b|X_b||} \\
&+ \frac{e^{i\phi_{X_t}} M_{\text{SUSY}}}{64\pi^2 v^2} \left(m_t|\widehat{X}_t| + m_b|\widehat{X}_b|\right)^3 \log\frac{M_{\text{SUSY}}^2}{|m_t|X_t| + m_b|X_b||} + \text{nonlog} = \\
&= \frac{3\alpha_t}{16\pi}\, m_t X_t\, |\widehat{X}_t|^2 \log\frac{M_{\text{SUSY}}^2}{M_t^2} + \frac{3\alpha_b}{16\pi}\, m_t X_t\, |\widehat{X}_b|^2 \log\frac{M_{\text{SUSY}}^2}{M_t^2} + \text{nonlog},
\end{aligned} \tag{4.4.9}$$

where $\widehat{X}_{t,b} = X_{t,b}/M_{\text{SUSY}}$. The large logarithms in Eq. (4.4.9) arise from diagrams involving the Goldstone bosons (see Fig. 4.1).[54] After evaluating these diagrams using

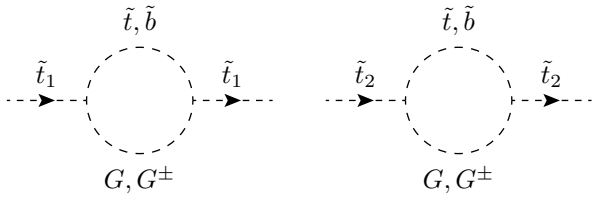

Figure 4.1: Diagrams generating the large logarithms in Eq. (4.4.9).

`FeynArts` [226] and `FormCalc` [227] in the gaugeless limit we found that the following terms transform into the first three lines of Eq. (4.4.9) after expansion in the ratio v/M_{SUSY},

$$\begin{aligned}
\delta^{(1)}(m_t X_t)\big|_{\text{fin}} \supset \frac{\alpha_t}{8\pi}\, m_t X_t\, \frac{|X_t|^2}{m_{\tilde{t}_1}^2 - m_{\tilde{t}_2}^2} \Big[&\text{Re}\{B_0(m_{\tilde{t}_1}^2, 0, m_{\tilde{t}_1}^2)\} - \text{Re}\{B_0(m_{\tilde{t}_2}^2, 0, m_{\tilde{t}_1}^2)\} \\
+ \;&\text{Re}\{B_0(m_{\tilde{t}_1}^2, 0, m_{\tilde{t}_2}^2)\} - \text{Re}\{B_0(m_{\tilde{t}_2}^2, 0, m_{\tilde{t}_2}^2)\} + \\
+ \Big(&\text{Re}\{B_0(m_{\tilde{t}_1}^2, 0, m_{\tilde{b}_1}^2)\} - \text{Re}\{B_0(m_{\tilde{t}_2}^2, 0, m_{\tilde{b}_1}^2)\}\Big) |\mathbf{U}_{\tilde{b},11}|^2 \\
+ \Big(&\text{Re}\{B_0(m_{\tilde{t}_1}^2, 0, m_{\tilde{b}_2}^2)\} - \text{Re}\{B_0(m_{\tilde{t}_2}^2, 0, m_{\tilde{b}_2}^2)\}\Big) |\mathbf{U}_{\tilde{b},12}|^2\Big]
\end{aligned} \tag{4.4.10}$$

[54] The counterterms $\delta^{(1)} m_{\tilde{t}_{12}}^2$ and $\delta^{(1)} m_{\tilde{t}_{21}}^2$ do not give rise to the large logarithms in Eq. (4.4.9).

$$
\begin{aligned}
&+\frac{\alpha_b}{8\pi}\, m_t X_t\, \frac{|X_b|^2}{m^2_{\tilde{t}_1}-m^2_{\tilde{t}_2}}\Big[\Big(\mathrm{Re}\{B_0(m^2_{\tilde{t}_1},0,m^2_{\tilde{b}_1})\}-\mathrm{Re}\{B_0(m^2_{\tilde{t}_2},0,m^2_{\tilde{b}_1})\}\Big)\,|\mathbf{U}_{\tilde{b},12}|^2\\
&\quad+\Big(\mathrm{Re}\{B_0(m^2_{\tilde{t}_1},0,m^2_{\tilde{b}_2})\}-\mathrm{Re}\{B_0(m^2_{\tilde{t}_2},0,m^2_{\tilde{b}_2})\}\Big)\,|\mathbf{U}_{\tilde{b},11}|^2\Big]\\
&-\frac{\alpha_b}{8\pi}\, m_t X_t\, \frac{|X_b|^2}{m^2_{\tilde{b}_1}-m^2_{\tilde{b}_2}}\Big[\mathrm{Re}\{B_0(m^2_{\tilde{t}_1},0,m^2_{\tilde{b}_1})\}-\mathrm{Re}\{B_0(m^2_{\tilde{t}_1},0,m^2_{\tilde{b}_2})\}\\
&\quad+\mathrm{Re}\{B_0(m^2_{\tilde{t}_2},0,m^2_{\tilde{b}_1})\}-\mathrm{Re}\{B_0(m^2_{\tilde{t}_2},0,m^2_{\tilde{b}_2})\}\Big],
\end{aligned}
$$

where $B_0(p^2,m_1^2,m_2^2)$ are Passarino-Veltman functions. Note that this expression involves only differences of the B_0 functions, therefore it does not depend on the renormalization scale. This means that the large logarithms arising from these terms have a different origin compared to the logarithm in Eq. (4.4.6).

Now let us expand the expression Eq. (4.4.10) in the ratio $v/M_{\rm SUSY}$ in the scenario where the soft-breaking masses of stops and sbottoms are all different [55]

$$
m_{\tilde{t}_L}\neq m_{\tilde{t}_R},\ m_{\tilde{b}_L}\neq m_{\tilde{b}_R},\ m_{\tilde{t}_R}\neq m_{\tilde{b}_R}. \tag{4.4.11}
$$

To obtain the leading term in this expansion, we can simply perform the following replacements in the Eq. (4.4.10),

$$
\begin{aligned}
&m_{\tilde{t}_1}\to m_{\tilde{t}_L},\quad m_{\tilde{t}_2}\to m_{\tilde{t}_R},\quad m_{\tilde{b}_1}\to m_{\tilde{t}_L},\quad m_{\tilde{b}_2}\to m_{\tilde{b}_R},\\
&|\mathbf{U}_{\tilde{b},11}|\to 1,\quad |\mathbf{U}_{\tilde{b},12}|\to 0,\quad |\mathbf{U}_{\tilde{b},21}|\to 0,\quad |\mathbf{U}_{\tilde{b},22}|\to 1.
\end{aligned} \tag{4.4.12}
$$

After applying these replacement rules to the expression given in the Eq. (4.4.10), we obtain

$$
\begin{aligned}
&\delta^{(1)}(m_tX_t)\Big|_{\rm fin}\supset \frac{\alpha_t}{8\pi}\, m_tX_t\,|\widehat{X}_t|^2\left(\frac{2m_{\tilde{t}_L}}{m_{\tilde{t}_R}}\log\frac{m^2_{\tilde{t}_L}}{|m^2_{\tilde{t}_L}-m^2_{\tilde{t}_R}|}+\frac{m_{\tilde{t}_R}}{m_{\tilde{t}_L}}\log\frac{m^2_{\tilde{t}_R}}{|m^2_{\tilde{t}_L}-m^2_{\tilde{t}_R}|}\right)\\
&+\frac{\alpha_b}{8\pi}\, m_tX_t\,|\widehat{X}_b|^2\left(-\frac{m_{\tilde{b}_R}(m^2_{\tilde{b}_R}-2m^2_{\tilde{t}_L}+m^2_{\tilde{t}_R})}{m_{\tilde{t}_L}(m^2_{\tilde{t}_L}-m^2_{\tilde{t}_R})}\log\frac{m^2_{\tilde{b}_R}}{|m^2_{\tilde{b}_R}-m^2_{\tilde{t}_L}|}\right.\\
&+\frac{m_{\tilde{b}_R}m_{\tilde{t}_L}(m^2_{\tilde{b}_R}-m^2_{\tilde{t}_R})^2}{(m^2_{\tilde{b}_R}-m^2_{\tilde{t}_L})m^2_{\tilde{t}_R}(m^2_{\tilde{t}_L}-m^2_{\tilde{t}_R})}\log\frac{m^2_{\tilde{b}_R}}{|m^2_{\tilde{b}_R}-m^2_{\tilde{t}_R}|}\\
&\left.-\frac{m_{\tilde{b}_R}m_{\tilde{t}_L}(m^2_{\tilde{t}_L}-m^2_{\tilde{t}_R})}{m^2_{\tilde{t}_R}(m^2_{\tilde{b}_R}-m^2_{\tilde{t}_L})}\log\frac{m^2_{\tilde{t}_L}}{|m^2_{\tilde{t}_L}-m^2_{\tilde{t}_R}|}+\frac{2m_{\tilde{b}_R}m_{\tilde{t}_L}}{m^2_{\tilde{b}_R}-m^2_{\tilde{t}_L}}\log\frac{m^2_{\tilde{b}_R}}{m^2_{\tilde{t}_L}}\right)\ ,
\end{aligned} \tag{4.4.13}
$$

where

$$
\widehat{X}_t=\frac{X_t}{\sqrt{m_{\tilde{t}_L}m_{\tilde{t}_R}}},\quad \widehat{X}_b=\frac{X_b}{\sqrt{m_{\tilde{b}_L}m_{\tilde{b}_R}}}\ . \tag{4.4.14}
$$

[55] Recall that $m_{\tilde{t}_L}=m_{\tilde{b}_L}$ due to $SU(2)_L$ invariance.

We note that contrary to the expression given in the Eq. (4.4.9), this expression does not contain any large logarithms $\log \frac{M_{\rm SUSY}^2}{M_t^2}$. This suggests that there is no smooth limit

$$m_{\tilde{t}_R} \to m_{\tilde{t}_L}, \quad m_{\tilde{b}_R} \to m_{\tilde{t}_L} \tag{4.4.15}$$

between the approximate expressions (4.4.9) and (4.4.13). Explicit calculation shows that $\delta^{(1)}(m_t X_t)\big|_{\rm fin}$ does not contain large logarithms also in the case

$$m_{\tilde{b}_R} = m_{\tilde{t}_R},\ m_{\tilde{t}_L} \neq m_{\tilde{t}_R}\ (\text{hence } m_{\tilde{b}_L} \neq m_{\tilde{b}_R}). \tag{4.4.16}$$

For MSSM scenarios with

$$m_{\tilde{b}_L} = m_{\tilde{b}_R},\ m_{\tilde{t}_L} \neq m_{\tilde{t}_R} \tag{4.4.17}$$

the quantity $\delta^{(1)}(m_t X_t)\big|_{\rm fin}$ contains the following large logarithm,

$$\delta^{(1)}(m_t X_t)\Big|_{\rm fin} \supset \frac{\alpha_b}{16\pi}\, m_t X_t\, \frac{|X_b|^2}{m_{\tilde{b}_L}^2} \log \frac{M_{\rm SUSY}^2}{M_t^2}. \tag{4.4.18}$$

Finally, in the case

$$m_{\tilde{t}_L} = m_{\tilde{t}_R},\ m_{\tilde{b}_L} \neq m_{\tilde{b}_R} \tag{4.4.19}$$

the large logarithm in the conversion formula takes the following form,

$$\delta^{(1)}(m_t X_t)\Big|_{\rm fin} \supset \frac{3\alpha_t}{16\pi}\, m_t X_t\, \frac{|X_t|^2}{m_{\tilde{t}_L}^2} \log \frac{M_{\rm SUSY}^2}{M_t^2}. \tag{4.4.20}$$

The unexpanded formula does not show this behavior. To illustrate it, we consider the MSSM scenario in which $\mu = 10$ TeV, all soft-breaking masses except for $m_{\tilde{t}_R}$, are equal to $M_{\rm SUSY} = 10$ TeV, the stop mixing parameter equals $X_t = M_{\rm SUSY}$ and $\tan\beta = 10$. In Fig. 4.2 we show the behaviour of the counterterm $\delta^{(1)}(m_t X_t)$, normalized by the top mass m_t and the soft mass $m_{\tilde{t}_L}$ neglecting corrections proportional to the bottom Yukawa and the strong gauge coupling for simplicity. The red curve corresponds to the full expression for $\delta^{(1)}(m_t X_t)/(m_t m_{\tilde{t}_L})$ of order $\mathcal{O}(\alpha_t)$. The blue curve corresponds to the approximate expression in Eq. (B.2.2c) and the green curve shows the behaviour of Eq. (B.1.2d). Since the SUSY scale is much heavier than the EW scale, the green curve approximates well the behavior of the red one for $\left|\frac{m_{\tilde{t}_R}}{m_{\tilde{t}_L}} - 1\right| \gtrsim 0.05$. On the other hand it starts to deviate from the red one for values of $m_{\tilde{t}_R}/m_{\tilde{t}_L}$ close to one, and for $m_{\tilde{t}_R}/m_{\tilde{t}_L} = 1$ its value is not defined. At this point the full expression is well approximated by the blue curve.

The one-loop contribution to the counterterm $\delta^{(1)}(m_t X_t)$ proportional to the strong gauge coupling does not exhibit the behavior described above. More specifically, there is no large logarithm emerging in the $\mathcal{O}(\alpha_s)$ expression for $\delta^{(1)}(m_t X_t)\big|_{\rm fin}$ in the heavy

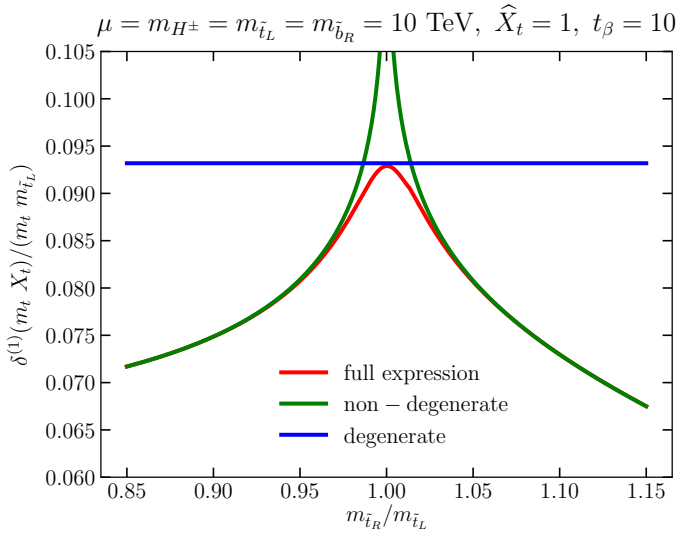

Figure 4.2: Numerical comparison of different expanded expressions for $\delta^{(1)}(m_t X_t)/(m_t m_{\tilde{t}_L})$.

SUSY limit regardless whether the squark soft-breaking masses are degenerate or non-degenerate. Furthermore, for the corrections of order $\mathcal{O}(\alpha_s)$ a smooth transition between the two mentioned scenarios exists (see Eq. (B.1.5d) and Eq. (B.2.4c)).

To summarize, the conversion formula for the stop mixing parameter X_t in the heavy SUSY limit for the case of the scenarios with fully degenerate squark soft-breaking masses defined in Eq. (4.4.8) reads,[56]

$$X_t^{\overline{\rm DR}}(M_{\rm SUSY}) = X_t^{\rm OS}\left\{1 + \left[\frac{\alpha_s}{\pi} - \frac{3\alpha_t}{16\pi}\left(1 - \frac{|X_t|^2}{M_{\rm SUSY}^2}\right) + \frac{3\alpha_b}{16\pi}\left(1 + \frac{|X_b|^2}{M_{\rm SUSY}^2}\right)\right]\log\frac{M_{\rm SUSY}^2}{M_t^2}\right\} + \text{nonlog}. \tag{4.4.21}$$

For the case where the stop soft-breaking masses are degenerate, but the sbottom soft-breaking masses are non-degenerate (see Eq. (4.4.19)), this formula takes the form,

$$X_t^{\overline{\rm DR}}(M_{\rm SUSY}) = X_t^{\rm OS}\left\{1 + \left[\frac{\alpha_s}{\pi} - \frac{3\alpha_t}{16\pi}\left(1 - \frac{|X_t|^2}{m_{\tilde{t}_L}^2}\right) + \frac{3\alpha_b}{16\pi}\right]\log\frac{M_{\rm SUSY}^2}{M_t^2}\right\} + \text{nonlog}. \tag{4.4.22}$$

If instead the sbottom soft-breaking masses are equal to each other but the stop soft-breaking masses are non-degenerate (see Eq. (4.4.17)), the logarithmic terms in

[56] We use the superscript "OS" in this formula, but it also holds if the running top mass $\overline{m}_t$ is used in the FO calculation.

the conversion formula read,

$$X_t^{\overline{\rm DR}}(M_{\rm SUSY}) = X_t^{\rm OS}\left\{1 + \left[\frac{\alpha_s}{\pi} - \frac{3\alpha_t}{16\pi} + \frac{3\alpha_b}{16\pi}\left(1 + \frac{|X_b|^2}{3m^2_{\tilde{b}_R}}\right)\right]\log\frac{M^2_{\rm SUSY}}{M_t^2}\right\} + \text{nonlog.} \tag{4.4.23}$$

In all other cases the conversion formula reads,

$$X_t^{\overline{\rm DR}}(M_{\rm SUSY}) = X_t^{\rm OS}\left\{1 + \left[\frac{\alpha_s}{\pi} - \frac{3\alpha_t}{16\pi} + \frac{3\alpha_b}{16\pi}\right]\log\frac{M^2_{\rm SUSY}}{M_t^2}\right\} + \text{nonlog.} \tag{4.4.24}$$

As we already mentioned above, the large logarithms originating from the top mass counterterm in Eqs. (4.4.21) – (4.4.24), i.e. the ones which are proportional only to the coupling constants α_t, α_b or α_s and not to the mixing parameters X_t ot X_b, arise from the RGE running of the top mass from $M_{\rm SUSY}$ to M_t. By using the top mass at the scale $M_{\rm SUSY}$ in the FO calculation this logarithm can be resummed to all orders. The situation with the large logarithms that are present only in certain "degenerate" scenarios and are absent in the others is much more difficult.[57] This logarithm is not connected to any RGE running and therefore other techniques have to be employed to resum it. Currently, the hybrid approach, as implemented into `FeynHiggs`, uses Eq. (4.4.21) with $\alpha_b \to 0$ in the hybrid approach if the input parameters for the top/stop sector are given in the OS scheme.[58] If the scenario under consideration involves non-degenerate stop breaking masses, this formula generates incorrect logarithmic terms at the three-loop level and above. The correct treatment of these logarithms lies beyond the scope of this thesis and is left for future study.

[57] Since the mentioned terms arise from the diagrams with virtual Goldstone bosons (see Fig. 4.1) one may ask a question if these terms are gauge-dependent. In this thesis, the expression (4.4.9) was derived in the gaugeless limit, so the mass of the Goldstone bosons equals zero in any R_ξ gauge. However, we also verified that this expression remains gauge-independent beyond the gaugeless limit.

[58] See Sec. 5.1 for a review of the current status of logarithmic resummation in `FeynHiggs`.

Chapter 5

Resummation of bottom quark contributions

In this Chapter, we discuss the resummation of logarithms controlled by the bottom Yukawa coupling and its combination with the existing fixed-order calculation. We find that the usage of the MSSM $\overline{DR}$ bottom mass is a suitable choice for merging the FO and the EFT results. In addition to that, we discuss the determination of the bottom Yukawa coupling in the MSSM itself.

5.1 Higgs mass calculation in `FeynHiggs`

`FeynHiggs` [21–23, 35, 90, 187, 228–231] is a `Fortran` code for calculating the MSSM Higgs boson masses. The latest version of the code, `FeynHiggs-2.16.0`, incorporates full one-loop fixed-order contributions [90] to the Higgs masses as well as two-loop corrections of order $\mathcal{O}(m_t^2\alpha_t\alpha_s + m_b^2\alpha_b\alpha_s + m_t^2\alpha_t^2 + m_t^2\alpha_t\alpha_b + m_b^2\alpha_t\alpha_b + m_b^2\alpha_b^2)$ computed in the gaugeless limit and in the approximation of vanishing external momenta [34, 129, 147, 148, 150].[59] For these corrections the following renormalization scheme is employed. The Higgs sector is renormalized in the mixed OS/$\overline{\text{DR}}$ scheme (see Sec. 3.2.1), the top/stop sector is renormalized in the OS scheme (see Sec. 3.2.2), and the bottom/sbottom is renormalized using the scheme denoted as **RS1** in Sec. 3.2.3. The Higgsino mass parameter μ and the ratio of vacuum expectation values of the Higgs doublets, $\tan\beta = v_2/v_1$ are by default renormalized in the $\overline{\text{DR}}$ scheme at the scale M_{SUSY}.[60] From version `2.14.0` on, an optional $\overline{\text{DR}}$ renormalization of the scalar top sector is possible. In this case, stop breaking masses $m_{\tilde{t}_L}$ and $m_{\tilde{t}_R}$ as well as stop mixing parameter X_t are defined in the $\overline{\text{DR}}$ scheme at M_{SUSY}.

[59] The two-loop corrections for non-zero external momentum have been computed in the rMSSM [211] and in the complex MSSM (cMSSM) [7, 211, 212].

[60] If the resummation of logarithm in case of $m_A \ll M_{\text{SUSY}}$ is invoked (`loglevel = 4`), $\tan\beta$ is defined in THDM at m_A.

Starting from version `2.10.0`, the code allows to resum large logarithms to all orders in the hybrid approach, as described in Sec. 4.3. The latest version of `FeynHiggs` allows the matching of the SM, split-SUSY model and Two-Higgs-Doublet Model (THDM) with or without light electroweakinos [16] to the MSSM at M_{SUSY}. The tower of EFTs is built depending on the hierarchy of mass scales. For instance, the THDM is matched to the SM at scale m_A.

If the SM or the SM with electroweakinos is matched to the MSSM, the currently implemented EFT calculation resums leading and next-to-leading (LL and NLL) logarithms as well next-to-next-to-leading logarithms (NNLL) in the limit of vanishing electroweak gauge couplings. This implies that the full one-loop threshold corrections of order $\mathcal{O}(\alpha_t^2 + \alpha_t\alpha)$ together with two-loop corrections of order $\mathcal{O}(\alpha_t^3 + \alpha_t^2\alpha_s)$ and the RGEs up to the three-loop order are implemented in the code.[61] So far, however, all corrections proportional to the bottom Yukawa coupling are set to zero.

5.2 Implementation of bottom Yukawa contributions

5.2.1 Fixed-order calculation

For our present study, we do not use the $\mathcal{O}(m_b^2\alpha_b\alpha_s + m_t^2\alpha_t\alpha_b + m_b^2\alpha_t\alpha_b + m_b^2\alpha_b^2)$ corrections already implemented in `FeynHiggs` [148, 149]. Instead, we employ the $\mathcal{O}(m_b^2\alpha_b\alpha_s + m_t^2\alpha_t\alpha_b + m_b^2\alpha_t\alpha_b + m_b^2\alpha_b^2)$ corrections presented in [9, 11].[62] These include also terms subleading in $\tan\beta$, allow for an easier control of the renormalization scheme and take $\mathcal{CP}$-violating phases fully into account. They will be part of an upcoming `FeynHiggs` release. For the present work, we evaluate them, however, externally and feed the numerical result back to `FeynHiggs`.[63]

In [9, 11] the corrections to the Higgs mass are computed in the scheme named **RS2** in Sec. 3.2.3: the stop masses and the stop mixing parameter are renormalized in the on-shell (OS) scheme. This also fixes the scheme for one of the sbottom masses. The other sbottom mass is defined in the on-shell scheme. The trilinear sbottom coupling, A_b, the Higgsino mass parameter, μ, and $\tan\beta$ are renormalized in the $\overline{\text{DR}}$ scheme. The result is parameterized in terms of the $\overline{\text{DR}}$ bottom mass of the MSSM.

[61] In case of THDM the NNLL resummation includes $\mathcal{O}(\alpha_t^2\alpha_s)$ threshold corrections to the quartic couplings at M_{SUSY} but does not include three-loop RGEs.
[62] The corrections computed in [11] also contain the momentum dependent pieces.
[63] In practice, we use the `FHAddSelf` functionality (see `feynhiggs.de`).

5.2.2 EFT calculation

At the stop mass scale, M_{SUSY}, all sfermions as well as the non-SM Higgs bosons are integrated out. After passing two additional independent thresholds for electroweakinos (charginos and neutralinos) and the gluino, the SM is recovered as EFT.

For the incorporation of the bottom Yukawa contributions, we aim to reach the same level of accuracy as for the other corrections. For implementing LL and NLL resummation, we include the bottom Yukawa contributions to the one-loop matching condition of the SM Higgs self-coupling, λ [13]. Also the two-loop RGEs are extended to include bottom Yukawa corrections. For the NNLL resummation, we implement the $\mathcal{O}(\alpha_b^2\alpha_s, (\alpha_t+\alpha_b)^3)$ threshold corrections for λ, which were derived in [15].[64] We also add the bottom Yukawa contributions to the three-loop SM RGEs in the limit of vanishing electroweak gauge couplings [232–236] and to the calculation of the SM $\overline{\text{MS}}$ vev. Threshold corrections for λ require computation of the MSSM bottom Yukawa coupling with Δ_b resummation. This procedure will be described in Sec. 5.2.4.

5.2.3 Combination in the hybrid approach

For the combination of the fixed-order and the EFT calculation, we follow the procedure described in Sec. 4.3. In order to ease this combination, we chose to define the sbottom input parameters in the same scheme in the fixed-order and the EFT calculations: We fix them in the $\overline{\text{DR}}$ scheme at the scale M_{SUSY}. Also $\tan\beta$ and μ are fixed in the $\overline{\text{DR}}$ scheme at the scale M_{SUSY}.

A complication arises through the use of the $\overline{\text{DR}}$ bottom quark mass in the EFT as well as the fixed-order calculation. After adding both results as shown in Eqs. (4.3.1) and (4.3.2) the Higgs pole masses are determined taking into account the momentum dependence of the fixed-order self-energy. As discussed in detail in [24], this momentum dependence comes only from SM-type corrections as well as contributions suppressed by the SUSY scale. To match the result of a pure EFT calculation, in which the Higgs pole mass is determined in the SM, we have to ensure that the SM-type corrections are evaluated using only SM quantities. The $\overline{\text{DR}}$ bottom quark mass, however, is a MSSM quantity. For this reason, we reparametrize the SM bottom quark contributions to the Higgs self-energies in terms of the SM $\overline{\text{MS}}$ bottom quark mass at the scale M_t. In our implementation it is achieved by subtracting the $\mathcal{O}(\alpha_b)$ self-energy $\widetilde{\Sigma}_{hh}^{\overline{\text{MS}},\text{SM}}(p^2)$, containing only the SM contributions (see Eq. (4.2.9)) and parametrized in terms of the MSSM bottom quark $m_b^{\overline{\text{DR}},\text{MSSM}}(M_{\text{SUSY}})$ and then adding back the same quantity but parametrized via $m_b^{\overline{\text{MS}},\text{SM}}(M_t)$. The explicit expression for the one-loop self-energy

[64] We independently calculated the same corrections and found agreement. See Chapter 6 for details

can be found with the help of `FeynArts` and `FormCalc`,

$$\widetilde{\Sigma}_{hh}^{\overline{\text{MS}},\text{SM}}(p^2) = \frac{3m_b^2}{16\pi^2 v^2}(p^2 - 4m_b^2)B_0(p^2, m_b^2, m_b^2). \tag{5.2.1}$$

Since the SM-like Higgs mass is determined via an iterative solution of the pole equation Eq. (4.1.8), the same procedure has to be applied to the derivative of $\widetilde{\Sigma}_{hh}^{\overline{\text{MS}},\text{SM}}(p^2)$ with respect to the external momentum. At the two-loop level, the $\mathcal{O}(m_b^2\alpha_b\alpha_s + m_t^2\alpha_t\alpha_b + m_b^2\alpha_t\alpha_b + m_b^2\alpha_b^2)$ self-energies computed in the SM and in the gaugeless limit are extracted from the code `FlexibleSUSY` [25, 27, 237, 238] and Refs. [239, 240]. The explicit expressions can be found in App. C.

In order to allow for an OS definition of the stop input parameters, a conversion of the OS parameters,[65] used in the fixed-order calculation, to the $\overline{\text{DR}}$ scheme, used in the EFT calculation, is necessary. As argued in Sec. 4.3, for this conversion only one-loop logarithmic terms should be taken into account. Only in the conversion formula for the stop mixing parameter, X_t, large logarithms appear. As was pointed out in Sec. 4.4, the conversion formula for X_t contains logarithms of two different origins: one of them comes from the RGE running of the top mass and another one originates from diagrams involving Goldstone bosons which are massless in the gaugeless limit. In Sec. 5.3, we will present the results for the SM-like Higgs boson mass in the case when all soft-breaking masses of the stop and sbottom sector are degenerate in masses. Therefore, we will make us of Eq. (4.4.21) to convert the stop mixing parameter X_t from the OS to the $\overline{\text{DR}}$ scheme.

In the next section we will consider the determination of the MSSM bottom Yukawa coupling in our EFT setup. This, in particular, requires the computation of the one-loop and two-loop Δ_b corrections which depend on $A_t^{\overline{\text{DR}}}(M_{\text{SUSY}})$. Since the Higgsino mass parameter μ and $\tan\beta$ are defined at M_{SUSY}, the conversion formula for A_t reads,

$$A_t^{\overline{\text{DR}}}(M_{\text{SUSY}}) = A_t^{\text{OS}} + X_t^{\overline{\text{DR}}}(M_{\text{SUSY}}) - X_t^{\text{OS}}, \tag{5.2.2}$$

where $X_t^{\overline{\text{DR}}}(M_{\text{SUSY}})$ is determined via Eq. (4.4.21).

Now we proceed with the explicit form for the subtraction terms proportional to the bottom Yukawa coupling and used to avoid double counting when merging the FO and the EFT calculations. As was pointed out in Sec. 4.2, the logarithmic subtraction terms can be obtained via iterative solution of the RGEs up to a certain order of perturbation theory. Since the bottom Yukawa coupling contributes at the

[65] As we discussed in Sec. 4.4, the OS definition of the stop mixing parameter X_t requires the OS definition of the $\delta m_{\tilde{t}_1}^2$, $\delta m_{\tilde{t}_2}^2$, $\delta m_{\tilde{t}_{12}}^2$ counterterms as well as of the top mass counterterm. In this Section, however, we will use a running top mass in the SM defined at M_t together with $\delta m_{\tilde{t}_1}^2$, $\delta m_{\tilde{t}_2}^2$, $\delta m_{\tilde{t}_{12}}^2$ defined OS. Strictly speaking, this choice corresponds to a different definition of X_t. However, in order to be consistent with the literature we will use the label "OS" also in this case.

one- and the two-loop level, we solve the system of RGEs only up to the two-loop level. The solution can be split into three parts,

$$\left[\Delta M_h^2\right]_{\rm sub}^{\rm log} = \left[\Delta M_h^2\right]_{\rm sub}^{\rm 1L,LL} + \left[\Delta M_h^2\right]_{\rm sub}^{\rm 2L,LL} + \left[\Delta M_h^2\right]_{\rm sub}^{\rm 2L,NLL}. \tag{5.2.3}$$

The one-loop leading logarithmic contribution reads,

$$\begin{aligned}\left[\Delta M_h^2\right]_{\rm sub}^{\rm 1L,LL} &= -2\,\lambda(M_t) v^2_{\overline{\rm MS},\rm SM}(M_t)\Big|_{\rm logs} = -2\,\lambda(M_t) v^2_{G_F}\Big|_{\rm logs} = \\ &= 2 v^2_{G_F}\beta_\lambda^{(1)}\kappa L = -6\kappa\frac{\overline{m}_b^2}{v^2_{G_F}}\left(2\overline{m}_b^2 - c^2_{2\beta} m_Z^2\right) L,\end{aligned} \tag{5.2.4}$$

where

$$\kappa = (16\pi^2)^{-1}, \quad L = \log\frac{M^2_{\rm SUSY}}{M_t^2}, \quad \overline{m}_b \equiv m_b^{\overline{\rm DR},\rm MSSM}(M_{\rm SUSY}), \tag{5.2.5}$$

and we omitted terms beyond the one-loop level. At the two-loop level the leading logarithmic terms have the following form (see Eq. (4.2.15)),

$$\left[\Delta M_h^2\right]_{\rm sub}^{\rm 2L,LL} = 2 v^2_{G_F}\beta_\lambda^{(1)}(M_{\rm SUSY})\kappa L - v^2_{G_F}\beta_\lambda^{(1,1)}(M_{\rm SUSY})\kappa L^2. \tag{5.2.6}$$

In this expression one has to take into account that the top mass entering $\beta_\lambda^{(1)}(M_{\rm SUSY})$ is the running mass defined at the scale $M_{\rm SUSY}$ in the SM, while the mass which enters the FO result is the SM top mass at the scale M_t, $m_t^{\overline{\rm MS},\rm SM}(M_t)$. The relation between the two masses contains a one-loop logarithm (and higher-order terms). The same argument applies to the vacuum expectation value, since the vev entering the right-hand side of Eq. (5.2.6) is the running vev at $M_{\rm SUSY}$, while the FO calculation uses v_{G_F}. The logarithmic terms in the relation between the mentioned parameters after insertion into $\beta_\lambda^{(1)}(M_{\rm SUSY})$ generate two-loop leading logarithms. The resulting explicit expression for the two-loop logarithms reads

$$\left[\Delta M_h^2\right]_{\rm sub}^{\rm 2L,LL} = 18\kappa^2\frac{\overline{m}_b^2}{v^4_{G_F}}\left(\overline{m}_b^4 - \overline{m}_b^2\overline{m}_t^2 + \overline{m}_t^4\right) L^2 - 96\kappa^2\frac{g_3^2\overline{m}_b^4}{v^2_{G_F}} L^2, \tag{5.2.7}$$

where

$$\overline{m}_t = m_t^{\overline{\rm MS},\rm SM}(M_t). \tag{5.2.8}$$

The two-loop next-to-leading logarithmic terms originate from the two-loop β-function for λ, $\beta_\lambda^{(2)}$, from the reparametrization of m_t and v in the one-loop threshold correction to $\lambda(M_{\rm SUSY})$ and m_b in $\beta_\lambda^{(1)}(M_{\rm SUSY})$, as well as from the one-loop conversion of the stop mixing parameter X_t if it is given in the OS scheme (see discussion in Sec. 4.4). Therefore, the explicit expression for the two-loop next-to-leading logarithms depends on the renormalization scheme used for the definition of X_t.

Here, we present the expressions in the special case

$$M_A = |M_3| = |\mu| = m_{\tilde{t}_L} = m_{\tilde{t}_R} = m_{\tilde{b}_R} \equiv M_{\rm SUSY}. \tag{5.2.9}$$

If X_t is renormalized in the OS scheme, the sub-leading logarithmic subtraction terms controlled by the bottom Yukawa coupling read[66]

$$\begin{aligned}\left[\Delta M_h^2\right]^{\rm 2L,NLL}_{\rm sub,OS} &= 3\kappa^2 \frac{\overline{m}_b^2\overline{m}_t^4}{v_{G_F}^4}\left(-10 + 6|\widehat{X}_t^{\rm OS}|^2 - |\widehat{X}_b|^2|\widehat{X}_t^{\rm OS}|^2(6 - |\widehat{X}_t^{\rm OS}|^2)\right) L \\ &+ 6\kappa^2 \frac{\overline{m}_b^4\overline{m}_t^2}{v_{G_F}^4}\left(3 + 4|\widehat{X}_t^{\rm OS}|^2 - 4|\widehat{X}_t^{\rm OS}||\widehat{Y}_t|\cos(\phi_{X_t} - \phi_{Y_t})\right. \\ &\left. + \frac{1}{t_\beta^2} + 12\log\frac{\overline{m}_t}{\overline{m}_b}\right) L + 6\kappa^2 \frac{\overline{m}_b^6}{v_{G_F}^4}\left(7 + 12\log\frac{\overline{m}_t}{\overline{m}_b} + 3t_\beta^2\right) L \\ &- 64\kappa^2 \frac{g_3^2\overline{m}_b^4}{v_{G_F}^2}\left(2 - |\widehat{X}_b|\cos(\phi_{X_b} - \phi_{M_3})\right) L,\end{aligned} \tag{5.2.10}$$

where $\widehat{Y}_t = \widehat{X}_t + \frac{2\widehat{\mu}^*}{\sin 2\beta}$ and $\phi_{X_t}, \phi_{Y_t}, \phi_{X_b}, \phi_{M_3}$ are the phases of the parameters X_t, Y_t, X_b and M_3, respectively. If X_t is renormalized in the $\overline{\rm DR}$ scheme at the scale $M_{\rm SUSY}$, we obtain

$$\begin{aligned}\left[\Delta M_h^2\right]^{\rm 2L,NLL}_{\rm sub,\overline{DR}} &= 3\kappa^2 \frac{\overline{m}_b^2\overline{m}_t^4}{v_{G_F}^4}\left(-10 + 6|\widehat{X}_t^{\overline{\rm DR}}|^2\right) L \\ &+ 6\kappa^2 \frac{\overline{m}_b^4\overline{m}_t^2}{v_{G_F}^4}\left(3 + 4|\widehat{X}_t^{\rm OS}|^2 - 4|\widehat{X}_t^{\rm OS}||\widehat{Y}_t|\cos(\phi_{X_t} - \phi_{Y_t})\right. \\ &\left. + \frac{1}{t_\beta^2} + 12\log\frac{\overline{m}_t}{\overline{m}_b}\right) L + 6\kappa^2 \frac{\overline{m}_b^6}{v_{G_F}^4}\left(7 + 12\log\frac{\overline{m}_t}{\overline{m}_b} + 3t_\beta^2\right) L \\ &- 64\kappa^2 \frac{g_3^2\overline{m}_b^4}{v_{G_F}^2}\left(2 - |\widehat{X}_b|\cos(\phi_{X_b} - \phi_{M_3})\right) L.\end{aligned} \tag{5.2.11}$$

A few comments are in order. First of all, different choices of the renormalization scheme for $\widehat{X}_t$ affect only the logarithmic terms proportional to $\overline{m}_b^2\overline{m}_t^4$. These terms, which are present in the first line of Eq. (5.2.10) and absent in Eq. (5.2.11), originate from the Goldstone boson contribution to the $\delta^{(1)}X_t$ counterterm (see Fig. 4.1). They are not related to the RGE running of the top-quark mass (see the discussion of this issue in Sec. 4.4). In particular, they vanish in scenarios with $m_{\tilde{b}_L} \neq m_{\tilde{b}_R}$.

Secondly, since the bottom mass is much smaller than the top-quark mass, the logarithmic terms proportional to it are numerically significant only if they are enhanced by powers of $\tan\beta$, X_b or Y_t. In this regard, we see that the only numerically significant terms are those which are contained in the next-to-leading logarithmic terms (and not in the leading one- and two-loop logs) and proportional to $\overline{m}_b^2\overline{m}_t^4$ in the

[66] As in Sec. 4.4, we define $\widehat{Y}_t = Y_t/M_{\rm SUSY}$, $\widehat{X}_t = X_t/M_{\rm SUSY}, \widehat{\mu} = \mu/M_{\rm SUSY}$

case of degenerate soft sbottom masses and X_t being renormalized in the OS scheme. We will illustrate the numerical significance of these terms in Sec. 5.3. The absence of $\tan\beta$-enhanced terms (i.e. terms proportional to $\sim \overline{m}_b^4 \tan^4\beta$ in Eq. (5.2.11)) might be surprising at first glance since the one-loop threshold correction of order $\mathcal{O}(\alpha_b^2)$ contains terms $\sim \overline{m}_b^4 \widehat{X}_b^4$. The reason for that is a cancellation between the two-loop terms proportional to $\Delta^{1l,\mathcal{O}(\alpha_b^2)}$ originating from the one-loop RGEs for λ and v. More precisely,

$$\begin{aligned}
&\lambda(M_t)^{\text{2L,NLL}} \supset \lambda(M_{\text{SUSY}}) - \beta_\lambda^{(1)}(M_{\text{SUSY}})\kappa L \supset \\
&\supset \Delta^{1l,\mathcal{O}(\alpha_b^2)}\left(1 + 4\beta_v^{(1)}\kappa L\right) - 6\lambda(M_{\text{SUSY}})(y_t^2 + y_b^2)\kappa L \supset \\
&\supset \Delta^{1l,\mathcal{O}(\alpha_b^2)}\left(4\beta_v^{(1)} - 6(y_t^2 + y_b^2)\right)\kappa L,
\end{aligned} \tag{5.2.12}$$

where y_t and y_b are the top and bottom Yukawa couplings, respectively, and we keep track only of the terms which are proportional to $\Delta^{1l,\mathcal{O}(\alpha_b^2)}$ and L. In addition to that, in the second line of Eq. (5.2.12) we exploited the fact that the one-loop threshold correction to λ of order $\mathcal{O}(\alpha_b^2)$ scales as $\overline{m}_b^4(M_{\text{SUSY}})/\overline{v}^4(M_{\text{SUSY}})$. Since the same bottom mass, $\overline{m}_b(M_{\text{SUSY}})$, is used in the FO result, we have to run only the vev. The one-loop RGE for the vacuum expectation value in the SM in the gaugeless limit can be found in [241] and reads,

$$\beta_v^{(1)} = \frac{3}{2}(y_t^2 + y_b^2). \tag{5.2.13}$$

By plugging Eq. (5.2.13) into Eq. (5.2.12) we see that the terms proportional to $\Delta^{1l,\mathcal{O}(\alpha_b^2)}$ cancel at the two-loop level. The terms in $\beta_\lambda^{(1)}$ and $\beta_v^{(1)}$ have a common origin – they arise from the external leg corrections to the vertex with four SM-like Higgses.

As a consistency check of our calculation, we have verified analytically and independently that the large logarithms arising in the EFT and in the FO calculation agree with each other at the one-loop level at orders $\mathcal{O}(m_t^2\alpha_t + m_b^2\alpha_b + m_t^2\alpha + m_b^2\alpha)$ [67] and at the two-loop level at orders $\mathcal{O}(m_t^2\alpha_t\alpha_s + m_b^2\alpha_b\alpha_s + m_t^2\alpha_t^2 + m_t^2\alpha_t\alpha_b + m_b^2\alpha_t\alpha_b + m_b^2\alpha_b^2)$.

Now let us proceed with the non-logarithmic subtraction terms. Since we merge the EFT calculation with the one- and two-loop fixed-order results, the subtraction terms also have to be derived up to the two-loop order,

$$\left[\Delta M_h^2\right]_{\text{sub}}^{\text{n/log}} = \left[\Delta M_h^2\right]_{\text{sub}}^{\text{n/log,1L}} + \left[\Delta M_h^2\right]_{\text{sub}}^{\text{n/log,2L}}. \tag{5.2.14}$$

As was argued in Sec. 4.3, the one-loop non-logarithmic subtraction terms are essentialy equal to the one-loop threshold corrections to the quartic coupling λ, multiplied

[67] Analogous checks at order $\mathcal{O}(m_t^2\alpha_t + m_t^2\alpha + M_W^2\alpha^2)$ have been performed in [22].

by $2v_{G_F}^2$.[68]

$$\begin{aligned}\left[\Delta M_h^2\right]_{\text{sub}}^{\text{n/log,1L}} &= -2v_{G_F}^2\Delta^{1l,\mathcal{O}(\alpha_b^2+\alpha_b\alpha)} = \\ &= -12\kappa\frac{\overline{m}_b^4}{v_{G_F}^2}\left(|\widehat{X}_b|^2 - \frac{|\widehat{X}_b|^4}{12}\right) + \kappa(g^2+g'^2)\,\overline{m}_b^2|\widehat{X}_b|^2\,c_{2\beta}(1+c_\beta^2).\end{aligned} \tag{5.2.15}$$

At the two-loop level, one has to subtract the two-loop threshold corrections Δ^{2l} of order $\mathcal{O}(\alpha_b^2\alpha_s + \alpha_t^2\alpha_b + \alpha_t\alpha_b^2 + \alpha_b^3)$ parametrized in terms of the fixed-order result parameters, i.e. in terms of $m_t^{\overline{\text{MS}},\text{SM}}(M_t)$, v_{G_F} and $m_b^{\overline{\text{DR}},\text{MSSM}}(M_{\text{SUSY}})$.

Additionally, as was argued in Sec. 4.3, one has to subtract the shifts caused by a different parametrization of the vacuum expectation value in the EFT and in the FO. Let us elaborate on this further. For the one-loop threshold correction of order $\mathcal{O}(\alpha_t^2)$ we use the same procedure as outlined in Eqs. (4.3.6) and (4.3.7). We only need to extend Eq. (4.3.7) by adding terms proportional to α_b and α_b^2 to $(\delta^{(1)}v^2)^{\text{SM}}$ (see Eqs. (B.1.2h) and (B.1.4) in App. B). For the terms, generated by $\Delta^{1l,\mathcal{O}(\alpha_b^2)}$, the situation is slightly different. These treshold corrections should be parametrized in terms of the MSSM bottom Yukawa coupling to avoid terms which contain powers of $\tan\beta$ that are higher than powers of y_b [15]. The non-logarithmic terms in the EFT result generated by $\Delta^{1l,\mathcal{O}(\alpha_b^2)}$ read

$$\begin{aligned}&\left[M_h^{2,\text{EFT}}\right]_{\text{n/log}}^{1l,\mathcal{O}(\alpha_b^2)} = 12\,\kappa\,v_{\overline{\text{MS}},\text{SM}}^2(M_t)\left(y_b^{\overline{\text{DR}},\text{MSSM}}(M_{\text{SUSY}})\right)^4\left(|\widehat{X}_b|^2 - \frac{|\widehat{X}_b|^4}{12}\right) \\ &= 12\,\kappa\,v_{\overline{\text{MS}},\text{SM}}^2(M_t)\left[\frac{\overline{m}_b}{v_{\overline{\text{DR}},\text{MSSM}}(M_{\text{SUSY}})}\right]^4\left(|\widehat{X}_b|^2 - \frac{|\widehat{X}_b|^4}{12}\right) = \\ &= 12\,\kappa\frac{\overline{m}_b^4}{v_{\overline{\text{MS}},\text{SM}}^2(M_t)}(1-2(\delta^{(1)}v^2)^{\text{n/SM}})\left(|\widehat{X}_b|^2 - \frac{|\widehat{X}_b|^4}{12}\right) + \text{logs} = \\ &= 12\,\kappa\frac{\overline{m}_b^4}{v_{G_F}^2}(1-(\delta^{(1)}v^2)^{\text{SM}} - 2(\delta^{(1)}v^2)^{\text{n/SM}})\left(|\widehat{X}_b|^2 - \frac{|\widehat{X}_b|^4}{12}\right) + \text{logs}.\end{aligned} \tag{5.2.16}$$

Note that we apply this procedure only to the one-loop threshold correction of order $\mathcal{O}(\alpha_b^2)$ and not to the correction of $\mathcal{O}(\alpha_b\alpha)$ since at the two-loop level the fixed-order corrections are derived in the gaugeless limit. This, in particular leads to a different parametrization of the corresponding piece in the FO and in the EFT. This difference is of $\mathcal{O}(m_t^2\alpha_b\alpha + m_b^2\alpha_b\alpha)$ and is formally beyond the order of perturbation theory which we consider in this thesis. As we will see in Sec. 5.3, this different parametrization induces a small difference in the Higgs mass at low M_{SUSY}.

[68] Here we already use the expressions for the one-loop threshold corrections in the MSSM with $\mathcal{CP}$-violation. They will be discussed in Chapter 6.

Summing up all the ingredients mentioned above, we arrive at the following subtraction terms controlled by the bottom Yukawa coupling.

$$\begin{aligned}\left[\Delta M_h^2\right]_{\text{sub}}^{\text{n/log,2L}} = -2v_{G_F}^2\Delta^{2l} + 18\kappa^2\Bigg\{\Bigg[4\left(\frac{\overline{m}_b^6}{v_{G_F}^4} + \frac{\overline{m}_t^2\overline{m}_b^4}{v_{G_F}^4}\right)\log\frac{\overline{m}_t}{\overline{m}_b} \\ -\frac{\overline{m}_b^2\overline{m}_t^4}{v_{G_F}^4}\left(1 - 2\log\frac{\overline{m}_t^2}{M_t^2}\right)\Bigg]\left(|\widehat{X}_t^{\text{FO}}|^2 - \frac{|\widehat{X}_t^{\text{FO}}|^4}{12}\right) \\ -\Bigg[\frac{\overline{m}_t^2\overline{m}_b^4}{v_{G_F}^4}\left(1 - 2\log\frac{\overline{m}_t^2}{M_t^2} + \frac{2|\widehat{X}_t^{\text{FO}}|^2}{3}\right) \\ +\frac{\overline{m}_b^6}{v_{G_F}^4}\left(1 - 2\log\frac{\overline{m}_t^2}{M_t^2} + \frac{2|\widehat{X}_b|^2}{3}\right)\Bigg]\left(|\widehat{X}_b|^2 - \frac{|\widehat{X}_b|^4}{12}\right)\Bigg\},\end{aligned} \tag{5.2.17}$$

where, in the expression above $\widehat{X}_t^{\text{FO}}$ is either $\widehat{X}_t^{\text{OS}}$ or $\widehat{X}_t^{\overline{\text{DR}}}$ depending on the renormalization scheme used for the stop sector.

5.2.4 Determination of the MSSM bottom quark mass and Yukawa coupling

Here, we describe how we obtain the $\overline{\text{DR}}$ bottom quark mass used in the fixed-order calculation as well as the $\overline{\text{DR}}$ bottom Yukawa coupling used in the EFT calculation. We start with the SM $\overline{\text{MS}}$ bottom Yukawa coupling, $y_b^{\overline{\text{MS}},\text{SM}}$, and the SM $\overline{\text{MS}}$ vev, $v^{\overline{\text{MS}},\text{SM}}$, at the scale M_t. Then, we evolve both quantities to the SUSY scale. At this scale we determine the MSSM $\overline{\text{DR}}$ bottom Yukawa coupling, $h_b^{\overline{\text{DR}},\text{MSSM}}$, and the MSSM $\overline{\text{DR}}$ vev, $v^{\overline{\text{DR}},\text{MSSM}}$, by matching the SM to the MSSM,

$$\left(h_b^{\overline{\text{DR}},\text{MSSM}}c_\beta\right)(M_{\text{SUSY}}) = y_b^{\overline{\text{MS}},\text{SM}}(M_{\text{SUSY}})\,(1+\Delta y_b)\,, \tag{5.2.18}$$

$$v^{\overline{\text{DR}},\text{MSSM}}(M_{\text{SUSY}}) = v^{\overline{\text{MS}},\text{SM}}(M_{\text{SUSY}})\,(1+\Delta v)\,. \tag{5.2.19}$$

The $\overline{\text{DR}}$ bottom quark mass is then determined by

$$m_b^{\overline{\text{DR}},\text{MSSM}}(M_{\text{SUSY}}) = \left(h_b^{\overline{\text{DR}},\text{MSSM}}c_\beta\right)(M_{\text{SUSY}})v^{\overline{\text{DR}},\text{MSSM}}(M_{\text{SUSY}}). \tag{5.2.20}$$

As was already discussed in Sec. 3.2.4, the corrections to the $\overline{\text{DR}}$ bottom quark mass, consisting of Δy_b and Δv, include terms proportional to $\tan\beta$. For large $\tan\beta$, the leading $\tan\beta$-enhanced terms can be resummed as described in [139, 148, 149, 189, 242–245]. Typically, this resummation is written in the form (see Eq. (3.2.65))

$$m_b^{\overline{\text{DR}},\text{MSSM}}(M_{\text{SUSY}}) = m_b^{\overline{\text{MS}},\text{SM}}(M_{\text{SUSY}})\frac{1+\epsilon_b}{|1-\Delta_b|}, \tag{5.2.21}$$

where Δ_b stands for the $\tan\beta$-enhanced terms and ϵ_b for terms not enhanced by $\tan\beta$.[69] We employ a similar relation for the matching of the bottom Yukawa coupling,

$$\left(h_b^{\overline{\text{DR}},\text{MSSM}} c_\beta\right)(M_{\text{SUSY}}) = y_b^{\overline{\text{MS}},\text{SM}}(M_{\text{SUSY}}) \frac{1+\epsilon_b-\Delta v}{|1-\Delta_b|}. \tag{5.2.22}$$

A similar procedure for the calculation of the MSSM bottom Yukawa coupling was adapted in [15]. There, however, non-enhanced terms, ϵ_b, and the threshold correction of the vev, Δv, were included into the definition of Δ_b. In our approach, we separate them to resum only $\tan\beta$ enhanced corrections to the bottom mass in the same way as in [149, 200]. This results only in a small numerical difference since the main contribution to $h_b^{\overline{\text{DR}},\text{MSSM}}(M_{\text{SUSY}})$ comes from Δ_b.

In our implementation, we include full one-loop corrections to Δ_b. The quantity Δv is calculated at the one-loop level in the gaugeless limit. In addition, we include the leading two-loop corrections to Δ_b. These two-loop corrections are based on the results from [29–31] (similar results have been obtained in [246–248]). We, however, expand the expression for large M_{SUSY} omitting terms of higher order in $\mathcal{O}(v^2/M_{\text{SUSY}}^2)$. In addition, we adapt the renormalization scheme to match our scheme. More precisely, in [29, 31] the soft supersymmetry breaking parameters in the stop and sbottom sectors as well as the gluino mass are renormalized on-shell. Moreover, the top-Yukawa coupling and the strong coupling are defined in Collins-Wilczek-Zee scheme (see Sec. 3.1.4.1) with 5 active flavours. This decoupling of the top quark and on-shell renormalization of the top sector induce large logarithms, $\log(M_{\text{SUSY}}^2/M_t^2)$, implying that the formulas in [29–31] are not directly applicable in our framework. Since in our case the low energy model is the SM with possibly light gluinos, we do not decouple the top-quark and the gluino. Also, to be compatible with the EFT computation we renormalize the gluino mass and stop/sbottom masses in the $\overline{\text{DR}}$ scheme at the scale Q. In the limit of all involved non-SM masses having the same mass, we obtain

$$\Delta_b^{2L} = \Delta_b^{2L,\text{QCD}} + \Delta_b^{2L,\text{EW}}, \tag{5.2.23a}$$

$$\Delta_b^{2L,\text{QCD}} = -\frac{\alpha_s(Q)^2 C_F}{12\pi^2}\frac{\mu}{M_{\text{SUSY}}} t_\beta \left(2C_A - C_F + 6T_R - (3C_A - 2C_F - 3T_R)\log\frac{M_{\text{SUSY}}^2}{Q^2}\right), \tag{5.2.23b}$$

$$\Delta_b^{2L,\text{EW}} = \frac{\alpha_s(Q) y_t^2(Q) C_F}{384\pi^3}\frac{A_t}{M_{\text{SUSY}}} t_\beta \left(7 + 10\log\frac{M_{\text{SUSY}}^2}{Q^2}\right). \tag{5.2.23c}$$

Here, Q is the renormalization scale, $C_A = 3, C_F = \frac{4}{3}$ and $T_R = \frac{1}{2}$.

[69] In principle, there are also terms in ϵ_b and Δv which are proportional to $m_b^2 \tan^2\beta$. We, however, checked that they are numerically irrelevant.

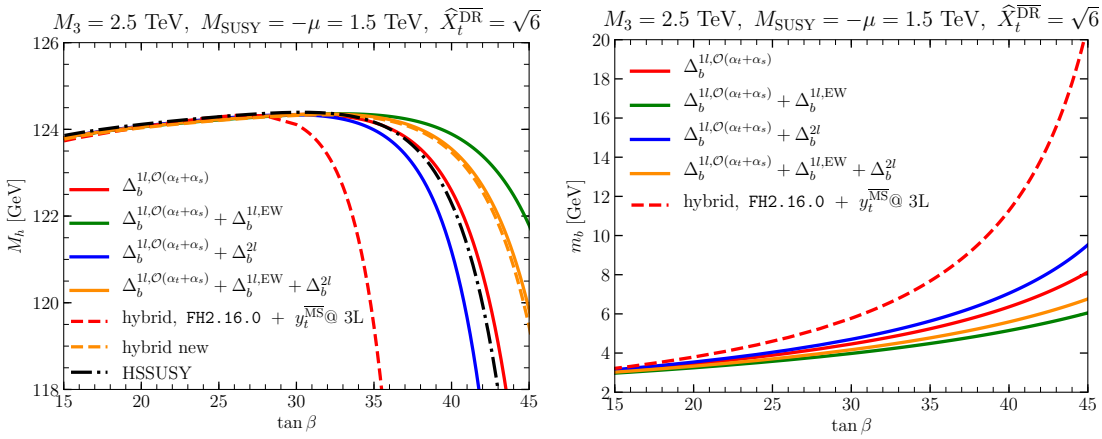

Figure 5.1: Predictions for M_h (*left*) and m_b (*right*) as a function of $\tan\beta$ for different accuracy levels in the calculation of Δ_b. For this plot we consider the same MSSM scenario as in Fig. 2 in [15].

5.3 Numerical results

Here, we investigate the numerical effect of resumming logarithmic contributions proportional to the bottom Yukawa coupling. First, we concentrate on a scenario presented in Ref. [15]. Namely, we assume that all soft SUSY masses are equal to $M_{\rm SUSY} = 1.5$ TeV except the gluino mass which is fixed by $M_3 = 2.5$ TeV. The stop mixing parameter is set by $X_t = \sqrt{6} M_{\rm SUSY}$ and the trilinear couplings of the third generation fermions are equal to each other, $A_b = A_\tau = A_t$. The Higgsino mass parameter, μ, is chosen to be equal to -1.5 TeV. Due to this choice of the signs of M_3, X_t and μ the MSSM bottom Yukawa coupling is enhanced by the one-loop threshold corrections proportional to the top Yukawa coupling and the strong Yukawa coupling. As in Ref. [15] all the input parameters listed above and $\tan\beta$ are assumed to be $\overline{\rm DR}$ parameters at the scale $M_{\rm SUSY}$.

On the left panel of Fig. 5.1 we present results for M_h in dependence on $\tan\beta$. In addition to showing results obtained with the calculation presented in this thesis, we display results obtained using the most recent public version of `FeynHiggs` (version `2.16.0`). Moreover, we show the result obtained in [15] for comparison. This result was obtained in a pure EFT framework using the code `HSSUSY` [25, 27]. On the right panel of the same figure we show the bottom mass, m_b, which is used in the corresponding calculations. In the case of the red dashed curve it is the bottom mass, $\widehat{m}_b$, defined by in Eq. (3.2.50) and in case of the blue, red, orange and green solid lines it is $m_b^{\overline{\rm DR},\rm MSSM}(M_{\rm SUSY})$.

First, we focus on the various EFT results in the left panel of Fig. 5.1: the solid red line on the plot corresponds to the solid red line in Fig. 2 of [15]; the blue, orange, green solid and black solid lines, to the results of our EFT calculation with

different approximation levels used in the calculation of the bottom Yukawa threshold correction. We should note here that the results presented in [15] have been obtained using the SM $\overline{\text{MS}}$ top Yukawa coupling extracted at the N^{3}LO level while we by default use the NNLO value. For a proper comparison with the results of [15], we adapted our calculation to use the same accuracy level (see also discussion in Chapter 7). We use this accuracy level for all curves of Fig. 5.1.

We observe a very good agreement between our EFT result using only $\mathcal{O}(\alpha_s + \alpha_t)$ corrections in the calculation of Δ_b (solid red curve), which is the same level of accuracy as used in [15], and the result of [15] (black dot-dashed curve). The absolute difference between the two curves equals ~ 0.04 GeV for $t_\beta = 15$ and ~ 0.7 GeV for $t_\beta = 42$. This difference comes mainly from the determination of the MSSM bottom Yukawa coupling at the scale M_{SUSY}. In [15], the threshold correction for the vacuum expectation value, Δv, and non-enhanced terms were included in the definition of Δ_b while we do not include them (see Eq. (5.2.22)). If we include them into Δ_b as in [15], the absolute difference between our calculation and the calculation presented in [15] shrinks down even further (~ 0.2 GeV for $t_\beta = 42$).

For the solid green curve in the left plot of Fig. 5.1, we take into account electroweak corrections in the calculation of Δ_b in addition to the $\mathcal{O}(\alpha_s, \alpha_t)$ corrections used for the solid red curve. As one can see from Eq. (A.1.8), this choice leads to a partial cancellation in the calculation of Δ_b and hence to a suppression of the MSSM bottom mass at the scale M_{SUSY} as one can see on the right panel of Fig. 5.1 showing $m_b^{\overline{\text{DR}},\text{MSSM}}(M_{\text{SUSY}})$ in dependence of $\tan\beta$. This in turn relaxes the suppression of the Higgs mass by the one-loop threshold corrections to the SM Higgs self-coupling, λ, proportional to the bottom Yukawa coupling.

The blue solid curve in the left plot of Fig. 5.1 shows the prediction for M_h neglecting the electroweak one-loop contributions to Δ_b but including the leading two-loop QCD corrections to Δ_b. For our parameter choice, these corrections increase the absolute value of Δ_b by approximately 5%. Correspondingly, also the MSSM bottom mass is increased as can be seen in the right plot of Fig. 5.1. This results in a significant change of the resulting Higgs mass for $\tan\beta \gtrsim 40$ where dependence on $\tan\beta$ is quite strong. The orange curves in the left plot of Fig. 5.1 correspond to the inclusion of all corrections to Δ_b mentioned above. For the considered parameter choice, the electroweak corrections to Δ_b are roughly three times larger by absolute value than the two-loop corrections to Δ_b. This explains why the orange and the green curves lie quite close to each other.

The orange dashed curve represents the result of the hybrid calculation of M_h. Namely, we have merged the $\mathcal{O}(m_t^2\alpha_t\alpha_s + m_b^2\alpha_b\alpha_s + m_t^2\alpha_t^2 + m_t^2\alpha_t\alpha_b + m_b^2\alpha_t\alpha_b + m_b^2\alpha_b^2)$ fixed-order result with the NNLL EFT calculation (see Sec. 5.2.3). The orange solid

and dashed curves differ essentially by the inclusion of terms that are suppressed by the ratio $v^2/M_{\rm SUSY}^2$ into the hybrid result. Since in our case $M_{\rm SUSY}$ is chosen above the TeV scale, the size is of these terms is quite small. Therefore, a good agreement between the two methods is expected and validates our hybrid calculation.

Finally, the red dashed curve shows the prediction for M_h obtained by `FeynHiggs-2.16.0` which we ran using default flags as explained in [231].[70] As only modification of this version, we have used the N^{3}LO instead of the NNLO SM $\overline{\rm MS}$ top Yukawa coupling to allow for a direct comparison to the result of [15]. We see that the agreement between all the seven curves is quite good for small values of $\tan\beta$ but for $\tan\beta \gtrsim 30$ the red dashed curve falls abruptly down for $\tan\beta \gtrsim 40$. The reason for this behaviour becomes clear when looking at the right panel of Fig. 5.1: the red dashed curve, which corresponds to $\widehat{m}_b$ defined in Eq. (3.2.50), increases much more rapidly for rising $\tan\beta$ than the other four lines.[71] This bottom mass is inserted in the leading one-loop fixed order result which has a negative impact on M_h [201, 249, 250],

$$(\Delta M_h^2)^{\rm 1l,bottom} \simeq -\frac{\widehat{m}_b^4 \tan^4\beta}{16\pi^2 v_{G_F}^2}. \tag{5.3.1}$$

This term grows rapidly in absolute value with increasing $\tan\beta$. The same argument applies to all other curves but there the dependence of the bottom mass on the $\tan\beta$ is much milder. This is a consequence of our choice of the renormalization scheme. Namely the bottom mass used in our setup is the $\overline{\rm DR}$ MSSM bottom mass calculated at the scale $M_{\rm SUSY}$. All the quantities entering the calculation of Δ_b and ϵ_b are also $\overline{\rm DR}$ MSSM quantities at this scale. The most important ones are the top Yukawa coupling α_t and the strong Yukawa coupling α_s (see Eq. (A.1.8) in App. A). Since their values decrease with increasing scale,[72] the Δ_b correction calculated in our approach is smaller than the corresponding correction in `FeynHiggs-2.16.0`. In this way our approach yields more stable results for large values of $\tan\beta$ and for regions of the MSSM parameter space where the signs of the products μM_3 and μA_t are negative.

Next, we discuss the numerical effect induced by the resummation of logarithms proportional to the bottom Yukawa coupling. First of all, to have an idea of how numerically important the effect is, it is instructive to have a look at the analytic one- and two-loop expressions that one can find in Sec. 5.2.3. As we pointed out there, the bottom mass we use in our calculation, even though being enhanced by Δ_b effects, is the smallest mass taken into account in our EFT calculation. The only way corrections containing the bottom mass may become sizeable is when these terms

[70] For reference, here we list the values of these input flags: `mssmpart` = 4, `higgsmix` = 2, `p2approx` = 4, `looplevel` = 2, `loglevel` = 3, `runningMT` = 1, `botResum` = 1, `tlCplxApprox` = 0.

[71] Note that the red dashed and the red solid lines have the same accuracy level of Δ_b.

[72] Note that we have also included the leading two-loop QCD corrections to Δ_b which mitigates its scale dependence.

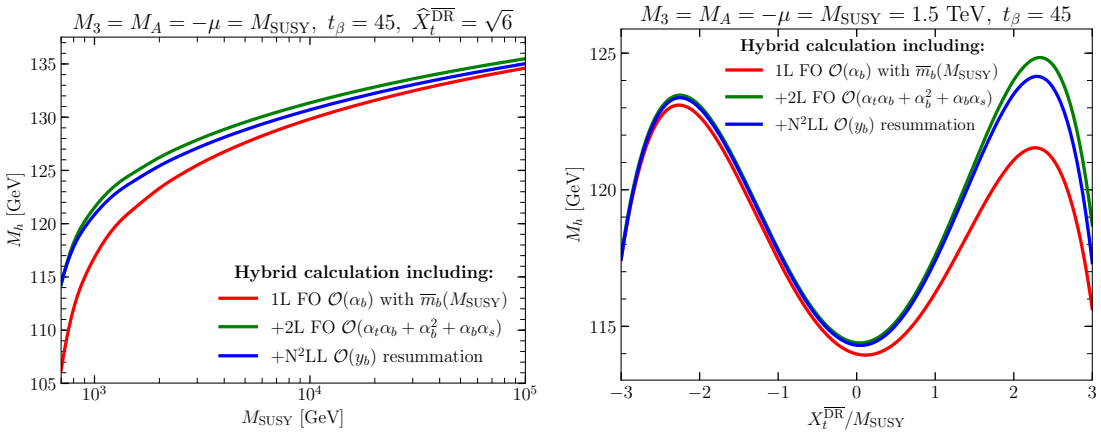

Figure 5.2: M_h as a function of $M_{\rm SUSY}$ (*left*) and $\widehat{X}_t^{\overline{\rm DR}}$ (*right*). The *red* lines show the prediction of our hybrid calculation including only the one-loop fixed-order $\mathcal{O}(\alpha_b)$ correction. For the *blue* lines, we additionally included the fixed-order $\mathcal{O}(m_t^2\alpha_t\alpha_b + m_b^2\alpha_t\alpha_b + m_b^2\alpha_b^2 + m_b^2\alpha_b\alpha_s)$ corrections. The *green* lines contain additionally the resummation of large logarithms proportional to the bottom Yukawa coupling.

are additionally proportional to $\tan\beta$. This is the case when m_b is, for example, multiplied by $\widehat{X}_b$, $\widehat{Y}_t$, t_β or $1/c_\beta$. We find such enhancements only in the two-loop next-to-leading logarithmic contributions when the stop mixing parameter, $\widehat{X}_t$, is renormalized in the OS scheme (see Eqs. (5.2.11) and (5.2.10)). In consequence, we expect the effect of the resummation to be small if we renormalize $\widehat{X}_t$ in the $\overline{\rm DR}$ scheme.

This preliminary consideration turns out to be qualitatively correct as one can see in the left panel of Fig. 5.2. The red curve corresponds to the hybrid result including the effects of the bottom Yukawa coupling only at the one-loop level in the fixed order calculation. The used MSSM $\overline{\rm DR}$ bottom mass, $m_b^{\overline{\rm DR},\rm MSSM}(M_{\rm SUSY})$, contains all the corrections discussed above (i.e. the level of accuracy corresponds to the orange curves in Fig. 5.1). The green curve includes additionally the $\mathcal{O}(m_t^2\alpha_t\alpha_b + m_b^2\alpha_t\alpha_b + m_b^2\alpha_b^2 + m_b^2\alpha_b\alpha_s)$ fixed-order corrections from [9, 11]. Finally, the blue curve also contains the resummation of LL, NLL and NNLL logarithms controlled by the bottom Yukawa coupling. The same color scheme also applies to the right panel of Fig. 5.2 and to both plots in Fig. 5.3. For these plots we have picked an MSSM scenario where all soft-breaking masses and μ are equal by absolute value to the common mass scale $M_{\rm SUSY}$. Moreover, we set $A_b = 2.5 M_{\rm SUSY}$ and $t_\beta = 45$. The bino, wino and gluino masses are chosen to be positive, $M_{1,2,3} > 0$, while the Higgsino mass parameter is negative, $\mu < 0$.

For the left plot of Fig. 5.2 we have chosen $\widehat{X}_t^{\overline{\rm DR}}(M_{\rm SUSY}) = \sqrt{6}$. First, we note that the green and the blue curves agree very well for low values of $M_{\rm SUSY}$ with the difference between the two being only equal to ~ 0.3 GeV for $M_{\rm SUSY} = 700$ GeV.

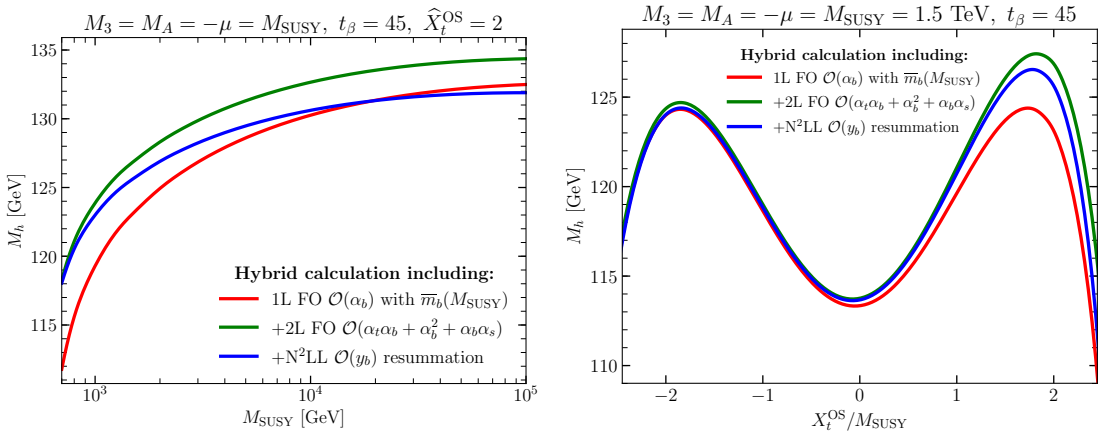

Figure 5.3: Same as Fig. 5.2 but X_t is renormalized in the OS scheme.

Indeed, since in this region the scale separation is relatively mild, one does not expect the resummation to contribute significantly to the final answer. However, the two curves lie quite close to each other for the whole range of scales, even for $M_{\rm SUSY}$ as high as 10^5 GeV. This is in line with our preliminary analysis above: the logarithms containing bottom Yukawa coupling are numerically negligible if we use $\widehat{X}_t^{\overline{\rm DR}}(M_{\rm SUSY})$ as an input parameter.

Next, we observe a significant gap of order $\mathcal{O}(10)$ GeV between the red and the blue lines on this figure which shrinks down as $M_{\rm SUSY}$ increases. This tells us that the Δ_b alone may not be a very good approximation for the higher-order effects controlled by the bottom Yukawa in the region of small $M_{\rm SUSY}$ since the bottom mass is large in this region and the two-loop fixed-order corrections are numerically important.[73] However, with the increase of $M_{\rm SUSY}$ the bottom mass $m_b^{\overline{\rm DR},\rm MSSM}(M_{\rm SUSY})$ decreases and all three curves give approximately the same answer.

On the right panel of Fig. 5.2 we fix $M_{\rm SUSY} = 1.5$ TeV and scan over $\widehat{X}_t^{\overline{\rm DR}}$. We notice that for negative $\widehat{X}_t^{\overline{\rm DR}}$ all three curves give roughly the same result. This due to the fact that the contributions to Δ_b proportional to the strong coupling and to the top Yukawa coupling partially cancel each other. Correspondingly, the bottom mass does not acquire any enhancement. Also the inclusion of the two-loop fixed-order corrections as well as the resummation of the logarithms is negligible. On the contrary, for positive $\widehat{X}_t$ the top Yukawa and strong corrections to Δ_b add up and enhance the bottom mass. In accordance with Eq. (5.3.1), this shifts the Higgs mass downwards at the one-loop level (red curve). The two-loop corrections increase it (blue curve).

In Fig. 5.3, we renormalize the stop sector in the OS scheme, fixing $\widehat{X}_t^{\rm OS} = 2$. This plot shares the same features at low $M_{\rm SUSY}$ as the corresponding plot in Fig. 5.2.

[73] It is worth noting that due to the parameter choices, which enhance Δ_b, different levels of approximation in Δ_b yield very different results for M_h.

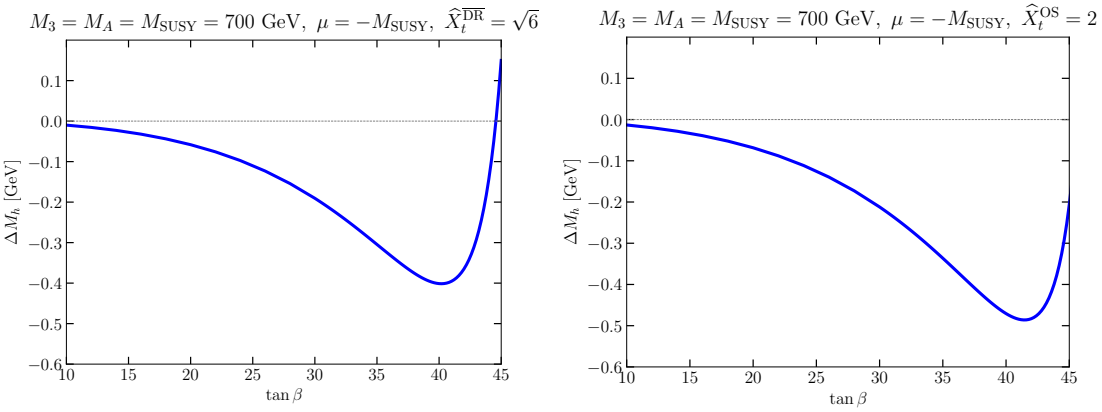

Figure 5.4: Difference $\Delta M_h = M_h^{\rm resum} - M_h^{\rm n/resum}$ as a function of $\tan\beta$ for $M_{\rm SUSY} = 700$ GeV.

However, for large $M_{\rm SUSY}$ the effect of the resummation becomes more prominent due to the presence of the logarithmic terms of order $\mathcal{O}(m_b^2 m_t^4)$ enhanced by $|\widehat{X}_b|^2 \simeq t_\beta^2$ (see Eq. (5.2.10)),

$$\left[\Delta M_h^2\right]_{\rm sub,OS}^{\rm 2L,NLL} \simeq -3\kappa^2 \frac{\overline{m}_b^2 \overline{m}_t^4}{v_{G_F}^4} t_\beta^2 |\widehat{A}_t|^2 (6 - |\widehat{A}_t|^2) L. \tag{5.3.2}$$

In the considered scenario, the resummation pushes the Higgs mass down by ~ 2 GeV for $M_{\rm SUSY} = 10$ TeV and by ~ 2.5 GeV for $M_{\rm SUSY} = 100$ TeV. On the right panel of this plot we show the result of the scan over $\widehat{X}_t^{\rm OS}$ with fixed $M_{\rm SUSY} = 1.5$ TeV. As in the case of the $\overline{\rm DR}$ stop input parameters all three lines essentialy coincide for $\widehat{X}_t^{\rm OS} < 0$ and the effect of the inclusion of the two-loop $\mathcal{O}(m_t^2\alpha_t\alpha_b + m_b^2\alpha_t\alpha_b + m_b^2\alpha_b^2 + m_b^2\alpha_b\alpha_s)$ fixed-order corrections and the resummation becomes sizeable only in the region $\widehat{X}_t^{\rm OS} \gtrsim 1$.

At the first glance the effect of resummation should be negligible for small values of $M_{\rm SUSY}$ since the logarithms $\log \frac{M_{\rm SUSY}^2}{M_t^2}$ are less important numerically in this region of parametere space. Indeed, we see that in the left panels of Fig. 5.2 and Fig. 5.3 the green and the blue curves are in good agreement for $M_{\rm SUSY} = 700$ GeV. Here, we investigate this region more closely. On Fig. 5.4 we present the difference ΔM_h between the predictions for the SM-like Higgs boson with and without resummation of bottom contributions, $\Delta M_h = M_h^{\rm resum} - M_h^{\rm n/resum}$ for the same scenario as was considered in Fig. 5.2 and Fig. 5.3 but now we fix $M_{\rm SUSY} = 700$ GeV and scan over $\tan\beta$. The blue curves on Fig. 5.4 corresponds to the difference between the blue and the green curves in Fig. 5.2 and Fig. 5.3. We see that for $\tan\beta = 45$ the effect of resummation is ~ 0.1 GeV for the $\overline{\rm DR}$ input parameters and essentially negligible for the OS input parameters in full agreement with plots on Fig. 5.2 and Fig. 5.3.

However, the difference is more prominent in both cases for $\tan\beta \sim 40$. The behavior of the curves on Fig. 5.4 can be explained as follows. As was discussed after Eq. (5.2.16), the vev is reparametrized only in the $\mathcal{O}(\alpha_b^2)$ and not to the $\mathcal{O}(\alpha_b\alpha)$ threshold corrections. The different treatment of the vacuum expectation value in the corresponding terms in the fixed-order – v_{G_F} is used – and the EFT calculation – $v^{\overline{\rm DR},\rm MSSM}(M_{\rm SUSY})$ is used – induces differences at order $\mathcal{O}(m_b^2\alpha(\alpha_t+\alpha_b))$. A similar effect was also discussed in [23]. Moreover, the different treatment of the vacuum expectation value in the two-loop threshold corrections and in the respective pieces of the fixed-order, inducing the difference at the three-loop order, contributes to the effect. This difference becomes sizeable for $\tan\beta \gtrsim 40$ and leads to the increase of curves in this region.

As a final phenomenological application of our improved calculation, we consider the $M_h^{125,\mu-}$ benchmark scenario recently defined in [251], accompanying the benchmark scenarios proposed in [138, 252]. In this scenario the SUSY input parameters are fixed as

$$M_{Q_3} = M_{U_3} = M_{D_3} = 1.5 \text{ TeV}, \quad M_{L_3} = M_{E_3} = 2 \text{ TeV},$$
$$\mu = -2 \text{ TeV}, \quad M_1 = 1 \text{ TeV}, \quad M_2 = 1 \text{ TeV}, \quad M_3 = 2.5 \text{ TeV},$$
$$X_t = 2.8 \text{ TeV}, \quad A_b = A_\tau = A_t \,.$$

For the SM parameters the ones recommended by the LHC-HXSWG [253] are used:

$$m_t^{\rm pole} = 172.5 \text{ GeV}, \quad \alpha_s(M_Z) = 0.118, \quad G_F = 1.16637 \cdot 10^{-5} \text{ GeV}^{-2},$$
$$m_b(m_b) = 4.18 \text{ GeV}, \quad M_Z = 91.1876 \text{ GeV}, \quad M_W = 80.385 \text{ GeV}\,.$$

The stop SUSY soft-breaking parameters are defined in the OS scheme. In [251], also the sbottom trilinear coupling is renormalized in the OS scheme. For better comparison with our previous results, we instead chose to fix them A_b in the $\overline{\rm DR}$ scheme. In addition, we define $\tan\beta$ at the scale $M_{\rm SUSY}$ instead of at the scale M_t, which was used in [251].

Note that for this scenario $\mu = -2$ TeV is chosen implying large Δ_b corrections which enhances the branching ratio of the heavy Higgs bosons decaying to a pair of bottom quarks. In addition, the large Δ_b corrections also affect the prediction for the SM-like Higgs boson, which we will investigate here.

The stop mass scale is equal to 1.5 TeV, so we do not expect the resummation of logarithms controlled by the bottom Yukawa coupling to have a major numerical impact in this case. However, large Δ_b corrections imply that the calculation might

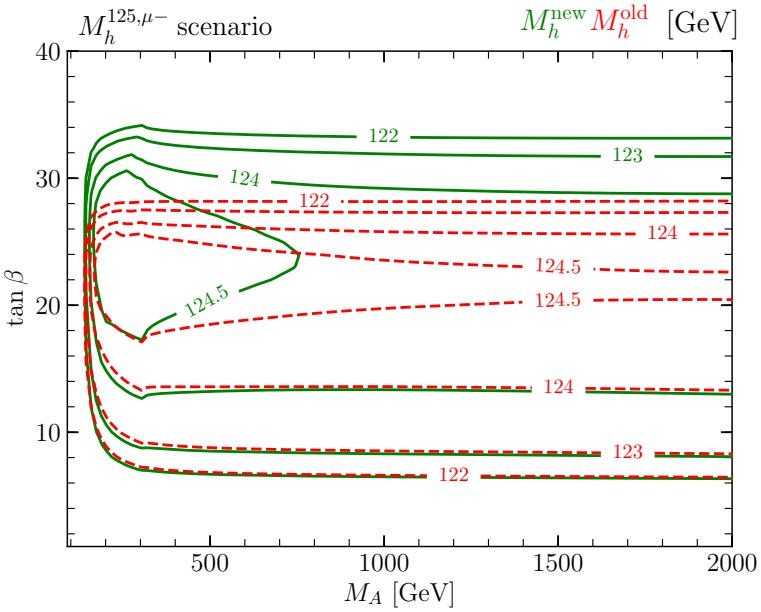

Figure 5.5: Results for M_h in the $M_h^{125,\mu-}$ scenario using a calculation including only the leading corrections to Δ_b, corresponding to the one used in [251] (red dashed), and our improved calculation presented in this thesis (green solid).

be sensitive to the level of accuracy in the determination of the bottom mass which is used in the fixed-order corrections at the one- and the two-loop level.

In Fig. 5.5 we present, in the $M_A - \tan\beta$ plane, the contour lines of the SM-like Higgs boson mass ranging from 122 GeV to 125 GeV. [74] We do not consider any experimental constraints described in detail in [138, 251, 252] and concentrate only on the mass of the lightest Higgs boson of the MSSM. The red and green lines correspond to two different computational setups. We calculated the red contours including only the leading one-loop corrections to Δ_b of $\mathcal{O}(\alpha_s, \alpha_t)$ as well as evaluating the bottom-quark mass at the scale M_t. Apart from the different definitions of some of the input parameters, as mentioned above, this corresponds to the default settings of `FeynHiggs-2.16.0`, which was used in [251] for the definition of the benchmark scenario. The green lines show the prediction of the improved calculation described in this thesis. In comparison to the red contours, we also include electroweak one-loop as well as the leading two-loop corrections to Δ_b, evaluate the bottom-quark mass at the SUSY scale and resum logarithms proportional to the bottom-Yukawa coupling.

We notice that in the region of small $\tan\beta$ both calculations agree very well since in this region the corrections from the bottom/sbottom sector are negligible. In this region the Higgs mass grows with increasing $\tan\beta$ mainly due to the growth of the tree-level mass. With a further increase of $\tan\beta$ the Higgs mass starts to decrease due to large Δ_b corrections and the rapid increase of the $\overline{\rm DR}$ bottom mass in the

[74] The 125 GeV contour is very small for the red lines and barely visible for the green lines.

MSSM. This is the behavior we already observed in the left plot of Fig. 5.1. As was discussed in the description for that plot the mass of the SM-like Higgs computed using `FeynHiggs-2.16.0` falls faster with increasing $\tan\beta$ than the mass computed using the calculation presented in this thesis due to the lower accuracy level in the calculation of Δ_b. Consequently, the region in which the SM-like Higgs mass is compatible with the experimentally measured value is enlarged. The upper bound on $\tan\beta$ is shifted from ~ 28 to ~ 33 .

Chapter 6

EFT calculation for complex input parameters

In this Chapter, we consider the SM as an effective field theory, assuming that the full theory, it is matched to, is the MSSM with $\mathcal{CP}$-violation. We derive one- and two-loop threshold corrections to the quartic coupling in the gaugeless limit in Sec. 6.1. In Sec. 6.2, we discuss the one-loop as well as the leading two-loop threshold corrections to the bottom Yukawa coupling between the SM and the MSSM with complex parameters. The numerical impact of the computed corrections is discussed in Sec. 6.3.

6.1 Threshold corrections to λ

In the fixed-order approach, the dependence on $\mathcal{CP}$-violating phases is known at the one- and two-loop level [90, 129, 130, 150, 254]. In the EFT framework, the phase dependence has so far only been considered in case of a low-energy Two-Higgs-Doublet-Model [19, 255]. In this Chapter, we work out the dependence on $\mathcal{CP}$-violating phases in the case of the SM (and the SM plus electroweakinos) as EFT, for which so far only an interpolation of the result in case of real input parameters is available [231].

We first discuss the case of the SM as low-energy EFT. Since the SM includes no phases (apart from the CKM phase, whose effect is negligible for the determination of the Higgs mass), $\mathcal{CP}$-violating effects in the full MSSM enter only via threshold corrections to real parameters. The threshold corrections to the quartic coupling λ can be obtained via the matching of the four-point vertex function involving external SM-like Higgs bosons. In this thesis, we, however, follow a different approach. Since in the SM the mass of the lightest Higgs boson is related to its quartic coupling via Eq. (1.2.11), the threshold corrections to λ can be obtained via the threshold

correction to the running Higgs mass.[75] Below we outline the method and derive the general formulas for the one- and two-loop threshold corrections to λ in the gaugeless limit. Similar discussions can be found in [13, 221].

In the limit $M_A \gg m_t$, The SM-like Higgs pole mass in the MSSM is given by the Eq. (4.1.14) up to the two-loop level,

$$\begin{aligned}(M_h)^2_{\rm MSSM} = m_h^2 &- \widehat{\Sigma}^{\rm MSSM,(1)}_{hh}(m_h^2) - \widehat{\Sigma}^{\rm MSSM,(2)}_{hh}(m_h^2) \\ &+ \widehat{\Sigma}^{\rm MSSM,(1)}_{hh}(m_h^2)\ \widehat{\Sigma}^{\rm MSSM,(1)\ \prime}_{hh}(m_h^2),\end{aligned} \tag{6.1.1}$$

where m_h is the tree-level mass given by Eq. (2.5.24) and the prime stands for the derivative with respect to the external momentum. The leading-order expression for m_h in the decoupling limit is given in Eq. (4.2.3). Since in this section we derive one- and two-loop corrections in the gaugeless limit, this mass is set to zero throughout this Section. All parameters entering self-energies $\widehat{\Sigma}^{\rm MSSM,(1)}_{hh}$ and $\widehat{\Sigma}^{\rm MSSM,(2)}_{hh}$ are renormalized in the $\overline{\rm DR}$ scheme. The self-energies entering Eq. (6.1.1) are assummed to be expanded in the limit $v/M_{\rm SUSY} \to 0$.

Below the matching scale Q, [76] the effective field theory is the SM. We write the matching condition for the SM running Higgs mass $\overline{m}_h^2$ as a loop expansion,

$$\overline{m}_h^2 = \overline{m}^2_{h,\rm tree} + (\overline{m}_h^{1l})^2 + (\overline{m}_h^{2l})^2 + \dots, \tag{6.1.2}$$

where the ellipsis denotes three-loop terms and higher. This relation is the same as Eq. (4.2.1) in Sec. 4.2 with the only difference that we have included the powers of the loop-counting factor κ into $(\overline{m}_h^{1l})^2$ and $(\overline{m}_h^{2l})^2$. From now on, we set $\overline{m}_{h,\rm tree} = 0$. The pole mass in the SM can be obtained via the solution of the pole equation

$$M_h^2 = \overline{m}_h^2 - \widetilde{\Sigma}^{\overline{\rm MS},\rm SM}_{hh}(M_h^2), \tag{6.1.3}$$

where $\widetilde{\Sigma}^{\overline{\rm MS},\rm SM}_{hh}$ is the SM Higgs boson self-energy renormalized in the $\overline{\rm MS}$ scheme with the tadpoles renormalized to zero (see Eq. (4.2.9)). Since the SM is treated as an effective field theory, its parameters are related to the corresponding parameters in the MSSM. This relation can be schematically written as follows,

$$P^{\rm SM} = P^{\rm MSSM} + \Delta P, \tag{6.1.4}$$

where P is a coupling constant, a running quark mass or the vacuum expectation value. Inserting this relation into the self-energy $\widetilde{\Sigma}^{\overline{\rm MS},\rm SM}_{hh}(M_h^2)$ induces a shift one

[75] This method is not sufficient to obtain the threshold correction for all quartic couplings if the EFT below $M_{\rm SUSY}$ is Two-Higgs-Doublet-Model.

[76] While the matching scale was set to $M_{\rm SUSY}$ in Sec. 4.2, we will keep it as a free variable in this Section.

order higher in the loop expansion.

$$\widetilde{\Sigma}_{hh}^{\overline{\rm MS},\rm SM} = \widetilde{\Sigma}_{hh}^{\rm SM}\Big|_{P^{\rm SM}\to P^{\rm MSSM}} + \widehat{\Sigma}_{hh}^{\rm SM,shifts}. \tag{6.1.5}$$

The first term on the right-hand side of this equation represents the self-energy which has the same analytic form as $\widetilde{\Sigma}_{hh}^{\overline{\rm MS},\rm SM}$ but with all $\overline{\rm MS}$ SM coupling constants and massesbeing replaced with their $\overline{\rm DR}$ MSSM counterparts. At the one-loop level the two self-energies are equal. The difference between them is encoded in the quantity $\widehat{\Sigma}_{hh}^{\rm SM,shifts}$ which is of two-loop order and higher.

The renormalized self-energy of the SM-like Higgs boson in the full MSSM can be split into parts,

$$\widehat{\Sigma}_{hh}^{\rm MSSM} = \widehat{\Sigma}_{hh}^{\rm SM} + \widehat{\Sigma}_{hh}^{\rm n/SM}, \tag{6.1.6}$$

where the SM part contains contributions from the diagrams with only SM particles and the non-SM part (indicated as "n/SM") originates from the diagrams with at least one non-SM particle. At the one-loop level, the following identity holds,

$$\widehat{\Sigma}_{hh}^{\rm SM,(1)} = \widetilde{\Sigma}_{hh}^{\rm SM,(1)}\Big|_{P^{\rm SM}\to P^{\rm MSSM}}. \tag{6.1.7}$$

At the two-loop level this holds for the Yukawa corrections to the Higgs mass, i.e. the corrections of order $\mathcal{O}(m_t^2\alpha_t^2+m_t^2\alpha_t\alpha_b+m_b^2\alpha_t\alpha_b+m_b^2\alpha_b^2)$. For the mixed Yukawa-QCD corrections, of $\mathcal{O}(m_t^2\alpha_t\alpha_s + m_b^2\alpha_b\alpha_s)$ the situation is slightly more elaborate. In this case the two different choices of the regularization scheme ($\overline{\rm MS}$ or $\overline{\rm DR}$) lead to two different expressions for the self-energy. This already can be anticipated since the running $\overline{\rm MS}$ and $\overline{\rm DR}$ quark masses are related to each other at the one-loop level via Eq. (3.2.62). By using `TwoCalc` [256] and the scripts described in [254] we explicitely checked the following relation,

$$\widetilde{\Sigma}_{hh}^{\overline{\rm MS},\rm SM,\mathcal{O}(m_t^2\alpha_t\alpha_s)} + \frac{\partial}{\partial m_t}\widetilde{\Sigma}_{hh}^{\overline{\rm MS},\rm SM,(1)}\cdot\Delta m_t^{\overline{\rm DR}\to\overline{\rm MS}} = \widetilde{\Sigma}_{hh}^{\overline{\rm DR},\rm SM,\mathcal{O}(m_t^2\alpha_t\alpha_s)}, \tag{6.1.8}$$

and the analogous relation for the $\mathcal{O}(m_b^2\alpha_b\alpha_s)$ self-energies. In Eq. (6.1.8),

$$\Delta m_t^{\overline{\rm DR}\to\overline{\rm MS}} = \frac{\alpha_s m_t}{3\pi}. \tag{6.1.9}$$

As explained above, the one-loop reparametrization of the couplings and masses in the one-loop SM self-energy induces shifts of the two-loop order,

$$\widehat{\Sigma}_{hh}^{\rm SM,shifts} = \sum_P \frac{\partial}{\partial P}\widetilde{\Sigma}_{hh}^{\overline{\rm MS},\rm SM,(1)}\Delta^{(1)}P. \tag{6.1.10}$$

Where P are all SM parameters which enter $\widetilde{\Sigma}_{hh}^{\overline{\rm MS},{\rm SM},(1)}$. The one-loop expression for $\widetilde{\Sigma}_{hh}^{\overline{\rm MS},{\rm SM},(1)}$ at zero external momentum of order $\mathcal{O}(m_t^2\alpha_t + m_b^2\alpha_b)$ reads (see also Eq. (5.2.1)),

$$\widetilde{\Sigma}_{hh}^{\overline{\rm MS},{\rm SM},(1)} = \sum_{q=t,b} \frac{3\overline{m}_q^4}{4\pi^2\overline{v}^2} \log \frac{\overline{m}_q^2}{Q^2}. \tag{6.1.11}$$

In this expression all masses and vacuum expectation values are SM $\overline{\rm MS}$ parameters evaluated at the scale Q,

$$\overline{m}_q \equiv m_q^{\overline{\rm MS},{\rm SM}}(Q), \quad \overline{v} \equiv v_{\overline{\rm MS},{\rm SM}}(Q). \tag{6.1.12}$$

They are related to the MSSM parameters in the $\overline{\rm DR}$ scheme at scale Q in the following way,

$$\begin{aligned} v^2_{\overline{\rm MS},{\rm SM}} &= v^2_{\overline{\rm DR},{\rm MSSM}} \left(1 - (\delta^{(1)}v^2)^{\rm n/SM}\right), \\ m_q^{\overline{\rm MS},{\rm SM}} &= m_q^{\overline{\rm DR},{\rm MSSM}} - (\delta^{(1)}m_q^{\rm OS})^{\rm n/SM}, \quad q = t, b, \end{aligned} \tag{6.1.13}$$

The one-loop shift $(\delta^{(1)}v^2)^{\rm n/SM}$ includes $\mathcal{O}(\alpha_t+\alpha_b)$ terms while $(\delta^{(1)}m_q^{\rm OS})^{\rm n/SM}$ includes $\mathcal{O}(\alpha_t+\alpha_b+\alpha_s)$ corrections. In our convention, $(\delta^{(1)}m_q^{\rm OS})^{{\rm n/SM},\mathcal{O}(\alpha_s)}$ includes in addition to the contribution of heavy particles also the transition between the $\overline{\rm DR}$ and $\overline{\rm MS}$ schemes. With these definitions and Eq. (6.1.7), the two-loop terms which account for the shifts between the SM and the MSSM quantities acquire the following form,[77]

$$\widehat{\Sigma}_{hh}^{\rm SM,shifts} = -\sum_{q=t,b} \frac{\partial}{\partial m_q} \widehat{\Sigma}_{hh}^{\rm SM,(1)} \, (\delta^{(1)}m_q^{\rm OS})^{\rm n/SM} + \widehat{\Sigma}_{hh}^{\rm SM,(1)} \, (\delta^{(1)}v^2)^{\rm n/SM}, \tag{6.1.14}$$

where we have exploited the fact that in the gaugeless limit $\widehat{\Sigma}_{hh}^{\rm SM,(1)}$ scales as $\propto 1/v^2$. In Ref. [23] it was shown that in the heavy SUSY limit the non-SM part of the vev shift can be expressed via the non-SM part of the Higgs self-energy derivative,

$$(\delta^{(1)}v^2)^{\rm n/SM} = -\widehat{\Sigma}_{hh}^{{\rm n/SM},(1)\prime}(m_h^2). \tag{6.1.15}$$

Using this relation, Eq. (6.1.14) can be rewritten as follows,

$$\widehat{\Sigma}_{hh}^{\rm SM,shifts} = -\sum_{q=t,b} \frac{\partial}{\partial m_q} \widehat{\Sigma}_{hh}^{\rm SM,(1)} \, (\delta^{(1)}m_q^{\rm OS})^{\rm n/SM} - \widehat{\Sigma}_{hh}^{\rm SM,(1)} \widehat{\Sigma}_{hh}^{{\rm n/SM},(1)\,\prime}. \tag{6.1.16}$$

[77] For clarity, we will omit arguments of the self-energies in the rest of this section, implying that it always equals zero.

Taking into account Eq. (6.1.5), Eq. (6.1.7) and Eq. (6.1.16), the pole equation Eq. (6.1.3) can be solved iteratively up to the two-loop level,

$$\begin{aligned}(M_h)^2_{\rm SM} &= (\overline{m}_h^{1l})^2 + (\overline{m}_h^{2l})^2 - \widehat{\Sigma}^{\rm SM,(1)}_{hh} - \widetilde{\Sigma}^{\overline{\rm MS},\rm SM,(2)}_{hh} \\ &- \widehat{\Sigma}^{\rm SM,(1)\prime}_{hh}\left((\overline{m}_h^{1l})^2 - \widehat{\Sigma}^{\rm SM,(1)}_{hh}\right) + \sum_{q=t,b}\frac{\partial}{\partial m_q}\widehat{\Sigma}^{\rm SM,(1)}_{hh}\,(\delta^{(1)}m_q^{\rm OS})^{\rm n/SM} \\ &+ \widehat{\Sigma}^{\rm SM,(1)}_{hh}\widehat{\Sigma}^{\rm n/SM,(1)\prime}_{hh}.\end{aligned} \tag{6.1.17}$$

At the matching scale Q, the predictions for the physical Higgs mass Mh in the SM and the MSSM have to be equal order by order,

$$(M_h)^2_{\rm SM} = (M_h)^2_{\rm MSSM}. \tag{6.1.18}$$

By equating the one-loop pieces in Eq. (6.1.18), and taking into account Eq. (6.1.1) and Eq. (6.1.17) we get,

$$(\overline{m}_h^{1l})^2 = -\widehat{\Sigma}^{\rm MSSM,(1)}_{hh} + \widehat{\Sigma}^{\rm SM,(1)}_{hh} = -\widehat{\Sigma}^{\rm n/SM,(1)}_{hh}. \tag{6.1.19}$$

After inserting this one-loop solution back into Eq. (6.1.17), we arrive at

$$\begin{aligned}(M_h)^2_{\rm SM} &= (\overline{m}_h^{2l})^2 - \widehat{\Sigma}^{\rm MSSM,(1)}_{hh} - \widetilde{\Sigma}^{\overline{\rm MS},\rm SM,(2)}_{hh} \\ &+ \widehat{\Sigma}^{\rm SM,(1)\prime}_{hh}\widehat{\Sigma}^{\rm MSSM,(1)}_{hh} + \sum_{q=t,b}\frac{\partial}{\partial m_q}\widehat{\Sigma}^{\rm SM,(1)}_{hh}\,(\delta^{(1)}m_q^{\rm OS})^{\rm n/SM} \\ &+ \widehat{\Sigma}^{\rm SM,(1)}_{hh}\widehat{\Sigma}^{\rm n/SM,(1)\prime}_{hh}.\end{aligned} \tag{6.1.20}$$

By equating the two-loop pieces in Eq. (6.1.18) and expanding the one-loop self-energies of the Higgs boson in the full MSSM according to Eq. (6.1.6), we get

$$\begin{aligned}(\overline{m}_h^{2l})^2 &= -\widehat{\Sigma}^{\rm MSSM,(2)}_{hh} + \widetilde{\Sigma}^{\overline{\rm MS},\rm SM,(2)}_{hh} \\ &- \sum_{q=t,b}\frac{\partial}{\partial m_q}\widehat{\Sigma}^{\rm SM,(1)}_{hh}\,(\delta^{(1)}m_q^{\rm OS})^{\rm n/SM} + \widehat{\Sigma}^{\rm n/SM,(1)}_{hh}\widehat{\Sigma}^{\rm n/SM,(1)\prime}_{hh}.\end{aligned} \tag{6.1.21}$$

The running Higgs-boson mass $\overline{m}_h^2$ can be related to the the threshold corrections to the quartic coupling λ via the relation

$$\overline{m}_h^2 = 2\Delta\lambda(Q)v^2_{\overline{\rm MS},\rm SM}(Q). \tag{6.1.22}$$

To express the one- and two-loop corrections in terms of the MSSM coupling constants we have to perform the shift of the vacuum expectation value in Eq. (6.1.22),

$$\overline{m}_h^2 = 2\Delta\lambda(Q)v^2_{\overline{\rm DR},\rm MSSM}(Q)(1 + \widehat{\Sigma}^{\rm n/SM,(1)\prime}_{hh}). \tag{6.1.23}$$

By solving this equation at the one- and two-loop levels, we obtain the expressions for the matching coefficients for the quartic coupling,

$$\Delta\lambda^{1l} = -\frac{\widehat{\Sigma}_{hh}^{\mathrm{n/SM},(1)}}{2v^2_{\overline{\mathrm{DR}},\mathrm{MSSM}}(Q)}, \tag{6.1.24a}$$

$$\Delta\lambda^{2l} = -\frac{1}{2v^2_{\overline{\mathrm{DR}},\mathrm{MSSM}}(Q)}\Big(\widehat{\Sigma}_{hh}^{\mathrm{MSSM},(2)} - \widetilde{\Sigma}_{hh}^{\overline{\mathrm{MS}},\mathrm{SM},(2)} - 2\,\widehat{\Sigma}_{hh}^{\mathrm{n/SM},(1)}\widehat{\Sigma}_{hh}^{\mathrm{n/SM},(1)\prime} + \sum_{q=t,b}\frac{\partial}{\partial m_q}\widehat{\Sigma}_{hh}^{\mathrm{SM},(1)}\,(\delta^{(1)}m_q^{\mathrm{OS}})^{\mathrm{n/SM}}\Big). \tag{6.1.24b}$$

As already mentioned in the expressions above all couplings are $\overline{\mathrm{DR}}$ MSSM couplings at the scale Q. Another option is to parametrize these treshold corrections in terms of the $\overline{\mathrm{MS}}$ SM couplings at Q. While for the bottom coupling this would lead to unacceptably large shifts, for the top Yukawa coupling the effect is relatively mild. In this thesis we will use the $\overline{\mathrm{MS}}$ top-Yukawa coupling in the SM and the $\overline{\mathrm{DR}}$ MSSM bottom-Yukawa coupling to parametrize the one- and two-loop threshold corrections. To express the two-loop threshold corrections in terms of the SM $\overline{\mathrm{MS}}$ top-Yukawa coupling we have to reparametrize the top mass and the vev in the one-loop $\mathcal{O}(\alpha_t^2)$ threshold correction. This generates the following two-loop terms,

$$\Delta\lambda\big|_{y_t^{\mathrm{MSSM}}\to y_t^{\mathrm{SM}}} = -\frac{1}{2v^2_{\overline{\mathrm{MS}},\mathrm{SM}}}\Big(\frac{\partial}{\partial m_t}\widehat{\Sigma}_{hh}^{\mathrm{n/SM},\mathcal{O}(m_t^2\alpha_t)}\,(\delta^{(1)}m_t^{\mathrm{OS}})^{\mathrm{n/SM},\mathcal{O}(\alpha_t+\alpha_b+\alpha_s)} + 2\,\widehat{\Sigma}_{hh}^{\mathrm{n/SM},(1),\mathcal{O}(m_t^2\alpha_t)}\,\widehat{\Sigma}_{hh}^{\mathrm{n/SM},(1),\mathcal{O}(\alpha_b+\alpha_t)\prime}\Big) \tag{6.1.25}$$

which has to be added to the Eq. (6.1.24b). The final results for the two-loop threshold corrections of $\mathcal{O}(\alpha_t^2\alpha_s + \alpha_b^2\alpha_s + (\alpha_t+\alpha_b)^3)$ read,

$$(\Delta\lambda)_{\alpha_t^3} = -\frac{1}{2v^2_{\overline{\mathrm{MS}},\mathrm{SM}}}\Big(\widehat{\Sigma}_{hh}^{\mathrm{MSSM},\mathcal{O}(m_t^2\alpha_t^2)} - \widetilde{\Sigma}_{hh}^{\overline{\mathrm{MS}},\mathrm{SM},\mathcal{O}(m_t^2\alpha_t^2)} + \frac{\partial}{\partial m_t}\widehat{\Sigma}_{hh}^{\mathrm{MSSM},\mathcal{O}(m_t^2\alpha_t)}\cdot\,(\delta^{(1)}m_t^{\mathrm{OS}})^{\mathrm{n/SM},\mathcal{O}(\alpha_t)}\Big), \tag{6.1.26a}$$

$$(\Delta\lambda)_{\alpha_t^2\alpha_b} = -\frac{1}{2v^2_{\overline{\mathrm{MS}},\mathrm{SM}}}\Big(\widehat{\Sigma}_{hh}^{\mathrm{MSSM},\mathcal{O}(m_t^2\alpha_t\alpha_b)} - \widetilde{\Sigma}_{hh}^{\overline{\mathrm{MS}},\mathrm{SM},\mathcal{O}(m_t^2\alpha_t\alpha_b)} + \frac{\partial}{\partial m_t}\widehat{\Sigma}_{hh}^{\mathrm{MSSM},\mathcal{O}(m_t^2\alpha_t)}\cdot\,(\delta^{(1)}m_t^{\mathrm{OS}})^{\mathrm{n/SM},\mathcal{O}(\alpha_b)}\Big), \tag{6.1.26b}$$

$$(\Delta\lambda)_{\alpha_t\alpha_b^2} = -\frac{1}{2v^2_{\overline{\mathrm{DR}},\mathrm{MSSM}}}\Big(\widehat{\Sigma}_{hh}^{\mathrm{MSSM},\mathcal{O}(m_b^2\alpha_t\alpha_b)} - \widetilde{\Sigma}_{hh}^{\overline{\mathrm{MS}},\mathrm{SM},\mathcal{O}(m_b^2\alpha_t\alpha_b)} - 2\,\widehat{\Sigma}_{hh}^{\mathrm{n/SM},(1),\mathcal{O}(m_b^2\alpha_b)}\widehat{\Sigma}_{hh}^{\mathrm{n/SM},(1),\mathcal{O}(\alpha_t)\prime} + \frac{\partial}{\partial m_b}\widehat{\Sigma}_{hh}^{\mathrm{SM},(1)}\cdot\,(\delta^{(1)}m_b^{\mathrm{OS}})^{\mathrm{n/SM},\mathcal{O}(\alpha_t)}\Big), \tag{6.1.26c}$$

$$(\Delta\lambda)_{\alpha_b^3} = -\frac{1}{2v^2_{\overline{\mathrm{DR}},\mathrm{MSSM}}}\Big(\widehat{\Sigma}_{hh}^{\mathrm{MSSM},\mathcal{O}(m_b^2\alpha_b^2)} - \widetilde{\Sigma}_{hh}^{\overline{\mathrm{MS}},\mathrm{SM},\mathcal{O}(m_b^2\alpha_b^2)} \tag{6.1.26d}$$

$$- 2\,\widehat{\Sigma}_{hh}^{\mathrm{n/SM},(1),\mathcal{O}(m_b^2\alpha_b)}\widehat{\Sigma}_{hh}^{\mathrm{n/SM},(1),\mathcal{O}(\alpha_b)\prime} + \frac{\partial}{\partial m_b}\widehat{\Sigma}_{hh}^{\mathrm{SM},(1)} \cdot \left(\delta^{(1)} m_b^{\mathrm{OS}}\right)^{\mathrm{n/SM},\mathcal{O}(\alpha_b)}\Big),$$

$$(\Delta\lambda)_{\alpha_t^2\alpha_s} = -\frac{1}{2v^2_{\overline{\mathrm{MS}},\mathrm{SM}}}\Big(\widehat{\Sigma}_{hh}^{\mathrm{MSSM},\mathcal{O}(m_t^2\alpha_t\alpha_s)} - \widetilde{\Sigma}_{hh}^{\overline{\mathrm{MS}},\mathrm{SM},\mathcal{O}(m_t^2\alpha_t\alpha_s)} \tag{6.1.26e}$$

$$+ \frac{\partial}{\partial m_t}\widehat{\Sigma}_{hh}^{\mathrm{MSSM},\mathcal{O}(m_t^2\alpha_t)} \cdot \left(\delta^{(1)} m_t^{\mathrm{OS}}\right)^{\mathrm{n/SM},\mathcal{O}(\alpha_s)}\Big),$$

$$(\Delta\lambda)_{\alpha_b^2\alpha_s} = -\frac{1}{2v^2_{\overline{\mathrm{DR}},\mathrm{MSSM}}}\Big(\widehat{\Sigma}_{hh}^{\mathrm{MSSM},\mathcal{O}(m_b^2\alpha_b\alpha_s)} - \widetilde{\Sigma}_{hh}^{\overline{\mathrm{MS}},\mathrm{SM},\mathcal{O}(m_b^2\alpha_b\alpha_s)} \tag{6.1.26f}$$

$$+ \frac{\partial}{\partial m_b}\widehat{\Sigma}_{hh}^{\mathrm{SM},\mathcal{O}(m_b^2\alpha_b)} \cdot \left(\delta^{(1)} m_b^{\mathrm{OS}}\right)^{\mathrm{n/SM},\mathcal{O}(\alpha_s)}\Big).$$

The non-SM part of the one-loop Higgs boson self-energy can be evaluated with the help of `FeynArts` and `FormCalc` and then expanded in the limit $m_{\tilde{t}_L}, m_{\tilde{t}_R}, m_{\tilde{b}_R} \gg m_t, m_b$. The explicit expression for them (and their derivatives) in the gaugeless limit and for the case $m_{\tilde{t}_L} = m_{\tilde{t}_R} = m_{\tilde{b}_R} \gg m_t, m_b$ reads,

$$\begin{aligned}
\widehat{\Sigma}_{hh}^{\mathrm{n/SM},(1)} &= -\sum_{q=t,b}\frac{3m_q^4}{4\pi^2 v^2}\left(\log\frac{M_{\mathrm{SUSY}}^2}{Q^2} + |\widehat{X}_q|^2 - \frac{|\widehat{X}_q|^4}{12}\right), \\
\widehat{\Sigma}_{hh}^{\mathrm{n/SM},(1)\prime} &= \sum_{q=t,b}\frac{m_q^2}{32\pi^2 v^2}\,|\widehat{X}_q|^2.
\end{aligned} \tag{6.1.27}$$

From this expressions and Eq. (6.1.24a) it is clear how the one-loop threshold corrections to λ computed in [15, 33] can be generalized to the case of the MSSM with $\mathcal{CP}$-violation. These corrections are polynomials in the squark mixing parameter $\widehat{X}_q$. To obtain the expression in the MSSM with $\mathcal{CP}$-violation $\widehat{X}_q$ has to replaced by $|\widehat{X}_q|$.

The two-loop self-energies were taken from [9, 11, 257] and expanded in the limit

$$m_{\tilde{t}_L}, m_{\tilde{t}_R}, m_{\tilde{b}_R}, m_A, |\mu|, |M_3| \gg m_t, m_b$$

without any additional assumptions on the internal masses.soft-breaking masses and the phases of X_t, X_b, μ and M_3. The two-loop SM self-energies in the $\overline{\mathrm{MS}}$ scheme are taken from Refs. [239, 240] and extracted from the code `FlexibleSUSY` [25, 27, 237, 238]. The explicit expressions for them can be found in App. C. Finally, the one-loop counterterms $(\delta^{(1)} m_t^{\mathrm{OS}})^{\mathrm{n/SM}}$ and $(\delta^{(1)} m_b^{\mathrm{OS}})^{\mathrm{n/SM}}$ have been computed using `FeynArts` and `FormCalc`. The explicit expressions for them in them are listed in the App. B. The resulting two-loop formulas for the threshold correcions are presented in App. A.

Knowing the expressions for the threshold corrections in the MSSM without $\mathcal{CP}$-violation the threshold corrections for the complex MSSM can be obtained via the following rules:

- $\mathcal{O}(\alpha_q^2\alpha_s)$ where $q = t, b$: The expression for zero phases is a polynomial in $\widehat{X}_q$. To get the expression for non-zero phases every odd power of $\widehat{X}_q$ has to be multiplied by $\cos(\phi_{X_q} - \phi_{M_3})$, and $\widehat{X}_q$ has to replaced by $|\widehat{X}_q|$.

- $\mathcal{O}(\alpha_q^3)$ where $q = t, b$: The expression for zero phases is a sum of monomials in the variables $\widehat{X}_q$ and $\widehat{Y}_q = \widehat{X}_q + \dfrac{2\widehat{\mu}^*}{\sin 2\beta}$ of one of three types: the monomials which contain only even powers of $\widehat{X}_q$, the ones which contain only even powers of $\widehat{Y}_q$ and the ones which contain both $\widehat{X}_q$ and $\widehat{Y}_q$. The latter contain only even or only odd powers of $\widehat{X}_q$ and $\widehat{Y}_q$ at the same time. To get the expression for non-zero phases, every monomial which contains odd powers of $\widehat{X}_q$ and $\widehat{Y}_q$ has to be multiplied by $\cos(\phi_{X_q} - \phi_{Y_q})$, and every $\widehat{X}_q$ and $\widehat{Y}_q$ has to be replaced by $|\widehat{X}_q|$ and $|\widehat{Y}_q|$, respectively.

The generalization of the $\mathcal{O}(\alpha_b^2\alpha_t)$ and $\mathcal{O}(\alpha_b\alpha_t^2)$ expressions from the $\mathcal{CP}$-conserving case to the $\mathcal{CP}$-violating case is slightly more complicated, since multiple different multiplicative factors arise.

If the low-energy is the SM plus electroweakinos, effective Higgs–Higgsino–gaugino couplings are induced. These are potentially complex-valued. An explicit matching calculation at the one-loop level, however, shows that their phase is zero even if one or more of the electroweakino phases in the MSSM is non-zero. Correspondingly, also the RGEs of the SM plus electroweakinos are not modified in the presence of non-zero phases. The phases, however, enter in the threshold correction for the bottom and top Yukawa coupling as well as the Higgs self-coupling when integrating out the electroweakinos (full expressions are listed in App. A).

6.2 Δ_b with phase dependence

In addition to the phase dependencies discussed above, also the Δ_b corrections (see Sec. 5.2.4) depend on ϕ_μ, $\phi_{M_{1,2,3}}$ and ϕ_{A_t}. The phase dependence of the one-loop correction has been derived in [191, 200]. The phase dependence of the two-loop correction, which we derived in the real case based upon the result of [29–31], has, however, been unknown so far. We find that this dependence is the same as for the one-loop result. This can be understood by looking at the explicit two-loop diagrams.

But first, let us consider the one-loop correction. The $\mathcal{O}(\alpha_t + \alpha_s)$ one-loop Δ_b correction in the heavy SUSY limit can be obtained by evaluating the diagrams in Fig. 6.1. These diagrams include the incoming and the outgoing b-quarks with different chirality. The diagrams which involve quarks with the same chirality are suppressed by additional factors of $\tan\beta$ and do not contribute to Δ_b [200]. The

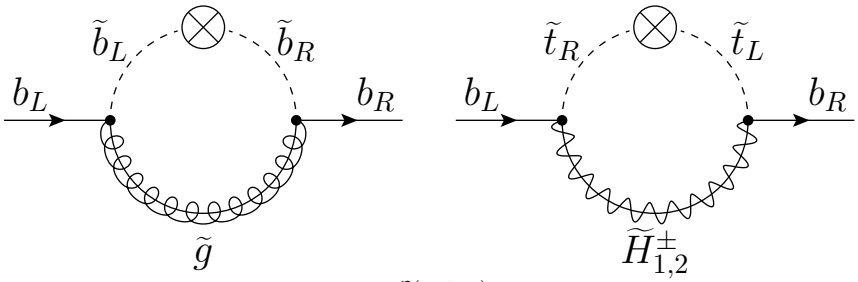

Figure 6.1: Diagrams contributing to $\Delta_b^{\mathcal{O}(\alpha_t+\alpha_s)}$ at the leading order in the chiral basis

diagrams are drawn using the chiral basis in which the "left" and the "right" squarks propagate and the off-diagonal mass term is interpreted as an additional interaction (denoted as $\otimes$) which flips the "chirality" of the squark. In the limit $M_{\text{SUSY}} \gg v$ only the diagrams with a single mass insertion contribute. This can be seen in the following way. The left diagram in Fig. 6.1 is proportional to

$$\propto \alpha_s \; m_b \; \mu \; t_\beta \; M_3 \; C_0(0,0,0,m^2_{\tilde{t}_L}, m^2_{\tilde{t}_R}, |M_3|^2), \tag{6.2.1}$$

where C_0 is a Passarino-Veltman function corresponding to the vertex function with three external legs. If all soft-breaking are equal M_{SUSY}, the expression in the Eq. (6.2.1) reduces to

$$\propto \alpha_s \; m_b \; t_\beta \frac{\mu \; M_3}{M^2_{\text{SUSY}}}. \tag{6.2.2}$$

The analogous diagram with two mass insertion is proportional to

$$\propto \alpha_s \; m_b \; \mu \; t_\beta \; M_3 \; D_0(0,0,0,0,0,0,m^2_{\tilde{t}_L}, m^2_{\tilde{t}_R}, m^2_{\tilde{t}_L}, |M_3|^2), \tag{6.2.3}$$

where D_0 is a Passarino-Veltman function corresponding to the vertex function with four external legs. If all soft-breaking are equal M_{SUSY} this diagrams behaves like

$$\propto \alpha_s \; m_b \; t_\beta \frac{\mu \; M_3}{M^2_{\text{SUSY}}} \times \frac{m_b \; \mu \; t_\beta}{M^2_{\text{SUSY}}}. \tag{6.2.4}$$

We see that it is suppressed by an additional factor m_b/M_{SUSY} compared to the diagram with one insertion and is therefore non-leading. Clearly, diagrams with more insertion will be suppressed by more additional factors of m_b/M_{SUSY}. Analogous arguments are applicable to the right diagram in Fig. 6.1.

The same argument applies to higher-order corrections to Δ_b [30] as can be proven by using the Kinoshita-Lee-Nauenberg theorem [258, 259]. Namely, the diagrams contributing to the two-loop quantity Δ_b of order $\mathcal{O}(\alpha_s^2 + \alpha_t\alpha_s)$ contain only one mass insertion.

The phases of the complex parameters A_t, μ and M_3 enter through the mass insertions and through $(b_L \tilde{b}^*_L \tilde{g})$ and $(b_L \tilde{t}^*_R \widetilde{H}^+_2)$ vertices. In particular, the mass

insertion in the left diagram in Fig. 6.1 yields the phase factor $\propto e^{+i\phi_\mu}$ while both vertices contain $e^{+i\frac{\phi_{M_3}}{2}}$ (see Sec. 2.5.4). The overall diagram is then $\propto e^{i\phi_{M_3}+i\phi_\mu}$. The result for the analogous diagram with incoming b_R and outgoing b_L leads to the phase factor $\propto e^{-i\phi_{M_3}-i\phi_\mu}$. The overall phase dependence is then $\propto \cos(\phi_{M_3}+\phi_\mu)$ (see Eq. (A.1.8) in App. A). The mass insertion in the right diagram in Fig. 6.1 gives phase factor $\propto e^{+i\phi_{A_t}}$, while $(b_L\widetilde{t}_R^*\widetilde{H}_2^+)$ and $(\bar{b}_R\widetilde{t}_L\widetilde{H}_2^-)$ vertices contain the entries of the chargino mixing matrices $\mathbf{V}_{22}^*$ and $\mathbf{U}_{22}^*$. In the gaugeless limit they are proportional to the phase factors $\propto e^{+i\frac{\phi_\mu}{2}}$. The overall diagram (together with its complex conjugated) is $\propto \cos(\phi_{A_t}+\phi_\mu)$ (see Eq. (A.1.8) in App. A).

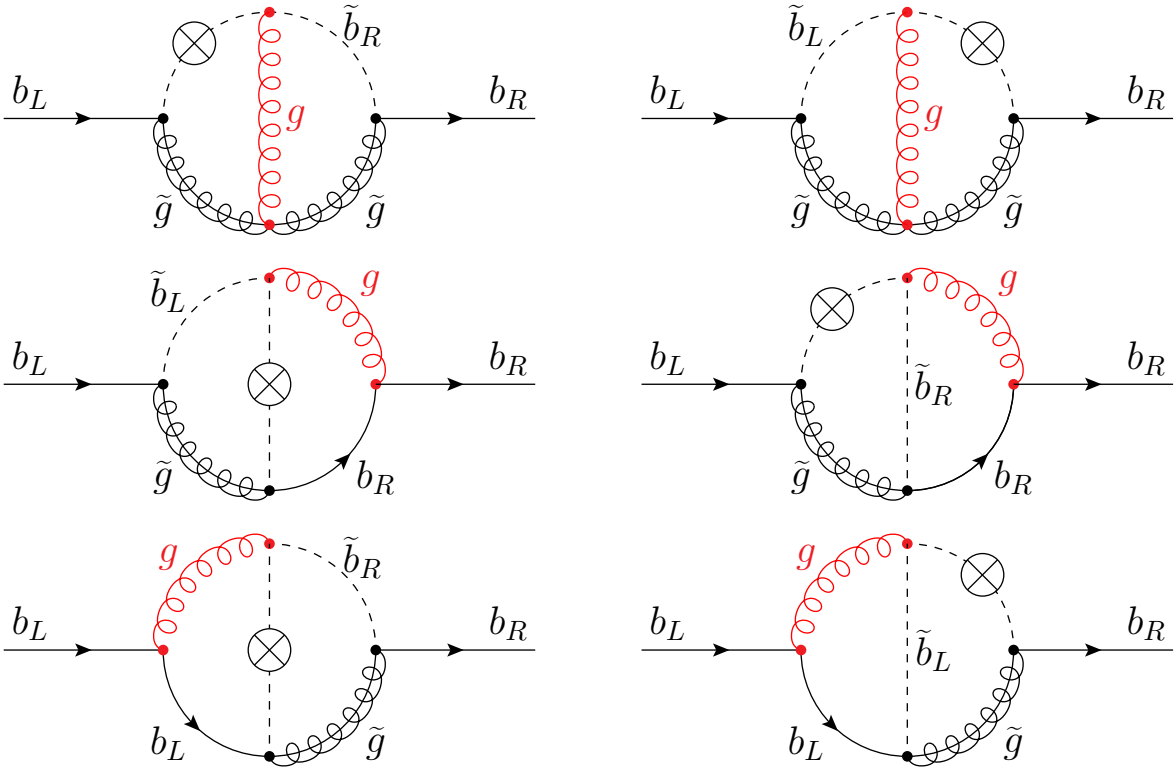

Figure 6.2: The first class of two-loop diagrams contributing to $\Delta_b^{2L,\mathcal{O}(\alpha_s^2)}$: a gluon is added to the $\mathcal{O}(\alpha_s)$ one-loop graph.

Two-loop diagrams contributing to the quantity Δ_b at order $\mathcal{O}(\alpha_s^2)$ can be split into three categories: either a gluon, a sbottom quark or a gluino is added to the one-loop $\mathcal{O}(\alpha_s)$ graph. Examples of the corresponding diagrams are depicted in Figs. 6.2 – 6.4. The particles which are added to the one-loop graph are highlighted with the red color.[78]

If a gluon is added, the phase dependence of the one-loop graph is obviously not changed, since the two additionally appearing strong gauge couplings do not include a phase dependence. The same is true if a sbottom quark is added coupled to the

[78] The rightmost diagram on Fig. 6.4 cannot be reduced to any one-loop diagram. This fact however does not change our argumentation.

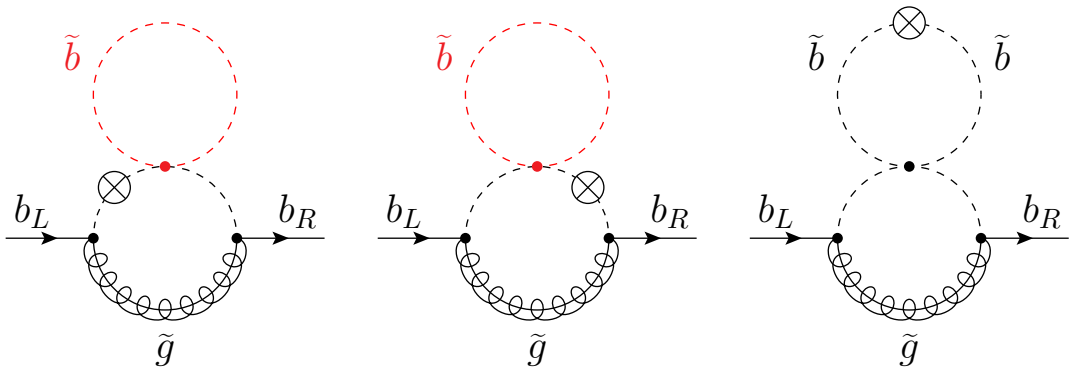

Figure 6.3: The second class of two-loop diagrams contributing to $\Delta_b^{2L,\mathcal{O}(\alpha_s^2)}$: a sbottom is added to the $\mathcal{O}(\alpha_s)$ graph.

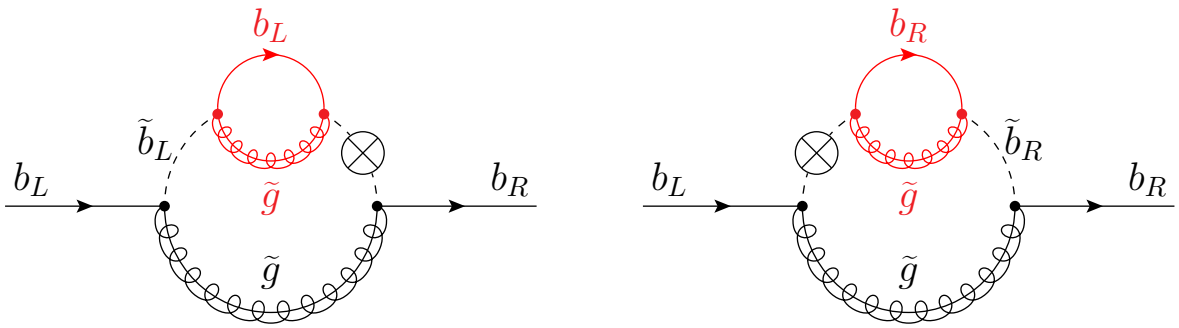

Figure 6.4: The third class of two-loop diagrams contributing to $\Delta_b^{2L,\mathcal{O}(\alpha_s^2)}$: a gluino is added to the one-loop $\mathcal{O}(\alpha_s)$ graph.

one-loop graph by a four-sfermion vertex. Working in the chiral basis, it is again obvious that this additional coupling does not induce an additional phase dependence. The case of adding a gluino (see Fig. 6.4) is slightly more complicated. The two additional gluon-gluino-sbottom couplings do depend on the phase of the gluino mass parameter. Working again in the chiral basis, it is obvious that one of these two additional couplings is a left-handed coupling and the other one is a right-handed coupling. The dependence on the gluino phase cancels between the left-handed and the right-handed coupling.

We conclude that in the case of the MSSM with complex parameters the two-loop Δ_b of $\mathcal{O}(\alpha_s^2)$ given in Eq. (5.2.23b) has to be multiplied by $\cos(\phi_\mu + \phi_{M_3})$. The same reasoning can be applied to the two-loop Δ_b at $\mathcal{O}(\alpha_t\alpha_s)$: Eq. (5.2.23c) has to be multiplied by $\cos(\phi_\mu + \phi_{A_t})$.[79]

[79] Corresponding two-loop diagrams can be found in the Appendix C of [30].

6.3 Numerical results

In this Section, we discuss the numerical effect of including the full phase dependence into the two-loop threshold corrections to the Higgs self-coupling. First, let us briefly review the method used in `FeynHiggs` to handle non-zero phases so far. The treatment of the two-loop corrections in the presence of the complex parameters is controlled by the flag `tlCplxApprox`. When it equals 3, the fixed-order $\mathcal{O}(m_t^2\alpha_t\alpha_s + m_t^2\alpha_t^2)$ corrections including the full phase dependence are activated and combined with the fixed-order $\mathcal{O}(m_t^2\alpha_t\alpha_b + m_b^2\alpha_t^2 + m_b^2\alpha_b^2 + m_b^2\alpha_b\alpha_s)$ corrections, interpolated in the phases. In this Section, we will assume that we run `FeynHiggs` in this mode. Interpolation occurs when the phases of μ, M_3, X_t or X_b are non-zero. The user can choose between interpolation in A_t or X_t, and A_b or X_b. In the EFT part of the code the interpolation is always carried out in the following way. First, the RGEs are integrated numerically and the subtraction terms are calculated for all possible combinations of $+|P|$ and $-|P|$ (where $P \in \{\mu, X_t/A_t, M_3\}$).[80] After that, linear interpolation is performed on the obtained grid. In this Section, we chose to interpolate X_t when the phase of X_t or A_t is non-zero.

The phases of the above-mentioned parameters enter the hybrid calculation via threshold corrections to the Higgs self-coupling and via the subtraction terms. As we mentioned in Sec. 6.1, both of them depend only on the absolute value $|\widehat{X}_t|$ at the one-loop level, so the interpolation would give a correct result if only LL and NLL resummation were included and the interpolation was performed in X_t. However, the two-loop threshold corrections to the Higgs self-coupling (and hence the two-loop non-logarithmic subtraction terms) do not depend just on the absolute value of X_t. For example, the $\mathcal{O}(\alpha_t^2\alpha_s)$ threshold correction also depends on the cosine of the phase difference, $\cos(\phi_{X_t} - \phi_{M_3})$, and the formula for the $\mathcal{O}(\alpha_t^3)$ threshold correction depends on $|\widehat{Y}_t|$ and $\cos(\phi_{X_t} - \phi_{Y_t})$. In comparison to the full formula, the usage of interpolation introduces an error at the next-to-next-to-leading logarithmic order. The phases also enter the expression for the two-loop threshold corrections of the bottom Yukawa coupling and Δ_b. First, we will, however, concentrate on MSSM scenarios in which the effect of the bottom Yukawa coupling on the Higgs mass is negligible and so we will switch off the two-loop corrections of $\mathcal{O}(m_t^2\alpha_t\alpha_b + m_b^2\alpha_t^2 + m_b^2\alpha_b^2 + m_b^2\alpha_b\alpha_s)$ by choosing the input flag `tlCplxApprox = 1` for the next three plots.

In order to test our approach we first consider the same MSSM scenario as in the Fig. 3 in [231]: all soft SUSY breaking masses and μ are equal to the common mass scale $M_{\rm SUSY} = 2$ TeV, $\tan\beta = 10$ and $\widehat{X}_t^{\overline{\rm DR}}(M_{\rm SUSY}) = \sqrt{6}$. We vary the phase of the gluino mass M3 in the interval $[-\pi, +\pi]$. All other input parameters are assumed

[80] The threshold corrections in `FH-2.16.0` do not depend on X_b or A_b.

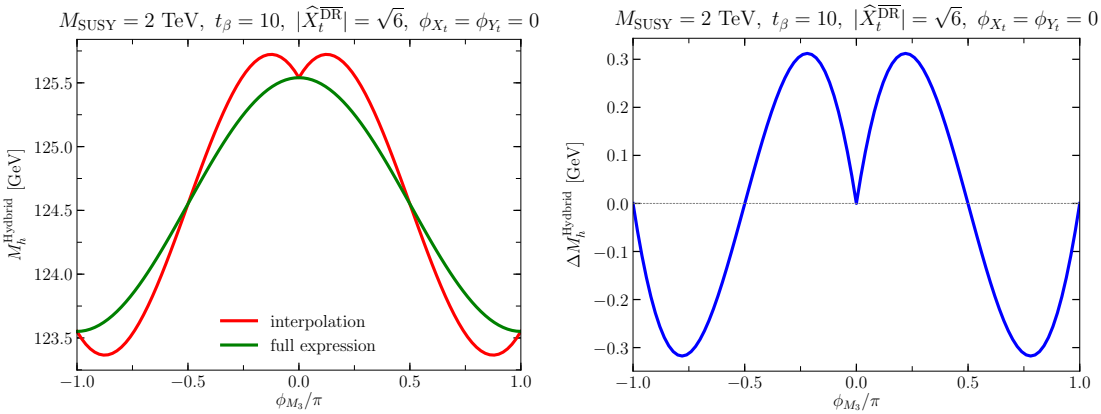

Figure 6.5: *Left:* M_h as a function of ϕ_{M_3} setting $\phi_{X_t} = \phi_{Y_t} = 0$. The results obtained by interpolating the EFT part of the hybrid calculation and by including the full phase dependence are compared. *Right:* Difference of the two curves in the left plot, $\Delta M_h^{\rm Hybrid} = M_h^{\rm interpolation} - M_h^{\rm full\ phase}$.

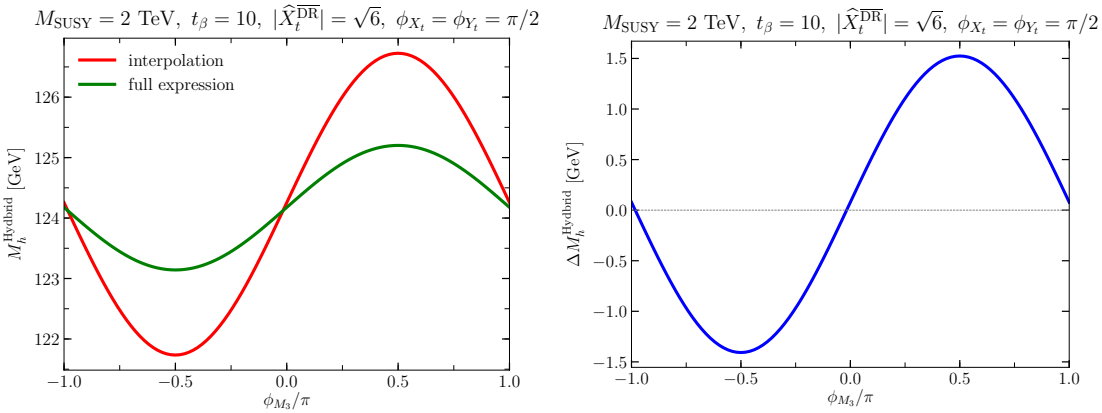

Figure 6.6: The same as in Fig. 6.5 but for $\phi_{X_t} = \phi_{Y_t} = \pi/2$.

to be real. In this way, we test the phase dependence of the $\mathcal{O}(\alpha_t^2\alpha_s)$ threshold correction.

In Fig. 6.5, we show the comparison between the prediction of `FeynHiggs-2.16.0` (red line) and our new calculation including the full phase dependence (green line). For clarity, in the right panel of the same Figure we present the difference between the two predictions. First, we notice that the two methods give the same answer for $\phi_{M_3} = 0, \pm\pi$ which is expected because in these cases M_3 is a real parameter. This serves as a cross-check for our implementation. Second, we see that the interpolation in this particular scenario is a fairly good approximation: the absolute difference between the two curves does not exceed ~ 0.3 GeV for $\phi_{M_3} \simeq \pm\frac{\pi}{4}$ or $\phi_{M_3} \simeq \pm\frac{3\pi}{4}$.

Next, we proceed with the scenario which is similar to the one described above, but we assume that $\widehat{X}_t$ and $\widehat{Y}_t$ are purely imaginary while keeping the same absolute value for $|\widehat{X}_t| = \sqrt{6}$ as before. As one can see in Fig. 6.6, the interpolation procedure overestimates the true Higgs mass for positive values of M_3 and underestimates it for

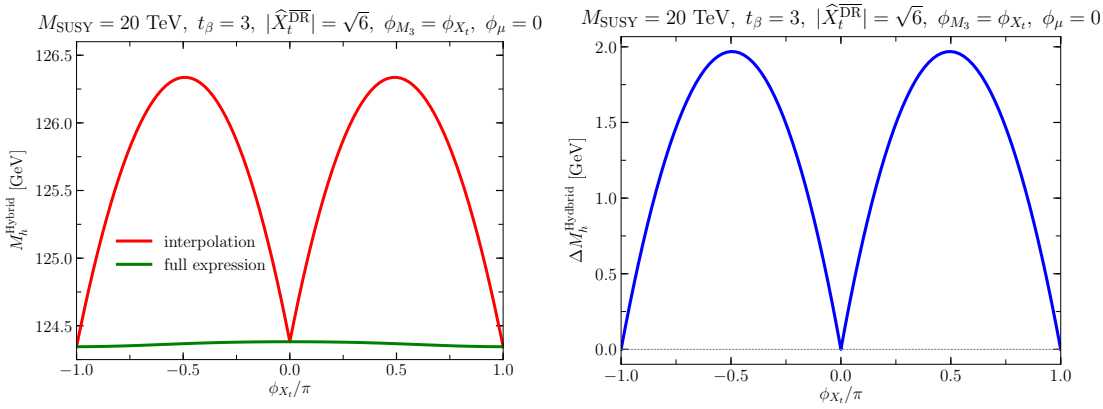

Figure 6.7: *Left:* M_h as a function of ϕ_{X_t} setting $\phi_{M_3} = \phi_{X_t}$ and $\phi_\mu = 0$. The results obtained by interpolating the EFT part of the hybrid calculation and by including the full phase dependence are compared. *Right:* Difference of the two curves in the left plot, $\Delta M_h^{\rm Hybrid} = M_h^{\rm interpolation} - M_h^{\rm full\ phase}$.

$M_3 < 0$. The absolute difference between the two approaches here may be as large as ~ 1.5 GeV for $\phi_{M_3} \simeq \pm\frac{\pi}{2}$.

As a next step, we investigate the effect of phase dependence in $\mathcal{O}(\alpha_t^3)$ threshold correction. To enhance the numerical value of this correction, we choose a low value for $\tan\beta = 3$. This choice, however, suppresses the tree-level Higgs mass, so to bring it back to the value around 125 GeV, we have to choose the scenario with particularly heavy $M_{\rm SUSY} = 20$ TeV. In order to isolate the effect of phase dependence in the considered corrections, we fix the phase of gluino mass to be equal to the phase of X_t. In consequence, the phase dependence in $\mathcal{O}(\alpha_s\alpha_t)$ threshold correction vanishes. We also choose the Higgsino mass parameter to be positive, $\phi_\mu = 0$. The result of the scan in ϕ_{X_t} is shown in Fig. 6.7. Again, as in the case of Fig. 6.5, we see that both methods give exactly the same result for $\phi_{X_t} = 0, \pm\pi$ since in these three points all parameters are real.[81] However, for other values of ϕ_{X_t} the interpolation procedure always overestimates the true value of M_h and, as one can see on the right panel of Fig. 6.7, the maximal difference between the two approaches can reach $\simeq 2$ GeV for $\phi_{X_t} = \phi_{M_3} = \pm\frac{\pi}{2}$.

Finally, in this section, we analyze the interplay between the resummation of the logarithms proportional to the bottom Yukawa coupling and the inclusion of the full phase dependence into the EFT part of our hybrid calculation. As a starting point we go back to the scenario discussed in the Sec. 5.3. Namely, we consider a single scale scenario, where all soft-breaking masses as well as the mass of the charged Higgs boson[82] are equal to 1 TeV, $A_b^{\overline{\rm DR}} = 2.5 M_{\rm SUSY}$, the Higgsino mass parameter is

[81] Even though we have chosen a very low value of $\tan\beta = 3$, the overall phase dependence is quite mild. The difference between the Higgs mass calculated at $\phi_{X_t} = 0$ and $\phi_{X_t} = \pi$ is only $\sim$ 0.05 GeV. Lowering the $\tan\beta$ even further (and pushing $M_{\rm SUSY}$ higher) does not lead to a stronger phase dependence.

[82] Due to the CP-violation $M_{H^\pm}$ is chosen as an input parameter instead of M_A.

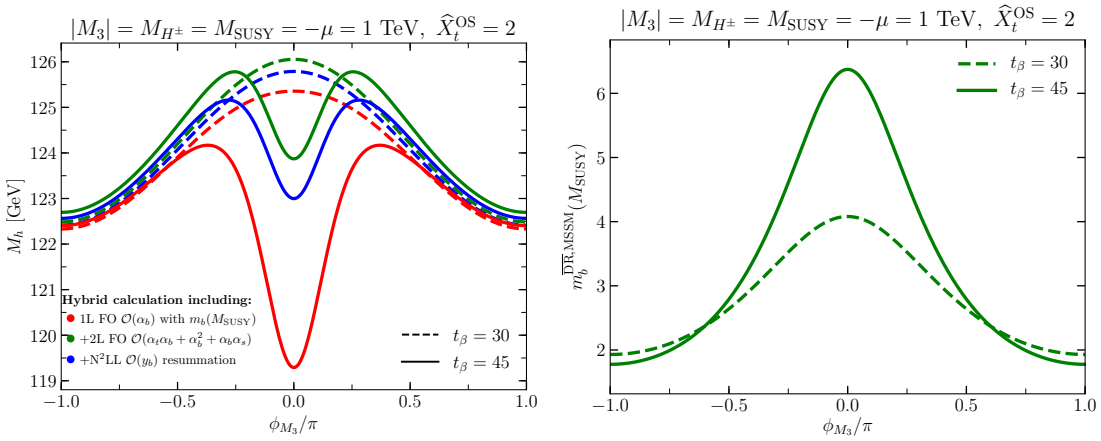

Figure 6.8: *Left:* M_h as a function of the phase of the gluino mass ϕ_{M_3}. The red, green and blue colors on this plot mean the same as in Fig. 5.2. The dashed curves correspond to $\tan\beta = 30$ and the solid curves to $\tan\beta = 45$. *Right:* $m_b^{\overline{\rm DR},{\rm MSSM}}(M_{\rm SUSY})$ as a function of ϕ_{M_3}.

negative $\mu = -M_{\rm SUSY}$, the bino and wino masses are chosen to be positive $M_{1,2} > 0$ and $\widehat{X}_t^{\rm OS} = 2$. The phase of the gluino mass is a free parameter and we scan over it in the interval from $-\pi$ to $+\pi$. We examine this scenario for $\tan\beta = 30$ and $\tan\beta = 45$.

The result of the scan in ϕ_{M_3} is shown in Fig. 6.8. The colors of the curves on the left panel correspond to the same levels of accuracy as in Fig. 5.2, solid lines correspond to $\tan\beta = 30$ and dashed lines correspond to $\tan\beta = 45$. For $\phi_{M_3} = \pm\pi$, all six lines agree within $\sim$ 0.4 GeV. Here, the strong and the top Yukawa contributions to Δ_b partially cancel each other and the MSSM bottom mass does not acquire any enhancement. In fact, in the mentioned points the Δ_b correction is positive and the bottom mass is even more suppressed. This is visible in the right panel of Fig. 6.8, where the solid line lies below the dashed line for $\phi_{M_3} \simeq \pm\pi$.

The red dashed curve resembles the cosine-shape line visible in Fig. 6.5. This is due to the fact that even for $\phi_{M_3} = 0$, where the bottom mass is maximal, it is still too small to have any sizeable effect on M_h. Here, the shape of the line can be explained by the phase dependence of the two-loop fixed-order corrections of $\mathcal{O}(m_t^2\alpha_t\alpha_s)$. Adding additionally the two-loop fixed-order corrections of $\mathcal{O}(m_t^2\alpha_t\alpha_b + m_b^2\alpha_t^2 + m_b^2\alpha_b^2 + m_b^2\alpha_b\alpha_s)$ (blue dashed) lifts the prediction for the Higgs mass by ~ 0.15 GeV for $\phi_{M_3} = \pm\pi$ and by ~ 0.7 GeV for $\phi_{M_3} = 0$. Additionally including resummation of logarithms proportional to the bottom Yukawa coupling (green dashed) is less sizable.

The picture is different for $\tan\beta = 45$. The red solid curve starts to grow when ϕ_{M_3} increases starting from $-\pi$, resembling the red dashed line in shape and reaching its maximal value at $\phi_{M_3} \simeq -\frac{2\pi}{5}$. At this point, the Δ_b correction becomes important leading to an increase of the MSSM bottom mass (see right plot of Fig. 6.8). In consequence, the one-loop corrections, involving the bottom mass, (see Eq. (5.3.1))

become important and they start to lower M_h. With a further increase of ϕ_{M_3} the bottom mass reaches ~ 6.4 GeV and the Higgs mass drops down to 119 GeV. The point $\phi_{M_3} = 0$ in this plot corresponds to the point where $M_{\rm SUSY} = 1$ TeV in the left plot of Fig. 5.3 and the discussion in Sec. 5.3 about the left plot in Fig. 5.3 applies here as well.

Chapter 7

Resummation of logarithms at order N^{3}LL

In this Chapter, we describe the implementation of partial N^{3}LL resummation into the code `FeynHiggs` *and discuss the numerical effect of this resummation.*

7.1 Implementation of N^{3}LL resummation

Up to now, the EFT calculation implemented in `FeynHiggs` was restricted to full LL and NLL resummation as well as NNLL resummation in the limit of vanishing electroweak gauge and bottom Yukawa couplings. In this Chapter, we discuss the implementation of N^{3}LL resummation at $\mathcal{O}(\alpha_s^2\alpha_t^2)$ based upon the work presented in [17]. As was argued in Sec. 4.2, N^{3}LL resummation at $\mathcal{O}(\alpha_s^2\alpha_t^2)$ requires three-loop $\mathcal{O}(\alpha_s^2\alpha_t^2)$ matching condition for the Higgs self-coupling between the SM and the MSSM. This matching condition was computed in [17] based upon the $\mathcal{O}(m_t^2\alpha_t\alpha_s^2)$ fixed-order calculation performed in [10, 219, 220]. The same level of accuracy has to be applied at the electroweak scale. First, the $\overline{\text{MS}}$ top Yukawa couplings have to extracted at the electroweak scale at order $\mathcal{O}(\alpha_s^3)$. Corresponding formulas can be found in [190]. Secondly, $\mathcal{O}(m_t^2\alpha_t\alpha_s^2)$ corrections the SM Higgs self-energy have to be included into the SM pole equation (see Eq. (4.2.8)). Finally, leading QCD corrections to the three-loop RGEs of the Higgs self-coupling, the strong gauge coupling as well as the top Yukawa couplings have to included.

The mentioned three-loop correction to λ is implemented in the publicly available code `Himalaya` [10, 17].[83] As discussed in [17], this calculation is based upon the expansion of three-loop diagrams for the following mass patterns:

$$\text{(h3)} \qquad m_{\tilde{q}} \approx m_{\tilde{t}_1} \approx m_{\tilde{t}_2} \approx m_{\tilde{g}}\,,$$

[83] https://github.com/Himalaya-Library/Himalaya

$$\begin{aligned}
&\text{(h4)} && m_{\tilde{q}} \gg m_{\tilde{t}_1} \approx m_{\tilde{t}_2} \approx m_{\tilde{g}}\,, \\
&\text{(h5)} && m_{\tilde{q}} \gg m_{\tilde{t}_2} \gg m_{\tilde{t}_1} \approx m_{\tilde{g}}\,, \\
&\text{(h6)} && m_{\tilde{q}} \gg m_{\tilde{t}_2} \approx m_{\tilde{g}} \gg m_{\tilde{t}_1}\,, \\
&\text{(h6b)} && m_{\tilde{q}} \approx m_{\tilde{t}_2} \approx m_{\tilde{g}} \gg m_{\tilde{t}_1}\,, \\
&\text{(h9)} && m_{\tilde{q}} \approx m_{\tilde{t}_1} \approx m_{\tilde{t}_2} \gg m_{\tilde{g}}\,,
\end{aligned} \tag{7.1.1}$$

where it is assumed that all squarks except for the top squarks are set equal to $m_{\tilde{q}}$. If one of the cases listed in (7.1.2) features a hierarchy between to masses (denoted as $\gg$), the loop integrals are expanded in the ratio of the respective masses. If two masses are assumed to be approximately equal to each other ($\approx$), the expressions are expanded in the corresponding mass differences. Additionally, in all cases (h3) – (h9) it is assumed that the masses of all squarks and the mass of gluino are much heavier than the mass of the top quark. For instance, if the MSSM scenario corresponds to the case (h3), all three-loop amplitudes are expanded in the following parameters,

$$1 - x_{12}^2, 1 - x_{1g}, 1 - x_{1q}^2, \tag{7.1.2}$$

up to $(1 - x_{12}^2)^3, (1 - x_{1g})^3$ and $(1 - x_{1q}^2)^3$, where

$$x_{12} = \frac{m_{\tilde{t}_1}^2}{m_{\tilde{t}_2}^2}, \quad x_{1g} = \frac{m_{\tilde{t}_1}}{m_{\tilde{g}}}, \quad x_{1q} = \frac{m_{\tilde{t}_1}}{m_{\tilde{q}}}. \tag{7.1.3}$$

If the stop SUSY soft-breaking masses are equal, $m_{\tilde{t}_L} = m_{\tilde{t}_R} \equiv M_{\text{SUSY}}$ the first parameter in Eq. (7.1.3) is equal to

$$1 - x_{12}^2 = \frac{2 M_t X_t}{M_{\text{SUSY}}^2}. \tag{7.1.4}$$

This implies that in the mentioned case the stop mixing parameter X_t is only included up to the power of three. On the other hand, the four-point function parametrized in terms of the MSSM top-Yukawa coupling includes terms proportional to X_t^4 [221]. The contribution of the missing $\sim \widehat{X}_t^4$ terms to the final answer is considered as an uncertainty and `Himalaya` provides an estimate for this uncertainty.

The calculation of three-loop corrections of $\mathcal{O}(m_t^2 \alpha_t \alpha_s^2)$ to the Higgs mass requires the one-loop renormalization of the gluino mass since this mass enters the two-loop $\mathcal{O}(m_t^2 \alpha_t \alpha_s)$ corrections. As we mentioned in Sec. 3.1.1, DRED preserves SUSY up to the three-loop level in the gaugeless limit. In this scheme loops with virtual ϵ-scalars – unphysical massless particles – have to be taken into account. Their computation requires the renormalization of the ϵ-scalars masses. Usually these masses are renormalized to zero in the OS scheme. This scheme is called $\overline{\text{DR}}'$-scheme.

We implemented all corrections mentioned into the EFT calculation of `FeynHiggs` (the link to `Himalaya` has already been implemented for the work presented in [35]). By default, `Himalaya` use the $\overline{\text{DR}}'$ scheme for the renormalization of the squark input parameters. Correspondingly, also the input parameters of `FeynHiggs` are defined in the $\overline{\text{DR}}'$ scheme if N^{3}LL resummation is activated. In case of complex input parameters, we interpolate the `Himalaya` result.[84]

The inclusion of N^{3}LL resummation in the EFT calculation can also be used together with the fixed-order calculation. In this case we, however, require that also in the fixed-order calculation the parameters entering the three-loop threshold correction are renormalized in the $\overline{\text{DR}}$ scheme. The needed two-loop conversion between OS parameters, potentially used in the fixed-order calculation, and $\overline{\text{DR}}$ parameters, used in the EFT calculation, is beyond the scope of this thesis.[85]

7.2 Numerical results

Here, we study the numerical effects of including N^{3}LL resummation at leading order in strong gauge coupling into our hybrid framework. We study a simple single scale scenario in which all non-SM masses are set to the common scale M_{SUSY}. Furthermore, we set all trilinear SUSY soft-breaking couplings, except for A_t, to zero. We define the stop parameters in the $\overline{\text{DR}}$ scheme at the scale M_{SUSY}. We set $\tan\beta = 10$.

In Fig. 7.1, we compare the results obtained using three different accuracy levels to each other: NNLL resummation with the SM top Yukawa coupling extracted at the two-loop level (blue), NNLL resummation with the SM top Yukawa coupling extracted at the three-loop level (red) and N^{3}LL resummation (green). In the upper plots, the different results are compared in dependence of M_{SUSY}. For vanishing stop mixing, all three results are in good agreement for low M_{SUSY}. If M_{SUSY} is raised, there is, however, an increasing difference between the NNLL (with the two-loop level SM top Yukawa coupling) and the N^{3}LL results of up to ~ 1 GeV for $M_{\text{SUSY}} \sim 100$ TeV. This shift is almost completely caused by including the three-loop corrections to the extraction of the SM top Yukawa coupling, since the NNLL result with the SM top Yukawa coupling extracted at the three-loop level and the N^{3}LL result are in very good agreement also for $M_{\text{SUSY}} \sim 100$ TeV. Also for $\widehat{X}_t = -\sqrt{6}$, the NNLL result with the SM top Yukawa coupling extracted at the three-loop level and the N^{3}LL result are in good agreement across the considered M_{SUSY} range (within ~ 0.3 GeV). The NNLL result with the SM top Yukawa coupling extracted at the two-loop level is shifted upwards by ~ 0.7 GeV. In the top right plot, also the estimate of the

[84] An interpolation in case of a complex M_3 is not possible since the expressions implemented in `Himalaya` are not dependent on the sign of M_3.

[85] The necessary two-loop squark self-energy corrections have in principle already been calculated in [222, 260].

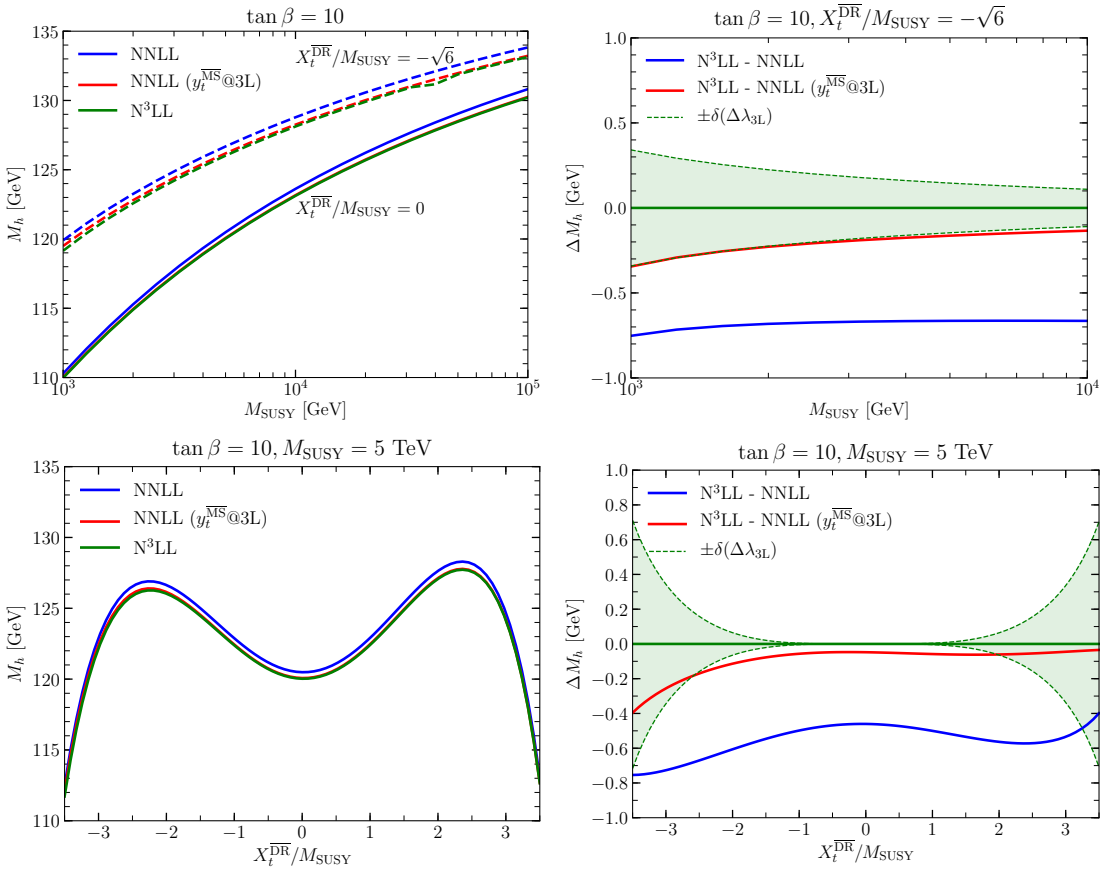

Figure 7.1: *Top left*: Prediction for M_h in dependence of $M_{\rm SUSY}$ for $\widehat{X}_t = 0$ (solid) and $\widehat{X}_t = -\sqrt{6}$ (dashed). The results using NNLL resummation (blue), NNLL resummation with the SM top Yukawa coupling extracted at the three-loop level (red) and N^{3}LL resummation (green) are compared. *Top right*: Differences of the M_h predictions using N^{3}LL and NNLL resummation (blue) as well as using N^{3}LL and NNLL resummation with the SM top Yukawa coupling extracted at the three-loop level (red) in dependence of $M_{\rm SUSY}$ for $\widehat{X}_t = -\sqrt{6}$. In addition, the estimate for the truncation error of the $\mathcal{O}(\alpha_s^2\alpha_t)$ Higgs self-coupling threshold correction is shown (green). *Bottom left*: Same as top left, but M_h is shown in dependence of $\widehat{X}_t$ for $M_{\rm SUSY} = 5$ TeV. *Bottom right*: Same as top right, but ΔM_h is shown in dependence of $\widehat{X}_t$ for $M_{\rm SUSY} = 5$ TeV

uncertainty associated with the truncation error in the calculation of the $\mathcal{O}(\alpha_s^2\alpha_t^2)$ threshold correction for the Higgs self-coupling is shown. This estimate is of the same size as the shift induced by including the $\mathcal{O}(\alpha_s^2\alpha_t^2)$ threshold correction.

In the lower plots of Fig. 7.1, the same curves as in the upper plots are shown but $M_{\rm SUSY}$ is set to 5 TeV and $\widehat{X}_t$ is varied. The shifts between the various results are only mildly dependent on $\widehat{X}_t$ (varying $\widehat{X}_t$ leads to shifts of up to 0.4 GeV). This dependence would be stronger for lower $M_{\rm SUSY}$ values. The estimate of the truncation error, however, shows a strong dependence on $\widehat{X}_t$. Whereas it is negligible for $-1 \lesssim \widehat{X}_t \lesssim 1$, it increases to up to 0.7 GeV for $|\widehat{X}_t| \sim 3.5$.

As expected, these results are in very good agreement with the results of [17, 28]. We observe that the main part of the shift induced by including N^{3}LL resummation is caused by taking into account the three-loop corrections to the extraction of the SM $\overline{\rm MS}$ top Yukawa coupling from the measured top mass. The shift caused by including the $\mathcal{O}(\alpha_s^2\alpha_t^2)$ threshold correction for the Higgs self-coupling is smaller and also associated with a large uncertainty for large $|\widehat{X}_t|$ values. For small $|\widehat{X}_t|$ values, the shift induced by including the $\mathcal{O}(\alpha_s^2\alpha_t^2)$ threshold correction for the Higgs self-coupling is found to be very small. Therefore, we suggest using the result obtained using NNLL resummation with the SM top Yukawa coupling extracted at the three-loop level as default result until the uncertainty in the calculation of the $\mathcal{O}(\alpha_s^2\alpha_t)$ threshold correction is further reduced.

Chapter 8

Higgs boson mass in case of heavy gluino

The two-loop QCD corrections to the lightest Higgs boson mass include terms which grow approximately quadratically when the gluino mass $|M_3|$ is increased (the two-loop correction also contains terms linear in $|M_3|$) if the result parametrized in the $\overline{DR}$ scheme. This leads to large theoretical uncertainties for scenarios where the gluinos are much heavier than the rest of the particles [35]. In the present Chapter, which is based on the paper [20], we demonstrate how the hybrid result that contains a resummation of higher-order logarithmic contributions can be consistently improved such that large theoretical uncertainties for the case of a heavy gluino are avoided. Our approach is based on the introduction of a suitable renormalization scheme for the EFT part of the hybrid result for which the occurrence of corrections power-enhanced by the gluino mass is avoided. In our numerical analysis which is presented in section 8.2, we show that reliable theoretical predictions can also be obtained for large hierarchies between the gluino mass and the stop masses.

8.1 Treatment of contributions enhanced by the gluino mass

The large theoretical uncertainties for the case where the gluino is heavier than the stop particles can be traced to corrections to the squared masses of the stops that are proportional to $|M_3|^2$ at the one-loop level in the $\overline{\text{DR}}$ scheme as well as corrections linear in $|M_3|$ originating from one-loop corrections to the stop mixing parameter X_t. If instead an on-shell (OS) renormalization for the stop masses and the stop mixing parameter (it is sufficient in this context to impose a condition on the renormalized off-diagonal self-energy of the two scalar top quarks) is employed, the momentum subtraction arising from the on-shell counterterms leads to a cancellation of the leading contributions that are proportional to $|M_3|^2$ and $|M_3|$. Accordingly, the

two-loop fixed-order prediction for the mass of the SM-like Higgs boson of the MSSM in the OS scheme depends only logarithmically on the gluino mass [34,187,212], while the corresponding $\overline{\text{DR}}$ result contains contributions that are enhanced by powers of $|M_3|$ [34]. However, for EFT calculations the OS scheme is not applicable. As a consequence, large non-decoupling effects for a heavy gluino occur both in pure EFT results (using a single SUSY scale) and also in the EFT parts of hybrid results via the threshold corrections at the SUSY scale that are evaluated in the $\overline{\text{DR}}$ scheme.

A possible solution would be the derivation of a complete EFT where the effects of a heavy gluino are systematically integrated out from the MSSM. While in the context of other observables such an approach has been investigated [261–263], a complete EFT calculation for a heavy gluino that could be applied for the Higgs-mass prediction in the MSSM has not been carried out so far. In [13] it was proposed to deal with this problem by reexpressing the threshold corrections in a pure (single-scale) EFT result derived in the $\overline{\text{DR}}$ scheme in terms of an "OS-like" renormalization scheme. However, this prescription is not a viable option since its derivation was based upon an incorrect result for the transition of the OS stop mixing parameter to the $\overline{\text{DR}}$ stop mixing parameter. If the correct formula is used, a large logarithm appears in the $\mathcal{O}(\alpha_t^3)$ threshold correction which should be avoided in the EFT approach.[86] Recently, the authors of [264,265] proposed a resummation of terms that are enhanced by powers of the gluino mass as a possibility to alleviate fine-tuning issues in the MSSM and the NMSSM.

In the following we present a systematic approach for the incorporation of terms that can be enhanced by powers of the gluino mass $|M_3|$ into the prediction for the mass of the SM-like Higgs boson in the MSSM. We will show that our results automatically incorporate the resummation of large gluino contributions that was recently proposed [264,265].

In a fixed-order calculation within the OS scheme the leading contributions that are enhanced by powers of the gluino mass cancel out between the unrenormalized diagrams and the counterterms as a consequence of the fact that the OS scheme is a momentum-subtraction scheme. As an example, it is well-known that the unrenormalized self-energies of the scalar top quarks, $\Sigma(p^2)$, receive contributions at the one-loop level that scale proportional to the squared gluino mass in the limit of a heavy gluino. These terms cancel, however, in the renormalized self-energies of the two stop mass eigenstates,

$$\Sigma^{\text{ren}}(p^2) = \Sigma(p^2) - \text{Re}\left(\Sigma(p^2 = m^2)\right) + \ldots, \tag{8.1.1}$$

[86] This is exactly the large logarithm in the formula for the conversion of the stop mixing parameter X_t which appears only in the scenarios with degenerate soft-breaking masses, see Sec. 4.4 for details.

where the ellipsis denotes terms involving the field renormalization constant and m is the mass of the scalar top quark. In the $\overline{\text{DR}}$ scheme, on the other hand, the mass counterterm does not have a finite part, and a cancellation like in eq. (8.1.1) does not occur.

In order to treat the case where the gluino is much heavier than the rest of the mass spectrum with EFT methods, the gluino should be integrated out. For this purpose, matching conditions between the full MSSM and the MSSM without gluino have to be calculated. In this matching procedure, all particles except the gluino can be treated as massless. Consequently, it follows purely from the dimensional analysis that no terms enhanced by powers of the gluino mass can enter the matching of the Higgs four-point function and also of all other dimensionless Green functions (terms depending logarithmically on the gluino mass are possible).

Contributions that are enhanced by powers of the gluino mass can, however, enter the matching of Green functions with a mass dimension greater than zero. If we perform the matching before electroweak symmetry breaking, these Green functions are all related to soft SUSY-breaking parameters which, apart from the gluino mass parameter M_3, can be treated as being zero at the tree-level in the heavy gluino limit. Diagrams involving gluinos generate non-zero contributions at the loop-level which are proportional to powers of the gluino mass. The highest possible power in M_3 is given by the mass dimension of the respective parameter.

In the context of the calculation of the lightest SM-like Higgs-boson mass, the soft SUSY-breaking parameters of the scalar top quarks are most relevant.[87] Their one-loop matching relations (not including terms suppressed by $|M_3|$) read

$$\left(m^{\text{MSSM}/\tilde{g}}_{\tilde{t}_{L,R}}\right)^2(Q) = \left(m^{\text{MSSM}}_{\tilde{t}_{L,R}}\right)^2(Q)\left[1+\frac{\alpha_s}{\pi}C_F\frac{|M_3|^2}{m^2_{\tilde{t}_{L,R}}}\left(1+\ln\frac{Q^2}{|M_3|^2}\right)-\right.$$
$$\left.-\frac{\alpha_s}{4\pi}C_F\left(1+2\ln\frac{Q^2}{|M_3|^2}\right)\right], \tag{8.1.2}$$
$$X_t^{\text{MSSM}/\tilde{g}}(Q) = X_t^{\text{MSSM}}(Q) - \frac{\alpha_s}{\pi}C_F M_3^*\left(1+\ln\frac{Q^2}{|M_3|^2}\right)+$$
$$+\frac{\alpha_s}{8\pi}C_F X_t\left(1-2\ln\frac{Q^2}{|M_3|^2}\right). \tag{8.1.3}$$

where MSSM/$\tilde{g}$ denotes the MSSM without the gluino, M_3 is the gluino mass parameter (we consider here the general case where M_3 can have complex values), $m_{\tilde{t}_{L,R}}$ are the left and right soft-breaking masses of the stop sector, X_t is the stop mixing

[87] The presented argumentation is straightforwardly transferable to other sectors having a smaller numerical impact (e.g. the sbottom sector), which are not discussed here. Note that also the Higgs soft-breaking masses receive threshold corrections (see [264, 265]). We work in the approximation of setting the electroweak gauge coupling to zero in the non-logarithmic two-loop corrections. Thus, the matching of the Higgs soft-breaking parameters does not enter the calculation of the SM-like Higgs mass.

parameter, $\alpha_s = g_3^2/(4\pi)$ (with g_3 being the strong gauge coupling), $C_F = 4/3$ and Q is the scale at which the matching is performed. Higher-order loop corrections to these relations are subleading (i.e., of the form $|M_3|^2\alpha_s^n$ with $n \geq 2$ in case of the mass parameters and of the form $|M_3|\alpha_s^n$ in the case of the stop mixing parameter).

After integrating out the gluino at the gluino mass scale, the parameters are evolved down to the stop mass scale, where in the simplest setup all other non-SM particles are integrated out. Since the gluino is not present in the EFT below the gluino mass scale, no terms enhanced by powers of the gluino mass can enter in all the parts of the calculation that are performed at a scale below the gluino mass scale.

Deriving all necessary matching conditions for integrating out the gluino as well as the corresponding RGEs is cumbersome. [88] Instead, we focus here specifically on terms that are enhanced by powers of the gluino mass. As argued above, these terms arise only in the matching relations of the soft SUSY-breaking masses. Instead of performing the full matching, we can also absorb the terms that are enhanced by powers of the gluino mass into the definition of the parameters. For the case of the mass parameters it is useful to adopt the $\overline{\text{MDR}}$ scheme employed in [220] for this purpose,

$$\left(m_{\tilde{t}_{L,R}}^{\overline{\text{MDR}}}\right)^2(Q) = \left(m_{\tilde{t}_{L,R}}^{\overline{\text{DR}}}\right)^2(Q)\left[1 + \frac{\alpha_s}{\pi}C_F\frac{|M_3|^2}{m_{\tilde{t}_{L,R}}^2}\left(1 + \ln\frac{Q^2}{|M_3|^2}\right)\right], \tag{8.1.4}$$

where here Q is the conversion scale at which the $\overline{\text{DR}}$ parameters are converted to the $\overline{\text{MDR}}$ ones.

We extend the $\overline{\text{MDR}}$ scheme by also defining it for the stop mixing parameter,

$$X_t^{\overline{\text{MDR}}}(Q) = X_t^{\overline{\text{DR}}}(Q) - \frac{\alpha_s}{\pi}C_F M_3^*\left(1 + \ln\frac{Q^2}{|M_3|^2}\right). \tag{8.1.5}$$

Using this scheme, the resummation formulas derived in [264,265] are easily recoverable (see App. D). Note also that the $\overline{\text{MDR}}$ parameters are scale independent at leading order in $|M_3|$.

If the EFT calculation is performed in the $\overline{\text{MDR}}$ scheme no terms enhanced by powers of the gluino mass appear.[89] At the same time the occurrence of large logarithms, $\ln M_{\text{SUSY}}/M_t$, in the threshold corrections which is not desirable in the EFT approach (as happens for the "OS-like" scheme proposed in [13]) is avoided in this way. It should be noted that the threshold corrections between the SM and the

[88] In the recent study [263] all one-loop matching conditions for operators of dimension four to six were derived for the MSSM without gluino in the gaugeless limit, but in addition also the appropriate two-loop threshold corrections and RGEs would be needed.

[89] If three-loop threshold corrections are taken into account, also subleading terms (i.e., terms of two-loop order) in the $\overline{\text{MDR}}$ definition have to be taken into account [220, 222].

MSSM still depend logarithmically on the gluino mass. These terms are, however, numerically less problematic.

If $\overline{\text{MDR}}$ parameters are given as input for the calculation, the application of the $\overline{\text{MDR}}$ scheme is obviously straightforward. It is, however, desirable to also allow for input parameters renormalized in other schemes. In order to incorporate the EFT calculation using the $\overline{\text{MDR}}$ scheme into a hybrid result involving on-shell parameters or into a framework using another scheme, for instance $\overline{\text{DR}}$ parameters, the respective parameters need to be related to the corresponding quantities in the $\overline{\text{MDR}}$ scheme. We briefly describe in the following how this can be achieved for the case of OS and $\overline{\text{DR}}$ parameters.

8.1.1 On-shell input parameters

Often the OS scheme is used for the definition of the stop parameters. It relates the mass parameters directly to physical observables (more precisely, pseudo-observables) and is therefore often used in phenomenological studies.

For the case of OS input parameters the incorporation of the EFT calculation using the $\overline{\text{MDR}}$ scheme can be carried out along the lines of the procedure that is employed in the hybrid framework of `FeynHiggs` for combining the fixed-order and EFT approaches [21–24]. As usual, the fixed-order corrections can be evaluated directly in the OS scheme.

As for the EFT part, there are, in principle, two strategies possible. One can convert the input parameters from the OS to the $\overline{\text{MDR}}$ scheme at some scale and then use the $\overline{\text{MDR}}$ quantities obtained in this way in the EFT calculation. However, a logarithm of the SUSY scale over the top mass scale appears in this conversion. As argued in [22, 23] only this logarithm has to be retained in the formula since it is sufficient to reproduce the logarithms emerging in the fixed-order result. Furthermore, the associated uncertainty from higher-order logarithmic terms is part of the uncertainty estimate presented in [35]. As an alternative to this method, one could consider using an "OS-like" scheme, similar to the one presented in [13], in the EFT calculation. This strategy, however, leads to a large logarithm, $\ln M_{\text{SUSY}}/M_t$, in the two-loop threshold-correction of the SM Higgs self-coupling. In order to avoid the occurrence of a large logarithm in this threshold correction, we prefer to use the procedure outlined above where such a logarithm appears only in the scheme conversion of the input parameters. To the best of our knowledge it has not yet been shown how logarithms of this kind could be properly resummed. We leave this issue for further study, but as mentioned above include it as part of the estimate of the remaining theoretical uncertainties.

We improve the hybrid result by carrying out the EFT calculation with the stop parameters defined in the $\overline{\text{MDR}}$ scheme rather than the $\overline{\text{DR}}$ scheme as it was used up to now (the subtraction terms are adapted accordingly). In order to obtain the input parameters of the EFT calculation in the $\overline{\text{MDR}}$ scheme we need to convert the input parameters given in the OS scheme to the $\overline{\text{MDR}}$ scheme. As we already mentioned above, we retain only large one-loop logarithms in this conversion. This implies that the incorporation of the EFT results using the $\overline{\text{MDR}}$ scheme instead of the $\overline{\text{DR}}$ scheme does not require changes in the conversion formulas presented in [22]. We perform the conversion at the scale M_{SUSY}. The matching scale between the SM and the MSSM can in principle be chosen independently of the conversion scale. We choose to use M_{SUSY}. Alternatively, converting at the scale $|M_3|$ (and also using $|M_3|$ as matching scale) does not lead to large shifts in M_h.

8.1.2 $\overline{\text{DR}}$ input parameters

For the study of high-scale SUSY breaking models, often the $\overline{\text{DR}}$ scheme is used as it is appropriate for running down the parameters from the high scale. This is also the scheme that is usually employed in pure EFT calculations. For the case of $\overline{\text{DR}}$ input parameters the following procedure should be employed. The high-scale $\overline{\text{DR}}$ parameters are run down to the conversion scale, where they are converted to the $\overline{\text{MDR}}$ scheme using eq. (8.1.4). After that the fixed-order as well as the EFT calculation can be carried out in the $\overline{\text{MDR}}$ scheme.

In principle, the conversion scale can be chosen arbitrarily. The result does not depend on it at the two-loop level. As argued above, the insertion of the $\overline{\text{MDR}}$ parameters into the one-loop threshold corrections is equivalent to the resummation of $|M_3|$-enhanced contributions to all orders. However, this insertion also generates large $|M_3|^2$-enhanced logarithmic contributions, see eq. (8.1.4), unless $Q = |M_3|$ is set. Therefore, in our approach, we perform the conversion between the $\overline{\text{DR}}$ and the $\overline{\text{MDR}}$ parameters at the gluino mass scale in order to avoid an unstable result. If $\overline{\text{DR}}$ parameters defined at a scale below $|M_3|$ are given as input, an unstable result cannot be avoided. In addition, we also set the scale where the SM is matched to the MSSM, which in principle is independent of the conversion scale, to the scale of the gluino mass.

8.2 Numerical results

In this Section, we discuss the numerical implications of using the $\overline{\text{MDR}}$ scheme in the EFT calculation. We focus on a single-scale scenario in which all non-SM mass

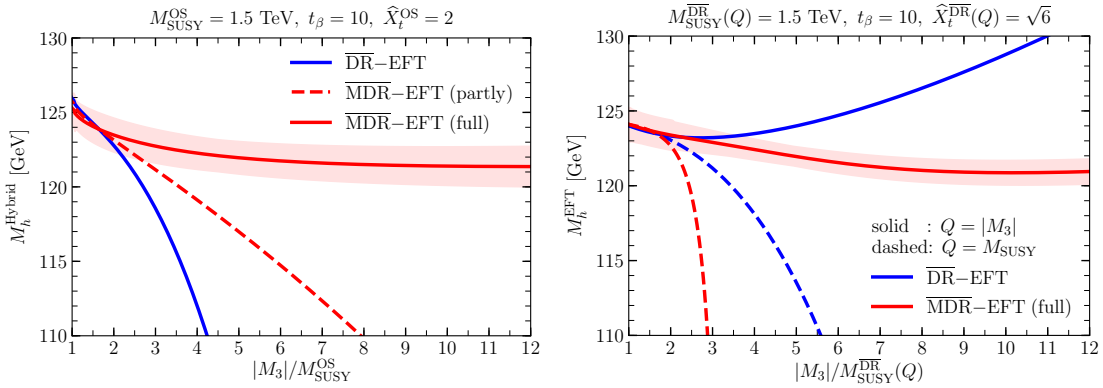

Figure 8.1: Prediction for M_h as a function of the ratio of the gluino mass over $M_{\rm SUSY}$. For the most accurate result, labelled as $\overline{\rm MDR}$–EFT (full), the estimate of the remaining theoretical uncertainties is shown as colored band. The result is compared with predictions using different renormalization schemes in the EFT calculation. *Left*: Prediction of the hybrid calculation using the OS scheme for the definition of the input parameters where for the EFT part the full $\overline{\rm MDR}$ scheme, a partial $\overline{\rm MDR}$ scheme (see text) and the $\overline{\rm DR}$ scheme are used. *Right*: Prediction of the pure EFT calculation using the $\overline{\rm DR}$ scheme for the definition of the input parameters. The result for the $\overline{\rm MDR}$ scheme with the conversion scale $Q = |M_3|$ is compared with the one for $Q = M_{\rm SUSY}$ and with the result for the $\overline{\rm DR}$ scheme with both scale choices.

parameters are chosen to be equal to a common mass scale named $M_{\rm SUSY}$, which is set to 1.5 TeV. As the only exception, we allow the gluino mass parameter M_3 to take a different value. We choose all soft SUSY-breaking trilinear couplings to be zero except for the stop trilinear coupling which is fixed by setting the stop mixing parameter X_t. The ratio of the Higgs vacuum expectation values, $\tan\beta$, is set to 10.

The left panel of fig. 8.1 shows the prediction for the lightest Higgs boson mass in the hybrid approach obtained by `FeynHiggs` (version `2.15.0`) as a function of the ratio $|M_3|/M_{\rm SUSY}$. In addition to the $\overline{\rm DR}$ scheme, which was used up to now by default in the EFT calculation of `FeynHiggs` for the definition of the stop parameters, we implemented the $\overline{\rm MDR}$ scheme as defined in Sec. 8.1. For this plot the input parameters of the stop sector are assumed to be defined in the OS scheme, setting $\widehat{X}_t^{\rm OS} = 2$, where $\widehat{X}_t = X_t/M_{\rm SUSY}$.

The blue solid line shows the result obtained using the $\overline{\rm DR}$ scheme in the EFT calculation. This means, in particular, that the stop parameters are $\overline{\rm DR}$ parameters defined at the scale $M_{\rm SUSY}$. Since the input parameters are defined in the OS scheme, there is no quadratic and linear dependence on M_3 at the two-loop level as the calculation up to this level is based on the fixed-order result in the OS scheme. However, terms that are enhanced by powers of the gluino mass emerge from the two-loop threshold correction to the Higgs quartic coupling of $\mathcal{O}(\alpha_t\alpha_s)$. This threshold correction generates three-loop NNLL (next-to-next-to-leading logarithmic) terms, involving $M_{\rm SUSY}$ and M_t, in the expression for the Higgs-boson mass. For $\widehat{X}_t^{\rm OS} = 2$, these power-enhanced terms in the $\overline{\rm DR}$-EFT result drive the Higgs-mass prediction

steeply downwards when $|M_3|$ increases as shown in the plot. The large numerical impact of the power-enhanced terms leads to a large increase of the theoretical uncertainty of the EFT result in the $\overline{\text{DR}}$ scheme (and consequently also of the hybrid result into which it is implemented), see the discussion in [35]. There a drastic increase of the uncertainty was found in the region $|M_3|/M_{\text{SUSY}} \gtrsim 2$ for the same scenario.

The red dashed curve on this plot corresponds to the result of the hybrid calculation in which in the EFT calculation the left and right stop soft-breaking masses are parametrized in the $\overline{\text{MDR}}$ scheme at the scale M_{SUSY}, while the stop mixing parameter X_t is still a $\overline{\text{DR}}$ parameter defined at the same scale. This corresponds to the version of the $\overline{\text{MDR}}$ scheme that was previously used in the literature. While for this result the Higgs-mass prediction falls less rapidly with increasing $|M_3|$ compared to the blue solid curve, the plot shows that there is a remaining approximately linear dependence of the squared Higgs mass on $|M_3|$ that leads to large theoretical uncertainties also for this result. The reason for the somewhat improved behaviour with respect to the result that is based on the $\overline{\text{DR}}$ scheme can be traced to the fact that the choice of $m_{\tilde{t}_{L,R}}$ in the $\overline{\text{MDR}}$ scheme absorbs the quadratic dependence $\sim |M_3|^2$ in the mentioned three-loop NNLL terms (and also of higher order terms).

The red solid curve in the left plot of fig. 8.1 shows the result of the hybrid calculation making use of the extended $\overline{\text{MDR}}$ scheme as described above. Accordingly, all the stop parameters entering the EFT part of the hybrid result are parametrized in the $\overline{\text{MDR}}$ scheme at the scale M_{SUSY}. In this case, all the terms scaling like powers of the gluino mass that would be induced by the two-loop $\mathcal{O}(\alpha_t\alpha_s)$ contribution to the threshold correction are absorbed into the definition of the soft-breaking parameters. We observe only a rather mild logarithmic dependence of the calculated Higgs-boson mass on $|M_3|/M_{\text{SUSY}}$. These logarithms could be resummed by performing the complete matching of the full MSSM to the MSSM without a gluino as low-energy theory above the stop mass scale. This, however, is numerically much less relevant and lies beyond the scope of the present paper.

For the full $\overline{\text{MDR}}$ result, we also show a coloured band indicating the remaining theoretical uncertainty estimated using the procedure developed in [35]. The comparison with the uncertainty estimate obtained in [35] for the case where the EFT part of the calculation is based on the $\overline{\text{DR}}$ scheme shows that the application of the (extended) $\overline{\text{MDR}}$ scheme to the EFT part of the calculation leads to a drastic reduction of the theoretical uncertainty. The uncertainty that we estimate for the full $\overline{\text{MDR}}$–EFT result stays approximately constant (~ 1.5 GeV) when $|M_3|$ is raised and shows no sharp increase as found in [35].

The right panel of fig. 8.1 shows the lightest Higgs-boson mass calculated in the pure EFT approach as implemented in `FeynHiggs` (version `2.15.0`) as a function of $|M_3|/M_{\rm SUSY}$ using the $\overline{\rm DR}$ scheme for the definition of the input parameters. We define these parameters at the conversion scale Q. For our result based on the (extended) $\overline{\rm MDR}$ scheme the parameters have to be defined at the scale $Q = |M_3|$ (red solid line) in order to obtain a numerical stable result (see also section 8.1). For comparison we also show the $\overline{\rm MDR}$–EFT result where the input parameters are defined at $M_{\rm SUSY}$, where also the conversion to the $\overline{\rm MDR}$ scheme is carried out (red dashed line). We furthermore display the $\overline{\rm DR}$–EFT result for both input scale choices. It should be noted that for $|M_3| \neq M_{\rm SUSY}$ the solid lines (input scale $|M_3|$) and the dashed lines (input scale $M_{\rm SUSY}$) cannot be directly compared to each other since they represent different physical situations. We fix $\widehat{X}_t^{\overline{\rm DR}} = \sqrt{6}$ for this plot.

Our result based on the (extended) $\overline{\rm MDR}$ scheme (red solid line) is parametrized in terms of $\overline{\rm MDR}$ quantities at the scale $|M_3|$, which are obtained from a one-loop conversion of the $\overline{\rm DR}$ parameters at the same scale using eqs. (8.1.4) and (8.1.5) and making the according adjustments to the $\mathcal{O}(\alpha_t\alpha_s)$ threshold correction (for more details see Sec. 8.1). We observe only a mild logarithmic dependence of the calculated Higgs-boson mass on $|M_3|/M_{\rm SUSY}$ for this result.

The coloured band shows the estimated size of unknown higher-order corrections for the $\overline{\rm MDR}$–EFT result with $Q = |M_3|$. The theoretical uncertainty of the EFT result is estimated following largely the procedure employed in [35]. As only differences we take into account the modified scale dependence of the $\overline{\rm MDR}$ parameters in comparison to the $\overline{\rm DR}$ parameters and an additional uncertainty associated with unknown higher-order corrections to the relations converting the parameters from the $\overline{\rm DR}$ to the $\overline{\rm MDR}$ scheme (see eqs. (8.1.4) and (8.1.5)). We estimate this uncertainty by replacing α_s by $\alpha_s\,[1 \pm \alpha_s/(4\pi)\,(1 + \ln Q^2/|M_3|^2)]$ in eqs. (8.1.4) and (8.1.5) (see also the discussion in [35]). As for the case of OS input parameters for the hybrid result, the total uncertainty stays approximately constant (~ 1 GeV) when $|M_3|$ is raised.

For comparison, the red dashed line shows the EFT result based on the (extended) $\overline{\rm MDR}$ scheme where the scale of the $\overline{\rm DR}$ input parameters is chosen as $Q = M_{\rm SUSY}$ instead of $Q = |M_3|$. It is clearly visible that using $\overline{\rm DR}$ parameters defined at the scale $M_{\rm SUSY}$ as input spoils the stability of the $\overline{\rm MDR}$–EFT result. Numerically, the sharp decrease of M_h is largely driven by the behaviour of the $\overline{\rm MDR}$ parameters. As one can see from eq. (8.1.4), in this scenario, the $\overline{\rm MDR}$ stop soft-breaking masses decrease with increasing $|M_3|$ while the stop mixing parameter $X_t^{\overline{\rm MDR}}(Q)$ increases. This results in the suppression of M_h with increasing $|M_3|$ visible for the dashed red line. In contrast, the $\overline{\rm MDR}$ stop soft-breaking masses increase and $X_t^{\overline{\rm MDR}}(Q)$ decreases for $Q = |M_3|$ (red solid line) resulting in the observed stability for rising

$|M_3|$.[90] As argued in section 8.1, the instability for $Q = M_{\text{SUSY}}$ is a consequence of the input parameters being defined in the MSSM and not in a valid EFT in which the gluino is integrated out at the scale $|M_3|$.

We now turn to the discussion of the $\overline{\text{DR}}$–EFT result (blue solid and dashed lines). It is obvious that neither input scale choice yields a reliable theoretical prediction of the $\overline{\text{DR}}$–EFT calculation. As explained above, this is caused by the power-enhanced gluino contributions that are present in this result. The blue dashed line shows the result where the input scale is chosen as M_{SUSY}. In this case, the two-loop threshold correction of $\mathcal{O}(\alpha_t\alpha_s)$ depends quadratically on $|M_3|$ and so does the squared Higgs mass which contains terms proportional to $\sim |M_3|^2\,(1 + \log M_{\text{SUSY}}^2/|M_3|^2)$.

The blue solid curve in the right plot of fig. 8.1 corresponds to the $\overline{\text{DR}}$–EFT result where the $\overline{\text{DR}}$ parameters are defined at the scale $|M_3|$. As explained above, there is a quadratic dependence on the gluino mass in the two-loop threshold correction. However, since for the choice $Q = |M_3|$ there is no additional negative logarithmic contribution to the threshold correction, in this case the Higgs mass grows with increasing $|M_3|$.

[90] This is true for the given choice of M_3 (i.e., $M_3 > 0$). For $M_3 < 0$ (or a complex-valued M_3), $|X_t^{\overline{\text{MDR}}}(|M_3|)|$ can increase but the ratio $|\widehat{X}_t| = |X_t/M_{\text{SUSY}}|$ will still decrease.

Chapter 9

Conclusions

A crucial prediction of the MSSM is the existence of a light Higgs boson. Its mass, which can be calculated in terms of the model parameters, is an important precision observable. Consequently, a precise theoretical prediction of this mass is required, with the goal to reach at least the same level of precision as currently achieved by the experimental measurements of the Higgs boson mass at the LHC. In order to reach this goal the theoretical uncertainties from unknown higher-order contributions as well as the parametric uncertainties that are induced by the experimental errors of the input parameters have to be significantly improved.

In this thesis, we discussed various improvements of the MSSM Higgs boson mass calculation relevant in certain regions of the MSSM parameter space. Namely, these are scenarios with large $\tan\beta$, with complex-valued soft SUSY-breaking parameters or the combination of the two. We performed these improvements in the hybrid approach, combining EFT and fixed-order calculations of the Higgs boson mass and including partial N^{3}LL resummation of large logarithms. This makes our result applicable to the scenarios with low, high, and intermediary SUSY scales. Also, we improved on the determination of the lightest Higgs boson mass in scenarios with a heavy gluino. Below we discuss the results obtained in this thesis in more detail.

Chapter 4 mainly serves as a review of the different methods for calculating the lightest Higgs boson mass. Sec. 4.4 contains the discussion of an issue which has so far not appeared in the literature. The hybrid approach requires the conversion of the input parameters from the on-shell (OS) to the $\overline{\text{DR}}$ scheme, and the conversion formulas may contain large logarithms. In particular, the conversion of the stop mixing parameter X_t contains logarithms of two types. The first type is related to the renormalization group running of the top-quark mass and in principle can be resummed. The logarithms of the second type originate from diagrams with the exchange of massless particles and are not related to the renormalization group running of parameters. These logarithms appear only in specific MSSM scenarios,

namely when the "left", and the "right" soft SUSY-breaking masses of the scalar quarks are equal to each other.

In **Chapter 5**, we presented an improved calculation of the lightest Higgs boson mass in the MSSM for scenarios with large $\tan\beta$. Instead of the bottom mass being defined via the relation between the sbottom mixing angle and the sbottom masses, we treated it as an independent parameter, renormalized in the $\overline{\text{DR}}$ scheme in the full MSSM at scale M_{SUSY}. This renormalization scheme yielded numerically more stable results and turned out to be more suitable for the combination with the EFT calculation. In the calculation of the bottom mass, we resummed corrections enhanced by $\tan\beta$ through Δ_b resummation. We incorporated full one-loop corrections to Δ_b. Moreover, we have adapted the leading two-loop QCD corrections to Δ_b obtained in [29–31] for our calculation framework. The inclusion of this correction is formally a three-loop effect. We, however, found it to be numerically relevant for scenarios with high $\tan\beta$, where it might lead to shifts in the prediction for the Higgs mass of roughly $\sim$ 2 GeV.

Moreover, we have included one- and two-loop threshold corrections to the SM Higgs self-coupling proportional to the bottom Yukawa as well as the corresponding RGE contributions up to the three-loop level. This allows resummation up to the next-to-next-leading-order. In contrast to the resummation of the logarithms proportional to the top Yukawa or electroweak couplings, here the one- and two-loop leading logarithms are numerically negligible due to the smallness of the bottom mass. However, at the two-loop level for the case where the stop sector is renormalized in the OS scheme and for large $\tan\beta$ the next-to-leading logarithms become parametrically enhanced. Their resummation can lead to a downward shift in the prediction for M_h of order of 2 GeV for $M_{\text{SUSY}} = 10$ TeV.

We applied our calculation to the $M_h^{125,\mu-}$ MSSM Higgs benchmark scenario, defined in [251]. In particular, we revisited the constraints on the $(M_A, \tan\beta)$ parameter plane from the requirement that the mass of the lightest Higgs-boson mass should lie in the range $[122; 128]$ GeV. Our calculation gave rise to an enlargement of the phenomenologically accessible space by lifting the maximal value of $\tan\beta$ from 28 to 33.

In **Chapter 6**, we used the two-loop fixed order results presented in Refs. [9, 11] to derive two-loop threshold corrections relating the self-coupling in the SM and the MSSM that are valid also for complex input parameters. We compared the results, including the full phase dependence, to the results obtained by the use of the interpolation routine adopted in `FeynHiggs` up to now. We have found that in some cases the interpolation procedure gives a prediction for M_h, which deviates from the full result by approximately 2 GeV.

In **Chapter 7**, we combined the publicly available code `Himalaya` with `FeynHiggs` in order to obtain a prediction for M_h including N^{3}LL resummation at leading order in the strong gauge coupling. A similar analysis was performed in [28], and we find a very good agreement with the results presented in this paper. The overall effect of the resummation is $\lesssim 1$ GeV, and it weakly depends on $M_{\rm SUSY}$. We also found that the extraction of the SM top Yukawa coupling at the three-loop level in the existing NNLL hybrid calculation approximates the N^{3}LL resummation well.

In **Chapter 8**, we have shown how an appropriate choice of the renormalization prescription for the stop sector of the MSSM leads to a significantly improved theoretical prediction for the mass of the SM-like Higgs boson in the region where the gluino is heavier than the scalar top quarks. This region is phenomenologically important in particular given the increasingly tight gluino mass limits form experimental searches.

In pure EFT calculations and in the EFT part of hybrid results making use of the $\overline{\rm DR}$ scheme for the renormalization of the stop sector leads to the appearance of terms enhanced by powers of the gluino mass. These large non-decoupling effects of the gluino, which are formally of three-loop order for a hybrid result where the fixed-order part is evaluated in the OS scheme up to the two-loop order, lead to unreliable predictions and correspondingly large theoretical uncertainties in the heavy-gluino region. We have shown how the occurrence of power-enhanced corrections from the gluino mass in the EFT part of the calculations can be avoided without spoiling the underlying assumptions of the EFT. In fact, we have demonstrated that the leading contributions from integrating out the gluino can be taken into account by absorbing them into the renormalization of the stop parameters. This scheme, called $\overline{\rm MDR}$, has already been used before in the literature. We have extended it to include also the stop mixing parameter. We have furthermore shown that the recently proposed resummation of large gluino contributions [264, 265] is taken into account in the (extended) $\overline{\rm MDR}$ scheme via the absorption of the contributions into the parameters of the model. We also discussed the implementation of the (extended) $\overline{\rm MDR}$ scheme into the public code `FeynHiggs` and its impact on the estimate of the remaining theoretical uncertainties from unknown higher-order corrections. The implementation will be publicly released in an upcoming version.

In our numerical analysis we have demonstrated that using the (extended) $\overline{\rm MDR}$ scheme for the EFT part of the hybrid result leads to a prediction for M_h that shows only a mild dependence on the gluino mass even for large hierarchies between the gluino mass and the stop masses. The theoretical uncertainties in the heavy-gluino region are vastly improved compared to the case where the EFT result is based on the $\overline{\rm DR}$ scheme. We have demonstrated that these features only hold for the extended $\overline{\rm MDR}$ scheme, while restricting the scheme to the masses — as previously used in the

literature — would not be sufficient for this purpose. We have furthermore stressed that in the case of $\overline{\text{DR}}$ input parameters the scale of the input parameters has to be $|M_3|$ (or larger) in order to allow for a stable M_h prediction for the case where $|M_3| > M_{\text{SUSY}}$. We have also pointed out that for the EFT approach using the $\overline{\text{DR}}$ scheme neither the input scale $|M_3|$ nor M_{SUSY} leads to a reliable prediction in the heavy-gluino region.

The improvements discussed above will become part of the public code `FeynHiggs`. In this way, the work presented in this thesis will facilitate more precise phenomenological studies probing the MSSM parameter space.

Acknowledgements

First of all, I want to express gratitude to my supervisor Georg Weiglein first for hiring me as a summer student and then as a PhD student, exciting projects, numerous discussions, explanations, and support. I thank Géraldine Servant for agreeing to be the referee of my thesis. I am grateful to Peter Schmelcher, Isabell Melzer-Pellmann, and Sven-Olaf Moch for being in the committee for my defense.

During my PhD, I was lucky to learn a lot about science from different people. First and foremost, I want to thank Henning Bahl for invaluable help, countless discussions on the projects, physics in general, and beyond, for carefully reading this manuscript, and numerous valuable suggestions on the text. I truly enjoyed this collaboration and hope to continue it in the future. Moreover, special thanks go to Sebastian Paßehr for providing two-loop corrections and countless explanations, which led to the results obtained in **Chapters 5** and **6**. I would like to thank Emanuele Bagnaschi and Pietro Slavich for providing the expressions of the two-loop threshold corrections for cross-checks.

I wish to thank all members of DESY Theory Group for making my stay here so enjoyable. Especially, Seva Chestnov – for motivating me to start doing jogging and a lot of conversations over the cup of coffee or the late dinner, Gleb Kotousov – for motivating me to run faster, Thomas Biekötter and Anton Sokolov – for numerous interesting discussions over lunch. Also, I want to thank my former and current officemates, Anne Ernst, Daniel Meuser, Troy Figiel, and Vincent Rothe, for creating a great atmosphere in the office. My special and deepest thanks go to my friends, Ruslan, Seva, Sergey, Semen, Anton, Dameli, Nastasia and Dmitry for crazy trips, parties, volleyball in the park, movie nights on the weekends and for making an amazing PhD Hat. Christina, thank you for you patience and support during these three years.

My special thanks go to my family: my parents Irina and Vladimir and my brother Sergey who always supported and motivated me.

Appendix A

Threshold corrections with phase dependence

A.1 One-loop threshold corrections

If integrating out the sfermions and heavy Higgses from the MSSM, effective Higgs–gaugino–Higgsino, $\tilde{g}_{1u,1d,2u,2d}$ couplings are generated (for their exact definition see e.g. [33]). In principle, they can be complex. An explicit calculation of their matching conditions at the SUSY scale, however, shows that they remain real if integrating out the sfermions and heavy Higgses. All other couplings of the EFT below the SUSY scale are also real-valued.

The only exception are the mass parameters of the EWinos themselves. The phases of these parameters become relevant if the EWinos are integrated out at the EWino mass scale, M_χ, and the SM is recovered as EFT.

The threshold corrections of the top and bottom Yukawa couplings originates completely from the corrections to the external Higgs leg. They read

$$y_t^{\mathrm{SM}}(M_\chi) = y_t^{\mathrm{SM+EWinos}}(M_\chi)\Big(1 + k\Delta_{\mathrm{WFR}}\Big), \tag{A.1.1}$$

$$y_b^{\mathrm{SM}}(M_\chi) = y_b^{\mathrm{SM+EWinos}}(M_\chi)\Big(1 + k\Delta_{\mathrm{WFR}}\Big), \tag{A.1.2}$$

$$\begin{aligned}\Delta_{\mathrm{WFR}} = -12\Bigg[&2g_{1u}g_{1d}\cos(\phi_{M_1}+\phi_\mu)f(r_1)\\ &+(g_{1u}^2+g_{1d}^2)\left(g(r_1)+3\ln\frac{|\mu|^2}{M_\chi^2}\right)\\ &+6g_{2u}g_{2d}\cos(\phi_{M_2}+\phi_\mu)f(r_2)\\ &+3(g_{2u}^2+g_{2d}^2)\left(g(r_2)+3\ln\frac{|\mu|^2}{M_\chi^2}\right)\Bigg]\end{aligned} \tag{A.1.3}$$

with

$$r_1 = \left|\frac{M_1}{\mu}\right|, \qquad r_2 = \left|\frac{M_2}{\mu}\right|. \tag{A.1.4}$$

The loop functions f and g are defined in the Appendix of [33]. Setting the phases to zero, we recover the result presented in [33].

Similarly, also the matching condition of the Higgs self-coupling is modified,

$$\lambda^{\mathrm{SM}}(M_\chi) = \lambda^{\mathrm{SM+EWinos}}(M_\chi) + \Delta\lambda \tag{A.1.5}$$

with

$$\begin{aligned}
(4\pi)^2\Delta\lambda = \frac{1}{2}\Big[&2\lambda\Big(g_{1u}^2+g_{1d}^2+3g_{2d}^2+3g_{2u}^2\Big) - g_{1u}^4 - g_{1d}^4 - 5g_{2u}^2 - 5g_{2d}^2 \\
&- 4g_{1u}g_{1d}g_{2u}g_{2d} - 2\Big(g_{1u}^2+g_{2d}^2\Big)\Big(g_{1d}^2+g_{2u}^2\Big)\Big]\ln\frac{|\mu|^2}{M_\chi^2} \\
&- \frac{7}{12}\Big(g_{1u}^4+g_{1d}^4\Big)f_1(r_1) - \frac{9}{4}f_2(r_2)\Big(g_{2u}^4+g_{2d}^4\Big) \\
&+ \frac{1}{6}g_{1u}^2g_{1d}^2\Big[2\cos(\phi_{M_1}+\phi_\mu)h_1(r_1) - 11h_2(r_1)\Big] \\
&+ \frac{1}{2}g_{2u}^2g_{2d}^2\Big[2\cos(\phi_{M_2}+\phi_\mu)h_1(r_2) - 9h_3(r_2)\Big] \\
&+ \frac{1}{3}g_{1u}g_{1d}g_{2u}g_{2d}\Big[\cos(\phi_{M_1}+\phi_{M_2}+2\phi_\mu)h_4(r_1,r_2) \\
&\qquad - 4\cos(\phi_{M_1}-\phi_{M_2})\frac{r_1r_2}{r_1+r_2}f_8(r_1,r_2) - 7h_5(r_1,r_2)\Big] \\
&- \frac{1}{3}\Big(g_{1u}^2g_{2u}^2+g_{1d}^2g_{2d}^2\Big)\Big[2\cos(\phi_{M_1}-\phi_{M_2})\frac{r_1r_2}{r_1+r_2}f_8(r_1,r_2) + \frac{5}{2}h_6(r_1,r_2)\Big] \\
&+ \frac{1}{6}\Big(g_{1u}^2g_{2d}^2+g_{1d}^2g_{2u}^2\Big)\Big[\cos(\phi_{M_1}+\phi_{M_2}+2\phi_\mu)h_4(r_1,r_2) - \frac{4}{r_1+r_2}f_8(r_1,r_2))\Big] \\
&- \frac{4}{3}\Big(g_{1u}g_{2u}+g_{1d}g_{2d}\Big)\Big(g_{1u}g_{2d}+g_{1d}g_{2u}\Big)\Big[\frac{r_1}{r_1+r_2}\cos(\phi_{M_1}+\phi_\mu) \\
&\qquad + \frac{r_2}{r_1+r_2}\cos(\phi_{M_2}+\phi_\mu)\Big]f_8(r_1,r_2) \\
&+ \frac{2}{3}g_{1u}g_{1d}\cos(\phi_{M_1}+\phi_\mu)\Big[\lambda - 2\Big(g_{1u}^2+g_{1d}^2\Big)\Big]f(r_1) \\
&+ 2g_{2u}g_{2d}\cos(\phi_{M_2}+\phi_\mu)\Big[\lambda - 2\Big(g_{2u}^2+g_{2d}^2\Big)\Big]f(r_2) \\
&+ \frac{1}{3}\lambda\Big(g_{1u}^2+g_{1d}^2\Big)g(r_1) + \lambda\Big(g_{2u}^2+g_{2d}^2\Big)g(r_2).
\end{aligned} \tag{A.1.6}$$

The loop functions f_i are defined in the Appendix of [33]. The loop functions h_i are defined by

$$h_1(r) = -\frac{6r^2}{(1-r^2)^3}\Big[2-2r^2+(1+r^2)\ln r^2\Big], \tag{A.1.7a}$$

$$h_2(r) = \frac{6}{11(1-r^2)^3}\Big[2+3r^2-4r^4-r^6+r^2(4+5r^2-r^4)\ln r^2\Big], \tag{A.1.7b}$$

$$h_3(r) = \frac{2}{9(1-r^2)^3}\Big[6+7r^2-8r^4-5r^6+r^2(12+13r^2-r^4)\ln r^2\Big], \tag{A.1.7c}$$

$$\begin{aligned} h_4(r_1,r_2) = -\frac{6r_1r_2}{(1-r_1^2)^2(1-r_2^2)^2(r_1^2-r_2^2)}\Big[&r_1^2(1-r_2^2)^2\ln r_1^2+(1-r_1^2)(1-r_2^2)(r_1^2-r_2^2)\\ &-(1-r_1^2)^2r_2^2\ln r_2^2\Big], \end{aligned} \tag{A.1.7d}$$

$$\begin{aligned} h_5(r_1,r_2) = \frac{6}{7(1-r_1^2)^2(1-r_2^2)^2(r_1^2-r_2^2)}\Big[&-r_1^6(1-r_2^2)^2-r_2^2(1-r_4^2)-r_1^4r_2^2(1-r_2^4)\\ &+r_1^2(1+r_2^4-2r_2^6)+r_1^4(1+r_1^2)(1-r_2^2)^2\ln r_1^2\\ &-(1-r_1^2)^2(1+r_2^2)r_2^4\ln r_2^2\Big], \end{aligned} \tag{A.1.7e}$$

$$\begin{aligned} h_6(r_1,r_2) = \frac{6}{5(1-r_1^2)^2(1-r_2^2)^2(r_1^2-r_2^2)}\Big[&-(1-r_1^2)(1-r_2^2)(r_2^4-r_1^2r_2^2-r_1^4+r_1^4r_2^2)\\ &+(1-r_2^2)^2r_1^6\ln r_1^2-(1-r_1^2)^2r_2^6\ln r_2^2\Big]. \end{aligned} \tag{A.1.7f}$$

In the limit of $r, r_1, r_2 \to 1$ all of the loop functions approach 1. Setting all phases to zero, we again recover the expression given in [33].

The corresponding expressions for the EWino contribution to the matching between SM and MSSM can be obtained by replacing the effective Higgs–Higgsino–gaugino couplings using their tree-level matching conditions.

The expressions for Δ_b, ϵ_b and Δv entering the one-loop threshold correction of the bottom Yukawa coupling (see Eq. (5.2.22)) read

$$\begin{aligned} (4\pi)^2\Delta_b^{1l} = &-C_F g_3^2 t_\beta \cos(\phi_{M_3}+\phi_\mu)\left|\frac{\mu}{M_3}\right|\widetilde{F}_9\left(\frac{m_{\tilde{t}_L}}{|M_3|},\frac{m_{\tilde{b}_R}}{|M_3|}\right)\\ &-\frac{1}{2}y_t^2 t_\beta\cos(\phi_{A_t}+\phi_\mu)\left|\frac{A_t}{\mu}\right|\widetilde{F}_9\left(\frac{m_{\tilde{t}_L}}{|\mu|},\frac{m_{\tilde{t}_R}}{|\mu|}\right)\\ &+\frac{3}{4}g^2 t_\beta\cos(\phi_{M_2}+\phi_\mu)\left|\frac{M_2}{\mu}\right|\widetilde{F}_9\left(\frac{m_{\tilde{t}_L}}{|\mu|},\left|\frac{M_2}{\mu}\right|\right)\\ &+\frac{g'^2}{6}t_\beta\cos(\phi_{M_1}+\phi_\mu)\left[\frac{1}{3}\left|\frac{\mu}{M_1}\right|\widetilde{F}_9\left(\frac{m_{\tilde{t}_L}}{|M_1|},\frac{m_{\tilde{b}_R}}{|M_1|}\right)\right.\\ &\qquad+\frac{1}{2}\left|\frac{M_1}{\mu}\right|\widetilde{F}_9\left(\frac{m_{\tilde{t}_L}}{|\mu|},\left|\frac{M_1}{\mu}\right|\right)\\ &\qquad\left.+\left|\frac{M_1}{\mu}\right|\widetilde{F}_9\left(\frac{m_{\tilde{b}_R}}{|\mu|},\left|\frac{M_1}{\mu}\right|\right)\right], \end{aligned} \tag{A.1.8}$$

$$(4\pi)^2\epsilon_b^{1l} = -C_F g_3^2\left[1+\log\frac{|M_3|^2}{Q^2}+\widetilde{F}_6\left(\frac{m_{\tilde{t}_L}}{|M_3|}\right)+\widetilde{F}_6\left(\frac{m_{\tilde{b}_R}}{|M_3|}\right)\right.$$

$$
\begin{aligned}
&\quad - \left|\frac{A_b}{M_3}\right| \cos(\phi_{A_b} - \phi_{M_3}) \widetilde{F}_9\left(\frac{m_{\tilde{t}_L}}{|M_3|}, \frac{m_{\tilde{b}_R}}{|M_3|}\right)\Bigg] \\
&- \frac{y_b^2}{c_\beta^2}\left[\frac{3}{4}\log\frac{|\mu|^2}{Q^2} + \frac{3}{8}s_\beta^2\left(2\log\frac{M_A^2}{Q^2} - 1\right) + \widetilde{F}_6\left(\frac{m_{\tilde{t}_L}}{|\mu|}\right) + \frac{1}{2}\widetilde{F}_6\left(\frac{m_{\tilde{b}_R}}{|\mu|}\right)\right] \\
&- \frac{y_t^2}{s_\beta^2}\left[\frac{1}{4}\log\frac{|\mu|^2}{Q^2} + \frac{1}{8}c_\beta^2\left(2\log\frac{M_A^2}{Q^2} - 1\right) + s_\beta^2\left(\log\frac{M_A^2}{Q^2} - 1\right) + \frac{1}{2}\widetilde{F}_6\left(\frac{m_{\tilde{t}_R}}{|\mu|}\right)\right. \\
&\qquad \left. + \frac{1}{2}\widetilde{F}_9\left(\frac{m_{\tilde{t}_L}}{|\mu|}, \frac{m_{\tilde{t}_R}}{|\mu|}\right)\left(\left|\frac{A_t}{\mu}\right|\cos(\phi_{A_t} + \phi_\mu)s_\beta c_\beta - 1\right)\right] \\
&- g^2\left[\frac{3}{8}\log\frac{|M_2|^2}{Q^2} - \frac{3}{2}\log\frac{|\mu|^2}{Q^2} + \frac{3}{4}\widetilde{F}_6\left(\frac{m_{\tilde{t}_L}}{|M_2|}\right) - \frac{3}{4}\widetilde{F}_8\left(\frac{m_{\tilde{t}_L}}{|\mu|}, \left|\frac{M_2}{\mu}\right|\right)\right] \\
&- g'^2\left[\frac{5}{72}\log\frac{|M_1|^2}{Q^2} - \frac{1}{2}\log\frac{|\mu|^2}{Q^2} + \frac{1}{36}\widetilde{F}_6\left(\frac{m_{\tilde{t}_L}}{|M_1|}\right) + \frac{1}{9}\widetilde{F}_6\left(\frac{m_{\tilde{b}_R}}{|M_1|}\right)\right. \\
&\qquad - \frac{1}{12}\widetilde{F}_8\left(\frac{m_{\tilde{t}_L}}{|\mu|}, \left|\frac{M_1}{\mu}\right|\right) - \frac{1}{6}\widetilde{F}_8\left(\frac{m_{\tilde{b}_R}}{|\mu|}, \left|\frac{M_1}{\mu}\right|\right) \\
&\qquad \left. + \frac{1}{18}\left|\frac{A_b}{M_1}\right|\cos(\phi_{A_b} - \phi_{M_1})\widetilde{F}_9\left(\frac{m_{\tilde{t}_L}}{|M_1|}, \frac{m_{\tilde{b}_R}}{|M_1|}\right)\right], \qquad \text{(A.1.9)}
\end{aligned}
$$

$$
(4\pi)^2\Delta v = -\frac{y_t^2}{4}\frac{|X_t|^2}{m_{\tilde{t}_L}m_{\tilde{t}_R}}\widetilde{F}_5\left(\frac{m_{\tilde{t}_L}}{m_{\tilde{t}_R}}\right) - \frac{y_b^2}{4}\frac{|X_b|^2}{m_{\tilde{t}_L}m_{\tilde{b}_R}}\widetilde{F}_5\left(\frac{m_{\tilde{t}_L}}{m_{\tilde{b}_R}}\right). \qquad \text{(A.1.10)}
$$

The functions $\widetilde{F}_{5,6,8,9}(x)$ are defined in Appendix A of [33]. Q is the renormalization scale, which we set equal to $M_{\rm SUSY}$. We neglect electroweak contributions to Δv.

In addition, we give the one-loop threshold correction for the top Yukawa coupling, which can be used to reexpress the two-loop threshold corrections of the Higgs self-coupling in terms of the MSSM top Yukawa coupling (see Sec. A.2). It is given by

$$
y_t^{\rm SM}(Q) = h_t^{\rm MSSM} s_\beta\,(1 + \Delta h_t)\,, \qquad \text{(A.1.11)}
$$

$$
\begin{aligned}
(4\pi)^2\Delta h_t = &\frac{4}{3}g_3^2\left[1 + \ln\frac{|M_3|^2}{Q^2} + \widetilde{F}_6\left(\frac{m_{\tilde{t}_L}}{|M_3|}\right) + \widetilde{F}_6\left(\frac{m_{\tilde{t}_R}}{|M_3|}\right)\right. \\
&\left. - \left|\frac{X_t}{M_3}\right|\cos(\phi_{M_3} - \phi_{X_t})\widetilde{F}_9\left(\frac{m_{\tilde{t}_L}}{|M_3|}, \frac{m_{\tilde{t}_R}}{|M_3|}\right)\right] \\
&+ \frac{y_t^2}{s_\beta^2}\left[\frac{3}{4}\ln\frac{|\mu|^2}{Q^2} + \frac{3}{8}c_\beta^2\left(2\ln\frac{M_A^2}{Q^2} - 1\right) - \frac{1}{4}s_\beta^2|\widetilde{X}_t|\widetilde{F}_5\left(\frac{m_{\tilde{t}_L}}{m_{\tilde{t}_R}}\right)\right. \\
&\left. + \widetilde{F}_6\left(\frac{m_{\tilde{t}_L}}{|\mu|}\right) + \frac{1}{2}\widetilde{F}_6\left(\frac{m_{\tilde{t}_R}}{|\mu|}\right)\right] \\
&+ \frac{y_b^2}{c_\beta^2}\left[\frac{1}{4}\ln\frac{|\mu|^2}{Q^2} + \frac{3}{8}s_\beta^2\left(2\ln\frac{M_A^2}{Q^2} - 1\right) - \frac{1}{4}c_\beta^2|\widetilde{X}_b|\widetilde{F}_5\left(\frac{m_{\tilde{t}_L}}{m_{\tilde{b}_R}}\right)\right.
\end{aligned}
$$

$$
\begin{aligned}
&+\frac{1}{2}\widetilde{F}_6\left(\frac{m_{\tilde{b}_R}}{|\mu|}\right)+\frac{1}{2}\frac{|X_b|}{|\mu|t_\beta}\cos(\phi_\mu+\phi_{X_b})\widetilde{F}_9\left(\frac{m_{\tilde{t}_L}}{|\mu|},\frac{m_{\tilde{b}_R}}{|\mu|}\right)\Bigg]\\
&+g^2\left[\frac{3}{8}\ln\frac{|M_2|^2}{Q^2}-\frac{3}{2}\ln\frac{|\mu|^2}{Q^2}+\frac{3}{4}\widetilde{F}_6\left(\frac{m_{\tilde{t}_L}}{|M_2|}\right)-\frac{3}{4}\widetilde{F}_8\left(\frac{m_{\tilde{t}_L}}{|\mu|},\frac{|M_2|}{|\mu|}\right)\right.\\
&\quad\left.-\frac{3}{4t_\beta}\frac{|M_2|}{|\mu|}\cos(\phi_{M_2}+\phi_\mu)\widetilde{F}_9\left(\frac{m_{\tilde{t}_L}}{|\mu|},\frac{|M_2|}{|\mu|}\right)-\frac{3}{8}\right]\\
&+g'^2\left[\frac{17}{12}\ln\frac{|M_1|^2}{Q^2}-\frac{1}{2}\ln\frac{|\mu|^2}{Q^2}+\frac{1}{36}\widetilde{F}_6\left(\frac{m_{\tilde{t}_L}}{|M_1|}\right)+\frac{4}{9}\widetilde{F}_6\left(\frac{m_{\tilde{t}_R}}{|M_1|}\right)\right.\\
&\quad+\frac{1}{12}\widetilde{F}_8\left(\frac{m_{\tilde{t}_L}}{|\mu|},\frac{|M_1|}{|\mu|}\right)-\frac{1}{3}\widetilde{F}_8\left(\frac{m_{\tilde{t}_R}}{|\mu|},\frac{|M_1|}{|\mu|}\right)\\
&\quad-\frac{1}{9}\frac{|X_t|}{|M_1|}\cos(\phi_{M_1}-\phi_{X_t})\widetilde{F}_9\left(\frac{m_{\tilde{t}_L}}{|M_1|},\frac{m_{\tilde{t}_R}}{|M_1|}\right)\\
&\quad+\frac{1}{3t_\beta}\frac{|M_1|}{|\mu|}\cos(\phi_{M_1}+\phi_\mu)\left(\frac{1}{4}\widetilde{F}_9\left(\frac{m_{\tilde{t}_L}}{|\mu|},\frac{|M_1|}{|\mu|}\right)-\widetilde{F}_9\left(\frac{m_{\tilde{t}_R}}{|\mu|},\frac{|M_1|}{|\mu|}\right)\right)\\
&\quad\left.-\frac{1}{72}\right]
\end{aligned}
\tag{A.1.12}
$$

Setting all phases to zero, we again recover the expression given in [33].

A.2 Two-loop threshold corrections

Here, we list the two-loop threshold corrections to the Higgs self-coupling in the limit of all involved non-SM particles expect for EWinos and gluinos having the same mass,

$$
\begin{aligned}
(4\pi)^4(\Delta\lambda)_{\alpha_t^3} = -y_t^6\Bigg\{&\frac{3|\widehat{X}_t|^6}{2}+\frac{1}{t_\beta^2}\Big(\cos(\phi_{X_t}-\phi_{Y_t})\Big(12(3+16K)|\widehat{X}_t|\\
&-12(1+4K)|\widehat{X}_t|^3\Big)|\widehat{Y}_t|+3(3+16K)|\widehat{Y}_t|^2\Big)\\
&-|\widehat{X}_t|^2\Big(2(7+36K)\frac{|\widehat{Y}_t|^2}{t_\beta^2}-\frac{3}{2s_\beta^2}\Big(7+24K\\
&-3(5-8K)c_{2\beta}+(32|\widehat{\mu}|^2-12|\widehat{\mu}|^4)f_2(|\widehat{\mu}|)\Big)\Big)\\
&+|\widehat{X}_t|^4\left(\frac{|\widehat{Y}_t|^2}{4t_\beta^2}(19+96K)-\frac{3}{8s_\beta^2}\Big(23-25c_{2\beta}+(16|\widehat{\mu}|^2-8|\widehat{\mu}|^4)\widetilde{f}_2(|\widehat{\mu}|)\Big)\right)\\
&+\frac{3}{4s_\beta^2}\Big(21+120K+32|\widehat{\mu}|^2+2\pi^2-(13-120K-2\pi^2)c_{2\beta}\\
&+\Big(-32+36|\widehat{\mu}|^2+8|\widehat{\mu}|^4\Big)\widetilde{f}_2(|\widehat{\mu}|)+16\widetilde{f}_3(|\widehat{\mu}|)\Big)\Bigg\},
\end{aligned}
\tag{A.2.1a}
$$

$$
(4\pi)^4(\Delta\lambda)_{\alpha_t^2\alpha_s} = g_3^2y_t^4\Bigg\{\frac{4}{3}\Big(-12|\widehat{X}_t|^2\Big(\widetilde{f}_1(|\widehat{M}_3|)-(1-7|\widehat{M}_3|^2+2|\widehat{M}_3|^4)\widetilde{f}_2(|\widehat{M}_3|)\Big)
$$

$$
\begin{aligned}
&+|\widehat{X}_t|^4\Big(\widetilde{f}_1(|\widehat{M}_3|)-(1-9|\widehat{M}_3|^2+4|\widehat{M}_3|^4)\widetilde{f}_2(|\widehat{M}_3|)\Big)\\
&-6\Big(3+4|\widehat{M}_3|^4\widetilde{f}_2(|\widehat{M}_3|)-|\widehat{M}_3|^2\Big(6\widetilde{f}_2(|\widehat{M}_3|)-8\widetilde{f}_4(|\widehat{M}_3|)\Big)\Big)\Big)\\
&+\frac{16}{3}\cos(\phi_{X_t}-\phi_{M_3})|\widehat{M}_3||\widehat{X}_t|\Big(\Big(2(8-|\widehat{M}_3|^2)|\widehat{X}_t|^2-|\widehat{X}_t|^4\Big)\widetilde{f}_2(|\widehat{M}_3|)\\
&-12\Big(1-\widetilde{f}_4(|\widehat{M}_3|)-|\widehat{M}_3|^2\widetilde{f}_5(|\widehat{M}_3|)\Big)\Big)\Big\},
\end{aligned}
\tag{A.2.1b}
$$

$$
\begin{aligned}
(4\pi)^4(\Delta\lambda)_{\alpha_b^2\alpha_s}=-\frac{8}{3}g_3^2y_b^4\Big\{&9+4|\widehat{X}_b|^3|\widehat{M}_3|\cos(\phi_{X_b}-\phi_{M_3})(-2+|\widehat{M}_3|^2)\widetilde{f}_2(|\widehat{M}_3|)\\
&-12|\widehat{X}_b|^2\Big(1+|\widehat{M}_3|^2(-2+|\widehat{M}_3|^2)\widetilde{f}_2(|\widehat{M}_3|)\Big)\\
&+|\widehat{X}_b|^4\Big(1+|\widehat{M}_3|^2(-3+2|\widehat{M}_3|^2)\widetilde{f}_2(|\widehat{M}_3|)\Big)\\
&+24|\widehat{X}_b||\widehat{M}_3|\cos(\phi_{X_b}-\phi_{M_3})\Big(1+\widetilde{f}_1(|\widehat{M}_3|)-2\widetilde{f}_4(|\widehat{M}_3|)\Big)\\
&+6|\widehat{M}_3|^2\Big((-3+2|\widehat{M}_3|^2)\widetilde{f}_2(|\widehat{M}_3|)+4\widetilde{f}_4(|\widehat{M}_3|)\Big)\Big\},
\end{aligned}
\tag{A.2.1c}
$$

$$
\begin{aligned}
(4\pi)^4(\Delta\lambda)_{\alpha_b\alpha_t^2}=y_t^4y_b^2\Big\{&-\frac{3}{2}+36K+3\pi^2+\frac{24K}{t_\beta^2}|\widehat{Y}_t|^2+\frac{1}{t_\beta^2}|\widehat{X}_b|^2|\widehat{Y}_t|^2+\frac{1}{t_\beta^2}|\widehat{X}_t|^2|\widehat{Y}_t|^2\\
&+\frac{2}{9}|\widehat{X}_t||\widehat{Y}_t||\widehat{X}_b||\widehat{Y}_b|\cos(\phi_{X_t}+\phi_{X_b}-\phi_{Y_t}-\phi_{Y_b})(18+(1+24K)|\widehat{X}_t|^2)\\
&-\frac{1}{6t_\beta^2}(11+48K)|\widehat{X}_b|^2|\widehat{X}_t|^2|\widehat{Y}_t|^2+\frac{48K}{c_\beta^2}\cos(\phi_{X_b}-\phi_{X_t})|\widehat{X}_b||\widehat{X}_t|\\
&+\frac{2}{s_\beta^2}|\widehat{Y}_t||\widehat{X}_b|\cos(\phi_{Y_t}-\phi_{X_b})(24K+|\widehat{X}_t|^2)+\frac{24}{s_\beta^2}(3K-\mathrm{Li}_2(1-|\widehat{\mu}|^2)+\widetilde{f}_1(|\widehat{\mu}|))\\
&+2\cos(\phi_{X_t}-\phi_{Y_t})|\widehat{X}_t||\widehat{Y}_t|\Big(\frac{|\widehat{X}_b|^2}{t_\beta^2}+6\Big(1+4K\Big(-3+\frac{1}{s_\beta^2}\Big)+2\widetilde{f}_1(|\widehat{\mu}|)\Big)\\
&+2|\widehat{X}_t|^2\Big(-\frac{1}{3}+4K-\widetilde{f}_1(|\widehat{\mu}|)-\widetilde{f}_2(|\widehat{\mu}|)\Big)\Big)\\
&+|\widehat{X}_b|^2|\widehat{X}_t|^4\Big(\frac{1}{2}-2\widetilde{f}_2(|\widehat{\mu}|)\Big)+\frac{3}{2}|\widehat{X}_b|^2|\widehat{X}_t|^2\Big(-2+\frac{1}{s_\beta^2}+16\widetilde{f}_2(|\widehat{\mu}|)\Big)\\
&+2\cos(\phi_{X_b}-\phi_{Y_b})|\widehat{X}_b||\widehat{Y}_b|(24K+|\widehat{X}_t|^2(1+(-12+|\widehat{X}_t|^2)\widetilde{f}_2(|\widehat{\mu}|))-24\widetilde{f}_4(|\widehat{\mu}|))\\
&+3|\widehat{X}_b|^2(5+8K-\frac{1}{s_\beta^2}(1+8K+2|\widehat{\mu}|^2\widetilde{f}_2(|\widehat{\mu}|))+16\widetilde{f}_4(|\widehat{\mu}|))\\
&+\frac{4}{3c_\beta^2}\cos(\phi_{X_t}-\phi_{Y_b})|\widehat{X}_t||\widehat{Y}_b|(-9+2|\widehat{X}_t|^2+12K(-6+|\widehat{X}_t|^2))\\
&+\frac{1}{c_\beta^2}\Big(36K+\Big(-6+\pi^2-|\widehat{\mu}|^2(-15+6|\widehat{\mu}|^2+\pi^2)\Big)\widetilde{f}_2(|\widehat{\mu}|)\\
&-(18+\pi^2)\widetilde{f}_4(|\widehat{\mu}|)+\Big(12+|\widehat{\mu}|^2(-6+\pi^2)\Big)\widetilde{f}_5(|\widehat{\mu}|)\Big)\\
&+3|\widehat{X}_t|^2\Big(-2(5+8K+4\widetilde{f}_1(|\widehat{\mu}|))-\frac{1}{s_\beta^2}(1+8K+2|\widehat{\mu}|^2\widetilde{f}_2(|\widehat{\mu}|))\\
&-\frac{2}{c_\beta^2}\Big(-1+4K+|\widehat{\mu}|^2\Big(1+\widetilde{f}_1(|\widehat{\mu}|)+\widetilde{f}_2(|\widehat{\mu}|)\Big)\Big)\Big)
\end{aligned}
$$

$$+|\widehat{X}_t|^4\Big(-\frac{3}{4}\Big(1+\frac{1}{c_\beta^2}\Big)+\Big(1+\widetilde{f}_1(|\widehat{\mu}|)+\widetilde{f}_2(|\widehat{\mu}|)\Big)\Big(4+\frac{|\widehat{\mu}|^2}{c_\beta^2}\Big)\Big) \tag{A.2.1d}$$

$$-3(1+8K)|\widehat{Y}_b|^2t_\beta^2+4(1+6K)|\widehat{X}_t|^2|\widehat{Y}_b|^2t_\beta^2-\frac{1}{36}(35+192K)|\widehat{X}_t|^4|\widehat{Y}_b|^2t_\beta^2\Big\},$$

$$(4\pi)^4(\Delta\lambda)_{\alpha_b^2\alpha_t}=y_t^2y_b^4\Big\{|\widehat{X}_b|^4|\widehat{X}_t|^2-\frac{3}{t_\beta^2}(1+8K)|\widehat{Y}_t|^2+\frac{4}{t_\beta^2}(1+6K)|\widehat{X}_b|^2|\widehat{Y}_t|^2$$

$$+\frac{2}{9}\cos(\phi_{X_t}+\phi_{X_b}-\phi_{Y_t}-\phi_{Y_b})|\widehat{X}_b||\widehat{X}_t||\widehat{Y}_b||\widehat{Y}_t|(18+(1+24K)|\widehat{X}_b|^2)$$

$$+\frac{4}{3s_\beta^2}\cos(\phi_{X_b}-\phi_{Y_t})|\widehat{X}_b||\widehat{Y}_t|(-9+2|\widehat{X}_b|^2+12K(-6+|\widehat{X}_b|^2))$$

$$+|\widehat{X}_b|^4\Big(1-4(-2+|\widehat{\mu}|^2)\widetilde{f}_2(|\widehat{\mu}|)-\frac{1}{4s_\beta^2}\Big(1-6|\widehat{\mu}|^2\widetilde{f}_2(|\widehat{\mu}|)+4|\widehat{\mu}|^4\widetilde{f}_2(|\widehat{\mu}|)\Big)\Big)$$

$$+2\cos(\phi_{X_t}-\phi_{Y_t})|\widehat{X}_t||\widehat{Y}_t|\Big(24K+|\widehat{X}_b|^2-24\widetilde{f}_4(|\widehat{\mu}|)\Big)-\frac{1}{36t_\beta^2}(35+192K)|\widehat{X}_b|^4|\widehat{Y}_t|^2$$

$$+\frac{48K}{c_\beta^2}\cos(\phi_{X_t}-\phi_{X_b})|\widehat{X}_b||\widehat{X}_t|+\frac{2}{c_\beta^2}\cos(\phi_{X_t}-\phi_{Y_b})(24K+|\widehat{X}_b|^2)|\widehat{X}_t||\widehat{Y}_b|$$

$$+\frac{3}{2}|\widehat{X}_b|^2|\widehat{X}_t|^2\Big(-6+\frac{1}{c_\beta^2}\Big)-\frac{1}{6}(11+48K)|\widehat{X}_b|^2|\widehat{X}_t|^2|\widehat{Y}_b|^2t_\beta^2$$

$$+\frac{1}{2}\Big(-3+72K+6\pi^2+\frac{2}{s_\beta^2}\Big(36K+\pi^2-3\Big(-6+\Big(8-11|\widehat{\mu}|^2+2|\widehat{\mu}|^4\Big)\widetilde{f}_2(|\widehat{\mu}|)$$

$$+(-4+8|\widehat{\mu}|^2)\widetilde{f}_4(|\widehat{\mu}|)\Big)\Big)+\frac{8}{c_\beta^2}\Big(-1+3K-\mathrm{Li}_2(1-|\widehat{\mu}|^2)+(1-|\widehat{\mu}|^2)\widetilde{f}_2(|\widehat{\mu}|)\Big)\Big)$$

$$+3|\widehat{X}_t|^2\Big(5+8K+16\widetilde{f}_3(|\widehat{\mu}|)-\frac{1}{c_\beta^2}\Big(1+8K+2|\widehat{\mu}|^2\widetilde{f}_2(|\widehat{\mu}|)\Big)\Big)$$

$$+3|\widehat{X}_b|^2\Big(9+16K-8(-1+|\widehat{\mu}|^2)\widetilde{f}_2(|\widehat{\mu}|)+\frac{1}{c_\beta^2}\Big(1+2|\widehat{\mu}|^4\widetilde{f}_2(|\widehat{\mu}|)$$

$$+\frac{2}{s_\beta^2}\Big(4K+|\widehat{\mu}|^2\widetilde{f}_2(|\widehat{\mu}|)-|\widehat{\mu}|^4\widetilde{f}_2(|\widehat{\mu}|)\Big)\Big)\Big)+(24K+|\widehat{X}_b|^2+|\widehat{X}_t|^2)|\widehat{Y}_b|^2t_\beta^2$$

$$+\frac{2}{3}\cos(\phi_{X_b}-\phi_{Y_b})|\widehat{X}_b||\widehat{Y}_b|\Big(2|\widehat{X}_b|^2\Big(2+12K+3(-2+|\widehat{\mu}|^2)\widetilde{f}_2(|\widehat{\mu}|)\Big)$$

$$+18\Big(1+2\widetilde{f}_1(|\widehat{\mu}|)+4K\Big(-3+\frac{1}{c_\beta^2}\Big)\Big)+3|\widehat{X}_t|^2t_\beta^2\Big)\Big\}, \tag{A.2.1e}$$

$$(4\pi)^4(\Delta\lambda)_{\alpha_b^3}=y_b^6\Big\{12\cos(\phi_{X_b}-\phi_{Y_b})|\widehat{X}_b||\widehat{Y}_b|t_\beta^2(4K(|\widehat{X}_b|^2-4)+|\widehat{X}_b|^2-3)$$

$$+\frac{1}{4}\Big(\frac{3}{c_\beta^2}\Big(48K(5-2|\widehat{X}_b|^2)+2|\widehat{\mu}|^2\Big(\widetilde{f}_2(|\widehat{\mu}|)\Big((3-2|\widehat{\mu}|^2)|\widehat{X}_b|^4$$

$$+4(3|\widehat{\mu}|^2-5)|\widehat{X}_b|^2+4|\widehat{\mu}|^2+18\Big)+16\Big)-32\widetilde{f}_2(|\widehat{\mu}|)$$

$$+16\widetilde{f}_3(|\widehat{\mu}|)+|\widehat{X}_b|^4-8|\widehat{X}_b|^2+4\pi^2+8\Big)$$

$$-|\widehat{Y}_b|^2t_\beta^2(|\widehat{X}_b|^2-2)\Big(96K(|\widehat{X}_b|^2-1)+19|\widehat{X}_b|^2-18\Big)$$

$$+ 2\Big(72K(2|\widehat{X}_b|^2 - 5) - 2|\widehat{X}_b|^2(|\widehat{X}_b|^2 - 6)^2 - 6\pi^2 + 39\Big)\Big)\Big\}. \tag{A.2.1f}$$

We assume that the one-loop $\mathcal{O}(\alpha_t^2, \alpha_b^2)$ corrections are expressed in terms of the SM $\overline{\text{MS}}$ top Yukawa coupling, y_t, and the MSSM $\overline{\text{DR}}$ bottom Yukawa coupling, y_b. Expressions to translate them to the MSSM $\overline{\text{DR}}$ top Yukawa coupling and the SM $\overline{\text{MS}}$ bottom Yukawa coupling, respectively, are provided in Sec. A.1.

In the expressions (A.2.1a) – (A.2.1f) $\widetilde{f}_{1,2,3,4,5}(x)$ are non-singular functions of $\widehat{\mu} = \dfrac{\mu}{M_S}$ or $\widehat{M}_3 = \dfrac{M_3}{M_S}$. The functions $\widetilde{f}_{1,2,3}(x)$ are the same as the functions $f_{1,2,3}(x)$ from [213]. We use a different notation for them since we have already used notations $f_i(x)$ for the functions in the threshold correction to the quartic coupling above in the Eq. (A.1.6),[91]

$$\widetilde{f}_1(x) = \frac{x^2 \log x^2}{1 - x^2} \tag{A.2.2a}$$

$$\widetilde{f}_2(x) = \frac{1}{1 - x^2}\left[1 + \frac{x^2}{1 - x^2}\log x^2\right] \tag{A.2.2b}$$

$$\widetilde{f}_3(x) = \frac{(-1 + 2x^2 + 2x^4)}{(1 - x^2)^2}\left[\log x^2 \log(1 - x^2) + \text{Li}_2(x^2) - \frac{\pi^2}{6} - x^2 \log x^2\right] \tag{A.2.2c}$$

$$\widetilde{f}_4(x) = \frac{x^2(\log x^2 + \text{Li}_2(1 - x^2))}{(1 - x^2)^2} \tag{A.2.2d}$$

$$\widetilde{f}_5(x) = \frac{x^2 \log x^2 + \text{Li}_2(1 - x^2)}{(1 - x^2)^2} \tag{A.2.2e}$$

with $\widetilde{f}_1(0) = 0,\ \widetilde{f}_2(0) = 1,\ \widetilde{f}_3(0) = \frac{\pi^2}{6},\ \widetilde{f}_4(0) = 0,\ \widetilde{f}_5(0) = \frac{\pi^2}{6}$ and $\widetilde{f}_1(1) = -1,\ \widetilde{f}_2(1) = \frac{1}{2},\ \widetilde{f}_3(1) = -\frac{9}{4},\ \widetilde{f}_4(1) = -\frac{1}{4},\ \widetilde{f}_5(1) = \frac{3}{4}$. The constant K is

$$K = -\frac{1}{\sqrt{3}}\int_0^{\pi/6} dx \log(2\cos x) \sim -0.1953256 \tag{A.2.3}$$

[91] These functions are not independent. For example, using the identities for the Spence's function $\text{Li}_2(x^2)$ one can show that $\widetilde{f}_3(x) = (1 - 2x^2 - 2x^4)\widetilde{f}_5(x)$, so it is enough to use only one of them. However, we decided to stick to the notations of [213], so we expressed our result in terms $\widetilde{f}_{1,2,3}$ and added two more functions for better readability of the results.

Appendix B

Counterterms in the heavy SUSY scenario

This Appendix contains explicit formulas for the finite parts of the counterterms $\delta^{(1)}m^2_{\tilde{t}_1}$, $\delta^{(1)}m^2_{\tilde{t}_2}$, $\delta^{(1)}m^2_{\tilde{t}_{12}}$, $\delta^{(1)}m_t$, $\delta^{(1)}m_b$, $\delta^{(1)}v^2$ and $\delta^{(1)}(m_tX_t)$ in the OS renormalization scheme described in Sec. 3.2.2, in the gaugeless limit and in the limit

$$m_{\tilde{t}_L}, m_{\tilde{t}_R}, m_{\tilde{b}_L}, m_{\tilde{b}_R}, |M_3|, m_{H^\pm}, |\mu| \gg m_t, m_b. \tag{B.0.1}$$

This in particular implies that the Goldstone boson masses and the mass of the SM-like Higgs boson are set to zero and the mass of the charged Higgs boson and the $\mathcal{CP}$-odd Higgs bosons are equal (see Sec. 3.2.1.1). The counterterm for the top and bottom quark mass is split into the SM and non-SM part as explained in Sec. 4.4,

$$\delta^{(1)}m_q^{\rm OS} = (\delta^{(1)}m_q^{\rm OS})^{\rm SM} + (\delta^{(1)}m_q^{\rm OS})^{\rm n/SM}, \quad q = t, b. \tag{B.0.2}$$

where the non-SM piece apart from the contribution of heavy particles, also includes the transition between the $\overline{\rm DR}$ and $\overline{\rm MS}$ schemes. In the same way, we split the counterterm for the vacuum expectation value, $\delta^{(1)}v^2$ in the SM and non-SM part. This counterterm can be related to the mass counterterm of the W-boson, as explained in Eq. (3.2.76) in Sec. 3.2.6,

$$\delta^{(1)}v^2 = (\delta^{(1)}v^2)^{\rm SM} + (\delta^{(1)}v^2)^{\rm n/SM}, \tag{B.0.3}$$

$$(\delta^{(1)}v^2)^{\rm SM} = \frac{(\delta^{(1)}M_W^2)^{\rm SM}}{M_W^2}, \quad \delta^{(1)}v^{2,\rm n/SM} = \frac{(\delta^{(1)}M_W^2)^{\rm n/SM}}{M_W^2}. \tag{B.0.4}$$

In all formulas below all Veltman-Passarino functions $A_0(m^2)$ and $B_0(p^2, m_1^2, m_2^2)$ contain only the finite part of the loop integral and the renormalization scale is denoted as Q.

B.1 Non-degenerate soft-breaking masses

In this Section we list the approximate expressions for the counterterms in the case

$$m_{\tilde{t}_L} \neq m_{\tilde{t}_R},\ m_{\tilde{b}_L} \neq m_{\tilde{b}_R},\ m_{\tilde{t}_R} \neq m_{\tilde{b}_R}. \tag{B.1.1}$$

B.1.1 $\mathcal{O}(\alpha_t + \alpha_b)$ contributions

$$\begin{aligned}
\delta^{(1)} m^2_{\tilde{t}_1}\Big|_{\text{fin}} = \frac{\alpha_t}{4\pi}\Bigg[&|X_t|^2\ \text{Re}\{B_0(m^2_{\tilde{t}_L},0,m^2_{\tilde{t}_R})\} + \frac{1}{t^2_\beta}\Big(A_0(m^2_{H^\pm}) + |Y_t|^2\ \text{Re}\{B_0(m^2_{\tilde{t}_L},m^2_{H^\pm},m^2_{\tilde{t}_R})\}\Big)\\
&+\frac{1}{s^2_\beta}\Big(A_0(m^2_{\tilde{t}_R}) - A_0(|\mu|^2) + (m^2_{\tilde{t}_L} - |\mu|^2)\ \text{Re}\{B_0(m^2_{\tilde{t}_L},0,|\mu|^2)\}\Big)\Bigg]\\
&+\frac{\alpha_b}{4\pi}\Bigg[|X_b|^2\ \text{Re}\{B_0(m^2_{\tilde{b}_L},0,m^2_{\tilde{b}_R})\} + t^2_\beta\Big(A_0(m^2_{H^\pm}) + |Y_b|^2\ \text{Re}\{B_0(m^2_{\tilde{b}_L},m^2_{H^\pm},m^2_{\tilde{b}_R})\}\Big)\\
&+\frac{1}{c^2_\beta}\Big(A_0(m^2_{\tilde{b}_R}) - A_0(|\mu|^2) + (m^2_{\tilde{b}_L} - |\mu|^2)\ \text{Re}\{B_0(m^2_{\tilde{b}_L},0,|\mu|^2)\}\Big)\Bigg],
\end{aligned} \tag{B.1.2a}$$

$$\begin{aligned}
\delta^{(1)} m^2_{\tilde{t}_2}\Big|_{\text{fin}} = \frac{\alpha_t}{2\pi}\Bigg[&|X_t|^2\ \text{Re}\{B_0(m^2_{\tilde{t}_R},0,m^2_{\tilde{t}_L})\} + \frac{1}{t^2_\beta}\Big(A_0(m^2_{H^\pm}) + |Y_t|^2\ \text{Re}\{B_0(m^2_{\tilde{t}_R},m^2_{H^\pm},m^2_{\tilde{t}_L})\}\Big)\\
&+\frac{1}{s^2_\beta}\Big(A_0(m^2_{\tilde{t}_L}) - A_0(|\mu|^2) + (m^2_{\tilde{t}_R} - |\mu|^2)\ \text{Re}\{B_0(m^2_{\tilde{t}_R},0,|\mu|^2)\}\Big)\Bigg],
\end{aligned} \tag{B.1.2b}$$

$$\begin{aligned}
\frac{\delta^{(1)} m^2_{\tilde{t}_{12}}}{m_t}\Bigg|_{\text{fin}} = \frac{\alpha_t}{8\pi} X_t^*\Bigg[&\frac{|X_t|^2}{m^2_{\tilde{t}_L} - m^2_{\tilde{t}_R}}\Big(2\ \text{Re}\{B_0(m^2_{\tilde{t}_L},0,m^2_{\tilde{t}_L})\} - \text{Re}\{B_0(m^2_{\tilde{t}_L},0,m^2_{\tilde{t}_R})\}\\
&+2\ \text{Re}\{B_0(m^2_{\tilde{t}_R},0,m^2_{\tilde{t}_L})\} - \text{Re}\{B_0(m^2_{\tilde{t}_R},0,m^2_{\tilde{t}_R})\}\Big) + 2\ \text{Re}\{B_0(m^2_{\tilde{t}_L},0,m^2_{\tilde{t}_L})\}\\
&+\text{Re}\{B_0(m^2_{\tilde{t}_L},0,m^2_{\tilde{t}_R})\} + 2\ \text{Re}\{B_0(m^2_{\tilde{t}_R},0,m^2_{\tilde{t}_L})\} + \text{Re}\{B_0(m^2_{\tilde{t}_R},0,m^2_{\tilde{t}_R})\}\Bigg]\\
+\frac{\alpha_t}{8\pi\ t^2_\beta}\Bigg[&\frac{X_t^*|Y_t|^2}{m^2_{\tilde{t}_L} - m^2_{\tilde{t}_R}}\Big(2\ \text{Re}\{B_0(m^2_{\tilde{t}_L},m^2_{H^\pm},m^2_{\tilde{t}_L})\} - \text{Re}\{B_0(m^2_{\tilde{t}_L},m^2_{H^\pm},m^2_{\tilde{t}_R})\}\\
&+2\ \text{Re}\{B_0(m^2_{\tilde{t}_R},m^2_{H^\pm},m^2_{\tilde{t}_L})\} - \text{Re}\{B_0(m^2_{\tilde{t}_R},m^2_{H^\pm},m^2_{\tilde{t}_R})\}\Big) + Y_t\Big(2\ \text{Re}\{B_0(m^2_{\tilde{t}_L},m^2_{H^\pm},m^2_{\tilde{t}_L})\}\\
&+\text{Re}\{B_0(m^2_{\tilde{t}_L},m^2_{H^\pm},m^2_{\tilde{t}_R})\} + 2\ \text{Re}\{B_0(m^2_{\tilde{t}_R},m^2_{H^\pm},m^2_{\tilde{t}_L})\} + \text{Re}\{B_0(m^2_{\tilde{t}_R},m^2_{H^\pm},m^2_{\tilde{t}_R})\}\Big)\Bigg]\\
+\frac{\alpha_t}{8\pi s^2_\beta}\frac{X_t^*}{m^2_{\tilde{t}_L} - m^2_{\tilde{t}_R}}\Bigg[&10A_0(m^2_{\tilde{t}_L}) - 8A_0(m^2_{\tilde{t}_R}) + 2A_0(m^2_{H^\pm})c^2_\beta - 2A_0(|\mu|^2)\\
&+(m^2_{\tilde{t}_L} - |\mu|^2)\ \text{Re}\{B_0(m^2_{\tilde{t}_L},0,|\mu|^2)\} + (m^2_{\tilde{t}_R} - |\mu|^2)\ \text{Re}\{B_0(m^2_{\tilde{t}_R},0,|\mu|^2)\}\Bigg]
\end{aligned}$$

$$
\begin{aligned}
&+\frac{\alpha_b}{8\pi}X_t^*\Bigg[\frac{|X_b|^2}{(m^2_{\tilde{b}_R}-m^2_{\tilde{t}_L})(m^2_{\tilde{t}_L}-m^2_{\tilde{t}_R})}\Big((m^2_{\tilde{t}_R}-m^2_{\tilde{b}_R})\ \mathrm{Re}\{B_0(m^2_{\tilde{t}_L},0,m^2_{\tilde{b}_R})\}\\
&\quad+(m^2_{\tilde{t}_L}-m^2_{\tilde{t}_R})\ \mathrm{Re}\{B_0(m^2_{\tilde{t}_L},0,m^2_{\tilde{t}_L})\}+(m^2_{\tilde{t}_R}-m^2_{\tilde{b}_R})\ \mathrm{Re}\{B_0(m^2_{\tilde{t}_R},0,m^2_{\tilde{b}_R})\}\\
&\quad+(m^2_{\tilde{t}_L}-m^2_{\tilde{t}_R})\ \mathrm{Re}\{B_0(m^2_{\tilde{t}_R},0,m^2_{\tilde{t}_L})\}\Big)-\mathrm{Re}\{B_0(m^2_{\tilde{t}_L},0,m^2_{\tilde{t}_L})\}-\mathrm{Re}\{B_0(m^2_{\tilde{t}_R},0,m^2_{\tilde{t}_L})\}\\
&\quad-\frac{1}{c^2_\beta(m^2_{\tilde{t}_L}-m^2_{\tilde{t}_R})}\Big(2A_0(m^2_{\tilde{b}_R})-2A_0(|\mu|^2)+2A_0(m^2_{H^\pm})s^2_\beta\\
&\quad+(m^2_{\tilde{t}_L}-|\mu|^2)\ \mathrm{Re}\{B_0(m^2_{\tilde{t}_L},0,|\mu|^2)\}+(m^2_{\tilde{t}_R}-|\mu|^2)\ \mathrm{Re}\{B_0(m^2_{\tilde{t}_R},0,|\mu|^2)\}\Big)\\
&\quad-\frac{|Y_b|^2t^2_\beta}{m^2_{\tilde{t}_L}-m^2_{\tilde{t}_R}}\Big(\mathrm{Re}\{B_0(m^2_{\tilde{t}_L},m^2_{H^\pm},m^2_{\tilde{b}_R})\}+\mathrm{Re}\{B_0(m^2_{\tilde{t}_R},m^2_{H^\pm},m^2_{\tilde{b}_R})\}\Big)\Bigg] \qquad \text{(B.1.2c)}\\
&+\frac{\alpha_b}{8\pi c^2_\beta}Y_b^*\Big(\mathrm{Re}\{B_0(m^2_{\tilde{t}_L},m^2_{H^\pm},m^2_{\tilde{b}_R})\}+\mathrm{Re}\{B_0(m^2_{\tilde{t}_R},m^2_{H^\pm},m^2_{\tilde{b}_R})\}\Big)\\
&+\frac{\alpha_b}{8\pi}\frac{X_bY_b^*Y_t^*}{m^2_{\tilde{b}_R}-m^2_{\tilde{t}_L}}\Big(\mathrm{Re}\{B_0(m^2_{\tilde{t}_L},m^2_{H^\pm},m^2_{\tilde{b}_R})\}-\mathrm{Re}\{B_0(m^2_{\tilde{t}_L},m^2_{H^\pm},m^2_{\tilde{t}_L})\}\\
&\quad+\mathrm{Re}\{B_0(m^2_{\tilde{t}_R},m^2_{H^\pm},m^2_{\tilde{b}_R})-\mathrm{Re}\{B_0(m^2_{\tilde{t}_R},m^2_{H^\pm},m^2_{\tilde{t}_L})\Big)\\
&-\frac{\alpha_b}{2\pi}\frac{\mu}{s_{2\beta}}\Big(\mathrm{Re}\{B_0(m^2_{\tilde{t}_L},0,|\mu|^2)\}+\mathrm{Re}\{B_0(m^2_{\tilde{t}_R},0,|\mu|^2)\}\Big)\\
&+\frac{\alpha_t}{8\pi}Y_t^*\Big(\mathrm{Re}\{B_0(m^2_{\tilde{t}_L},m^2_{H^\pm},m^2_{\tilde{t}_L})\}+\mathrm{Re}\{B_0(m^2_{\tilde{t}_R},m^2_{H^\pm},m^2_{\tilde{t}_L})\}\Big),
\end{aligned}
$$

$$
\begin{aligned}
&\delta^{(1)}(m_tX_t)\big|_{\mathrm{fin}}=\frac{\alpha_t}{8\pi}m_tX_t\Bigg[\frac{|X_t|^2}{m^2_{\tilde{t}_L}-m^2_{\tilde{t}_R}}\Big(2\ \mathrm{Re}\{B_0(m^2_{\tilde{t}_L},0,m^2_{\tilde{t}_L})\}+\mathrm{Re}\{B_0(m^2_{\tilde{t}_L},0,m^2_{\tilde{t}_R})\}\\
&-2\ \mathrm{Re}\{B_0(m^2_{\tilde{t}_R},0,m^2_{\tilde{t}_L})\}-\mathrm{Re}\{B_0(m^2_{\tilde{t}_R},0,m^2_{\tilde{t}_R})\}\Big)+2\ \mathrm{Re}\{B_0(m^2_{\tilde{t}_L},0,m^2_{\tilde{t}_L})\}\\
&+\mathrm{Re}\{B_0(m^2_{\tilde{t}_L},0,m^2_{\tilde{t}_R})\}+2\ \mathrm{Re}\{B_0(m^2_{\tilde{t}_R},0,m^2_{\tilde{t}_L})\}+\mathrm{Re}\{B_0(m^2_{\tilde{t}_R},0,m^2_{\tilde{t}_R})\}\Bigg]\\
&+\frac{\alpha_t}{8\pi t^2_\beta}m_tY_t\Bigg[\frac{X_tY_t^*}{m^2_{\tilde{t}_L}-m^2_{\tilde{t}_R}}\Big(2\ \mathrm{Re}\{B_0(m^2_{\tilde{t}_L},m^2_{H^\pm},m^2_{\tilde{t}_L})\}+\mathrm{Re}\{B_0(m^2_{\tilde{t}_L},m^2_{H^\pm},m^2_{\tilde{t}_R})\}\\
&-2\ \mathrm{Re}\{B_0(m^2_{\tilde{t}_R},m^2_{H^\pm},m^2_{\tilde{t}_L})\}-\mathrm{Re}\{B_0(m^2_{\tilde{t}_R},m^2_{H^\pm},m^2_{\tilde{t}_R})\}\Big)+2\ \mathrm{Re}\{B_0(m^2_{\tilde{t}_L},m^2_{H^\pm},m^2_{\tilde{t}_L})\}\\
&+\mathrm{Re}\{B_0(m^2_{\tilde{t}_L},m^2_{H^\pm},m^2_{\tilde{t}_R})\}+2\ \mathrm{Re}\{B_0(m^2_{\tilde{t}_R},m^2_{H^\pm},m^2_{\tilde{t}_L})\}+\mathrm{Re}\{B_0(m^2_{\tilde{t}_R},m^2_{H^\pm},m^2_{\tilde{t}_R})\}\Bigg]\\
&+\frac{3\alpha_t}{8\pi s^2_\beta}\frac{m_tX_t}{m^2_{\tilde{t}_L}-m^2_{\tilde{t}_R}}\Bigg[2\ A_0(m^2_{\tilde{t}_L})-2\ A_0(m^2_{\tilde{t}_R})+(m^2_{\tilde{t}_L}-|\mu|^2)\ \mathrm{Re}\{B_0(m^2_{\tilde{t}_L},0,|\mu|^2)\}\\
&-(m^2_{\tilde{t}_R}-|\mu|^2)\ \mathrm{Re}\{B_0(m^2_{\tilde{t}_R},0,|\mu|^2)\}\Bigg] \qquad \text{(B.1.2d)}\\
&+\frac{\alpha_b}{8\pi}\ m_tX_t\ \Bigg[\frac{|X_b|^2}{m^2_{\tilde{t}_L}-m^2_{\tilde{t}_R}}\Big(\mathrm{Re}\{B_0(m^2_{\tilde{t}_L},0,m^2_{\tilde{b}_R})\}-\mathrm{Re}\{B_0(m^2_{\tilde{t}_R},0,m^2_{\tilde{b}_R})\}\Big)
\end{aligned}
$$

$$
\begin{aligned}
&+\frac{|X_b|^2}{m^2_{\tilde{t}_L}-m^2_{\tilde{b}_R}}\Big(\mathrm{Re}\{B_0(m^2_{\tilde{t}_L},0,m^2_{\tilde{b}_R})\}-\mathrm{Re}\{B_0(m^2_{\tilde{t}_L},0,m^2_{\tilde{t}_L})\}+\mathrm{Re}\{B_0(m^2_{\tilde{t}_R},0,m^2_{\tilde{b}_R})\}\\
&-\mathrm{Re}\{B_0(m^2_{\tilde{t}_R},0,m^2_{\tilde{t}_L})\}\Big)-\frac{|Y_b|^2t^2_\beta}{m^2_{\tilde{t}_L}-m^2_{\tilde{t}_R}}\Big(\mathrm{Re}\{B_0(m^2_{\tilde{t}_R},m^2_{H^\pm},m^2_{\tilde{b}_R})\}-\mathrm{Re}\{B_0(m^2_{\tilde{t}_L},m^2_{H^\pm},m^2_{\tilde{b}_R})\}\Big)\\
&-\Big(\mathrm{Re}\{B_0(m^2_{\tilde{t}_R},0,m^2_{\tilde{t}_L})\}+\mathrm{Re}\{B_0(m^2_{\tilde{t}_L},0,m^2_{\tilde{t}_L})\}\Big)\\
&+\frac{1}{c^2_\beta(m^2_{\tilde{t}_L}-m^2_{\tilde{t}_R})}\Big((m^2_{\tilde{t}_L}-|\mu|^2)\ \mathrm{Re}\{B_0(m^2_{\tilde{t}_L},0,|\mu|^2)\}-(m^2_{\tilde{t}_R}-|\mu|^2)\ \mathrm{Re}\{B_0(m^2_{\tilde{t}_R},0,|\mu|^2)\Big)\Big]\\
&+\frac{\alpha_b}{8\pi}\ m_tY_t\ \Bigg[\frac{Y_bX^*_b}{m^2_{\tilde{b}_R}-m^2_{\tilde{t}_L}}\Big(\mathrm{Re}\{B_0(m^2_{\tilde{t}_L},m^2_{H^\pm},m^2_{\tilde{b}_R})\}-\mathrm{Re}\{B_0(m^2_{\tilde{t}_L},m^2_{H^\pm},m^2_{\tilde{t}_L})\}\\
&+\mathrm{Re}\{B_0(m^2_{\tilde{t}_R},m^2_{H^\pm},m^2_{\tilde{b}_R})\}-\mathrm{Re}\{B_0(m^2_{\tilde{t}_R},m^2_{H^\pm},m^2_{\tilde{t}_L})\}\Big)+\mathrm{Re}\{B_0(m^2_{\tilde{t}_L},m^2_{H^\pm},m^2_{\tilde{t}_L})\}\\
&+\mathrm{Re}\{B_0(m^2_{\tilde{t}_R},m^2_{H^\pm},m^2_{\tilde{t}_L})\}\Bigg]\\
&+\frac{\alpha_b}{8\pi c^2_\beta}\ m_tY_b\ \Big(\mathrm{Re}\{B_0(m^2_{\tilde{t}_L},m^2_{H^\pm},m^2_{\tilde{b}_R})\}+\mathrm{Re}\{B_0(m^2_{\tilde{t}_R},m^2_{H^\pm},m^2_{\tilde{b}_R})\}\Big)\\
&-\frac{\alpha_b}{4\pi s_\beta c_\beta}\ m_t\mu^*\ \Big(\mathrm{Re}\{B_0(m^2_{\tilde{t}_L},0,|\mu|^2)\}+\mathrm{Re}\{B_0(m^2_{\tilde{t}_R},0,|\mu|^2)\}\Big),
\end{aligned}
$$

$$
\begin{aligned}
\frac{(\delta^{(1)}m_t^{\mathrm{OS}})^{\mathrm{n/SM}}}{m_t}\Big|_{\mathrm{fin}}&=-\frac{\alpha_t}{4\pi s^2_\beta}\Big[\frac{3}{8}(1-2B_0(0,0,m^2_{H^\pm}))c^2_\beta\\
&-\frac{1}{4(|\mu|^2-m^2_{\tilde{t}_L})^2}\Big(3|\mu|^4-4|\mu|^2m^2_{\tilde{t}_L}+m^4_{\tilde{t}_L}+2m^2_{\tilde{t}_L}(2|\mu|^2-m^2_{\tilde{t}_L})\log\frac{m^2_{\tilde{t}_L}}{|\mu|^2}\Big)\\
&-\frac{1}{8(|\mu|^2-m^2_{\tilde{t}_R})^2}\Big(3|\mu|^4-4|\mu|^2m^2_{\tilde{t}_R}+m^4_{\tilde{t}_R}+2m^2_{\tilde{t}_R}(2|\mu|^2-m^2_{\tilde{t}_R})\log\frac{m^2_{\tilde{t}_R}}{|\mu|^2}\Big)\\
&+\frac{3}{4}\log\frac{|\mu|^2}{Q^2}\Big]-\frac{\alpha_b}{4\pi c^2_\beta}\Big[\frac{1}{8}\Big(s^2_\beta-(2+6c^2_\beta)B_0(0,0,m^2_{H^\pm})\Big)\\
&-\frac{1}{8(|\mu|^2-m^2_{\tilde{b}_R})^2}\Big(3|\mu|^4-4|\mu|^2m^2_{\tilde{b}_R}+m^4_{\tilde{b}_R}+2m^2_{\tilde{b}_R}(2|\mu|^2-m^2_{\tilde{b}_R})\log\frac{m^2_{\tilde{b}_R}}{|\mu|^2}\Big)\\
&-\frac{\mu X_b+\mu^*X^*_b}{2t_\beta}\frac{B_0(0,|\mu|^2,m^2_{\tilde{b}_R})-B_0(0,|\mu|^2,m^2_{\tilde{t}_L})}{m^2_{\tilde{b}_R}-m^2_{\tilde{t}_L}}\\
&+\frac{1}{4}\log\frac{|\mu|^2}{Q^2}\Big],
\end{aligned}
\tag{B.1.2e}
$$

$$
\begin{aligned}
\frac{(\delta^{(1)}m_t^{\mathrm{OS}})^{\mathrm{SM}}}{m_t}\Big|_{\mathrm{fin}}&=\frac{\alpha_t}{8\pi}\left(2+B_0(0,0,m^2_t)+\frac{1}{2}\left(1-\frac{m^2_b}{m^2_t}\right)^2\mathrm{Re}\{B_0(m^2_t,0,m^2_b)\}\right)\\
&-\frac{\alpha_b}{16\pi}\left(1+\frac{m^2_b}{m^2_t}\right)B_0(0,0,m^2_b),
\end{aligned}
\tag{B.1.2f}
$$

$$(\delta^{(1)}v^2)^{\mathrm{n/SM}}\Big|_{\mathrm{fin}} = \frac{3\alpha_t}{8\pi}\frac{|X_t|^2}{(m^2_{\tilde{t}_R}-m^2_{\tilde{t}_L})^3}\left(m^4_{\tilde{t}_L}-m^4_{\tilde{t}_R}-2m^2_{\tilde{t}_L}m^2_{\tilde{t}_R}\log\frac{m^2_{\tilde{t}_L}}{m^2_{\tilde{t}_R}}\right)$$
$$+\frac{3\alpha_b}{8\pi}\frac{|X_b|^2}{(m^2_{\tilde{b}_R}-m^2_{\tilde{t}_L})^3}\left(m^4_{\tilde{t}_L}-m^4_{\tilde{b}_R}-2m^2_{\tilde{t}_L}m^2_{\tilde{b}_R}\log\frac{m^2_{\tilde{t}_L}}{m^2_{\tilde{b}_R}}\right), \tag{B.1.2g}$$

$$(\delta^{(1)}v^2)^{\mathrm{SM}}\Big|_{\mathrm{fin}} = -\left(\frac{3\alpha_t}{8\pi}+\frac{3\alpha_b}{8\pi}\right)\left(1-2\log\frac{m_t^2}{Q^2}\right)-\frac{3\alpha_b}{2\pi}\frac{m_b^2}{m_b^2-m_t^2}\log\frac{m_t}{m_b}, \tag{B.1.2h}$$

$$\frac{(\delta^{(1)}m_b^{\mathrm{OS}})^{\mathrm{n/SM}}}{m_b}\Big|_{\mathrm{fin}} = -\frac{\alpha_b}{4\pi c_\beta^2}\Big[\frac{3}{8}(1-2B_0(0,0,m^2_{H^\pm}))s_\beta^2$$
$$-\frac{1}{4(|\mu|^2-m^2_{\tilde{t}_L})^2}\Big(3|\mu|^4-4|\mu|^2m^2_{\tilde{t}_L}+m^4_{\tilde{t}_L}+2m^2_{\tilde{t}_L}(2|\mu|^2-m^2_{\tilde{t}_L})\log\frac{m^2_{\tilde{t}_L}}{|\mu|^2}\Big)$$
$$-\frac{1}{8(|\mu|^2-m^2_{\tilde{b}_R})^2}\Big(3|\mu|^4-4|\mu|^2m^2_{\tilde{b}_R}+m^4_{\tilde{b}_R}+2m^2_{\tilde{b}_R}(2|\mu|^2-m^2_{\tilde{b}_R})\log\frac{m^2_{\tilde{b}_R}}{|\mu|^2}\Big)$$
$$+\frac{3}{4}\log\frac{|\mu|^2}{Q^2}\Big]-\frac{\alpha_t}{4\pi s_\beta^2}\Big[\frac{1}{8}\left(c_\beta^2-(2+6s_\beta^2)B_0(0,0,m^2_{H^\pm})\right) \tag{B.1.2i}$$
$$-\frac{1}{8(|\mu|^2-m^2_{\tilde{t}_R})^2}\Big(3|\mu|^4-4|\mu|^2m^2_{\tilde{t}_R}+m^4_{\tilde{t}_R}+2m^2_{\tilde{t}_R}(2|\mu|^2-m^2_{\tilde{t}_R})\log\frac{m^2_{\tilde{t}_R}}{|\mu|^2}\Big)$$
$$-\frac{(\mu X_t+\mu^* X_t^*)t_\beta}{2}\frac{B_0(0,|\mu|^2,m^2_{\tilde{t}_R})-B_0(0,|\mu|^2,m^2_{\tilde{t}_L})}{m^2_{\tilde{t}_R}-m^2_{\tilde{t}_L}}$$
$$+\frac{1}{4}\log\frac{|\mu|^2}{Q^2}\Big],$$

$$\frac{(\delta^{(1)}m_b^{\mathrm{OS}})^{\mathrm{SM}}}{m_b}\Big|_{\mathrm{fin}} = \frac{\alpha_b}{8\pi}\left(2+B_0(0,0,m_b^2)+\frac{1}{2}\left(1-\frac{m_t^2}{m_b^2}\right)^2\mathrm{Re}\{B_0(m_b^2,0,m_t^2)\}\right)$$
$$-\frac{\alpha_t}{16\pi}\left(1+\frac{m_t^2}{m_b^2}\right)B_0(0,0,m_t^2). \tag{B.1.2j}$$

Since $m_b \ll m_t$, the epxressions for $\delta^{(1)}m_t^{\mathrm{OS,SM}}$ and $\delta^{(1)}v^{2,\mathrm{SM}}$ can be expanded in the ratio m_b/m_t.

$$\frac{(\delta^{(1)}m_t^{\mathrm{OS}})^{\mathrm{SM}}}{m_t}\Big|_{\mathrm{fin}} = \frac{\alpha_t}{16\pi}\left(8-3\log\frac{m_t^2}{Q^2}\right)+\frac{\alpha_b}{16\pi}\left(-4+3\log\frac{m_t^2}{Q^2}\right.$$
$$\left.-\frac{3m_b^2}{2m_t^2}\left(1+4\log\frac{m_t}{m_b}\right)+\frac{m_b^4}{6m_t^4}\left(11+12\log\frac{m_t}{m_b}\right)+\mathcal{O}\left(\frac{m_b^6}{m_t^6}\right)\right), \tag{B.1.3}$$
$$(\delta^{(1)}v^2)^{\mathrm{SM}}\Big|_{\mathrm{fin}} = -\left(\frac{3\alpha_t}{8\pi}+\frac{3\alpha_b}{8\pi}\right)\left(1-2\log\frac{m_t^2}{Q^2}\right)$$

$$+\frac{3\alpha_b}{2\pi}\left(\frac{m_b^2}{m_t^2}+\frac{m_b^4}{m_t^2}+\mathcal{O}\left(\frac{m_b^6}{m_t^6}\right)\right)\log\frac{m_t}{m_b}. \tag{B.1.4}$$

B.1.2 $\mathcal{O}(\alpha_s)$ contributions

$$\delta^{(1)}m^2_{\tilde{t}_1}\Big|_{\text{fin}} = -\frac{2\alpha_s}{3\pi}\Big(A_0(m^2_{\tilde{g}})+A_0(m^2_{\tilde{t}_L})+2m^2_{\tilde{t}_L} + \text{Re}\{B_0(m^2_{\tilde{t}_L},m^2_{\tilde{g}},0)\}(m^2_{\tilde{g}}-m^2_{\tilde{t}_L})\Big), \tag{B.1.5a}$$

$$\delta^{(1)}m^2_{\tilde{t}_2}\Big|_{\text{fin}} = -\frac{2\alpha_s}{3\pi}\Big(A_0(m^2_{\tilde{g}})+A_0(m^2_{\tilde{t}_R})+2m^2_{\tilde{t}_R} + \text{Re}\{B_0(m^2_{\tilde{t}_R},m^2_{\tilde{g}},0)\}(m^2_{\tilde{g}}-m^2_{\tilde{t}_R})\Big), \tag{B.1.5b}$$

$$\frac{\delta^{(1)}m^2_{\tilde{t}_{12}}}{m_t}\bigg|_{\text{fin}} = \frac{2\alpha_s}{3\pi}\Big(-X_t^*\text{Re}\{B_0(0,m^2_{\tilde{t}_L},m^2_{\tilde{t}_R})\} + M_3^*(\text{Re}\{B_0(m^2_{\tilde{t}_L},m^2_{\tilde{g}},0)\}+\text{Re}\{B_0(m^2_{\tilde{t}_R},m^2_{\tilde{g}},0)\})\Big), \tag{B.1.5c}$$

$$\begin{aligned}\delta^{(1)}(m_tX_t)\Big|_{\text{fin}} = \frac{2\alpha_s}{3\pi}m_t\Big[&\frac{X_t}{m^2_{\tilde{t}_L}-m^2_{\tilde{t}_R}}\Big((m^2_{\tilde{t}_L}-m^2_{\tilde{g}})\,\text{Re}\{B_0(m^2_{\tilde{t}_L},m^2_{\tilde{g}},0)\}\\ &-(m^2_{\tilde{t}_R}-m^2_{\tilde{g}})\,\text{Re}\{B_0(m^2_{\tilde{t}_R},m^2_{\tilde{g}},0)\}\Big)-2X_t\left(1+B_0(0,m^2_{\tilde{t}_L},m^2_{\tilde{t}_R})\right)\\ &+M_3\left(\text{Re}\{B_0(m^2_{\tilde{t}_L},m^2_{\tilde{g}},0)\}+\text{Re}\{B_0(m^2_{\tilde{t}_R},m^2_{\tilde{g}},0)\}\right)\Big],\end{aligned} \tag{B.1.5d}$$

$$\begin{aligned}\frac{(\delta^{(1)}m_t^{\text{OS}})^{\text{n/SM}}}{m_t}\bigg|_{\text{fin}} = -\frac{\alpha_s}{3\pi}\Big[&\frac{M_3^*X_t+M_3X_t^*}{m^2_{\tilde{t}_L}-m^2_{\tilde{t}_R}}\Big(B_0(0,m^2_{\tilde{g}},m^2_{\tilde{t}_L})-B_0(0,m^2_{\tilde{g}},m^2_{\tilde{t}_R})\Big)\\ &-\frac{1}{4(m^2_{\tilde{g}}-m^2_{\tilde{t}_L})^2}\Big(3m^4_{\tilde{g}}-4m^2_{\tilde{g}}m^2_{\tilde{t}_L}+m^4_{\tilde{t}_L}+2m^2_{\tilde{t}_L}(2m^2_{\tilde{g}}-m^2_{\tilde{t}_L})\log\frac{m^2_{\tilde{t}_L}}{m^2_{\tilde{g}}}\Big)\\ &-\frac{1}{4(m^2_{\tilde{g}}-m^2_{\tilde{t}_R})^2}\Big(3m^4_{\tilde{g}}-4m^2_{\tilde{g}}m^2_{\tilde{t}_R}+m^4_{\tilde{t}_R}+2m^2_{\tilde{t}_R}(2m^2_{\tilde{g}}-m^2_{\tilde{t}_R})\log\frac{m^2_{\tilde{t}_R}}{m^2_{\tilde{g}}}\Big)\\ &+\log\frac{m^2_{\tilde{g}}}{Q^2}+1\Big],\end{aligned} \tag{B.1.5e}$$

$$\frac{(\delta^{(1)}m_t^{\text{OS}})^{\text{SM}}}{m_t}\bigg|_{\text{fin}} = -\frac{\alpha_s}{3\pi}\left(1+3B_0(0,0,m_t^2)\right), \tag{B.1.5f}$$

$$\frac{(\delta^{(1)}m_b^{\text{OS}})^{\text{n/SM}}}{m_b}\bigg|_{\text{fin}} = -\frac{\alpha_s}{3\pi}\Big[\frac{M_3^*X_b+M_3X_b^*}{m^2_{\tilde{t}_L}-m^2_{\tilde{b}_R}}\Big(B_0(0,m^2_{\tilde{g}},m^2_{\tilde{t}_L})-B_0(0,m^2_{\tilde{g}},m^2_{\tilde{b}_R})\Big)$$

$$- \frac{1}{4(m_{\tilde{g}}^2 - m_{\tilde{t}_L}^2)^2}\Big(3m_{\tilde{g}}^4 - 4m_{\tilde{g}}^2 m_{\tilde{t}_L}^2 + m_{\tilde{t}_L}^4 + 2m_{\tilde{t}_L}^2(2m_{\tilde{g}}^2 - m_{\tilde{t}_L}^2)\log\frac{m_{\tilde{t}_L}^2}{m_{\tilde{g}}^2}\Big) \tag{B.1.5g}$$
$$- \frac{1}{4(m_{\tilde{g}}^2 - m_{\tilde{b}_R}^2)^2}\Big(3m_{\tilde{g}}^4 - 4m_{\tilde{g}}^2 m_{\tilde{b}_R}^2 + m_{\tilde{b}_R}^4 + 2m_{\tilde{b}_R}^2(2m_{\tilde{g}}^2 - m_{\tilde{b}_R}^2)\log\frac{m_{\tilde{b}_R}^2}{m_{\tilde{g}}^2}\Big)$$
$$+ \log\frac{m_{\tilde{g}}^2}{Q^2} + 1\Big],$$

$$\frac{(\delta^{(1)} m_b^{\rm OS})^{\rm SM}}{m_b}\Big|_{\rm fin} = -\frac{\alpha_s}{3\pi}\left(1 + 3B_0(0,0,m_b^2)\right). \tag{B.1.5h}$$

B.2 Degenerate soft-breaking masses

In this Section we outline the epxression for the finite parts of the counterterms for the scenario,

$$m_{\tilde{t}_L} = m_{\tilde{t}_R} = m_{\tilde{b}_L} = m_{\tilde{b}_R} \equiv M_{\rm SUSY}. \tag{B.2.1}$$

B.2.1 $\mathcal{O}(\alpha_t + \alpha_b)$ contributions

$$\delta^{(1)} m_{\tilde{t}_{1/2}}^2\Big|_{\rm fin} = \frac{3\alpha_t}{8\pi}\Big[|X_t|^2 B_0(M_{\rm SUSY}^2, 0, M_{\rm SUSY}^2)$$
$$+ \frac{1}{t_\beta^2}\left(A_0(m_{H^\pm}^2) + |Y_t|^2 B_0(M_{\rm SUSY}^2, m_{H^\pm}^2, M_{\rm SUSY}^2)\right) \tag{B.2.2a}$$
$$+ \frac{1}{s_\beta^2}\left(A_0(M_{\rm SUSY}^2) - A_0(|\mu|^2) + (M_{\rm SUSY}^2 - |\mu|^2)\ {\rm Re}\{B_0(M_{\rm SUSY}^2, 0, |\mu|^2)\}\right)\Big]$$
$$+ \frac{\alpha_b}{8\pi}\Big[|X_b|^2 B_0(M_{\rm SUSY}^2, 0, M_{\rm SUSY}^2) + t_\beta^2\left(A_0(m_{H^\pm}^2) + |Y_b|^2 B_0(M_{\rm SUSY}^2, m_{H^\pm}^2, M_{\rm SUSY}^2)\right)$$
$$+ \frac{1}{c_\beta^2}\left(A_0(M_{\rm SUSY}^2) - A_0(|\mu|^2) + (M_{\rm SUSY}^2 - |\mu|^2)\ {\rm Re}\{B_0(M_{\rm SUSY}^2, 0, |\mu|^2)\}\right)\Big],$$

$$\delta^{(1)} m_{\tilde{t}_{12}}^2\Big|_{\rm fin} = \frac{\alpha_t}{8\pi} e^{i\phi_{X_t}}\Big[|X_t|^2 B_0(M_{\rm SUSY}^2, 0, M_{\rm SUSY}^2)$$
$$+ \frac{1}{t_\beta^2}\left(A_0(m_{H^\pm}^2) + |Y_t|^2 B_0(M_{\rm SUSY}^2, m_{H^\pm}^2, M_{\rm SUSY}^2)\right) \tag{B.2.2b}$$
$$+ \frac{1}{s_\beta^2}\left(A_0(M_{\rm SUSY}^2) - A_0(|\mu|^2) + (M_{\rm SUSY}^2 - |\mu|^2){\rm Re}\{B_0(M_{\rm SUSY}^2, 0, |\mu|^2)\}\right)\Big]$$
$$- \frac{\alpha_b}{8\pi} e^{i\phi_{X_t}}\Big[|X_b|^2 B_0(M_{\rm SUSY}^2, 0, M_{\rm SUSY}^2) + t_\beta^2\left(A_0(m_{H^\pm}^2) + |Y_b|^2 B_0(M_{\rm SUSY}^2, m_{H^\pm}^2, M_{\rm SUSY}^2)\right)$$
$$+ \frac{1}{c_\beta^2}\left(A_0(M_{\rm SUSY}^2) - A_0(|\mu|^2) + (M_{\rm SUSY}^2 - |\mu|^2){\rm Re}\{B_0(M_{\rm SUSY}^2, 0, |\mu|^2)\}\right)\Big],$$

$$
\begin{aligned}
\delta^{(1)}(m_t X_t)\big|_{\rm fin} &= \frac{\alpha_b}{4\pi}\, m_t X_t\, |\widehat{X}_b|^2 + \frac{\alpha_t}{4\pi}\, m_t X_t\, |\widehat{X}_t|^2\, \log\frac{M^2_{\rm SUSY}}{2m_t|X_t|} + \\
&+ \frac{e^{i\phi_{X_t}} M_{\rm SUSY}}{64\pi^2 v^2}\left(m_t|\widehat{X}_t| - m_b|\widehat{X}_b|\right)^3 \log\frac{M^2_{\rm SUSY}}{|m_t|X_t| - m_b|X_b||} \\
&+ \frac{e^{i\phi_{X_t}} M_{\rm SUSY}}{64\pi^2 v^2}\left(m_t|\widehat{X}_t| + m_b|\widehat{X}_b|\right)^3 \log\frac{M^2_{\rm SUSY}}{|m_t|X_t| + m_b|X_b||} \qquad \text{(B.2.2c)} \\
&+ \frac{3\alpha_t}{4\pi}\, m_t X_t\, B_0(M^2_{\rm SUSY}, 0, M^2_{\rm SUSY}) - \frac{\alpha_b}{4\pi}\, m_t X_t\, B_0(M^2_{\rm SUSY}, 0, M^2_{\rm SUSY}) \\
&+ \frac{3\alpha_t}{4\pi t_\beta^2}\, m_t Y_t\, B_0(M^2_{\rm SUSY}, m^2_{H^\pm}, M^2_{\rm SUSY}) + \frac{\alpha_b}{4\pi}\, m_t \left(Y_t + \frac{Y_b}{c_\beta^2}\right)\, B_0(M^2_{\rm SUSY}, m^2_{H^\pm}, M^2_{\rm SUSY}) \\
&- \frac{3\alpha_t}{8\pi t_\beta^2}\, m_t X_t\, \frac{|\widehat{Y}_t|^2}{x^2_{H^\pm} - 4}\left[(x^2_{H^\pm} - 3)\left(B_0(M^2_{\rm SUSY}, m^2_{H^\pm}, M^2_{\rm SUSY}) + \log\frac{M^2_{\rm SUSY}}{Q^2}\right)\right. \\
&\left. - (x^2_{H^\pm} - 2)\left(1 + \log\frac{M^2_{\rm SUSY}}{m^2_{H^\pm}}\right)\right] \\
&- \frac{\alpha_b}{8\pi}\frac{m_t}{x^2_{H^\pm} - 4}\left[\left(t_\beta^2(x^2_{H^\pm} - 3)X_t|\widehat{Y}_b|^2 + 2Y_b\widehat{X}_b^*\widehat{Y}_t\right)\left(B_0(M^2_{\rm SUSY}, m^2_{H^\pm}, M^2_{\rm SUSY}) + \log\frac{M^2_{\rm SUSY}}{Q^2}\right)\right. \\
&\left. - \left(t_\beta^2(x^2_{H^\pm} - 2)X_t|\widehat{Y}_b|^2 + 4Y_b\widehat{X}_b^*\widehat{Y}_t\right)\left(1 + \log\frac{M^2_{\rm SUSY}}{m^2_{H^\pm}}\right)\right] - \frac{3\alpha_t}{4\pi s_\beta^2}\, m_t X_t\, \log\frac{M^2_{\rm SUSY}}{Q^2} \\
&- \frac{3\alpha_t}{8\pi s_\beta^2}\, m_t X_t\, \left(1 + \frac{A_0(|\mu|^2)}{M^2_{\rm SUSY}} - \left(1 + \frac{|\mu|^2}{M^2_{\rm SUSY}}\right)\mathrm{Re}\{B_0(M^2_{\rm SUSY}, |\mu|^2, 0)\}\right) \\
&- \frac{\alpha_b}{8\pi c_\beta^2}\, m_t X_t\, \left(1 + \frac{A_0(|\mu|^2)}{M^2_{\rm SUSY}} - \left(1 + \frac{|\mu|^2}{M^2_{\rm SUSY}}\right)\mathrm{Re}\{B_0(M^2_{\rm SUSY}, |\mu|^2, 0)\}\right) \\
&- \frac{\alpha_b}{2\pi s_\beta c_\beta}\, m_t \mu^*\, \mathrm{Re}\{B_0(M^2_{\rm SUSY}, 0, |\mu|^2)\},
\end{aligned}
$$

$$
\begin{aligned}
\frac{(\delta^{(1)} m_t^{\rm OS})^{\rm n/SM}}{m_t}\bigg|_{\rm fin} &= -\frac{\alpha_t}{4\pi s_\beta^2}\left[\frac{3}{8}(1 - 2B_0(0, 0, m^2_{H^\pm}))c_\beta^2\right. \\
&- \frac{3}{8(1 - |\widehat{\mu}|^2)^2}\left(1 - 4|\widehat{\mu}|^2 + 3|\widehat{\mu}|^4 + 2(2|\widehat{\mu}|^2 - 1)\log\frac{M^2_{\rm SUSY}}{|\mu|^2}\right) \\
&\left. + \frac{3}{4}\log\frac{|\mu|^2}{Q^2}\right] - \frac{\alpha_b}{4\pi c_\beta^2}\left[\frac{1}{8}\left(s_\beta^2 - (2 + 6c_\beta^2)B_0(0, 0, m^2_{H^\pm})\right)\right. \qquad \text{(B.2.2d)} \\
&- \frac{1}{8(1 - |\widehat{\mu}|^2)^2}\left(1 - 4|\widehat{\mu}|^2 + 3|\widehat{\mu}|^4 + 2(2|\widehat{\mu}|^2 - 1)\log\frac{M^2_{\rm SUSY}}{|\mu|^2}\right) \\
&\left. + \frac{\widehat{\mu}\widehat{X}_b + \widehat{\mu}^*\widehat{X}_b^*}{2t_\beta}\frac{1 - |\widehat{\mu}|^2 - |\widehat{\mu}|^2\log\frac{M^2_{\rm SUSY}}{|\mu|^2}}{(1 - |\widehat{\mu}|^2)^2} + \frac{1}{4}\log\frac{|\mu|^2}{Q^2}\right],
\end{aligned}
$$

$$
\begin{aligned}
\frac{(\delta^{(1)} m_t^{\rm OS})^{\rm SM}}{m_t}\bigg|_{\rm fin} &= \frac{\alpha_t}{8\pi}\left(2 + B_0(0, 0, m_t^2) + \frac{1}{2}\left(1 - \frac{m_b^2}{m_t^2}\right)^2 \mathrm{Re}\{B_0(m_t^2, 0, m_b^2)\}\right) \\
&- \frac{\alpha_b}{16\pi}\left(1 + \frac{m_b^2}{m_t^2}\right) B_0(0, 0, m_b^2), \qquad \text{(B.2.2e)}
\end{aligned}
$$

$$(\delta^{(1)}v^2)^{\mathrm{n/SM}}\Big|_{\mathrm{fin}} = -\frac{\alpha_t}{8\pi}|\widehat{X}_t|^2 - \frac{\alpha_b}{8\pi}|\widehat{X}_b|^2, \tag{B.2.2f}$$

$$(\delta^{(1)}v^2)^{\mathrm{SM}}\Big|_{\mathrm{fin}} = -\left(\frac{3\alpha_t}{8\pi}+\frac{3\alpha_b}{8\pi}\right)\left(1-2\log\frac{m_t^2}{Q^2}\right) - \frac{3\alpha_b}{2\pi}\frac{m_b^2}{m_b^2-m_t^2}\log\frac{m_t}{m_b}, \tag{B.2.2g}$$

$$\begin{aligned}\frac{(\delta^{(1)}m_b^{\mathrm{OS}})^{\mathrm{n/SM}}}{m_b}\Big|_{\mathrm{fin}} &= -\frac{\alpha_b}{4\pi c_\beta^2}\Big[\frac{3}{8}(1-2B_0(0,0,m_{H^\pm}^2))s_\beta^2 \\ &- \frac{3}{8(1-|\widehat{\mu}|^2)^2}\Big(1-4|\widehat{\mu}|^2+3|\widehat{\mu}|^4+2(2|\widehat{\mu}|^2-1)\log\frac{M_{\mathrm{SUSY}}^2}{|\mu|^2}\Big) \\ &+ \frac{3}{4}\log\frac{|\mu|^2}{Q^2}\Big] - \frac{\alpha_t}{4\pi s_\beta^2}\Big[\frac{1}{8}\Big(c_\beta^2-(2+6s_\beta^2)B_0(0,0,m_{H^\pm}^2)\Big) \\ &- \frac{1}{8(1-|\widehat{\mu}|^2)^2}\Big(1-4|\widehat{\mu}|^2+3|\widehat{\mu}|^4+2(2|\widehat{\mu}|^2-1)\log\frac{M_{\mathrm{SUSY}}^2}{|\mu|^2}\Big) \\ &+ \frac{(\widehat{\mu}\widehat{X}_t+\widehat{\mu}^*\widehat{X}_t^*)t_\beta}{2}\frac{1-|\widehat{\mu}|^2-|\widehat{\mu}|^2\log\frac{M_{\mathrm{SUSY}}^2}{|\mu|^2}}{(1-|\widehat{\mu}|^2)^2}+\frac{1}{4}\log\frac{|\mu|^2}{Q^2}\Big],\end{aligned} \tag{B.2.2h}$$

$$\begin{aligned}\frac{(\delta^{(1)}m_b^{\mathrm{OS}})^{\mathrm{SM}}}{m_b}\Big|_{\mathrm{fin}} &= \frac{\alpha_b}{8\pi}\left(2+B_0(0,0,m_b^2)+\frac{1}{2}\left(1-\frac{m_t^2}{m_b^2}\right)^2\mathrm{Re}\{B_0(m_b^2,0,m_t^2)\}\right) \\ &- \frac{\alpha_t}{16\pi}\left(1+\frac{m_t^2}{m_b^2}\right)B_0(0,0,m_t^2).\end{aligned} \tag{B.2.2i}$$

where

$$\widehat{X}_{t,b} = \frac{X_{t,b}}{M_{\mathrm{SUSY}}}, \quad \widehat{Y}_{t,b} = \frac{Y_{t,b}}{M_{\mathrm{SUSY}}}, \quad x_{H^\pm} = \frac{m_{H^\pm}}{M_{\mathrm{SUSY}}}, \quad \widehat{\mu} = \frac{\mu}{M_{\mathrm{SUSY}}}. \tag{B.2.3}$$

B.2.2 $\mathcal{O}(\alpha_s)$ contributions

$$\begin{aligned}\delta^{(1)}m_{\tilde{t}_{1/2}}^2\Big|_{\mathrm{fin}} &= -\frac{2\alpha_s}{3\pi}\Big(A_0(m_{\tilde{g}}^2)+A_0(M_{\mathrm{SUSY}}^2)+2M_{\mathrm{SUSY}}^2 \\ &\quad + \mathrm{Re}\{B_0(M_{\mathrm{SUSY}}^2,m_{\tilde{g}}^2,0)\}(m_{\tilde{g}}^2-M_{\mathrm{SUSY}}^2)\Big),\end{aligned} \tag{B.2.4a}$$

$$\delta^{(1)}m_{\tilde{t}_{12}}^2\Big|_{\mathrm{fin}} = \frac{2\alpha_s}{3\pi}\left(M_3-e^{2i\phi_{X_t}}M_3^*\right)\ \mathrm{Re}\{B_0(M_{\mathrm{SUSY}}^2,m_{\tilde{g}}^2,0)\}, \tag{B.2.4b}$$

$$\delta^{(1)}(m_tX_t)\Big|_{\mathrm{fin}} = \frac{2\alpha_s}{3\pi}m_t\Big[X_t\Big(-3+\left(1+\frac{m_{\tilde{g}}^2}{M_{\mathrm{SUSY}}^2}\right)\mathrm{Re}\{B_0(M_{\mathrm{SUSY}}^2,m_{\tilde{g}}^2,0)\}$$

$$- 2B_0(0, M^2_{\rm SUSY}, M^2_{\rm SUSY}) - \frac{A_0(m^2_{\tilde g})}{M^2_{\rm SUSY}}\Big) + M_3\ {\rm Re}\{B_0(M^2_{\rm SUSY}, m^2_{\tilde g}, 0)\}\Big], \tag{B.2.4c}$$

$$\frac{(\delta^{(1)} m_t^{\rm OS})^{\rm n/SM}}{m_t}\bigg|_{\rm fin} = \frac{\alpha_s}{3\pi}\Big[(\widehat{M}_3^* \widehat{X}_t + \widehat{M}_3 \widehat{X}_t^*)\frac{1 - \widehat{m}^2_{\tilde g} - \widehat{m}^2_{\tilde g}\log\frac{M^2_{\rm SUSY}}{m^2_{\tilde g}}}{(1-\widehat{m}^2_{\tilde g})^2}$$
$$+ \frac{1}{2(1-\widehat{m}^2_{\tilde g})^2}\Big(1 - 4\widehat{m}^2_{\tilde g} + 3\widehat{m}^4_{\tilde g} + 2(2\widehat{m}^2_{\tilde g} - 1)\log\frac{M^2_{\rm SUSY}}{m^2_{\tilde g}}\Big) \tag{B.2.4d}$$
$$- \log\frac{m^2_{\tilde g}}{Q^2} - 1\Big],$$

$$\frac{(\delta^{(1)} m_t^{\rm OS})^{\rm SM}}{m_t}\bigg|_{\rm fin} = -\frac{\alpha_s}{3\pi}\left(1 + 3B_0(0,0,m_t^2)\right), \tag{B.2.4e}$$

$$\frac{(\delta^{(1)} m_b^{\rm OS})^{\rm n/SM}}{m_b}\bigg|_{\rm fin} = \frac{\alpha_s}{3\pi}\Big[(\widehat{M}_3^* \widehat{X}_b + \widehat{M}_3 \widehat{X}_b^*)\frac{1 - \widehat{m}^2_{\tilde g} - \widehat{m}^2_{\tilde g}\log\frac{M^2_{\rm SUSY}}{m^2_{\tilde g}}}{(1-\widehat{m}^2_{\tilde g})^2}$$
$$+ \frac{1}{2(1-\widehat{m}^2_{\tilde g})^2}\Big(1 - 4\widehat{m}^2_{\tilde g} + 3\widehat{m}^4_{\tilde g} + 2(2\widehat{m}^2_{\tilde g} - 1)\log\frac{M^2_{\rm SUSY}}{m^2_{\tilde g}}\Big) \tag{B.2.4f}$$
$$- \log\frac{m^2_{\tilde g}}{Q^2} - 1\Big], \tag{B.2.4g}$$

$$\frac{(\delta^{(1)} m_b^{\rm OS})^{\rm SM}}{m_b}\bigg|_{\rm fin} = -\frac{\alpha_s}{3\pi}\left(1 + 3B_0(0,0,m_b^2)\right). \tag{B.2.4h}$$

where

$$\widehat{M}_3 = \frac{M_3}{M_{\rm SUSY}}, \quad \widehat{m}_{\tilde g} = \frac{m_{\tilde g}}{M_{\rm SUSY}} \equiv |\widehat{M}_3|. \tag{B.2.5}$$

Appendix C

Two-loop Higgs boson self-energies in the SM

Equations (6.1.26a) – (6.1.26f) in Chapter 6 contain the expressions for the $\mathcal{O}(\alpha_t^2\alpha_s + \alpha_b^2\alpha_s + (\alpha_t+\alpha_b)^3)$ two-loop threshold corrections to λ. These expressions involve two-loop $\mathcal{O}(m_t^2\alpha_t\alpha_s + m_b^2\alpha_b\alpha_s + m_t^2\alpha_t^2 + m_t^2\alpha_t\alpha_b + m_b^2\alpha_t\alpha_b + m_b^2\alpha_b^2)$ self-energies of the SM-like Higgs boson computed in the $\overline{\text{MS}}$ scheme in the SM. In this Appendix we provide the explicit expressions for these self-energies,

$$\widetilde{\Sigma}_{hh}^{\overline{\text{MS}},\text{SM},\mathcal{O}(m_t^2\alpha_t\alpha_s)} = -\frac{\alpha_s \overline{m}_t^4}{2\pi^3 \overline{v}^2} \log\frac{\overline{m}_t^2}{Q^2}\left(1 + 3\log\frac{\overline{m}_t^2}{Q^2}\right), \tag{C.0.1a}$$

$$\widetilde{\Sigma}_{hh}^{\overline{\text{MS}},\text{SM},\mathcal{O}(m_b^2\alpha_b\alpha_s)} = -\frac{\alpha_s \overline{m}_b^4}{2\pi^3 \overline{v}^2} \log\frac{\overline{m}_b^2}{Q^2}\left(1 + 3\log\frac{\overline{m}_b^2}{Q^2}\right), \tag{C.0.1b}$$

$$\widetilde{\Sigma}_{hh}^{\overline{\text{MS}},\text{SM},\mathcal{O}(m_t^2\alpha_t^2)} = \frac{3\overline{m}_t^6}{128\pi^4 \overline{v}^4}\left(2 - 7\log\frac{\overline{m}_t^2}{Q^2} + 3\log^2\frac{\overline{m}_t^2}{Q^2} + 2\,\text{Li}_2\left(1 - \frac{\overline{m}_b^2}{\overline{m}_t^2}\right)\right), \tag{C.0.1c}$$

$$\widetilde{\Sigma}_{hh}^{\overline{\text{MS}},\text{SM},\mathcal{O}(m_t^2\alpha_t\alpha_b)} = -\frac{3\overline{m}_t^4\overline{m}_b^2}{128\pi^4 \overline{v}^4}\left(-2 + 2\log\frac{\overline{m}_b^2}{\overline{m}_t^2} + \log\frac{\overline{m}_t^2}{Q^2} + 3\log^2\frac{\overline{m}_t^2}{Q^2} + 6\,\text{Li}_2\left(1 - \frac{\overline{m}_b^2}{\overline{m}_t^2}\right)\right), \tag{C.0.1d}$$

$$\begin{aligned}\widetilde{\Sigma}_{hh}^{\overline{\text{MS}},\text{SM},\mathcal{O}(m_b^2\alpha_t\alpha_b)} = -\frac{3\overline{m}_t^2\overline{m}_b^4}{128\pi^4 \overline{v}^4}\Bigg(&-2 + \log\frac{\overline{m}_t^2}{Q^2} + 3\log^2\frac{\overline{m}_t^2}{Q^2} \\ &+ \log\frac{\overline{m}_b^2}{\overline{m}_t^2}\left(6\log\frac{\overline{m}_t^2}{Q^2} - 1\right) - 6\,\text{Li}_2\left(1 - \frac{\overline{m}_b^2}{\overline{m}_t^2}\right)\Bigg),\end{aligned} \tag{C.0.1e}$$

$$\widetilde{\Sigma}_{hh}^{\overline{\rm MS},{\rm SM},\mathcal{O}(m_b^2\alpha_b^2)} = \frac{3\overline{m}_b^6}{128\pi^4\overline{v}^4}\left(2 + 2\log^2\frac{\overline{m}_b^2}{\overline{m}_t^2} - 7\log\frac{\overline{m}_t^2}{Q^2} + 3\log^2\frac{\overline{m}_t^2}{Q^2} + \log\frac{\overline{m}_b^2}{\overline{m}_t^2}\left(6\log\frac{\overline{m}_t^2}{Q^2} - 7\right) - 2\,\mathrm{Li}_2\left(1 - \frac{\overline{m}_b^2}{\overline{m}_t^2}\right)\right) \tag{C.0.1f}$$

where $\overline{m}_t = m_t^{\overline{\rm MS},{\rm SM}}(Q),\ \overline{m}_b = m_b^{\overline{\rm MS},{\rm SM}}(Q), \overline{v} = v^2_{\overline{\rm MS},{\rm SM}}(Q)$.

If the computation is performed in the $\overline{\rm DR}$ scheme, the result for the $\mathcal{O}(m_t^2\alpha_t^2 + m_t^2\alpha_t\alpha_b + m_b^2\alpha_t\alpha_b + m_b^2\alpha_b^2)$ self-energies does not change, while the expressions for the $\mathcal{O}(m_t^2\alpha_t\alpha_s + m_b^2\alpha_b\alpha_s)$ self-energies read,

$$\widetilde{\Sigma}_{hh}^{\overline{\rm DR},{\rm SM},\mathcal{O}(m_t^2\alpha_t\alpha_s)} = \frac{\alpha_s\overline{m}_t^4}{2\pi^3\overline{v}^2}\left(1 + \log\frac{\overline{m}_t^2}{Q^2} - 3\log^2\frac{\overline{m}_t^2}{Q^2}\right), \tag{C.0.2a}$$

$$\widetilde{\Sigma}_{hh}^{\overline{\rm DR},{\rm SM},\mathcal{O}(m_b^2\alpha_b\alpha_s)} = \frac{\alpha_s\overline{m}_b^4}{2\pi^3\overline{v}^2}\left(1 + \log\frac{\overline{m}_b^2}{Q^2} - 3\log^2\frac{\overline{m}_b^2}{Q^2}\right). \tag{C.0.2b}$$

Appendix D

From the $\overline{\text{MDR}}$ scheme to the resummation of gluino contributions

Here, we discuss how the resummation formulas given in [264] can be recovered from the expressions in the $\overline{\text{MDR}}$ scheme. The authors of [264] considered two sets of diagrams contributing to the matching of the soft SUSY-breaking Higgs mass parameter m_{22}.

The left diagram of Fig. 1 in [264] corresponds to an A_0 Passarino–Veltman loop function. In the $\overline{\text{MDR}}$ scheme, we do not have to consider any stop self-energy insertions beyond the one-loop diagram. Following [264], we define $\xi_{L,R}$ via

$$(m_{\tilde{t}_{L,R}}^{\overline{\text{MDR}}})^2 = (m_{\tilde{t}_{L,R}}^{\overline{\text{DR}}})^2 \, (1 - \xi_{L,R}) \tag{D.0.1}$$

we obtain for the finite part of the diagram (with Q being a generic renormalization scale)

$$\begin{aligned}
&A_0^{\text{fin}}\left((m_{\tilde{t}_{L,R}}^{\overline{\text{MDR}}})^2\right) = \\
&= A_0^{\text{fin}}\left((m_{\tilde{t}_{L,R}}^{\overline{\text{DR}}})^2\right) - (m_{\tilde{t}_{L,R}}^{\overline{\text{DR}}})^2 \left(-\xi_{L,R} \ln \frac{(m_{\tilde{t}_{L,R}}^{\overline{\text{DR}}})^2}{Q^2} + \frac{1}{2}\xi_{L,R}^2 + \frac{1}{6}\xi_{L,R}^3 + \dots\right) \\
&= A_0^{\text{fin}}\left((m_{\tilde{t}_{L,R}}^{\overline{\text{DR}}})^2\right) - (m_{\tilde{t}_{L,R}}^{\overline{\text{DR}}})^2 \left(-\xi_{L,R} \ln \frac{(m_{\tilde{t}_{L,R}}^{\overline{\text{DR}}})^2}{Q^2} + \sum_{k=2}^{\infty} \frac{\xi_{L,R}^k}{k(k-1)}\right) \\
&= A_0^{\text{fin}}\left((m_{\tilde{t}_{L,R}}^{\overline{\text{DR}}})^2\right) - (m_{\tilde{t}_{L,R}}^{\overline{\text{DR}}})^2 \left(-\xi_{L,R} \ln \frac{(m_{\tilde{t}_{L,R}}^{\overline{\text{DR}}})^2}{Q^2} + \xi_{L,R} + (1 - \xi_{L,R}) \ln(1 - \xi_{L,R})\right),
\end{aligned} \tag{D.0.2}$$

recovering the resummation in Eq. (10) of [264].[92]

The right diagram of Fig. 1 in [264] corresponds to a B_0 Passarino–Veltman loop function. Analogously to the A_0 loop function above, we obtain for the special case where $m_{\tilde{t}_L}^{\overline{\text{MDR}}} = m_{\tilde{t}_R}^{\overline{\text{MDR}}}$.

$$\begin{aligned} B_0\left(0, (m_{\tilde{t}_L}^{\overline{\text{MDR}}})^2, (m_{\tilde{t}_R}^{\overline{\text{MDR}}})^2\right) &= B_0\left(0, (m_{\tilde{t}_L}^{\overline{\text{DR}}})^2, (m_{\tilde{t}_R}^{\overline{\text{DR}}})^2\right) + \xi_{L,R} + \frac{1}{2}\xi_{L,R}^2 + \frac{1}{3}\xi_{L,R}^3 + \dots \\ &= B_0\left(0, (m_{\tilde{t}_L}^{\overline{\text{DR}}})^2, (m_{\tilde{t}_R}^{\overline{\text{DR}}})^2\right) + \sum_{k=1}^{\infty} \frac{\xi_{L,R}^k}{k} \\ &= B_0\left(0, (m_{\tilde{t}_L}^{\overline{\text{DR}}})^2, (m_{\tilde{t}_R}^{\overline{\text{DR}}})^2\right) - \ln(1 - \xi_{L,R}), \end{aligned} \tag{D.0.3}$$

recovering the expression given in Eq. (11) of [264].

[92] The additional two-loop terms found in Eq. (9) [264] originate from the matching of the soft SUSY-breaking Higgs mass parameter m_{22} and are not related to the matching of the soft SUSY-breaking stop masses. This additional contribution, however, does not affect the calculation of the SM-like Higgs mass at the considered order.

List of Figures

List of Tables

Bibliography

[1] ATLAS collaboration, G. Aad et al., *Observation of a new particle in the search for the Standard Model Higgs boson with the ATLAS detector at the LHC*, *Phys. Lett.* **B716** (2012) 1–29, [1207.7214].

[2] CMS collaboration, S. Chatrchyan et al., *Observation of a New Boson at a Mass of 125 GeV with the CMS Experiment at the LHC*, *Phys. Lett.* **B716** (2012) 30–61, [1207.7235].

[3] ATLAS, CMS collaboration, G. Aad et al., *Combined Measurement of the Higgs Boson Mass in pp Collisions at $\sqrt{s} = 7$ and 8 TeV with the ATLAS and CMS Experiments*, *Phys. Rev. Lett.* **114** (2015) 191803, [1503.07589].

[4] Particle Data Group collaboration, M. Tanabashi et al., *Review of Particle Physics*, *Phys. Rev. D* **98** (2018) 030001.

[5] CMS collaboration, A. M. Sirunyan et al., *A measurement of the Higgs boson mass in the diphoton decay channel*, *Phys. Lett. B* **805** (2020) 135425, [2002.06398].

[6] M. Cepeda et al., *Report from Working Group 2: Higgs Physics at the HL-LHC and HE-LHC*, vol. 7, pp. 221–584. 12, 2019. 1902.00134. 10.23731/CYRM-2019-007.221.

[7] S. Borowka, T. Hahn, S. Heinemeyer, G. Heinrich and W. Hollik, *Renormalization scheme dependence of the two-loop QCD corrections to the neutral Higgs-boson masses in the MSSM*, *Eur. Phys. J.* **C75** (2015) 424, [1505.03133].

[8] M. D. Goodsell and F. Staub, *The Higgs mass in the CP violating MSSM, NMSSM, and beyond*, *Eur. Phys. J.* **C77** (2017) 46, [1604.05335].

[9] S. Paßehr and G. Weiglein, *Two-loop top and bottom Yukawa corrections to the Higgs-boson masses in the complex MSSM*, *Eur. Phys. J. C* **78** (2018) 222, [1705.07909].

[10] R. V. Harlander, J. Klappert and A. Voigt, *Higgs mass prediction in the MSSM at three-loop level in a pure $\overline{DR}$ context*, *Eur. Phys. J.* **C77** (2017) 814, [1708.05720].

[11] S. Borowka, S. Paßehr and G. Weiglein, *Complete two-loop QCD contributions to the lightest Higgs-boson mass in the MSSM with complex parameters*, *Eur. Phys. J. C* **78** (2018) 576, [1802.09886].

[12] A. Fazio and E. Reyes R., *The Lightest Higgs Boson Mass of the MSSM at Three-Loop Accuracy*, *Nucl. Phys. B* **942** (2019) 164–183, [1901.03651].

[13] J. Pardo Vega and G. Villadoro, *SusyHD: Higgs mass Determination in Supersymmetry*, *JHEP* **07** (2015) 159, [1504.05200].

[14] G. Lee and C. E. M. Wagner, *Higgs bosons in heavy supersymmetry with an intermediate m_A*, *Phys. Rev.* **D92** (2015) 075032, [1508.00576].

[15] E. Bagnaschi, J. Pardo Vega and P. Slavich, *Improved determination of the Higgs mass in the MSSM with heavy superpartners*, *Eur. Phys. J.* **C77** (2017) 334, [1703.08166].

[16] H. Bahl and W. Hollik, *Precise prediction of the MSSM Higgs boson masses for low M_A*, *JHEP* **07** (2018) 182, [1805.00867].

[17] R. V. Harlander, J. Klappert, A. D. Ochoa Franco and A. Voigt, *The light CP-even MSSM Higgs mass resummed to fourth logarithmic order*, *Eur. Phys. J.* **C78** (2018) 874, [1807.03509].

[18] E. Bagnaschi, G. Degrassi, S. Paßehr and P. Slavich, *Full two-loop QCD corrections to the Higgs mass in the MSSM with heavy superpartners*, *Eur. Phys. J.* **C79** (2019) 910, [1908.01670].

[19] N. Murphy and H. Rzehak, *Higgs-Boson Masses and Mixings in the MSSM with CP Violation and Heavy SUSY Particles*, 1909.00726.

[20] H. Bahl, I. Sobolev and G. Weiglein, *Precise prediction for the mass of the light MSSM Higgs boson for the case of a heavy gluino*, 1912.10002.

[21] T. Hahn, S. Heinemeyer, W. Hollik, H. Rzehak and G. Weiglein, *High-Precision Predictions for the Light CP -Even Higgs Boson Mass of the Minimal Supersymmetric Standard Model*, *Phys. Rev. Lett.* **112** (2014) 141801, [1312.4937].

[22] H. Bahl and W. Hollik, *Precise prediction for the light MSSM Higgs boson mass combining effective field theory and fixed-order calculations*, *Eur. Phys. J. C* **76** (2016) 499, [1608.01880].

[23] H. Bahl, S. Heinemeyer, W. Hollik and G. Weiglein, *Reconciling EFT and hybrid calculations of the light MSSM Higgs-boson mass*, *Eur. Phys. J. C* **78** (2018) 57, [1706.00346].

[24] H. Bahl, *Pole mass determination in presence of heavy particles*, *JHEP* **02** (2019) 121, [1812.06452].

[25] P. Athron, J. Park, T. Steudtner, D. Stöckinger and A. Voigt, *Precise Higgs mass calculations in (non-)minimal supersymmetry at both high and low scales*, *JHEP* **01** (2017) 079, [1609.00371].

[26] F. Staub and W. Porod, *Improved predictions for intermediate and heavy Supersymmetry in the MSSM and beyond*, *Eur. Phys. J. C* **77** (2017) 338, [1703.03267].

[27] P. Athron, M. Bach, D. Harries, T. Kwasnitza, J.-h. Park, D. Stöckinger et al., *FlexibleSUSY 2.0: Extensions to investigate the phenomenology of SUSY and non-SUSY models*, *Comput. Phys. Commun.* **230** (2018) 145–217, [1710.03760].

[28] R. Harlander, J. Klappert and A. Voigt, *The light CP-even MSSM Higgs mass including N^3LO+N^3LL QCD corrections*, *Eur. Phys. J. C* **80** (2020) 186, [1910.03595].

[29] D. Noth and M. Spira, *Higgs Boson Couplings to Bottom Quarks: Two-Loop Supersymmetry-QCD Corrections*, *Phys. Rev. Lett.* **101** (2008) 181801, [0808.0087].

[30] D. Noth, *Supersymmetric precision calculations of Bottom Yukawa couplings*, *PhD thesis, University of Zürich, 2008*, https://www.zora.uzh.ch/id/eprint/17033/ .

[31] D. Noth and M. Spira, *Supersymmetric Higgs Yukawa Couplings to Bottom Quarks at next-to-next-to-leading Order*, *JHEP* **06** (2011) 084, [1001.1935].

[32] G. F. Giudice and A. Strumia, *Probing High-Scale and Split Supersymmetry with Higgs Mass Measurements*, *Nucl. Phys.* **B858** (2012) 63–83, [1108.6077].

[33] E. Bagnaschi, G. F. Giudice, P. Slavich and A. Strumia, *Higgs Mass and Unnatural Supersymmetry*, *JHEP* **09** (2014) 092, [1407.4081].

[34] G. Degrassi, P. Slavich and F. Zwirner, *On the neutral Higgs boson masses in the MSSM for arbitrary stop mixing*, *Nucl. Phys.* **B611** (2001) 403–422, [hep-ph/0105096].

[35] H. Bahl, S. Heinemeyer, W. Hollik and G. Weiglein, *Theoretical uncertainties in the MSSM Higgs boson mass calculation*, 1912.04199.

[36] ATLAS collaboration, M. Aaboud et al., *Search for squarks and gluinos in final states with jets and missing transverse momentum using 36 fb^{-1} of $\sqrt{s} = 13$ TeV pp collision data with the ATLAS detector*, *Phys. Rev.* **D97** (2018) 112001, [1712.02332].

[37] ATLAS collaboration, G. Aad et al., *Search for squarks and gluinos in final states with same-sign leptons and jets using 139 fb^{-1} of data collected with the ATLAS detector*, 1909.08457.

[38] ATLAS collaboration, *Search for squarks and gluinos in final states with jets and missing transverse momentum using 139 fb^{-1} of $\sqrt{s}$ =13 TeV pp collision data with the ATLAS detector*, Tech. Rep. ATLAS-CONF-2019-040, CERN, Geneva, Aug, 2019.

[39] CMS collaboration, A. M. Sirunyan et al., *Search for supersymmetry in proton-proton collisions at 13 TeV using identified top quarks*, *Phys. Rev.* **D97** (2018) 012007, [1710.11188].

[40] CMS collaboration, A. M. Sirunyan et al., *Search for natural and split supersymmetry in proton-proton collisions at $\sqrt{s} = 13$ TeV in final states with jets and missing transverse momentum*, *JHEP* **05** (2018) 025, [1802.02110].

[41] CMS collaboration, A. M. Sirunyan et al., *Search for supersymmetry in proton-proton collisions at 13 TeV in final states with jets and missing transverse momentum*, *JHEP* **10** (2019) 244, [1908.04722].

[42] CMS collaboration, A. M. Sirunyan et al., *Searches for physics beyond the standard model with the M_{T2} variable in hadronic final states with and without disappearing tracks in proton-proton collisions at $\sqrt{s} = 13$ TeV*, 1909.03460.

[43] CMS collaboration, A. M. Sirunyan et al., *Search for supersymmetry in pp collisions at $\sqrt{s} = 13$ TeV with 137 fb^{-1} in final states with a single lepton using the sum of masses of large-radius jets*, 1911.07558.

[44] CMS collaboration, *Search for physics beyond the standard model in events with two same-sign leptons or at least three leptons and jets in proton-proton*

collisions at $\sqrt{s} = 13$ TeV., Tech. Rep. CMS-PAS-SUS-19-008, CERN, Geneva, 2019.

[45] F. Englert and R. Brout, *Broken Symmetry and the Mass of Gauge Vector Mesons*, *Phys. Rev. Lett.* **13** (1964) 321–323.

[46] P. W. Higgs, *Broken symmetries, massless particles and gauge fields*, *Phys. Lett.* **12** (1964) 132–133.

[47] P. W. Higgs, *Broken Symmetries and the Masses of Gauge Bosons*, *Phys. Rev. Lett.* **13** (1964) 508–509.

[48] P. W. Higgs, *Spontaneous Symmetry Breakdown without Massless Bosons*, *Phys. Rev.* **145** (1966) 1156–1163.

[49] MuLan collaboration, V. Tishchenko et al., *Detailed Report of the MuLan Measurement of the Positive Muon Lifetime and Determination of the Fermi Constant*, *Phys. Rev.* **D87** (2013) 052003, [1211.0960].

[50] N. Cabibbo, *Unitary Symmetry and Nonleptonic Decays*, *Phys. Rev. Lett.* **12** (1964) 62–63.

[51] M. Kobayashi and T. Maskawa, *CP Violation in the Renormalizable Theory of Weak Interaction*, *Prog. Theor. Phys.* **49** (1973) 652–657.

[52] J. H. Christenson, J. W. Cronin, V. L. Fitch and R. Turlay, *Evidence for the* 2π *Decay of the* K_2^0 *Meson*, *Phys. Rev. Lett.* **13** (1964) 138–140.

[53] R. Davis, Jr., D. S. Harmer and K. C. Hoffman, *Search for neutrinos from the sun*, *Phys. Rev. Lett.* **20** (1968) 1205–1209.

[54] SNO collaboration, Q. R. Ahmad et al., *Measurement of the rate of* $\nu_e + d \to p + p + e^-$ *interactions produced by* ^8B *solar neutrinos at the Sudbury Neutrino Observatory*, *Phys. Rev. Lett.* **87** (2001) 071301, [nucl-ex/0106015].

[55] M. C. Gonzalez-Garcia and M. Maltoni, *Phenomenology with Massive Neutrinos*, *Phys. Rept.* **460** (2008) 1–129, [0704.1800].

[56] Double Chooz collaboration, Y. Abe et al., *Indication of Reactor* $\bar{\nu}_e$ *Disappearance in the Double Chooz Experiment*, *Phys. Rev. Lett.* **108** (2012) 131801, [1112.6353].

[57] Daya Bay collaboration, F. P. An et al., *Observation of electron-antineutrino disappearance at Daya Bay*, *Phys. Rev. Lett.* **108** (2012) 171803, [1203.1669].

[58] RENO collaboration, J. K. Ahn et al., *Observation of Reactor Electron Antineutrino Disappearance in the RENO Experiment*, *Phys. Rev. Lett.* **108** (2012) 191802, [1204.0626].

[59] L. D. Faddeev and V. N. Popov, *Feynman Diagrams for the Yang-Mills Field*, *Phys. Lett.* **25B** (1967) 29–30.

[60] C. Becchi, A. Rouet and R. Stora, *The Abelian Higgs-Kibble Model. Unitarity of the S Operator*, *Phys. Lett.* **52B** (1974) 344–346.

[61] C. Becchi, A. Rouet and R. Stora, *Renormalization of the Abelian Higgs-Kibble Model*, *Commun. Math. Phys.* **42** (1975) 127–162.

[62] C. Becchi, A. Rouet and R. Stora, *Renormalization of Gauge Field Models*, in *Marseille Colloq.,1974:6*, p. 6, 1974.

[63] I. V. Tyutin, *Gauge Invariance in Field Theory and Statistical Physics in Operator Formalism*, 0812.0580.

[64] G. 't Hooft, *Renormalizable Lagrangians for Massive Yang-Mills Fields*, *Nucl. Phys.* **B35** (1971) 167–188.

[65] F. R. Klinkhamer and N. S. Manton, *A Saddle Point Solution in the Weinberg-Salam Theory*, *Phys. Rev.* **D30** (1984) 2212.

[66] L. Zeune, *Precise predictions for the W boson mass in models beyond the Standard Model*, Master's thesis, Gottingen U., 2011.

[67] S. Heinemeyer, W. Hollik, G. Weiglein and L. Zeune, *Implications of LHC search results on the W boson mass prediction in the MSSM*, *JHEP* **12** (2013) 084, [1311.1663].

[68] L. Zeune, *Constraining supersymmetric models using Higgs physics, precision observables and direct searches*, *PhD thesis, U. Hamburg, Dept. Phys., 2014*, *http://www-library.desy.de/cgi-bin/showprep.pl?thesis14-020* .

[69] O. Stål, G. Weiglein and L. Zeune, *Improved prediction for the mass of the W boson in the NMSSM*, *JHEP* **09** (2015) 158, [1506.07465].

[70] J. Erler and M. Schott, *Electroweak Precision Tests of the Standard Model after the Discovery of the Higgs Boson*, *Prog. Part. Nucl. Phys.* **106** (2019) 68–119, [1902.05142].

[71] F. Zwicky, *Die Rotverschiebung von extragalaktischen Nebeln*, *Helv. Phys. Acta* **6** (1933) 110–127.

[72] K. C. Freeman, *On the disks of spiral and SO Galaxies*, *Astrophys. J.* **160** (1970) 811.

[73] V. C. Rubin and W. K. Ford, Jr., *Rotation of the Andromeda Nebula from a Spectroscopic Survey of Emission Regions*, *Astrophys. J.* **159** (1970) 379–403.

[74] D. Clowe, M. Bradac, A. H. Gonzalez, M. Markevitch, S. W. Randall, C. Jones et al., *A direct empirical proof of the existence of dark matter*, *Astrophys. J.* **648** (2006) L109–L113, [astro-ph/0608407].

[75] Planck collaboration, N. Aghanim et al., *Planck 2018 results. VI. Cosmological parameters*, 1807.06209.

[76] Troitsk collaboration, V. N. Aseev et al., *An upper limit on electron antineutrino mass from Troitsk experiment*, *Phys. Rev.* **D84** (2011) 112003, [1108.5034].

[77] KATRIN collaboration, M. Aker et al., *Improved Upper Limit on the Neutrino Mass from a Direct Kinematic Method by KATRIN*, *Phys. Rev. Lett.* **123** (2019) 221802, [1909.06048].

[78] S. Weinberg, *Baryon and Lepton Nonconserving Processes*, *Phys. Rev. Lett.* **43** (1979) 1566–1570.

[79] M. J. Dolinski, A. W. P. Poon and W. Rodejohann, *Neutrinoless Double-Beta Decay: Status and Prospects*, *Ann. Rev. Nucl. Part. Sci.* **69** (2019) 219–251, [1902.04097].

[80] S. Weinberg, *Implications of Dynamical Symmetry Breaking*, *Phys. Rev.* **D13** (1976) 974–996.

[81] E. Gildener, *Gauge Symmetry Hierarchies*, *Phys. Rev.* **D14** (1976) 1667.

[82] L. Susskind, *Dynamics of Spontaneous Symmetry Breaking in the Weinberg-Salam Theory*, *Phys. Rev.* **D20** (1979) 2619–2625.

[83] J. C. Pati and A. Salam, *Lepton Number as the Fourth Color*, *Phys. Rev.* **D10** (1974) 275–289.

[84] H. Georgi and S. L. Glashow, *Unity of All Elementary Particle Forces*, *Phys. Rev. Lett.* **32** (1974) 438–441.

[85] A. G. Cohen, A. De Rujula and S. L. Glashow, *A Matter - antimatter universe?*, *Astrophys. J.* **495** (1998) 539–549, [astro-ph/9707087].

[86] A. D. Sakharov, *Violation of CP Invariance, C asymmetry, and baryon asymmetry of the universe*, *Pisma Zh. Eksp. Teor. Fiz.* **5** (1967) 32–35.

[87] M. Drees, R. Godbole and P. Roy, *Theory and phenomenology of Sparticles: an account of four-dimensional N=1 supersymmetry in high-energy physics*. World Scientific, Singapore, 2004, 10.1142/4001.

[88] S. P. Martin, *A Supersymmetry primer*, hep-ph/9709356.

[89] Bertolini, "Lectures on supersymmetry." https://people.sissa.it/~bertmat/susycourse.pdf, 2019.

[90] M. Frank, T. Hahn, S. Heinemeyer, W. Hollik, H. Rzehak and G. Weiglein, *The Higgs Boson Masses and Mixings of the Complex MSSM in the Feynman-Diagrammatic Approach*, *JHEP* **02** (2007) 047, [hep-ph/0611326].

[91] S. Paßehr, *Two-Loop Corrections to the Higgs-Boson Masses in the Minimal Supersymmetric Standard Model with CP-Violation*, *PhD thesis, Münich, Tech. U., 2014*, http://mediatum.ub.tum.de?id=1223795 .

[92] H. K. Dreiner, H. E. Haber and S. P. Martin, *Two-component spinor techniques and Feynman rules for quantum field theory and supersymmetry*, *Phys. Rept.* **494** (2010) 1–196, [0812.1594].

[93] Yu. A. Golfand and E. P. Likhtman, *Extension of the Algebra of Poincare Group Generators and Violation of p Invariance*, *JETP Lett.* **13** (1971) 323–326.

[94] D. V. Volkov and V. P. Akulov, *Possible universal neutrino interaction*, *JETP Lett.* **16** (1972) 438–440.

[95] J. Wess and B. Zumino, *A Lagrangian Model Invariant Under Supergauge Transformations*, *Phys. Lett.* **49B** (1974) 52.

[96] S. R. Coleman and J. Mandula, *All Possible Symmetries of the S Matrix*, *Phys. Rev.* **159** (1967) 1251–1256.

[97] R. Haag, J. T. Lopuszanski and M. Sohnius, *All Possible Generators of Supersymmetries of the s Matrix*, *Nucl. Phys.* **B88** (1975) 257.

[98] N. Seiberg, *Naturalness versus supersymmetric nonrenormalization theorems*, *Phys. Lett.* **B318** (1993) 469–475, [hep-ph/9309335].

[99] J. Wess and B. Zumino, *Supergauge Transformations in Four-Dimensions*, *Nucl. Phys.* **B70** (1974) 39–50.

[100] J. Wess and B. Zumino, *Supergauge Invariant Extension of Quantum Electrodynamics*, *Nucl. Phys.* **B78** (1974) 1.

[101] H. P. Nilles, *Supersymmetry, Supergravity and Particle Physics*, *Phys. Rept.* **110** (1984) 1–162.

[102] H. E. Haber and G. L. Kane, *The Search for Supersymmetry: Probing Physics Beyond the Standard Model*, *Phys. Rept.* **117** (1985) 75–263.

[103] R. Barbieri, *Looking Beyond the Standard Model: The Supersymmetric Option*, *Riv. Nuovo Cim.* **11N4** (1988) 1–45.

[104] R. Barbier et al., *R-parity violating supersymmetry*, *Phys. Rept.* **420** (2005) 1–202, [hep-ph/0406039].

[105] B. Bajc, J. Hisano, T. Kuwahara and Y. Omura, *Threshold corrections to dimension-six proton decay operators in non-minimal SUSY SU (5) GUTs*, *Nucl. Phys.* **B910** (2016) 1–22, [1603.03568].

[106] H. Goldberg, *Constraint on the Photino Mass from Cosmology*, *Phys. Rev. Lett.* **50** (1983) 1419.

[107] J. R. Ellis, J. S. Hagelin, D. V. Nanopoulos, K. A. Olive and M. Srednicki, *Supersymmetric Relics from the Big Bang*, *Nucl. Phys.* **B238** (1984) 453–476.

[108] L. J. Hall, J. D. Lykken and S. Weinberg, *Supergravity as the Messenger of Supersymmetry Breaking*, *Phys. Rev.* **D27** (1983) 2359–2378.

[109] S. K. Soni and H. A. Weldon, *Analysis of the Supersymmetry Breaking Induced by N=1 Supergravity Theories*, *Phys. Lett.* **126B** (1983) 215–219.

[110] I. Affleck, M. Dine and N. Seiberg, *Dynamical Supersymmetry Breaking in Four-Dimensions and Its Phenomenological Implications*, *Nucl. Phys.* **B256** (1985) 557–599.

[111] H. P. Nilles, *Dynamically Broken Supergravity and the Hierarchy Problem*, *Phys. Lett.* **115B** (1982) 193.

[112] A. H. Chamseddine, R. L. Arnowitt and P. Nath, *Locally Supersymmetric Grand Unification*, *Phys. Rev. Lett.* **49** (1982) 970.

[113] P. Nath, R. L. Arnowitt and A. H. Chamseddine, *Gauge Hierarchy in Supergravity Guts*, *Nucl. Phys.* **B227** (1983) 121–133.

[114] R. Barbieri, S. Ferrara and C. A. Savoy, *Gauge Models with Spontaneously Broken Local Supersymmetry*, *Phys. Lett.* **119B** (1982) 343.

[115] M. Dine and A. E. Nelson, *Dynamical supersymmetry breaking at low-energies*, *Phys. Rev.* **D48** (1993) 1277–1287, [hep-ph/9303230].

[116] M. Dine, A. E. Nelson, Y. Nir and Y. Shirman, *New tools for low-energy dynamical supersymmetry breaking*, *Phys. Rev.* **D53** (1996) 2658–2669, [hep-ph/9507378].

[117] G. F. Giudice and R. Rattazzi, *Theories with gauge mediated supersymmetry breaking*, *Phys. Rept.* **322** (1999) 419–499, [hep-ph/9801271].

[118] D. E. Kaplan, G. D. Kribs and M. Schmaltz, *Supersymmetry breaking through transparent extra dimensions*, *Phys. Rev.* **D62** (2000) 035010, [hep-ph/9911293].

[119] Z. Chacko, M. A. Luty, A. E. Nelson and E. Ponton, *Gaugino mediated supersymmetry breaking*, *JHEP* **01** (2000) 003, [hep-ph/9911323].

[120] L. Girardello and M. T. Grisaru, *Soft Breaking of Supersymmetry*, *Nucl. Phys.* **B194** (1982) 65.

[121] G. D'Ambrosio, G. F. Giudice, G. Isidori and A. Strumia, *Minimal flavor violation: An Effective field theory approach*, *Nucl. Phys.* **B645** (2002) 155–187, [hep-ph/0207036].

[122] A. J. Buras, *Minimal flavor violation*, *Acta Phys. Polon.* **B34** (2003) 5615–5668, [hep-ph/0310208].

[123] R. Barbieri, G. Isidori, J. Jones-Perez, P. Lodone and D. M. Straub, $U(2)$ *and Minimal Flavour Violation in Supersymmetry*, *Eur. Phys. J.* **C71** (2011) 1725, [1105.2296].

[124] A. C. Fowler, *Higher order and CP-violating effects in the neutralino and Higgs boson sectors of the MSSM*, *PhD thesis, Durham U., 2010*, *http://etheses.dur.ac.uk/449/* .

[125] R. Peccei and H. R. Quinn, *CP Conservation in the Presence of Instantons*, *Phys. Rev. Lett.* **38** (1977) 1440–1443.

[126] R. Peccei and H. R. Quinn, *Constraints Imposed by CP Conservation in the Presence of Instantons*, *Phys. Rev. D* **16** (1977) 1791–1797.

[127] J. E. Kim and H. P. Nilles, *The mu Problem and the Strong CP Problem*, *Phys. Lett.* **138B** (1984) 150–154.

[128] U. Ellwanger, C. Hugonie and A. M. Teixeira, *The Next-to-Minimal Supersymmetric Standard Model*, *Phys. Rept.* **496** (2010) 1–77, [0910.1785].

[129] W. Hollik and S. Paßehr, *Two-loop top-Yukawa-coupling corrections to the Higgs boson masses in the complex MSSM*, *Phys. Lett.* **B733** (2014) 144–150, [1401.8275].

[130] W. Hollik and S. Paßehr, *Higgs boson masses and mixings in the complex MSSM with two-loop top-Yukawa-coupling corrections*, *JHEP* **10** (2014) 171, [1409.1687].

[131] S. Heinemeyer, O. Stal and G. Weiglein, *Interpreting the LHC Higgs Search Results in the MSSM*, *Phys. Lett.* **B710** (2012) 201–206, [1112.3026].

[132] A. Bottino, N. Fornengo and S. Scopel, *Phenomenology of light neutralinos in view of recent results at the CERN Large Hadron Collider*, *Phys. Rev.* **D85** (2012) 095013, [1112.5666].

[133] R. Benbrik, M. Gomez Bock, S. Heinemeyer, O. Stal, G. Weiglein and L. Zeune, *Confronting the MSSM and the NMSSM with the Discovery of a Signal in the two Photon Channel at the LHC*, *Eur. Phys. J.* **C72** (2012) 2171, [1207.1096].

[134] P. Bechtle, S. Heinemeyer, O. Stal, T. Stefaniak, G. Weiglein and L. Zeune, *MSSM Interpretations of the LHC Discovery: Light or Heavy Higgs?*, *Eur. Phys. J.* **C73** (2013) 2354, [1211.1955].

[135] M. Drees, *A Supersymmetric Explanation of the Excess of Higgs–Like Events at the LHC and at LEP*, *Phys. Rev.* **D86** (2012) 115018, [1210.6507].

[136] M. Carena, S. Heinemeyer, O. Stål, C. E. M. Wagner and G. Weiglein, *MSSM Higgs Boson Searches at the LHC: Benchmark Scenarios after the Discovery of a Higgs-like Particle*, *Eur. Phys. J.* **C73** (2013) 2552, [1302.7033].

[137] P. Bechtle, H. E. Haber, S. Heinemeyer, O. Stål, T. Stefaniak, G. Weiglein et al., *The Light and Heavy Higgs Interpretation of the MSSM*, *Eur. Phys. J.* **C77** (2017) 67, [1608.00638].

[138] E. Bagnaschi et al., *MSSM Higgs Boson Searches at the LHC: Benchmark Scenarios for Run 2 and Beyond*, *Eur. Phys. J.* **C79** (2019) 617, [1808.07542].

[139] M. Carena, D. Garcia, U. Nierste and C. E. M. Wagner, *Effective Lagrangian for the $\bar{t}bH^+$ interaction in the MSSM and charged Higgs phenomenology*, *Nucl. Phys.* **B577** (2000) 88–120, [hep-ph/9912516].

[140] T. Takagi, *On an algebraic problem related to an analytic theorem of Carathéodory and Fejér and on an allied theorem of Landau*, *Japanese J.Math.* **1** (1927) 83.

[141] T. Hahn, *Routines for the diagonalization of complex matrices*, physics/0607103.

[142] S. Y. Choi, J. Kalinowski, G. A. Moortgat-Pick and P. M. Zerwas, *Analysis of the neutralino system in supersymmetric theories*, *Eur. Phys. J.* **C22** (2001) 563–579, [hep-ph/0108117].

[143] J. F. Gunion and H. E. Haber, *Two-body Decays of Neutralinos and Charginos*, *Phys. Rev.* **D37** (1988) 2515.

[144] H. Bahl, *Resummation of logarithmic contributions in mssm higgs-boson mass calculations*, Master's thesis, Technische Universität München, 2015.

[145] T.-F. Feng, *The Two-loop gluino's corrections on the inclusive B —> X(s) gamma decay in the CP violation MSSM with large tan beta*, *Phys. Rev.* **D70** (2004) 096012, [hep-ph/0405192].

[146] A. Denner, *Techniques for calculation of electroweak radiative corrections at the one loop level and results for W physics at LEP-200*, *Fortsch. Phys.* **41** (1993) 307–420, [0709.1075].

[147] A. Brignole, G. Degrassi, P. Slavich and F. Zwirner, *On the O(alpha(t)**2) two loop corrections to the neutral Higgs boson masses in the MSSM*, *Nucl. Phys.* **B631** (2002) 195–218, [hep-ph/0112177].

[148] A. Dedes, G. Degrassi and P. Slavich, *On the two loop Yukawa corrections to the MSSM Higgs boson masses at large tan beta*, *Nucl. Phys.* **B672** (2003) 144–162, [hep-ph/0305127].

[149] A. Brignole, G. Degrassi, P. Slavich and F. Zwirner, *On the two loop sbottom corrections to the neutral Higgs boson masses in the MSSM*, *Nucl. Phys.* **B643** (2002) 79–92, [hep-ph/0206101].

[150] S. Heinemeyer, W. Hollik, H. Rzehak and G. Weiglein, *The Higgs sector of the complex MSSM at two-loop order: QCD contributions*, *Phys. Lett.* **B652** (2007) 300–309, [0705.0746].

[151] T. Fritzsche, S. Heinemeyer, H. Rzehak and C. Schappacher, *Heavy Scalar Top Quark Decays in the Complex MSSM: A Full One-Loop Analysis*, *Phys. Rev. D* **86** (2012) 035014, [1111.7289].

[152] R. P. Feynman, *Space-time approach to nonrelativistic quantum mechanics*, *Rev. Mod. Phys.* **20** (1948) 367–387.

[153] R. P. Feynman, *Relativistic cutoff for quantum electrodynamics*, *Phys. Rev.* **74** (1948) 1430–1438.

[154] R. P. Feynman, *A Relativistic cutoff for classical electrodynamics*, *Phys. Rev.* **74** (1948) 939–946.

[155] N. N. Bogolyubov and O. S. Parasyuk, *A theory of multiplication of causative singular functions,*, *Doklady Akademii Nauk SSSR* **100** (1955) 25–28.

[156] K. Hepp, *Proof of the Bogolyubov-Parasiuk theorem on renormalization*, *Commun. Math. Phys.* **2** (1966) 301–326.

[157] W. Zimmermann, *Convergence of Bogolyubov's method of renormalization in momentum space*, *Commun. Math. Phys.* **15** (1969) 208–234.

[158] M. D. Schwartz, *Quantum Field Theory and the Standard Model*. Cambridge University Press, 2014.

[159] G. 't Hooft and M. J. G. Veltman, *Regularization and Renormalization of Gauge Fields*, *Nucl. Phys.* **B44** (1972) 189–213.

[160] C. G. Bollini and J. J. Giambiagi, *Lowest order divergent graphs in nu-dimensional space*, *Phys. Lett.* **40B** (1972) 566–568.

[161] G. M. Cicuta and E. Montaldi, *Analytic renormalization via continuous space dimension*, *Lett. Nuovo Cim.* **4** (1972) 329–332.

[162] J. F. Ashmore, *A Method of Gauge Invariant Regularization*, *Lett. Nuovo Cim.* **4** (1972) 289–290.

[163] W. Siegel, *Supersymmetric Dimensional Regularization via Dimensional Reduction*, *Phys. Lett.* **84B** (1979) 193–196.

[164] D. M. Capper, D. R. T. Jones and P. van Nieuwenhuizen, *Regularization by Dimensional Reduction of Supersymmetric and Nonsupersymmetric Gauge Theories*, *Nucl. Phys.* **B167** (1980) 479–499.

[165] D. Stockinger, *Regularization by dimensional reduction: consistency, quantum action principle, and supersymmetry*, *JHEP* **03** (2005) 076, [hep-ph/0503129].

[166] W. Hollik and D. Stockinger, *MSSM Higgs-boson mass predictions and two-loop non-supersymmetric counterterms*, *Phys. Lett.* **B634** (2006) 63–68, [hep-ph/0509298].

[167] D. Stöckinger and J. Unger, *Three-loop MSSM Higgs-boson mass predictions and regularization by dimensional reduction*, *Nucl. Phys. B* **935** (2018) 1–16, [1804.05619].

[168] A. Denner and S. Dittmaier, *Electroweak Radiative Corrections for Collider Physics*, 1912.06823.

[169] M. Bohm, A. Denner and H. Joos, *Gauge theories of the strong and electroweak interaction*. 2001.

[170] T. Appelquist and J. Carazzone, *Infrared Singularities and Massive Fields*, *Phys. Rev.* **D11** (1975) 2856.

[171] J. C. Collins, F. Wilczek and A. Zee, *Low-Energy Manifestations of Heavy Particles: Application to the Neutral Current*, *Phys. Rev.* **D18** (1978) 242.

[172] W. Bernreuther and W. Wetzel, *Decoupling of Heavy Quarks in the Minimal Subtraction Scheme*, *Nucl. Phys.* **B197** (1982) 228–236.

[173] D. J. Gross and F. Wilczek, *Ultraviolet Behavior of Nonabelian Gauge Theories*, *Phys. Rev. Lett.* **30** (1973) 1343–1346.

[174] H. D. Politzer, *Reliable Perturbative Results for Strong Interactions?*, *Phys. Rev. Lett.* **30** (1973) 1346–1349.

[175] Y. Schroder and M. Steinhauser, *Four-loop decoupling relations for the strong coupling*, *JHEP* **01** (2006) 051, [hep-ph/0512058].

[176] K. G. Chetyrkin, J. H. Kuhn and C. Sturm, *QCD decoupling at four loops*, *Nucl. Phys.* **B744** (2006) 121–135, [hep-ph/0512060].

[177] R. Harlander, L. Mihaila and M. Steinhauser, *Two-loop matching coefficients for the strong coupling in the MSSM*, *Phys. Rev.* **D72** (2005) 095009, [hep-ph/0509048].

[178] A. Bauer, L. Mihaila and J. Salomon, *Matching coefficients for alpha(s) and m(b) to O(alpha**2(s)) in the MSSM*, *JHEP* **02** (2009) 037, [0810.5101].

[179] A. Brignole, *Radiative corrections to the supersymmetric neutral Higgs boson masses*, *Phys. Lett.* **B281** (1992) 284–294.

[180] M. Frank, S. Heinemeyer, W. Hollik and G. Weiglein, *FeynHiggs1.2: Hybrid MS-bar / on-shell renormalization for the CP even Higgs boson sector in the MSSM*, hep-ph/0202166.

[181] A. Freitas and D. Stockinger, *Gauge dependence and renormalization of tan beta in the MSSM*, *Phys. Rev.* **D66** (2002) 095014, [hep-ph/0205281].

[182] P. H. Chankowski, S. Pokorski and J. Rosiek, *One loop corrections to the supersymmetric Higgs boson couplings and LEP phenomenology*, *Phys. Lett.* **B286** (1992) 307–314.

[183] P. H. Chankowski, S. Pokorski and J. Rosiek, *Complete on-shell renormalization scheme for the minimal supersymmetric Higgs sector*, *Nucl. Phys.* **B423** (1994) 437–496, [hep-ph/9303309].

[184] A. Dabelstein, *The One loop renormalization of the MSSM Higgs sector and its application to the neutral scalar Higgs masses*, *Z. Phys.* **C67** (1995) 495–512, [hep-ph/9409375].

[185] A. Dabelstein, *Fermionic decays of neutral MSSM Higgs bosons at the one loop level*, *Nucl. Phys.* **B456** (1995) 25–56, [hep-ph/9503443].

[186] H. Bahl, *Precise prediction of MSSM Higgs boson masses combining fixed-order and effective field theory calculations*, *PhD thesis, Münich, Tech. U., 2018*, *http://mediatum.ub.tum.de?id=1444430* .

[187] S. Heinemeyer, W. Hollik and G. Weiglein, *The Masses of the neutral CP - even Higgs bosons in the MSSM: Accurate analysis at the two loop level*, *Eur. Phys. J.* **C9** (1999) 343–366, [hep-ph/9812472].

[188] Y. Yamada, *Gauge dependence of the on-shell renormalized mixing matrices*, *Phys. Rev.* **D64** (2001) 036008, [hep-ph/0103046].

[189] S. Heinemeyer, W. Hollik, H. Rzehak and G. Weiglein, *High-precision predictions for the MSSM Higgs sector at O(alpha(b) alpha(s))*, *Eur. Phys. J.* **C39** (2005) 465–481, [hep-ph/0411114].

[190] D. Buttazzo, G. Degrassi, P. P. Giardino, G. F. Giudice, F. Sala, A. Salvio et al., *Investigating the near-criticality of the Higgs boson*, *JHEP* **12** (2013) 089, [1307.3536].

[191] K. E. Williams, H. Rzehak and G. Weiglein, *Higher order corrections to Higgs boson decays in the MSSM with complex parameters*, *Eur. Phys. J.* **C71** (2011) 1669, [1103.1335].

[192] C. Weber, H. Eberl and W. Majerotto, *Improved full one loop corrections to A0 —> tilde-f(1) anti-tilde-f(2) and tilde-f(2) —> tilde-f(1) A0*, *Phys. Rev. D* **68** (2003) 093011, [hep-ph/0308146].

[193] C. Weber, H. Eberl and W. Majerotto, *Improved full one loop corrections to A0 —> squark(1) anti-squark(2) and squark(2) —> squark(1) A0*, *Phys. Lett. B* **572** (2003) 56–67, [hep-ph/0305250].

[194] C. Weber, K. Kovarik, H. Eberl and W. Majerotto, *Complete one-loop corrections to decays of charged and CP-even neutral Higgs bosons into sfermions*, *Nucl. Phys. B* **776** (2007) 138–169, [hep-ph/0701134].

[195] S. Heinemeyer, H. Rzehak and C. Schappacher, *Proposals for Bottom Quark/Squark Renormalization in the Complex MSSM*, *Phys. Rev.* **D82** (2010) 075010, [1007.0689].

[196] P. Slavich. Private communication.

[197] T. Fritzsche, T. Hahn, S. Heinemeyer, F. von der Pahlen, H. Rzehak and C. Schappacher, *The Implementation of the Renormalized Complex MSSM in FeynArts and FormCalc*, *Comput. Phys. Commun.* **185** (2014) 1529–1545, [1309.1692].

[198] L. V. Avdeev and M. Yu. Kalmykov, *Pole masses of quarks in dimensional reduction*, *Nucl. Phys.* **B502** (1997) 419–435, [hep-ph/9701308].

[199] H. Baer, J. Ferrandis, K. Melnikov and X. Tata, *Relating bottom quark mass in DR-BAR and MS-BAR regularization schemes*, *Phys. Rev.* **D66** (2002) 074007, [hep-ph/0207126].

[200] L. Hofer, U. Nierste and D. Scherer, *Resummation of tan-beta-enhanced supersymmetric loop corrections beyond the decoupling limit*, *JHEP* **10** (2009) 081, [0907.5408].

[201] P. Draper, G. Lee and C. E. M. Wagner, *Precise estimates of the Higgs mass in heavy supersymmetry*, *Phys. Rev.* **D89** (2014) 055023, [1312.5743].

[202] A. Sirlin, *Radiative Corrections in the $SU(2)_L \times U(1)$ Theory: A Simple Renormalization Framework*, *Phys. Rev. D* **22** (1980) 971–981.

[203] A. Freitas, W. Hollik, W. Walter and G. Weiglein, *Electroweak two loop corrections to the $M_W - M_Z$ mass correlation in the standard model*, *Nucl. Phys. B* **632** (2002) 189–218, [hep-ph/0202131].

[204] P. H. Chankowski, A. Dabelstein, W. Hollik, W. M. Mosle, S. Pokorski and J. Rosiek, *Delta R in the MSSM*, *Nucl. Phys. B* **417** (1994) 101–129.

[205] S. Heinemeyer, W. Hollik, D. Stockinger, A. Weber and G. Weiglein, *Precise prediction for M(W) in the MSSM*, *JHEP* **08** (2006) 052, [hep-ph/0604147].

[206] E. Fuchs and G. Weiglein, *Breit-Wigner approximation for propagators of mixed unstable states*, *JHEP* **09** (2017) 079, [1610.06193].

[207] E. Fuchs, *Interference effects in new physics processes at the LHC*, *PhD thesis, U. Hamburg, Dept. Phys., 2015*, *http://bib-pubdb1.desy.de/record/224288* .

[208] P. H. Chankowski, S. Pokorski and J. Rosiek, *Charged and neutral supersymmetric Higgs boson masses: Complete one loop analysis*, *Phys. Lett. B* **274** (1992) 191–198.

[209] R.-J. Zhang, *Two loop effective potential calculation of the lightest CP even Higgs boson mass in the MSSM*, *Phys. Lett.* **B447** (1999) 89–97, [hep-ph/9808299].

[210] J. R. Espinosa and R.-J. Zhang, *MSSM lightest CP even Higgs boson mass to O(alpha(s) alpha(t)): The Effective potential approach*, *JHEP* **03** (2000) 026, [hep-ph/9912236].

[211] G. Degrassi, S. Di Vita and P. Slavich, *Two-loop QCD corrections to the MSSM Higgs masses beyond the effective-potential approximation*, *Eur. Phys. J.* **C75** (2015) 61, [1410.3432].

[212] S. Borowka, T. Hahn, S. Heinemeyer, G. Heinrich and W. Hollik, *Momentum-dependent two-loop QCD corrections to the neutral Higgs-boson masses in the MSSM*, *Eur. Phys. J.* **C74** (2014) 2994, [1404.7074].

[213] J. R. Espinosa and R.-J. Zhang, *Complete two loop dominant corrections to the mass of the lightest CP even Higgs boson in the minimal supersymmetric standard model*, *Nucl. Phys.* **B586** (2000) 3–38, [hep-ph/0003246].

[214] B. C. Allanach, A. Djouadi, J. L. Kneur, W. Porod and P. Slavich, *Precise determination of the neutral Higgs boson masses in the MSSM*, *JHEP* **09** (2004) 044, [hep-ph/0406166].

[215] S. P. Martin, *Two Loop Effective Potential for the Minimal Supersymmetric Standard Model*, *Phys. Rev.* **D66** (2002) 096001, [hep-ph/0206136].

[216] S. P. Martin, *Complete Two Loop Effective Potential Approximation to the Lightest Higgs Scalar Boson Mass in Supersymmetry*, *Phys. Rev.* **D67** (2003) 095012, [hep-ph/0211366].

[217] S. P. Martin, *Strong and Yukawa two-loop contributions to Higgs scalar boson self-energies and pole masses in supersymmetry*, *Phys. Rev.* **D71** (2005) 016012, [hep-ph/0405022].

[218] M. D. Goodsell, K. Nickel and F. Staub, *The Higgs Mass in the MSSM at two-loop order beyond minimal flavour violation*, *Phys. Lett. B* **758** (2016) 18–25, [1511.01904].

[219] R. V. Harlander, P. Kant, L. Mihaila and M. Steinhauser, *Higgs boson mass in supersymmetry to three loops*, *Phys. Rev. Lett.* **100** (2008) 191602, [0803.0672].

[220] P. Kant, R. V. Harlander, L. Mihaila and M. Steinhauser, *Light MSSM Higgs boson mass to three-loop accuracy*, *JHEP* **08** (2010) 104, [1005.5709].

[221] T. Kwasnitza, D. Stöckinger and A. Voigt, *Improved MSSM Higgs mass calculation using the 3-loop FlexibleEFTHiggs approach including x_t-resummation*, 2003.04639.

[222] S. P. Martin, *Refined gluino and squark pole masses beyond leading order*, *Phys. Rev. D* **74** (2006) 075009, [hep-ph/0608026].

[223] M. D. Goodsell and S. Paßehr, *All two-loop scalar self-energies and tadpoles in general renormalisable field theories*, 1910.02094.

[224] G. Passarino and M. Veltman, *One Loop Corrections for e+ e- Annihilation Into mu+ mu- in the Weinberg Model*, *Nucl. Phys. B* **160** (1979) 151–207.

[225] G. 't Hooft and M. Veltman, *Scalar One Loop Integrals*, *Nucl. Phys. B* **153** (1979) 365–401.

[226] T. Hahn, *Generating Feynman diagrams and amplitudes with FeynArts 3*, *Comput. Phys. Commun.* **140** (2001) 418–431, [hep-ph/0012260].

[227] T. Hahn and M. Perez-Victoria, *Automatized one loop calculations in four-dimensions and D-dimensions*, *Comput. Phys. Commun.* **118** (1999) 153–165, [hep-ph/9807565].

[228] G. Degrassi, S. Heinemeyer, W. Hollik, P. Slavich and G. Weiglein, *Towards high precision predictions for the MSSM Higgs sector*, *Eur. Phys. J. C* **28** (2003) 133–143, [hep-ph/0212020].

[229] S. Heinemeyer, W. Hollik and G. Weiglein, *FeynHiggs: A Program for the calculation of the masses of the neutral CP even Higgs bosons in the MSSM*, *Comput. Phys. Commun.* **124** (2000) 76–89, [hep-ph/9812320].

[230] T. Hahn, S. Heinemeyer, W. Hollik, H. Rzehak and G. Weiglein, *FeynHiggs: A program for the calculation of MSSM Higgs-boson observables - Version 2.6.5*, *Comput. Phys. Commun.* **180** (2009) 1426–1427.

[231] H. Bahl, T. Hahn, S. Heinemeyer, W. Hollik, S. Paßehr, H. Rzehak et al., *Precision calculations in the MSSM Higgs-boson sector with FeynHiggs 2.14*, *Comput. Phys. Commun.* **249** (2020) 107099, [1811.09073].

[232] L. N. Mihaila, J. Salomon and M. Steinhauser, *Renormalization constants and beta functions for the gauge couplings of the Standard Model to three-loop order*, *Phys. Rev.* **D86** (2012) 096008, [1208.3357].

[233] A. V. Bednyakov, A. F. Pikelner and V. N. Velizhanin, *Anomalous dimensions of gauge fields and gauge coupling beta-functions in the Standard Model at three loops*, *JHEP* **01** (2013) 017, [1210.6873].

[234] A. V. Bednyakov, A. F. Pikelner and V. N. Velizhanin, *Yukawa coupling beta-functions in the Standard Model at three loops*, *Phys. Lett.* **B722** (2013) 336–340, [1212.6829].

[235] K. G. Chetyrkin and M. F. Zoller, *β-function for the Higgs self-interaction in the Standard Model at three-loop level*, *JHEP* **04** (2013) 091, [1303.2890].

[236] A. V. Bednyakov, A. F. Pikelner and V. N. Velizhanin, *Higgs self-coupling beta-function in the Standard Model at three loops*, *Nucl. Phys.* **B875** (2013) 552–565, [1303.4364].

[237] P. Athron, J.-h. Park, D. Stöckinger and A. Voigt, *FlexibleSUSY—A spectrum generator generator for supersymmetric models*, *Comput. Phys. Commun.* **190** (2015) 139–172, [1406.2319].

[238] D. Meuser and A. Voigt, *Investigating multiple solutions to boundary value problems in constrained minimal and non-minimal SUSY models*, *Eur. Phys. J. C* **79** (2019) 821, [1907.07686].

[239] G. Degrassi, S. Di Vita, J. Elias-Miro, J. R. Espinosa, G. F. Giudice, G. Isidori et al., *Higgs mass and vacuum stability in the Standard Model at NNLO*, *JHEP* **08** (2012) 098, [1205.6497].

[240] S. P. Martin and D. G. Robertson, *Higgs boson mass in the Standard Model at two-loop order and beyond*, *Phys. Rev. D* **90** (2014) 073010, [1407.4336].

[241] M. Sperling, D. Stöckinger and A. Voigt, *Renormalization of vacuum expectation values in spontaneously broken gauge theories*, *JHEP* **07** (2013) 132, [1305.1548].

[242] R. Hempfling, *Yukawa coupling unification with supersymmetric threshold corrections*, *Phys. Rev.* **D49** (1994) 6168–6172.

[243] L. J. Hall, R. Rattazzi and U. Sarid, *The Top quark mass in supersymmetric SO(10) unification*, *Phys. Rev.* **D50** (1994) 7048–7065, [hep-ph/9306309].

[244] M. Carena, M. Olechowski, S. Pokorski and C. E. M. Wagner, *Electroweak symmetry breaking and bottom - top Yukawa unification*, *Nucl. Phys.* **B426** (1994) 269–300, [hep-ph/9402253].

[245] J. Guasch, P. Hafliger and M. Spira, *MSSM Higgs decays to bottom quark pairs revisited*, *Phys. Rev.* **D68** (2003) 115001, [hep-ph/0305101].

[246] S. P. Martin, *Fermion self-energies and pole masses at two-loop order in a general renormalizable theory with massless gauge bosons*, *Phys. Rev.* **D72** (2005) 096008, [hep-ph/0509115].

[247] L. Mihaila and C. Reisser, $\mathcal{O}(\alpha_s^2)$ *corrections to fermionic Higgs decays in the MSSM*, *JHEP* **08** (2010) 021, [1007.0693].

[248] M. Ghezzi, S. Glaus, D. Müller, T. Schmidt and M. Spira, *Refinements of the Bottom and Strange MSSM Higgs Yukawa Couplings at NNLO*, 1711.02555.

[249] M. Carena, J. R. Espinosa, M. Quiros and C. E. M. Wagner, *Analytical expressions for radiatively corrected Higgs masses and couplings in the MSSM*, *Phys. Lett.* **B355** (1995) 209–221, [hep-ph/9504316].

[250] M. Carena, H. E. Haber, S. Heinemeyer, W. Hollik, C. E. M. Wagner and G. Weiglein, *Reconciling the two loop diagrammatic and effective field theory computations of the mass of the lightest CP - even Higgs boson in the MSSM*, *Nucl. Phys.* **B580** (2000) 29–57, [hep-ph/0001002].

[251] H. Bahl, P. Bechtle, S. Heinemeyer, S. Liebler, T. Stefaniak and G. Weiglein, *HL-LHC and ILC sensitivities in the hunt for heavy Higgs bosons*, 2005.14536.

[252] H. Bahl, S. Liebler and T. Stefaniak, *MSSM Higgs benchmark scenarios for Run 2 and beyond: the low* $\tan\beta$ *region*, *Eur. Phys. J. C* **79** (2019) 279, [1901.05933].

[253] LHC Higgs Cross Section Working Group collaboration, D. de Florian et al., *Handbook of LHC Higgs Cross Sections: 4. Deciphering the Nature of the Higgs Sector*, 1610.07922.

[254] T. Hahn and S. Paßehr, *Implementation of the* $\mathcal{O}(\alpha_t^2)$ *MSSM Higgs-mass corrections in* FeynHiggs, *Comput. Phys. Commun.* **214** (2017) 91–97, [1508.00562].

[255] M. Carena, J. Ellis, J. S. Lee, A. Pilaftsis and C. E. M. Wagner, *CP Violation in Heavy MSSM Higgs Scenarios*, *JHEP* **02** (2016) 123, [1512.00437].

[256] G. Weiglein, R. Scharf and M. Bohm, *Reduction of general two loop selfenergies to standard scalar integrals*, *Nucl. Phys. B* **416** (1994) 606–644, [hep-ph/9310358].

[257] S. Paßehr and G. Weiglein. Private communication.

[258] T. Kinoshita, *Mass singularities of Feynman amplitudes*, *J. Math. Phys.* **3** (1962) 650–677.

[259] T. Lee and M. Nauenberg, *Degenerate Systems and Mass Singularities*, *Phys. Rev.* **133** (1964) B1549–B1562.

[260] S. P. Martin, *Two-loop scalar self-energies and pole masses in a general renormalizable theory with massless gauge bosons*, *Phys. Rev.* **D71** (2005) 116004, [hep-ph/0502168].

[261] M. Muhlleitner, H. Rzehak and M. Spira, *MSSM Higgs Boson Production via Gluon Fusion: The Large Gluino Mass Limit*, *JHEP* **04** (2009) 023, [0812.3815].

[262] J. Aebischer, A. Crivellin, C. Greub and Y. Yamada, *The MSSM without Gluinos; an Effective Field Theory for the Stop Sector*, *Eur. Phys. J. C* **77** (2017) 740, [1703.08061].

[263] M. Krämer, B. Summ and A. Voigt, *Completing the scalar and fermionic Universal One-Loop Effective Action*, *JHEP* **01** (2020) 079, [1908.04798].

[264] T. Deppisch and U. Nierste, *Little hierarchies solve the little fine-tuning problem: a case study in supersymmetry with heavy guinos*, 1908.01222.

[265] T. L. Deppisch, *A Tale of Scales - Fermion Masses and Mixing in Minimal Supersymmetric $SO(_{10})$ and Resummation of Gluino Contributions to the MSSM Higgs Potential*. PhD thesis, KIT, Karlsruhe, 2019. 10.5445/IR/1000094546.